Steering Control Characteristics of Human Driver Coupled with an Articulated Commercial Vehicle

Siavash Taheri

A Thesis
In the Department
of
Mechanical and Industrial Engineering

Presented in Partial Fulfillment of the Requirements
For the Degree of
Doctor of Philosophy (Mechanical Engineering) at
Concordia University
Montreal, Quebec, Canada

January 2014

CONCORDIA UNIVERSITY

School of Graduate Studies

This is to certify that the thesis prepared

By : **Siavash Taheri**

Entitled: **Steering Control Characteristics of Human Driver Coupled With an Articulated Commercial Vehicle**

and submitted in partial fulfilment of the requirements for the degree of

DOCTOR OF PHILOSOPHY (Mechanical Engineering)

complies with the regulations of the University and meets the accepted standards with respect to originality and quality.

Signed by the final examining committee:

Dr. H. Akbari	Chair
Dr. Y. He	External Examiner
Dr. V. Ramachandran	External to program
Dr. Y. Zhang	Examiner
Dr. R. Sedaghati	Examiner
Dr. S. Rakheja	Co-supervisor
Dr. H. Hong	Co-supervisor

Approved by

Dr. A. Dolatabadi, Graduate Program Director

Januavry 17, 2014

Dr. C. Trueman, Interim Dean
Faculty of Engineering & Computer Science

ABSTRACT

Steering Control Characteristics of Human Driver Coupled With an Articulated Commercial Vehicle

Siavash Taheri,
Concordia University, 2013

Road safety associated with vehicle operation is a complex function of dynamic interactions between the driver, vehicle, road and the environment. Using different motion perceptions, the driver performs as a controller to satisfy key guidance and control requirements of the vehicle system. Considerable efforts have been made to characterize cognitive behavior of the human drivers in the context of vehicle control. The vast majority of the reported studies on driver-vehicle interactions focus on automobile drivers with little or no considerations of the control limits of the human driver. The human driver's control performance is perhaps of greater concern for articulated vehicle combinations, which exhibit significantly lower stability limits. The directional dynamic analyses of such vehicles, however, have been limited either to open-loop steering and braking inputs or simplified path-following driver models. The primary motivations for this dissertation thus arise from the need to characterize human driving behavior coupled with articulated vehicles, and to identify essential human perceptions for developments in effective driver-assist systems and driver-adaptive designs.

In this dissertation research, a number of reported driver models employing widely different control strategies are reviewed and evaluated to identify the contributions of different control strategies as well as the most effective error prediction and compensation strategies for applications to heavy vehicles. A series of experiments was

performed on a driving simulator to measure the steering and braking reaction times, and steering and control actions of the drivers with varying driving experience at different forward speeds. The measured data were analyzed and different regression models are proposed to describe driver's steering response time, peak steer angle and peak steer rate as functions of driving experience and forward speed.

A two-stage preview driver model incorporating curved path geometry in addition to essential human driver cognitive elements such as path preview/prediction, error estimation, decision making and hand-arm dynamics, is proposed. The path preview of the model is realized using near and far preview points on the roadway to simultaneously maintain central lane position and vehicle orientation. The driver model is integrated to yaw-plane models of a single-unit vehicle and an articulated vehicle. The coupled driver-articulated vehicle model is studied to investigate the influences of variations in selected vehicle design parameters and driving speed on the path tracking performance and control characteristics of the human driver. The driver model parameters are subsequently identified through minimization of a composite cost function of path and orientation errors and target directional dynamic responses subject to limit constraints on the driver control characteristics. The significance of enhancing driver's perception of vehicle motion states on path tracking and control demands of the driver are then examined by involving different motion cues for the driver. The results suggest that the proposed model structure could serve as an effective tool to identify human control limits and to determine the most effective motion feedback cues that could yield improved directional dynamic performance and the control demands. The results are discussed so as to serve as guidance towards developments in DAS technologies for future commercial vehicles.

Acknowledgments

My greatest appreciations to my parents and sisters for their constant support and love in my endeavors throughout my lifetime.

I am sincerely grateful to my supervisors, Dr. Subhash Rakheja and Dr. Henry Hong for initiating this research study as well as for their continued technical guidance and great financial support during the completion of this thesis work.

I would also wish to acknowledge Dr. Pierro Hirsch, Mr. Stéphane Desrosiers and all my friends who have volunteered their help and their great corporation during the experimental stages of this work.

Last but not the least, I greatly thank all colleagues, faculty and staff at the department of Mechanical and Industrial Engineering, and my dear friends, specially, Alireza Pazooki, Roham Mactabi and Sining Liu, whose pure friendship has motivated my social and academic life in Canada.

LIST OF CONTENTS

List of Figures xi

List of Tables xviii

Nomenclature xxiv

Abbreviations xxxi

CHAPTER 1

LITERATURE REVIEW AND SCOPE OF THE DISSERTATION

1.1 Introduction 1

1.2 Review of Relevant Literature 3

1.2.1 Perception and Prediction Process 5

1.2.2 Path Preview Process 10

1.2.3 Decision Making Process 15

1.2.4 Response/Reaction Time 24

1.2.5 Limb Motion and Steering Dynamic 27

1.2.6 Performance Index and Identification of the Driver's Control Parameters 30

1.3 Scope and Objective of the Dissertation 32

1.3.1 Objectives of the Dissertation Research 34

1.3.2 Organization of the Dissertation 34

CHAPTER 2

RELATIVE PERFORMANCE ANALYSIS OF DRIVER MODELS

2.1 Introduction 37

2.2 Yaw-Plane Vehicle Model 38

2.3 Mathematical Formulations of the Selected Driver Control Strategies 43

2.3.1 Compensatory Driver Model 44

2.3.2 Preview Compensatory Driver Model 47

2.3.3 Anticipatory/Compensatory Driver Model 50

2.4 Identification of Driver Models Control Parameters 52

2.5 Sensitivity Analysis 54

2.6 Results and Discussions 56

2.6.1 Influences of Variations in Vehicle Speed 56

2.6.2 Influence of Variations in Vehicle Mass 66

2.6.3 Influence of Understeer Coefficient of the Vehicle 72

2.7 Summary 78

2.8 Conclusion 79

CHAPTER 3

EXPERIMENTAL CHARACTERIZATION OF DRIVER CONTROL PROPERTIES

3.1 Introduction 81

3.2 Driving Simulator 82

3.2.1 Experiment Procedures 83

3.2.2 Identification of Outliers 85

3.3 Skill Classification 86

3.3.1 Maneuver Accomplishment 87

3.3.2 Peak Steer Angle and Steer Rate 89

3.3.3 Steer Angle and Steer Rate Crest Factors 93

3.3.4 Steering Profile Area 96

3.3.5 Mean and Peak Speed Deviations from the Target Speed 98

3.3.6 Summary of the Skill Classification 99

3.4 Measurement of the Braking and Steering Response Times 100

3.4.1 Abrupt Braking Maneuver 101

3.4.2 Obstacle Avoidance Maneuver 102

3.5 Results and Discussions 103

3.5.1 Braking Response Time 103

3.5.2 Steering Response Time 106

3.6 Characterization of Drivers' Control Properties 108

3.6.1 Peak Steer angle 109

3.6.2 Peak Steer Rate 111

3.6.3 Coupled Driver-Vehicle responses - Clear Visual Situation 113

3.6.4 Coupled Driver-Vehicle responses - Restricted Visual Situation 115

3.7 Summary 116

CHAPTER 4

DEVELOPMENT OF THE COUPLED DRIVER-VEHICLE MODEL

4.1 Introduction 118

4.2 Yaw-Plane Vehicle Models 119

4.3.1 Yaw-Plane Model of the Articulated Vehicle 120

4.3 Formulation of the Two-Stage Preview Driver Model 123

4.3.1 Driver's Perception and Prediction ……..... 123

4.3.2 Two-stage Preview and Parameters Estimations 125

4.3.3 Decision Making Process 130

4.4 Coupled Driver-Single-Unit Vehicle Model 132

4.4.1 The Generalized Performance Index 133

4.4.2 Validation of the Coupled Driver-Vehicle Model - Clear Visual Field ... 135

4.4.3 Validation of the Coupled Driver-Vehicle Model - Limited Visual Field 138

4.5 Coupled Driver-Articulated Vehicle Model 142

4.6 Summary 147

CHAPTER 5

IDENTIFICATION OF DRIVER'S CONTROL LIMITS

5.1 Introduction 148

5.2 Identification of the Driver's Control Parameters 149

5.3 Sensitivity Analysis - Driver Model Parameters 152

5.4 Sensitivity Analysis - Variations in Speed and Vehicle Design Parameters 155

5.5 Identification of Control Limits of the Driver 159

5.5.1 Variations of the Forward Speed 160

5.5.2 Variations in Tractor Design Parameters ……..... 165

5.5.3 Variations in Semi-Trailer Design Parameters ……..... 173

5.6 Summary 181

CHAPTER 6

IDENTIFICATION OF EFFECTIVE MOTION CUES PERCEPTION

6.1 Introduction 183

6.2 Perception of Different Vehicle States by the Human Driver 184

6.3 Identification of Effective Motion Cues Perception …….. 186

6.3.1 Influence of Additional Feedback Cues - High Speed Driving …..... 187

6.3.2 Influence of Additional Feedback Cues - Heavier Tractor Unit …… 193

6.3.3 Influence of Additional Feedback Cues - Longer Tractor Unit ……. 196

6.3.4 Influence of Additional Feedback Cues - Higher Tractor Tandem Spread 198

6.3.5 Influence of Additional Feedback Cues - Heavier Trailer Unit …… 200

6.3.6 Influence of Additional Feedback Cues - Longer Trailer Unit …….. 203

6.3.7 Influence of Additional Feedback Cues - Higher Trailer Tandem Spread 205

6.4 Summary 207

CHAPTER 7

CONCLUSIONS AND RECOMMENDATIONS

7.1 Highlights and Major Contributions of the Dissertation Research 209

7.2 Conclusions 211

7.3 Recommendations for Future Studies 213

REFERENCES ……..... 216

APENDIX A

A.1 Yaw-Plane Model of the Single-Track Articulated Vehicle …….…..... 229

A.2 Yaw-Plane Articulated Vehicle Model ……...…... 211

A.3 Simulation Results of Tire Cornering and Aligning Properties ……..…….. 213

LIST OF FIGURES

Figure 1.1:	Overall structure of the coupled driver/vehicle system ……	4
Figure 1.2:	The dead-zone model used to describe perception threshold of the human body sensory feedbacks ……	7
Figure 1.3:	Prediction of vehicle motion at a future instant using first-order and second-order prediction models …….	9
Figure 1.4:	The compensatory driver model structure ……	17
Figure 1.5:	The anticipatory/compensatory driver model structure ……	18
Figure 1.6:	The preview compensatory structure involving the driver's preview and prediction …….	19
Figure 1.7:	Estimation of the vehicle orientation deviation ……	20
Figure 1.8:	Visual angle of the lead car in a forward speed control system …..	21
Figure 1.9:	Basic components and schematic of neuromuscular system ……	27
Figure 1.10:	Limb motion dynamics coupled with the steering system dynamics	28
Figure 2.1:	Two DoF yaw-plane model of a single-unit vehicle ……	39
Figure 2.2:	Comparisons of directional responses of the yaw plane vehicle model with the simulator measured data under a double lane-change maneuver at 30 km/h ……	40
Figure 2.3:	Comparisons of directional responses of the yaw plane vehicle model with the simulator measured data under a double lane-change maneuver at 50 km/h ……	41
Figure 2.4:	Comparisons of directional responses of the yaw plane vehicle model (solid line) with the simulator measured data (dashed line) under a double lane-change maneuver at 70 km/h ……...	42
Figure 2.5:	The compensatory driver model employing lateral position feedback ……	46
Figure 2.6:	The compensatory driver model employing lateral position and orientation feedbacks ……	47

Figure 2.7: The preview compensatory model employing second-order path prediction …….. 48

Figure 2.8: The preview compensatory driver model employing 'internal vehicle model' path prediction strategy ……... 49

Figure 2.9: The preview compensatory driver model employing multi-point preview strategy …… 50

Figure 2.10: The preview compensatory driver model employing multi-point preview strategy together with the muscular dynamic ……. 51

Figure 2.11: The anticipatory/compensatory driver model structure proposed by Donges …….. 52

Figure 2.12: Comparisons of the lead time constant, lateral position gain constant (log scale) and orientation gain constant of the selected driver models during a double-lane change maneuver at three different speeds ……. 57

Figure 2.13: Comparison of the lead time constant, lateral position gain constant and orientation gain constant of selected driver models during a double-lane change maneuver subject to variations in the vehicle mass (speed= 20 m/s) ……... 67

Figure 2.14: Comparison of the lead time constant, lateral position gain constant and orientation gain constant of selected driver models subject to variations of understeer coefficient (speed= 20 m/s) ….. 74

Figure 3.1: Open cabin of the limited-motion driving simulator …… 81

Figure 3.2: The standard slalom course used in the experiments ……... 86

Figure 3.3: Correlations of number of hit or missed cones with the driving experience during slalom maneuvers at 70 km/h ……. 87

Figure 3.4: Correlations of mean peak steer angle, and $r2$ values and variations in CoV when data corresponding to a certain subject was removed during slalom maneuver slalom at 30 km/h, 50 km/h and 70 km/h …….. 90

Figure 3.5: Correlations of mean peak steer rate during slalom maneuvers at 30 km/h, 50 km/h and 70 km/h ...…….. 91

Figure 3.6: Correlations of mean steer angle crest factor, mean steering rate crest factor with the driving experience during slalom maneuvers at three selected target speed 30, 50 and 70 km/h ……... 94

Figure 3.7: Steering profile of the driver, steering profile area, indicated by the grey-shaded area ……... 95

Figure 3.8: Correlations of mean steering profile area with the driving experience during slalom maneuvers at three target speeds ...…….. 96

Figure 3.9: Correlations of mean speed deviations and peak speed deviations with the driving experience during slalom maneuvers at 70 km/h ... 98

Figure 3.10: Braking response time in an abrupt braking maneuver …… 101

Figure 3.11: Steering response time observed during an obstacle avoidance maneuver …….. 102

Figure 3.12: Variations in mean perception-processing times, mean foot movement time and mean overall brake response time with forward speed ……... 104

Figure 3.13: Variations in mean perception-processing and movement time with participants' driving experience ……... 104

Figure 3.14: Variations in the steering response time due to variations in the forward speeds and driving experience …… 106

Figure 3.15: Standard course of the double-lane change maneuver ……. 108

Figure 3.16: Peak steer angle and peak steer rate as functions of the forward speed and driving experience during double-lane change maneuvers ……. 112

Figure 3.17: Comparisons of path tracking and steering responses of 'average' (solid line) and 'experience' (dashed line) drivers groups under a double lane-change maneuver at different speeds: 30 km/h, 50 km/h and 70 km/h (clear visual situation) …… 113

Figure 3.18: Comparisons of mean path tracking and steering responses of average (solid line) and experience (dashed line) drivers groups under a double lane-change maneuver at different speeds: 30 km/h, 50 km/h and 70 km/h (limited visibility condition) ……. 115

Figure 4.1: Three DoF yaw-plane model of the articulated vehicle ……... 121

Figure 4.2: Comparisons of directional responses of the single-track yaw-plane vehicle model (dashed line) and the nonlinear yaw-plane vehicle model (solid line) with the measured data (dotted line) during a lane-change maneuver at a constant speed of 68.8 km/h ... 121

Figure 4.3: The structure of the proposed two-stage preview driver model ….. 122

Figure 4.4: Estimation of the near and far preview points on a straight-line roadway and a curved path ……... 126

Figure 4.5: Estimation of the lateral position error ……. 128

Figure 4.6: The two-stage preview driver coupled with a single-unit vehicle model …… 131

Figure 4.7: Variations in control parameters of the driver model during a double lane-change maneuver at different speeds for 'experienced' and 'average' drivers (clear visual field) ……. 134

Figure 4.8: Comparisons of measured path tracking and steering responses (solid line) with the model responses (dashed line) for the 'average' driver group under a double lane-change maneuver at different speeds: 30, 50 and 70 km/h (clear visual field) ……. 136

Figure 4.9: Comparisons of measured path tracking and steering responses (solid line) with the model responses (dashed line) for the 'experienced' driver group under a double lane-change maneuver at different speeds: 30, 50 and 70 km/h (clear visual field) ……. 137

Figure 4.10: Variations in control parameters of the driver models during a double lane-change maneuver at different speeds for 'experienced' and 'average' driver (limited visibility field) ……... 138

Figure 4.11: Comparisons of measured path tracking and steering responses (solid line) with the model responses (dashed line) for the 'average' driver group under a double lane-change maneuver at different speeds: 30, 50 and 70 km/h (limited visual field) …….. 140

Figure 4.12: Comparisons of measured path tracking and steering responses (solid line) with the model responses (dashed line) for the 'experienced' driver group under a double lane-change maneuver at different speeds: 30, 50 and 70 km/h (limited visual field) …….. 141

Figure 4.13: The coupled baseline driver-articulated vehicle system (solid line) and the additional perceived motion states of the vehicle (dashed line) corresponding to structures 2 to 10 …… 142

Figure 4.14: Comparisons of (a) path tracking response; and (b) front wheel steer angle of the coupled driver-articulated vehicle model (solid line) with the measured data (dashed line) during a lane-change maneuver at a constant speed of 68.8 km/h …….. 145

Figure 5.1: Schematic of a tractor and semi-trailer combination illustrating geometric and inertial parameters of interest ……... 149

Figure 5.2: Variations in the optimization problem solutions corresponding to three different sets of initial values: (a) lateral position and orientation gains; (b) far and near preview times; and (c) lead and lag time constants ……. 151

Figure 5.3: Path coordinates of the tractor cg during an open-loop step-steer maneuver at 100 km/h with 20% increase in selected geometric and inertial parameters ……. 157

Figure 5.4: Influence of variations in the forward speed on the driver control parameters during a double lane-change maneuver (50, 80, 100 and 120 km/h) ……... 161

Figure 5.5: Influence of variations in the forward speed on: (a) path tracking response; and (b) steer angle of the tractor unit during double lane-change maneuvers …… 161

Figure 5.6: Path deviation and orientation error of the articulated vehicle ……. 162

Figure 5.7: Influence of variations in the tractor mass on the driver control parameters during a double lane-change maneuver (speed=100 km/h) …… 165

Figure 5.8: Influence of variations in the tractor mass on: (a) path tracking response; and (b) steer angle during a double lane-change maneuver (speed=100 km/h) …… 165

Figure 5.9: Influence of variations in the tractor wheelbase on the driver control parameters during a double lane-change maneuver (speed=100 km/h) ……. 168

Figure 5.10: Influence of variations in the tractor wheelbase on: (a) path tracking response; and (b) steer angle during a double lane-change maneuver (speed=100 km/h) …… 168

Figure 5.11: Influence of variations in the tractor axle spreads on the driver control parameters during a double lane-change maneuver (speed=100 km/h) ……. 170

Figure 5.12: Influence of variations in the tractor axle spreads on: (a) path tracking response; and (b) steer angle during a double lane-change maneuver (speed=100 km/h) …… 170

Figure 5.13: Influence of variations in the semi-trailer mass on the driver control parameters during a double lane-change maneuver (speed=100 km/h) ……. 173

Figure 5.14: Influence of variations in the semi-trailer mass on: (a) path tracking response; and (b) steer angle during a double lane-change maneuver (speed=100 km/h) …… 173

Figure 5.15: Influence of variations in the semi-trailer wheelbase on the driver control parameters during a double lane-change maneuver (speed=100 km/h) ……. 176

Figure 5.16: Influence of variations in the semi-trailer wheelbase on: (a) path tracking response; and (b) steer angle during a double lane-change maneuver (speed=100 km/h) …… 176

Figure 5.17: Influence of variations in the semi-trailer axle spreads on the driver control parameters during a double lane-change maneuver (speed=100 km/h) ……. 178

Figure 5.18: Influence of variations in the semi-trailer axle spreads on: (a) path tracking response; and (b) steer angle during a double lane-change maneuver (speed=100 km/h) …… 179

Figure 6.1: Influence of employing different combinations of feedback cues on variations in the lag time constant (T_l) at a constant speed of 120 km/h ……... 191

Figure A.1: Three DoF yaw-plane model of the single-track articulated vehicle 229

Figure A.2: Dimensional parameters of the yaw-plane articulated vehicle model …… 233

Figure A.3: Cornering forces of the tires and articulation forces of the yaw-plane articulated vehicle model …… 234

Figure A.4: Comparison of the measured data (circle dotes) and estimated profile of the cornering forces and aligning moments of the tire subject to the three different normal loads ……... 236

LIST OF TABLES

Table 1.1: Different driver sensory feedbacks which is employed in the reported studies ……. 6

Table 1.2: Summary of studies reporting objectively measured human driver preview time ……. 13

Table 1.3: Summary of studies reporting indirectly identified preview time … 15

Table 1.4: Summary of reported driver model strategies related to the steering behavior of the human driver ……... 22

Table 1.5: Studies reporting indirectly identified reaction times …….. 25

Table 1.6: Summary of studies reported measured reaction times of human drivers …….. 26

Table 1.7: Range of human driver's control variables …….. 31

Table 2.1: Simulation parameters of the single-unit vehicle model …….. 39

Table 2.2: Summary of selected driver models ……. 45

Table 2.3: Range of vehicle parameters and the nominal values employed in sensitivity analysis …… 55

Table 2.4: Influences of variations in vehicle speed on the identified driver model parameters and corresponding performance measures of the selected driver-vehicle models ……. 58

Table 2.5: Sensitivity of directional responses and steering effort of selected driver-vehicle models to variations in forward speed …….. 63

Table 2.6: Sensitivity of total performance index and its constituents of the selected driver-vehicle models to variations in forward speed …… 64

Table 2.7: Influences of variations in vehicle mass on the identified driver model parameters and corresponding performance measures …….. 66

Table 2.8: Variation in peak directional responses of the selected driver models to variations in the vehicle mass (speed=20 m/s) …… 70

Table 2.9: Variation in total performance index and its constituents of the selected driver models to variations in the vehicle mass (speed=20 m/s) ……... 70

Table 2.10: Influences of variations in understeer coefficient of the vehicle on the identified driver model parameters and corresponding performance measures …….. 73

Table 2.11: Variation in the peak directional responses of the selected driver models to changes in the understeer coefficient (speed=20 m/s) …. 76

Table 2.12: Variation in the total performance index and its constituents of the selected driver models to changes in the understeer coefficient (speed=20 m/s) ……. 77

Table 3.1: List of subject information ……... 82

Table 3.2: Total number of 'hit' or 'missed' cones during all trials of slalom maneuvers ……. 87

Table 3.3: Peak front wheels steer angle measured during constant speed slalom maneuvers ……. 88

Table 3.4: Peak rate of steering input measured during constant speed slalom maneuvers ……. 89

Table 3.5: Crest factor of the steer angle measured during slalom maneuvers.. 93

Table 3.6: Crest factor of rate of steering input measured during slalom maneuvers ……. 94

Table 3.7: Steering profile area during slalom maneuvers …… 96

Table 3.8: Mean of 'mean' and 'peak' speed deviations during slalom maneuvers ……. 98

Table 3.9: Summary of driving skill classification based upon the measures considered during a slalom maneuvers ……. 99

Table 3.10: Mean perception-processing and movement times of each participant performing a straight-line braking maneuver at three different speeds ……. 103

Table 3.11: Mean steering response time of each participant performing an obstacle avoidance maneuver at three different speeds …… 105

Table 3.12: Peak steer angle measured during the first two trials of constant speed double-lane change maneuvers …….. 109

Table 3.13: Peak rate of steering input measured during the first two trials of constant speed double-lane change maneuvers ……. 111

Table 4.1: The steering system and the limb dynamic parameters, and the identified control parameters of the coupled driver-articulated model during a lane-change maneuver at 68.8 km/h …… 145

Table 5.1: Percentage change of the total performance index and its constituents with variations in the driver model parameters …… 153

Table 5.2: Range of vehicle parameters and the nominal values employed in sensitivity analysis …… 155

Table 5.3: Percent changes in peak directional responses of the articulated vehicle with 20% increase in the selected parameters …….. 158

Table 5.4: Influence of variations in the forward speed of the vehicle on peak errors in path tracking measures tracking responses of the driver-vehicle system …….. 163

Table 5.5: Influence of variations in the forward speed of the vehicle on peak directional responses of the driver-vehicle system ……... 163

Table 5.6: Influence of variations in the tractor mass on peak errors in path tracking measures of the driver-vehicle system (speed=100 km/h).. 166

Table 5.7: Influence of variations in tractor mass on peak directional responses of the driver-vehicle system (speed=100 km/h) …….. 166

Table 5.8: Influence of variations in tractor wheelbase on peak errors in path tracking measures of the driver-vehicle system (speed=100 km/h).. 169

Table 5.9: Influence of variations in tractor wheelbase on peak directional responses of the driver-vehicle system (speed=100 km/h) …….. 169

Table 5.10: Influence of variations in tractor axle spreads on peak errors in path tracking measures of the driver-vehicle system (speed=100 km/h) …… 171

Table 5.11: Influence of variations in tractor axle spreads on peak directional responses of the driver-vehicle system (speed=100 km/h) …….. 171

Table 5.12: Influence of variations in semi-trailer mass on peak errors in path tracking measures of the driver-vehicle system (speed=100 km/h).. 174

Table 5.13: Influence of variations in semi-trailer mass on peak directional responses of the driver-vehicle system (speed=100 km/h) …….. 174

Table 5.14: Influence of variations in semi-trailer wheelbase on peak errors in path tracking measures of the driver-vehicle system (speed=100 km/h) …… 177

Table 5.15: Influence of variations in semi-trailer wheelbase on peak directional responses of the driver-vehicle system (speed=100 km/h) …… 177

Table 5.16: Influence of variations in semi-trailer axle spread on peak errors in path tracking measures of the driver-vehicle system (speed=100 km/h) …… 179

Table 5.17: Influence of variations in semi-trailer axle spread on peak directional responses of the driver-vehicle system (speed=100 km/h) …… 180

Table 5.18: Influences of variations in the forward speed and vehicle design parameters on path tracking performance and steering response of the driver …….. 181

Table 6.1: The proposed driver model structures employing driver's perceptions of different motion cue ……. 184

Table 6.2: Range of human driver's control parameters ……... 186

Table 6.3: Variations in the total performance index and its constituents by considering different driver model structures considering nominal vehicle parameters at a constant speed of 100 km/h …… 187

Table 6.4: Relative changes in path tracking and directional response measures of the coupled driver-vehicle system integrating different feedback cues compared to those obtained from the baseline model (structure 1) considering nominal vehicle parameters at constant speed of 100 km/h …… 188

Table 6.5: Variations in the total performance index and its constituents by considering different driver model structures considering nominal vehicle parameters at a constant speed of 120 km/h …… 189

Table 6.6: Relative changes in path tracking and directional response measures of the coupled driver-vehicle system integrating different feedback cues compared to those obtained from the baseline model (structure 1) considering nominal vehicle parameters at a constant speed of 120 km/h …… 190

Table 6.7: Variations in the total performance index and its constituents by considering different driver model structures for a heavier tractor unit (100 km/h) …… 192

Table 6.8: Relative changes in path tracking and directional response measures of the coupled driver-vehicle system with respect to those obtained from the baseline model (structure 1) considering different feedback cues for a heavier tractor unit (100 km/h) …….. 194

Table 6.9: Variations in the total performance index and its constituents by considering different driver model structures for a longer tractor unit (100 km/h) ……. 196

Table 6.10: Relative changes in path tracking and directional response measures of the coupled driver-vehicle system with respect to those obtained from the baseline model (structure 1) considering different feedback cues for a longer tractor unit (100 km/h) …… 197

Table 6.11: Variations in the total performance index and its constituents by considering different driver model structures for higher tandem axle spread of the tractor (100 km/h) ……... 198

Table 6.12: Relative changes in path tracking and directional response measures of the coupled driver-vehicle system with respect to those obtained from the baseline model (structure 1) considering different feedback cues for higher tandem axle spread of the tractor (100 km/h) ……. 199

Table 6.13: Variations in the total performance index and its constituents by considering different driver model structures for a heavier trailer unit (100 km/h) ……. 200

Table 6.14: Relative changes in path tracking and directional response measures of the coupled driver-vehicle system with respect to those obtained from the baseline model (structure 1) considering different feedback cues for a heavier trailer unit (100 km/h) ……... 201

Table 6.15: Variations in the total performance index and its constituents by considering different driver model structures for a longer trailer unit (100 km/h) ……. 202

Table 6.16: Relative changes in path tracking and directional response measures of the coupled driver-vehicle system with respect to those obtained from the baseline model (structure 1) considering different feedback cues for a longer trailer unit (100 km/h) …… 203

Table 6.17: Variations in the total performance index and its constituents by considering different driver model structures for higher tandem axle spread of the trailer (100 km/h) …… 204

Table 6.18: Relative changes in path tracking and directional response measures of the coupled driver-vehicle system with respect to those obtained from the baseline model (structure 1) considering different feedback cues for higher tandem axle spread of the trailer (100 km/h) …… 206

Table 6.19: The most effective combinations of feedback cues to improve the path deviation, steering effort and the total performance index of the coupled driver-vehicle system …… 207

Table A.1: Geometric and Inertial parameters of the selected articulated vehicle combination ……..…… 234

NOMENCLATURE

SYMBOL	DESCRIPTION
a	Longitudinal distance of the front axle from the cg of the single-unit vehicle, m
a_k	Longitudinal distance from k^{th} axle to the center of gravity of the associated unit (k=1,2,3,4,5), m
a_y	Lateral acceleration of the single-unit vehicle, m/s^2
a_{yj}	Lateral acceleration of unit j for the articulated vehicle combinations (j=1 for the tractor and j=2 for the semi-trailer unit), m/s^2
$a_{y,maxl}$	Maximum allowable lateral acceleration of the vehicle (l=1 for the single-unit vehicle, and l=2 for the articulated vehicle), m/s^2
$[A_l]$	State matrix of the states-space model of the vehicle (l=1 for the single-unit vehicle, and l=2 for the articulated vehicle)
b	Longitudinal distance of the rear axle from the cg of the single-unit vehicle, m
B_r	Damping coefficient of the reflex system, N.m.s/rad
B_{dr}	Damping coefficient of the drivers' hand-arm system, N.m.s/rad
B_{st}	Damping coefficient of the steering system, N.m.s/rad
$[B_l]$	Input matrix of the states-space model of the vehicle (l=1 for the single-unit vehicle, and l=2 for the articulated vehicle)
c_j	Longitudinal distance between the articulation joint and the center of gravity of unit j (j=1 for the tractor and j=2 for the semi-trailer unit), m
C	Curvatures of the predicted coordinate of the vehicle trajectory, 1/m
C_d	Instantaneous path curvature, 1/m
$C_{d,Tp}$	Curvature of the previewed path at a future instant T_p, 1/m
C_e	Instantaneous path curvature error, 1/m
C_k	Cornering stiffness of tires mounted on k^{th} axle of the articulated vehicle (k=1,2,3,4,5), N/rad
C_{xk}	Longitudinal stiffness of tires mounted on k^{th} axle of the articulated vehicle (k=1,2,3,4,5), N

C_δ	Crest factor of the steer angle
$C_{\dot{\delta}}$	Crest factor of the rate of steering input
D	Dual tire spacing, m
D_p	Preview distance of the driver, m
D_{PN} and D_{PF}	Near and Far preview distances, respectively
F_{yf} and F_{yr}	Cornering forces acting on the front and rear tires of the single-unit vehicle, respectively, N
F_{yk}	Cornering force of the k^{th} axle tires for the single-track articulated vehicle (k=1,2,3,4,5), N
F_{yki}	Cornering force of the i^{th} tire on axle k for the articulated vehicle (i=1,2 for k=1; i=1,2,3,4 for k=2,3,4,5), N
F_{zk}	Normal load on the tire corresponding to k^{th} axle for the single-track articulated vehicle (k=1,2,3,4,5), N
F_{zki}	Normal load on the i^{th} tire on axle k for the articulated vehicle (i=1,2 for k=1; i=1,2,3,4 for k=2,3,4,5), N
F_{XA} and F_{YA}	Longitudinal and lateral forces at the articulation point, respectively, N
G_{st}	Steering ratio of the vehicle steering system
I_{zz}	Yaw moment of inertia of the single-unit vehicle, kg.m/sec^2
I_{zzj}	Yaw moment of inertia of the unit j for articulated vehicle combinations (j=1 for the tractor and j=2 for the semi-trailer unit), kg.m/sec^2
J_{dr}	The inertia of the drivers' hand-arm system
J_{st}	The inertia of the steering system
J_t	Generalized performance index, summation of all indices
J_Y	Weighted mean squared lateral position error of the vehicle
J_Ψ	Weighted mean squared orientation error of the vehicle
J_δ	Weighted mean squared steer angle of the human driver
$J_{\dot{\delta}}$	Weighted mean squared steer rate of the human driver
J_{a_y}	Weighted mean squared lateral acceleration of the single-unit vehicle

$J_{a_{yj}}$	Weighted mean squared lateral acceleration of unit *j* for the articulated vehicle combinations (*j*=1 for the tractor and *j*=2 for the semi-trailer unit)
J_r	Weighted mean squared yaw rate of the single-unit vehicle
J_{r_j}	Weighted mean squared yaw rate of unit *j* for the articulated vehicle combinations (*j*=1 for the tractor and *j*=2 for the semi-trailer unit)
$J_{\dot{\gamma}}$	Weighted mean squared articulation rate for the articulated vehicle combinations
K_{dr}	The stiffness of the drivers' hand-arm system, Nm/rad
K_r	The stiffness constants of the reflex system, Nm/rad
K_{st}	The stiffness of the steering system, Nm/rad
K_C	Curvature error compensatory gain, rad.m
K_y	Lateral position error compensatory gain, rad/m
K_Ψ	Orientation error compensatory gain, rad/rad
K_i	Proportional compensatory actions of the driver with respect to the estimated path deviation (*i*=1) and orientation error (*i*=2) of the tractor unit, and the selected perceived motion states of both the tractor and the semi-trailer units, (*i*=3 to 7).
m	Mass of the single-unit vehicle, kg
m_j	Mass of unit *j* for articulated vehicle combinations (*j*=1 for the tractor and *j*=2 for the semi-trailer unit), kg.m/sec^2
M_{yf} and M_{yr}	Aligning moment acting on the front and rear tires of the single-unit vehicle, respectively, N.m
M_k	Aligning moment of the k^{th} axle tires for the single-track articulated vehicle combinations (*k*=1,2,3,4,5), N.m
M_{ki}	Aligning moment of the i^{th} tire on axle *k* for the articulated vehicle combinations (*i*=1,2 for *k*=1; *i*=1,2,3,4 for *k*=2,3,4,5), N.m
M_{DTk}	Dual tire moment of the k^{th} axle tires for the single-track articulated vehicle combinations (*k*=1,2,3,4,5), N.m
r	Yaw rate of the single-unit vehicle, rad/s
r_j	Yaw rate of unit *j* for the articulated vehicle combinations (*j*=1 for the tractor and *j*=2 for the semi-trailer unit), rad/s

r_{maxl}	Maximum allowable yaw rate of the vehicle (l=1 for the single-unit vehicle, and l=2 for articulated vehicle), rad/s
t	Time, s
t_k	Pneumatic trail of tires on k^{th} axle for the articulated vehicle (k=1,2,3,4,5), m
T_p	Preview time of the human driver, s
T_{fb}	Torque feedback of the steering system, N.m
T_L	Lead time constant, s
$T_{L\Psi}$	Lead time constant of the driver corresponding to the orientation error of the vehicle, s
T_{Ly}	Lead time constant of the driver corresponding to the lateral position error of the vehicle, s
T_I	Lag time constant, s
$T_{I\Psi}$	Lag time constant of the driver corresponding to the orientation error of the vehicle, s
T_{Iy}	Lag time constant of the driver corresponding to the lateral position error of the vehicle, s
T_{Nm}	Lag time of the neuromuscular system, s
T_{PN} and T_{PF}	Near and Far preview times, respectively, s
$\vec{u}$	Input vector of the state-space model of the vehicle
v_x	Longitudinal velocity of the vehicle in the vehicle-fixed coordinate (xy), m/s
v_{xj}	Longitudinal velocity of unit j for the articulated vehicle combinations (j=1 for the tractor and j=2 for the semi-trailer unit) in the vehicle-fixed coordinate, m/s
v_y	Lateral velocity of the vehicle in the vehicle-fixed coordinate (xy), m/s
v_{yj}	Lateral velocity of unit j for the articulated vehicle combinations (j=1 for the tractor and j=2 for the semi-trailer unit) in the vehicle-fixed coordinate, m/s
$\vec{x}$	State vector of the state-space model of the vehicle
X_D and Y_D	Longitudinal and lateral coordinates of the driver's seat in the global axis system (XY), respectively, m

X_g and Y_g	Longitudinal and lateral coordinates of the driver's seat in the global axis system (XY), respectively, m
X_P and Y_P	Longitudinal and lateral coordinates of the predicted position of the tractor cg in the global axis system (XY), respectively, m
X_N and Y_N	Longitudinal and lateral coordinates of the near target point in the global axis system (XY), respectively, m
X_F and Y_F	Longitudinal and lateral coordinates of the far target point in the global axis system (XY), respectively, m
X_T and Y_T	Longitudinal and lateral coordinates of the tangent point in the global axis system (XY), respectively, m
Y	Instantaneous lateral position of the vehicle, m
$\dot{Y}$	Instantaneous lateral velocity of the vehicle in the global axis system (XY), m/s
$\ddot{Y}$	Instantaneous lateral acceleration of the vehicle in the global axis system (XY), m/s^2
Y_e	Instantaneous lateral position error of the vehicle in the global axis system (XY), m
Y_{Tp}	Predicted lateral coordinates of the vehicle in the global axis system (XY), m
$Y_{d,Tp}$	Previewed path coordinates at a future instant T_p in the global axis system (XY), m
$Y_{e,Tp}$	Perceived path error between the previewed path and predicted coordinates of the vehicle in the global axis system (XY), m
$Y_{e,max}$	Maximum allowable lateral position error, m
α_{kj}	Average side-slip angle developed at the tires mounted on k^{th} axle of the unit j (j=1 for tractor and 2 for semi-trailer unit), (k=1,2,3 for j=1; k=4,5 for j=2), rad
Ψ	Orientation of the single-unit vehicle, rad
Ψ_j	Orientation of unit j for the articulated vehicle combinations (j=1 for the tractor and j=2 for the semi-trailer unit), rad
Ψ_c	Visual angle of the sight point, rad
Ψ_d	Instantaneous orientation of the desired path, rad

Ψ_e	Instantaneous orientation error, rad
$\Psi_{e,max}$	Maximum allowable orientation error, rad
Ψ_v	Visual angle of the predicted path, rad
ϕ	Roll angle of the vehicle, rad
Φ	Human driver's overall visual field, rad
$\emptyset(t)$	State-transition matrix
δ_d	Steering angle command of the human driver, rad
δ_F	Vehicle's front wheels steering angle, rad
δ_S	Human driver steering wheel angle, rad
$\delta_{F,max}$	Peak steer angle during double lane-change maneuver, rad
$\dot{\delta}_{F,max}$	Peak steer rate during double lane-change maneuver, rad/s
$\Delta\delta_F$	Peak steer angle in accordance with the known drivers' limits, rad
$\Delta\dot{\delta}_F$	Peak steer rate in accordance with the known drivers' limits, rad/s
$\Delta v_{x,mean}$	Deviation of the average speed from the target speed, m/s
$\Delta v_{x,peak}$	Peak difference between the instantaneous speed and the average speed, m/s
τ_b	Overall braking response time of the human driver, s
τ_s	Overall steering response time of the human driver, s
τ_p	Processing delay time of the human driver, s
τ_r	The transport lag in sending messages to and from the spinal cord, s
τ_{pd}	Perception delay time of the driver, s
τ_m	Movement delay time, s
ζ	The damping ratio of the combined manipulator and the limb muscles
ω_n	The natural frequency of the combined manipulator and the limb muscles, rad/s
ω_c	The cut-off frequency of the reflex system, rad/s
γ	Articulation angle of the articulated vehicle combination, rad

$\dot{\gamma}$	Articulation rate of the articulated vehicle combination, rad/s
$\dot{\gamma}_{max}$	Maximum allowable articulation rate for the articulated vehicle combinations, rad/s

ABBREVIATIONS

ANOVA	Analysis of variance
ADAS	Active driver assist system
BACs	Blood alcohol concentration
CCD	Charge-coupled device
DAS	Driver-assist system
DoF	Degree of freedom
EMG	Electromyography
MOU	Memorandum of understanding

CHAPTER 1

LITERATURE REVIEW AND SCOPE OF THE DISSERTATION

1.1 Introduction

The directional control performance of road vehicles is primarily influenced by the driver's control actions that arise from the driver's interactions with the vehicle, road and the environment. The main objective of the driver is to satisfy the control and guidance requirements of the driving task in a controlled and stable manner. Generally, these would include reducing the path tracking error to a permissible threshold level, and rejection of the environmental and road disturbances. The human driver is known to exhibit limited control performance, particularly in situations demanding critical steering maneuvers, which has been associated with unsafe vehicle operations and vast majority of the road accidents [1]. During 2009, nearly 5.5 million motor vehicle crashes leading to nearly 1.5 million injuries and 31,000 fatalities were reported in the US alone [2,3]. The reported highway accident data suggest that nearly 90% of such accidents are primarily attributable to errors related to drivers' perception of risk situations, decision making process and control actions [4]. Although the number of crashes have been steadily declining in recent years, the costs of such accidents associated with fatalities, compensation and loss of quality of life remain unacceptable. Considerable efforts have thus been made to characterize cognitive behavior of human drivers in the context of vehicle control [5-7]. A number of experimental and analytical studies have attempted to characterize human control and driving behavior, over the past five decades. These studies generally focus on identifications of essential control characteristics of the driver

through objective measurements and formulations of mathematical models that describe the driver as a controller considering the human perception, prediction, preview and compensation abilities [7-9]. The resulting models have been applied for: (i) identification of control characteristics of the human driver coupled with a vehicle, e.g., [10-12]; (ii) identification of control limits of the human driver, e.g., [13,14]; (iii) developments in driver-adaptive vehicle designs, e.g., [15,16]; and (iv) developments in effective driver-assist systems (DAS), e.g., [17,18]. The reported coupled driver-vehicle models range from single-feedback closed-loop lateral position control models, e.g., [10,19], to multi-loop control models incorporating comprehensive sensory feedback cues, e.g., [9,11,20,21]. Irrespective of the control structure, reported models generally consider the driver as an ideal controller that can readily adjust its driving strategy to adapt to a desired vehicle path with little or no considerations of control limits of the human driver [9]. Thus, the model parameters, reported in such studies may be considered valid only in the vicinity of the vehicle design and operating conditions selected for identification of the driver model. The reported models, depending upon the control strategies, may exhibit substantial path deviation and even instabilities under higher operating speeds or emergency type of path change maneuvers. These may be in-part attributed to the selected feedback cues that are integrated with different control strategies.

It has been widely accepted that perception of the path information through visual channel and vehicle motion prediction significantly influences the path tracking performance and steering response of the coupled driver-vehicle system [22-24]. The reported models, with only a few exceptions [11,25,26], however, have been developed

considering dynamics of automobiles only. The driver behavior characterization, however, is far more vital for articulated commercial vehicles that exhibit substantially different dynamics and lower control limits compared to automobiles.

In this dissertation research, a two-point preview strategy is used to develop a driver model. The proposed model involves essential elements of the human driver, such as perception, prediction, path preview, error estimation, decision making and hand-arm system dynamics in conjunction with a directional dynamics of a single-unit as well as an articulated freight vehicle. The driver model parameters are identified by minimizing a composite performance index subject to constraints imposed by the human driver's control and compensation limits. Subsequently, the control demands on the driver are evaluated through enhanced perception of different vehicle states so as to identify secondary cues that could facilitate vehicle path tracking while limiting the control demands. The vehicle states that help reduce path deviation could be utilized as additional sensory feedbacks in a driver-assist system (DAS) for enhanced path tracking performance of the coupled driver-vehicle system.

1.2 Review of Relevant Literature

A number of mathematical representations of the human driving behavior have evolved since the 1950s. These models generally aim to describe human driving behavior in terms of four essential elements, namely: (i) perception and prediction; (ii) preview; (iii) decision making process; and (iv) limbs motions (Figure 1.1) [6,7,27]. Drivers' perception of the instantaneous states of the vehicle help to predict the future vehicle trajectory in a qualitative sense [22,28], while the roadway coordinates are previewed through the visual field, which is described as the preview process. Using the previewed

path coordinates and predicted vehicle trajectory, the driver estimates the error of the vehicle trajectory with respect to the desired roadway. The driver subsequently imparts required compensatory control to minimize the tracking error subject to control performance limits, response delays, muscular dynamics and the vehicle steering system dynamics.

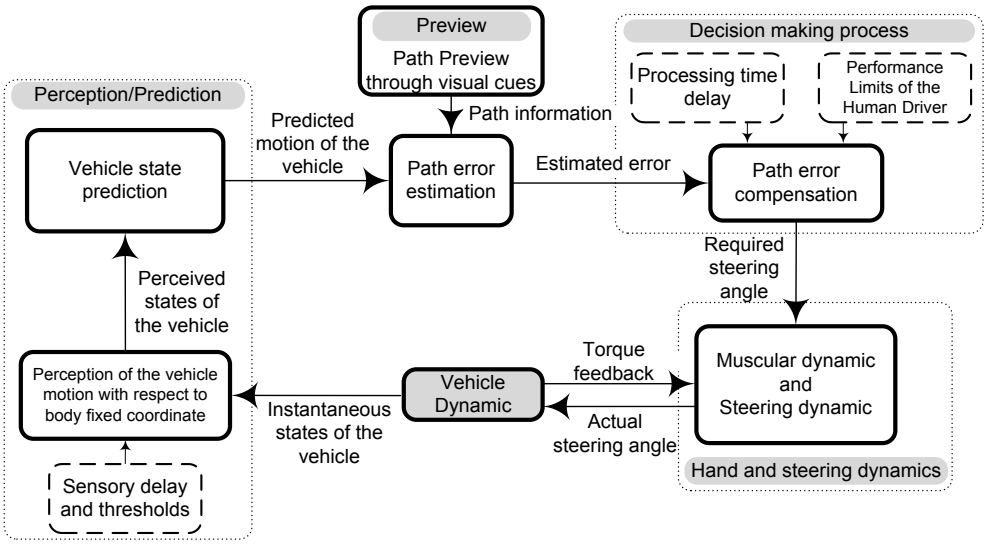

Figure 1.1: Overall structure of the coupled driver/vehicle system

Early studies were mostly attempted to estimate the human control actions by minimizing instantaneous perceived error between the vehicle trajectory and the desired path coordinates, using simplified single-loop compensatory models. These models, however, yield considerable path deviation, particularly under high speed directional maneuvers [7,9]. It has been suggested that a coupled driver/vehicle model would exhibit superior control performance through formulation of driver's preview ability and perhaps involving additional sensory feedback [29,30]. A few earlier studies and the majority of the recent studies, have thus employed involve driver's preview and multiple feedback variables, so as to enhance the path tracking performance. Further, a number of studies have been concerned with the role of hand-arm system and muscular dynamics. The

reported driver models employed widely different strategies to formulate these essential components. In the following subsection each essential elements of a generalized driver model will be described and relevant reported studies will be briefly reviewed and discussed in terms of model formulations. The limitations of different control strategies are further discussed in view of the driver control limits and vehicle path tracking performance to build the essential knowledge and formulate the scope of the dissertation research.

1.2.1 Perception and Prediction Process

It is established that the vehicle driver can sense instantaneous vehicle motion states through its visual, vestibular and kinesthetic cues [29]. Perceived motion states of the vehicle assist the driver to undertake the required steering control actions. A number of studies are thus focused on identification and characterization of required sensory cues related to human perception together with their mathematical descriptions [29,31]. The reported studies invariably consider that the instantaneous coordinates and orientation of the vehicle relative to its surroundings is perceived by the driver through visual sensory cues, suggesting that visual aspects of driving are of the highest significance [29,31-33]. Experimental studies have suggested that without specific training, even high-skilled drivers are unable to perform a good driving task in the absence of visual feedback [34]. It is also suggested that human driver can perceive linear and rotational accelerations as well as rotational velocities of the vehicle in a qualitative manner through vestibular and body-distributed kinesthetic cues [29]. The reported studies, however, mostly focus on single-unit vehicles and employ lateral coordinate and heading angle of the vehicle as the two primary cues, which can be more precisely perceived by the human driver. In case of

articulated vehicle combinations, it has been suggested that drivers' perception of secondary cues related to additional motion states of the vehicle could further assist the driver to undertake the required steering control actions more effectively. These may include articulation rate, lateral acceleration and yaw velocity of both the tractor and the semi-trailer units. Table 1.1 summarizes the range of sensory feedbacks considered in reported studies on human steering behavior, where the studies are identified by the lead author alone.

Table 1.1: Different driver sensory feedbacks which is employed in the reported studies

First Author	Driver's sensory cues							
	Lateral position Y	Heading angle Ψ	Lateral velocity v_y	Lateral acceleration a_y	Yaw rate r	Path curvature C_d	Roll angle ϕ	Articulation rate $\dot{\gamma}$
Kondo (1985)	■							
Weir (1968)	■	■	■	■	■			
Yoshimoto (1969)	■							
McRuer (1975)	■	■						
Donges (1978)	■	■				■		
Hess (1980)	■							
Reid (1981)	■	■				■		
MacAdam (1981)	■							
Garrot (1982)	■	■						
Legouis (1987)	■							
Allen (1988)	■	■						
Hess (1989)	■	■						
Mojtahedzadeh(1993)	■							
Mitschke (1993)						■		
Horiuchi (2000)	■	■						
Sharp (2000)	■	■						
Yang (2002)	■	■		■	■		■	■
Guo (2004)	■	■	■					
Edelmann (2007)	■					■		
Ishio (2008)	■							
Pick (2008)	■	■						
Menhour (2009)	■	■				■		
Sentouh (2009)	■	■			■			

The human perception of instantaneous vehicle states can be described considering two essential characteristics: (i) perception delay time [5]; and (ii) a perception threshold

that relates to minimum value of a state that can be sensed by the human driver [32]. The delay time to perceive vehicle states, denoted as the driver's perception delay time τ_{pd}, could vary from 0.1 to 0.2 depending upon the driver's sensory channels and environmental factors [1,29,33]. The magnitude of a vehicle state, however, must exceed its threshold value to be detected by the human driver. The threshold values, however, vary for different sensory channels. For instance, it has been reported that human can detect linear acceleration exceeding 0.06 m/s^2 through the vestibular system [29,33,35-38]. The perception threshold of the human driver can be mathematically expressed by a dead-zone operator (Figure 1.2), such that [29]:

$$S_j(I_j, T_j) = \begin{cases} \max\{I_j - T_j, 0\} & ; \quad T_j > 0 \\ I_j & ; \quad T_j = 0 \\ \min\{I_j - T_j, 0\} & ; \quad T_j < 0 \end{cases} \tag{1.1}$$

where I_j and S_j are instantaneous and perceived motion states, and T_j is the perceptive threshold of vehicle state j (j=1,…, n); n being the number of motion states to be perceived.

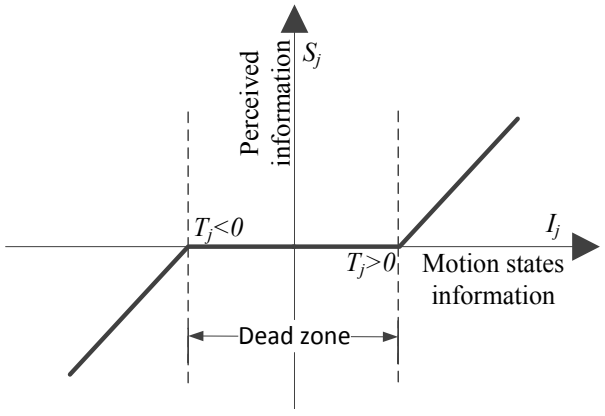

Figure 1.2: The dead-zone model used to describe perception threshold of the human body sensory feedbacks

The human driver continually predicts vehicle coordinates at a future instant in a qualitative sense on the basis of the perceived information such as heading angle, forward speed, lateral acceleration and lateral coordinates of the vehicle. The driver subsequently undertakes a control or corrective action on the basis of anticipated deviations between the predicted and previewed paths [28,39,40]. A number of attempts have been made to characterize the driver prediction capability through different prediction models [41,42]. Assuming a constant lateral velocity and heading angle of the vehicle within the preview interval, a first-order prediction model is used to estimate the future lateral coordinate of the vehicle, such that [41]:

$$Y_{Tp} = Y\left(t + T_p\right) = Y(t) + T_p v_x \, sin(\Psi) \tag{1.2}$$

where $Y\left(t + T_p\right)$ is the predicted lateral coordinate of the vehicle at a future instant T_p in the global X-Y frame, as shown in Figure 1.3(a), t represent time, and $Y(t)$, Ψ and v_x are, respectively the instantaneous lateral position, orientation and forward speed of the vehicle. The preview distance in the figure is indicated by D_p=$T_p v_x$. The term $v_x \, sin \, \Psi(t)$ can be approximated by the instantaneous lateral velocity of the vehicle, $\dot{Y}(t)$, in the global X-Y frame, such that:

$$Y_{Tp} = Y\left(t + T_p\right) = Y(t) + T_p \dot{Y}(t) \tag{1.3}$$

Owing to the constant lateral velocity assumption within the preview interval, this approach is considered accurate for predicting first order trajectories. Alternatively, the second-order prediction model considering constant lateral acceleration of the vehicle within the preview interval has been formulated, as (Figure 1.3b) [42]:

$$Y_{Tp} = Y\left(t + T_p\right) = Y(t) + T_p \, \dot{Y}(t) + \frac{T_P^2}{2} \ddot{Y}(t) \tag{1.4}$$

It is suggested that the second-order prediction yield improved predictability of the vehicle motion compared to the first-order model [8,42]. A third-order prediction model has been also reported in a few studies. However, it has been shown that the third-order prediction model is usually over-demanding and leads to directional instability of the coupled driver-vehicle system [8].

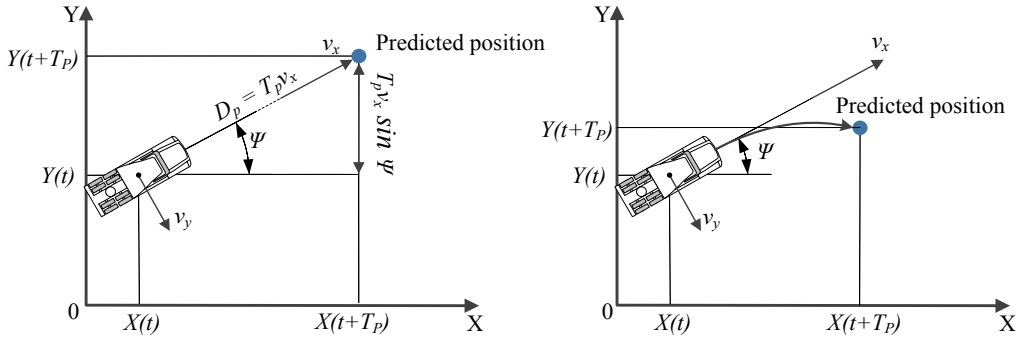

Figure 1.3: Prediction of vehicle motion at a future instant using (a) first-order prediction model; and (b) second-order prediction model

A number of studies have employed a more elaborated formulation of the human driver's prediction ability through the so-called 'internal vehicle model'. These suggest that the human drivers may employ prior knowledge of the vehicle response trends to predict vehicle coordinates at a future instant [18,22,28]. A linear state-space model of the vehicle has thus been proposed for determination of future coordinates of a vehicle, such that [40]:

$$\dot{\vec{x}}(t) = [A_1]\vec{x}(t) + [B_1]\vec{u}(t) \tag{1.5}$$

where $\vec{x}$ and $\vec{u}$ are the state and input vectors of the state-space model of vehicle, and $[A_1]$ and $[B_1]$ are respectively the state and input matrices for a single-unit vehicle. The homogenous and non-homogenous solutions of the vehicle motion can be obtained from:

$$\vec{x}(t) = [\emptyset(t - t_0)]\vec{x}(t_0) + \int_{t_0}^{t} [\emptyset(t - \tau)][B_1]\vec{u}(\tau)d\tau \tag{1.6}$$

where t_0 is the initial time. Assuming time invariant vehicle parameters, the state transition matrix $[\emptyset(t)] = e^{[A_1]t}$ is estimated using the Taylor series approximation:

$$e^{[A_1]t} = \sum_{n=0}^{\infty} \frac{([A_1]t)^n}{n!} \tag{1.7}$$

Combining Eqs. (1.6) and (1.7), the predicted motion states of the vehicle at a future instant T_p are obtained as follow:

$$\vec{x}(t + T_p) = \left(\sum_{n=0}^{\infty} \frac{([A_1]T_p)^n}{n!}\right)\vec{x}(t) + T_p\left(\sum_{n=0}^{\infty} \frac{([A_1]T_p)^n}{(n+1)!}\right)[B_1]\vec{u}(t) \tag{1.8}$$

Using the above equation the predicted coordinates of the vehicle cg at a future instance T_p can be determined. The above formulation employs linear approximations of the tire and vehicle dynamics and thus could yield considerable inaccuracies. A few recent studies have attempted to incorporate driver experience and skill in order to account for variations in the tire-vehicle characteristics under different driving conditions, so as to enhance the accuracy of the linear state-space vehicle model [22,28].

1.2.2 Path Preview Process

Many theoretical and empirical studies have shown that human driver tends to compensate for its perception/response delays through preview of future path information [31,43,44]. This path preview process involves assessment of the lateral coordinate, orientation and curvature of the desired roadway at a pre-set sight point, denoted as the preview point [41,45]. The preview distance (D_P), the distance from the preview point to the driver's position, is strongly influenced by the vehicle forward speed, maneuver

severity, path curvature and driver's path preview strategy [41,44,46,47]. The preview distance is generally expressed in terms of preview time (T_P), which can account for the speed effect assuming constant driving speed within the preview interval, which could range from 0.5 to 9 s [7,11,18,48].

A number of experimental and analytical studies have been performed either in the field or on driving simulators to identify ranges of drivers preview distances and preview times under different driving situations. For instance, an experimental study [49], showed that the optimum preview distance on straight path driving is 21 m at constant forward speeds ranging from 30 to 50 km/h. The reported studies have employed two different methods to characterize driver preview distance based on: (i) direct measurements; and (ii) indirect identification.

- **Direct measurement method**

The driver preview distances have been measured directly using three different techniques: (i) the slit method; (ii) the sight-point camera; and (iii) eye movement tracking. In the slit method the driver is asked to drive while seeing through a horizontal slit placed in front of the driver's eyes. Under this condition the driver observes a certain distance ahead of the road through the slit. The preview distance is then determined from driver's eye and slit position [41]. In this approach the driver's normal visual scene is obstructed, which may affect human driving behavior, particularly at higher speeds [50,51]. In the sight-point camera measurement technique, an aperture device is used to restrict driver's field of vision, while the preview distance is estimated from the width of the previewed path [52,53]. The use of this method has been limited since it requires driver's effort to focus at the sight point through the aperture. In eye movement tracking

method, the driver uses a helmet equipped with a camera to record the road scene and a charge-coupled device (CCD) camera to capture the pupil movement [31,47,54-56]. The preview distance is then captured from the instantaneous change in pupil and road orientation. These studies show two main characteristics of driver's path preview: (i) driver mainly looks at the tangent point on the inside edge of the bend during a cornering maneuver [57-59]; and (ii) driver's head movement performs most of the required movements to observe road information [57]. This approach, however, has limitations in differentiating between the eye and the head movements, and contribution of the driver's peripheral vision [60-62]. Table 1.2 lists some of the experimental studies on human driver preview process to identify the preview time of the human driver, where the studies are identified by the lead author alone. Wide variability in the reported values may be attributable to driver-, vehicle- and environmental-related factors such as differences in measurement methods, driving task, participants' skill and vehicle speed. An examination of the reported results, however, revealed a number of important and consistent findings. For instance, a higher forward speed, generally, requires a longer preview distance, which tends to enhance directional stability of the vehicle. Further, the preview distance tends to decrease considerably with increase in path curvature [46].

Table 1.2: Summary of studies reporting objectively measured human driver preview time

Author	Apparatus	Method of measurement	Velocity (m/s)	Preview time (s)	Number of subjects†	Driving task	Major finding(s)
Gordon (1966)	Automobile	Sight point camera	6 - 6.5	6.9	7(M) 3(F)	Curve negotiation	Preview time independent of speed.
Mclean (1973)	Automobile	Sight point camera	9 – 13.5	1.6 - 2.4	8(M) 2(F)	Straight course	Preview time independent of speed.
Kondo (1978)	Automobile	Slit method	3 - 16.5	2 - 9	10	Straight course	Preview time linearly increasing with speed.
	Automobile	Sight point camera	3 – 7.5	2 - 4	10	Curve negotiation	
Reid (1981)	Automobile	Eye movement tracking	14	2 - 3.5	3 (M)	Obtacle avoidance	Average previw time: 2.6 s
	Driving simulator	Eye movement tracking	14	1 - 3.5	3 (M)	Obtacle avoidance	Average previw time: 2.8 s
	Driving simulator	Indirect identification	14	0.7 - 0.9	6 (M)	Lane tracking	Indirect identifcation by minimzing the error between the response quantity and the measured data.
	Driving simulator	Indirect identification	14	1.5 - 3.3	4 (M)	Obtacle avoidance	
Afonso (1993)	Automobile	Eye movement tracking	11 - 22	1.6 - 2.5	20	Curve negotiation	Preview distance as a function of path curvature and speed.
Land (1994)	Automobile	Slit method	~12	1 - 2	3	Curve negotiation	Significance of the tangent point during curve negotiation.
Land (1995)	Driving simulator	Slit method	16.9	0.93 far 0.53 near	3	Curve negotiation	Effectivenss of two preview points at high speeds.
Boer (1996)	Driving simulator	Indirect identification	25	0.4 - 0.5	5	Curve negotiation	Significance of the tangent point during curve negotiation.
Zwahlen (1997)	Automobile	Eye movement tracking	23.5	0.5 - 1.8	11	Straight course	Driving behavior in low visibility condition.
Wilkie (2003)	Driving simulator	Eye movement tracking	8	1 - 2.5	6	Curve negotiation	Particiapants did not look toward the tangent point of the bends at low speeds.
Billington (2010)	Driving simulator	Eye movement tracking	8	1.5	7(M) 7(F)	Curve negotiaton	Participants used the distant road edges to improve their heading judgments.

† M- Male subjects; F - Female subjects

- **Indirect identification methods**

Considering wide variability in the reported preview time, vast majority of studies have relied on indirect identifications of the preview time for formulating the driver models. The indirect method is, invariably, employs a coupled vehicle-driver model, where the parameters identification techniques are applied to achieve minimal error between a response quantity and the corresponding measured data [45,63-65]. Indirect identification of the preview characteristics, however, necessitates a reliable driver model. The reported studies have thus been limited to identification of the preview distances for particular set of driver control measures and vehicle dynamic variables, and would be considered valid only for certain driving situations. Considerable discrepancies among the reported results are evident, which are attributed to variations in methodology used, driving conditions and the objectives. Table 1.3 lists some of the reported studies that employ indirect identification of preview characteristics together with the ranges of preview time.

The vast majority of the studies on human driving behavior have employed a single-point preview ahead of the vehicle to obtain the required path information. A single-point preview strategy, however, may lead to unsatisfactory path tracking performance and instability, particularly under high speed directional maneuvers coupled with a relatively short preview distance [66]. A human driver would exhibit superior control performance when a preview of the entire roadway is available. Only a few studies have proposed multi-point preview strategy for enhanced directional control performance of the driver [15,18]. A multi-point preview strategy involves simultaneous preview of a number of equally spaced target points for mapping of the required path information [15,67]. Further, it has been experimentally illustrated that novice drivers tend to use near preview

points of the desired path to obtain the required information, while drivers with relatively higher driving skills tend to employ farther preview points [66]. Consequently, a concept of weighted multi-point preview has been used in a few studies [18,66,68,69]. Measurements performed under restricted visual situations have shown that human drivers observing only two segments of the roadway achieve improved path tracking performance that is similar to that could be realized with entire roadway visibility [31,56,70,71]. A two-point strategy is thus considered adequate for describing driver preview opposed to the more complex multi-point approach. A few studies have employed two-point preview strategy to develop coupled single-unit vehicle-driver models [21,45,65,72,73], which suggest that only two target points ahead of the vehicle are sufficient to obtain the roadway coordinates [34,45,56].

Table 1.3: Summary of studies reporting indirectly identified preview time

Author	Forward speed (m/s)	Preview time (s)	Description	Control Strategy
Weir (1968)	26.8	5	Error minimzation	Cross-over
Yoshimoto (1968)	10 - 30	2.2 - 3.5	Error minimzation	Proportional
McRuer (1975)	26.8	2.7	Error minimzation	Cross-over
Donges (1978)	8.3 - 16.6	1 - 1.3	Error minimzation	Two-level
MacAdam (1981)	26.8	1.3	Error minimzation	Optimal preview
Hess (1985)	30	0.2	Error minimzation	Lead compensation
Mitschke (1993)	14 - 30	0.6 - 0.75	Based on vehicle design parameters	Two-level
Sharp (2000)	60	0.5	Error minimzation	Multi-point previrw
Yang (2002)	27.7	1.51 - 2.88	Based on driving skill	Multi-loop compensatory
Guo (2004)	22	1.4	Error minimzation	Preview-follower
Edelmann (2007)	< 8	0.4 – 0.8	Based on vehicle design parameters	Two-level

1.2.3 Decision Making Process

The decision making process involves driver's control strategy to compensate for the perceived error between the previewed path and predicted trajectory of the vehicle, which may depend upon the driving task, driver's skill and various situational conditions

[11,22,29]. The reported driver's control strategies can be grouped under four categories, namely: (i) compensatory control strategy; (ii) anticipatory/compensatory strategy; (iii) preview compensatory strategy; and (iv) forward speed control strategies. While the first three categories focus on steering strategies under constant forward speed, the last group of studies aim at longitudinal speed control models.

- **Compensatory Control Strategy**

The compensatory strategy aims to track the desired path by minimizing instantaneous lateral position error (Y_e) between the perceived trajectory (Y) and the desired path (Y_d), as shown in Figure 1.4. The compensatory control strategy has been widely expressed by the well-known crossover model [10], which implies that the driver undertakes compensations to realize a stable and well-damped non-oscillatory vehicle response in the vicinity of the crossover frequency, ranging from 2 to 4 rad/s [29,75]. This model suggests that the dynamic response of the open-loop driver-vehicle system can be described by a delay time and an integrator. The required model parameters are thus determined in accordance with dynamic response of the vehicle. The crossover model strategy exhibits good correlation with the measured data in immediate vicinity of the gain crossover frequency but it can cause substantial tracking errors and a directional instability at frequencies distant from the crossover frequency [7,76].

The vast majority of the reported compensatory models have employed instantaneous lateral position of the vehicle as the main sensory feedback to the driver. This, however, may lead to substantial tracking errors and a directional instability of the coupled driver-vehicle system, particularly under emergency type of steering maneuvers [7,29,43]. It is suggested that, the addition of the driver preview and/or driver's secondary sensory

feedbacks helps realized stable vehicle response [20,29,30,77,78]. A consideration of additional sensory feedbacks, such as heading angle of the vehicle, helps to enhance the path tracking performance of the coupled driver-vehicle system [7,11,71,78]. A number of studies have also considered the previewed path information attained from the human driver's visual channel, which will be discussed in the following subsection.

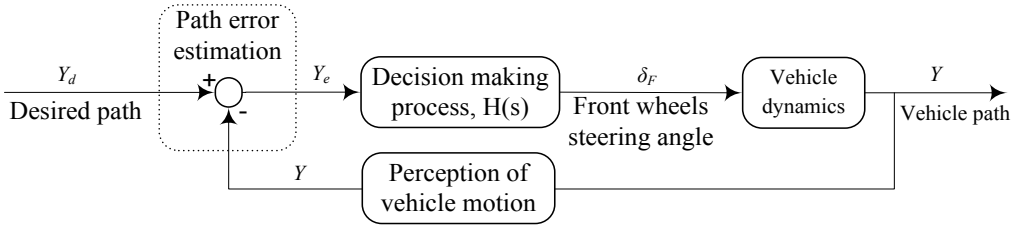

Figure 1.4: The compensatory driver model structure

- **Anticipatory/Compensatory Control Strategy**

It is suggested that skilled drivers can simultaneously employ open-loop anticipatory and closed-loop compensatory strategies to satisfy the control and guidance requirements of a driving task [12,21,45,65]. One of the earliest anticipatory/compensatory models was proposed by Donges [45]. The two-level driver model generates: (i) an anticipatory steering action δ_a based on perception of the future course of driving; and (ii) a compensatory steering δ_c, as shown in Figure 1.5, to maintain instantaneous central lane position. The anticipatory open-loop strategy, attained through a learning process, is related to the predictive steering action of the driver, while the closed-loop compensatory steering enhanced the path tracking performance of the coupled vehicle-driver system [21,45,79].

The anticipatory control action is primarily obtained from the perceived path curvature, C_d, considering single or multiple preview points, while the compensatory

steering is based on an instantaneous lateral position, orientation and curvature error. Edelmann et al. [12] and Mitschke [65] have employed Donges' [45] two-level driver model to stuyd the driver-vehicle lateral dynamics. These models, invariably, obtain the previewd pah information on the basis of the previewed path curvature. However, it has been experimentally shown that the human driver exhibit limited ability to estimate the previewed path curvature with a reasonably good accuracy due to the so-called 'illusive curve phenomenon', where the curvature of short-radius curves is mainly underestimated [56,79,80].

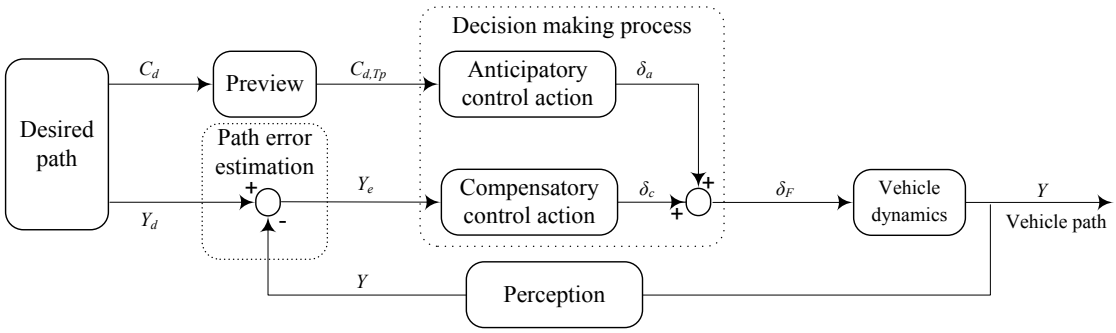

Figure 1.5: The anticipatory/compensatory driver model structure

- **Preview Compensatory Control Strategy**

The preview compensatory driver models consider both the preview and prediction ability of the human driver to minimize the perceived path tracking error $Y_{e,Tp}$ between the previewed path information $Y_{d,Tp}$ and predicted motion of the vehicle Y_{Tp}, as shown in Figure 1.6 [20,30,40,]. One of the first preview compensatory models was introduced by Kondo and Ajimine [41], which employed a proportional controller to minimize the lateral position error between the preview path and the predicted vehicle trajectory using a first order prediction model. Guo and Guan [8] demonstrated enhanced path tracking performance of the vehicle using a preview-follower concept in conjunction with a

second order prediction model. The concept involves variations in the required model parameters in accordance with the driver's preview process *P(s)* and coupled driver-vehicle system *F(s)*, as shown in Figure 1.6. MacAdam [40] proposed a more elaborate preview/prediction formulation incorporating a linear state-space internal vehicle model. An optimal control approach was employed to minimize a performance index comprising lateral position error between the previewed path coordinate and predicted trajectory of the vehicle.

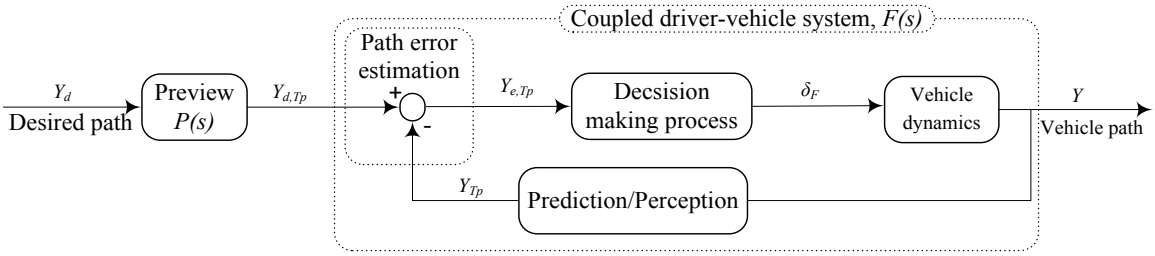

Figure 1.6: The preview compensatory structure involving the driver's preview and prediction

Considering the single-point preview strategy, Allen et al. [81] formulated a driver model to compensate for the orientation error between the previewed and the predicted path, which is defined as the visual angle, as shown in Figure 1.7 [81,82]. Steering control action is then realized as a function of the visual angle Ψ_c of the sight point, visual angle of the predicted path Ψ_v, lateral position error Y_e and vehicle heading angle Ψ between the previewed and predicted paths of the vehicle:

$$\delta_F = K_\Psi \frac{2}{D_p}(\Psi_c + \frac{Y_e}{D_p} + \Psi - \Psi_v)\mathrm{e}^{-\tau_s \mathrm{s}} \tag{1.9}$$

where D_p and K_Ψ are the preview distance and compensatory gain constant, respectively, and τ_s represents the human driver steering response time.

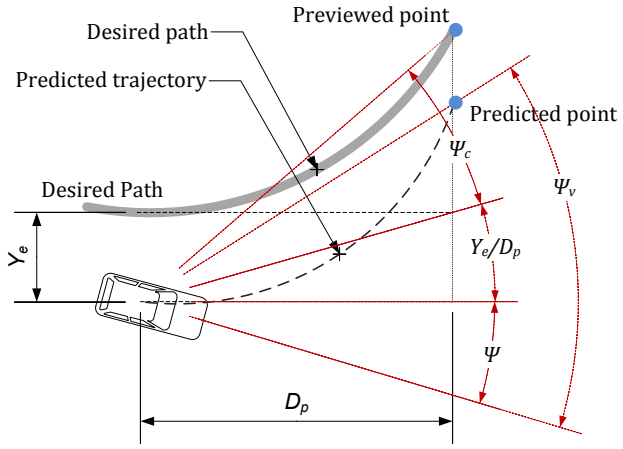

Figure 1.7: Estimation of the vehicle orientation deviation proposed by Allen et al. [81]

Some recent studies have employed a two-level control strategy using two parallel closed-loop compensatory actions considering simualtaneous compensation of the precieved errors associtaed with a far and a near preview point. It is suggested that the far target point satisfies the guidance requirement of the driving task, while the near target preview point minimizes the instantaneous path deviation and assures adequate disturbance rejection [70,71]. Salvucci and Gray [79] proposed a driver model to simultaneously generate steering action in response to the previewed path and to maintain a central lane position. Similarly, Sentouh et al. [72] proposed a two-level driver model employing two closed-loop compensatory control strategies to satisfy the path tracking task. Reported studies have employed widely different methods to acheive minimal error between the previewed and predicted paths [18,21,22,42,67,73]. Table 1.4 summarizes the strategies employed in the reported studies, which are identified by the lead author alone.

- **Forward Speed Control Driver Models**

The vast majority of the reported driver models assume constant forward speed. The human driver, however, tends to vary vehicle speed in order to maintain lane position in

response to vehicle motion and road/environmental condition. A few studies have attempted to consider human driver's adaptation to the instantaneous vehicle responses and road/environmental conditions through forward speed variations. It has been recognized that human driver invariably adjusts the vehicle forward speed in order to maintain safe levels of lateral acceleration during curve negotiation [83] and distance with respect to a moving object ahead of the vehicle [84-86]. Savkoor and Ausejo [83] proposed a curve negotiation driver model employing the previewed path curvature to predict the future lateral acceleration of the vehicle, while the vehicle speed was adjusted to a predetermined level of lateral acceleration. In a similar manner, Reymond et al. [87] used human driver model to predict lateral path deviation and adjust the forward speed to maintain a predetermined level of lateral position error. Forward speed control models have also been proposed on the basis of relative velocity with respect to a lead vehicle, which would be similar to the adaptive cruise control (ACC) concept [84], relative position [85], and visual angle [86], as seen in Figure 1.8.

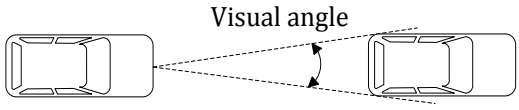

Figure 1.8: Visual angle of the lead car in a forward speed control system proposed by Pipes [86]

Table 1.4: Summary of reported driver model strategies related to the steering behavior of the human driver

Author	Control strategy	Formulation of the decision making process	Sensory cues	Description
Iguchi (1959)	Compensatory model	PID controller	Lateral position	Neglects driver's response time
McRuer (1967)	Compensatory model	Proportional compensatory gain and an integrator	Lateral position	Consider the cross-over control strategy
McRuer (1970)	Compensatory model	Lead-lag controller	Lateral position	Consider the cross-over control strategy and a first-order lag to formulate muscle dynamic
McRuer (1975)	Compensatory model	Proportional compensatory gain for lateral position error and a lead controller for the heading error	Lateral position and heading angle	Consider the cross-over control strategy
Donges (1978)	Anticipatory/Compensatory model	Two-level controller: open-loop anticipatory for the previewed curvature of the path and closed-loop proportional compensatory gains for instantaneous lateral position, heading angle and curvature errors	Lateral position, heading angle and curvature	Consider two-target points and a pure time delay to formulate driver's response time.
Reid (1981)	Preview compensatory model	Lead-lag controller	Lateral position, heading angle and curvature	Consider a pure time delay to formulate driver's response time.
MacAdam (1981)	Preview compensatory model	Linear Quadratic Riccati regulator (LQR)	Lateral position	Consider a performance index comprising the previewed path deviation, and the internal vehicle model to formulate driver's prediction process
Guo (1983)	Preview compensatory model	Lead-lag controller	Lateral position and heading angle	Consider a second-order prediction model to formulate driver's prediction process
Allen (1988)	Preview compensatory model	Proportional compensatory gain	Lateral position and heading angle	-
Mojtahedzadeh (1993)	Preview compensatory model	Lead controller	Lateral position	Incorporate neuromuscular dynamic of human driver
Mitschke (1993)	Anticipatory/Compensatory model	Two-level controller: open-loop anticipatory for the previewed curvature of the path; and a closed-loop lead-lag controller for instantaneous curvature error	Curvature	Internal vehicle model to formulate driver's prediction process

Table 1.4 (Cont.): Summary of reported driver model strategies related to the steering behavior of the human driver

Author	Control strategy	Formulation of the decision making process	Sensory cues	Description
Sharp (2000)	Preview compensatory model	Proportional compensatory gain	Lateral position and heading angle	Incorporate the instantaneous heading error and lateral deviation related to multiple target points
Horiuchi (2000)	Compensatory model	A lead compensatory controller for the lateral position error and a lead-lag controller for heading error	Lateral position and heading angle	Consider a performance index comprising the lateral position error, steer angle and two lead time constants
Yang (2002)	Preview compensatory model	Proportional compensatory gain	Lateral position and orientation errors, and lateral acceleration, yaw rate and roll angle of the tractor and the trailing units	The preview time and the response time vary depending upon driver's skill level. Employing the constraint minimization technique to determine the model parameters
Ungoren (2005)	Preview compensatory model	Linear quadratic riccati regulator (LQR)	Lateral position and heading angle	Consider a tunable parameter to assign relative importance of lateral position and heading errors. Consider a performance index comprising the magnitude and rate of path deviation
Edelmann (2007)	Anticipatory/Compensatory model	Two-level controller: open-loop anticipatory for the preview path curvature; and compensatory lead-lag controller for perceived lateral position error	Lateral position and curvature	-
Ishio (2008)	Compensatory model	Lead-Lag controller	Lateral position	Considering a performance index comprising the lateral position error and lateral velocity together with steer angle and steer rate
Sentouh (2009)	Anticipatory/Compensatory model	Two-level controller: closed-loop proportional controller related to the heading angle error for the far preview point; and compensatory lead-lag controller related to the perceived heading angle error for the near preview point;	Lateral position and heading angle	Incorporates neuromuscular dynamic

1.2.4 Response/Reaction Time

The human reactions to external stimuli, in-general, exhibit time delays depending upon the decision-making abilities, depth of the required mental processing, awareness, expectancy and neuromuscular dynamics [1,7]. Conceptually, the driver's reaction time (τ) may be decomposed into the perception-processing time and the movement time. The perception-processing time defines the time interval between observing a stimulus and initiation of a discernible muscular response [33,38,88].

The perception-processing time may be further divided into four distinct stages, namely: (i) detection; (ii) identification; (iii) decision making; and (iv) response time [89]. The initial detection stage involves interval where the driver develops a conscious awareness of a sudden stimulus. In the identification stage, the driver acquires sufficient information to identify the nature of the event. Following the detection and identification of a stimulus, the driver undertakes the decision stage involving information processing and desirable control actions such as steering or braking [1]. In the final stage, denoted as the response stage, the control command is transmitted by the motor center of the brain to appropriate muscles to carry out the required actions [90]. It is extremely complex to quantify the time intervals associated with each stage. The overall perception-processing time, however, is mostly related to the depth of the required mental processing, age, awareness and expectancy of the stimuli, and may vary among the different receptors [33,91-93].

Movement time defines the interval to perform the intended action by the driver, which mostly depends on the muscles dynamic, age, blood alcohol concentration (BACs) and fatigue [91,94-99]. In the context of human driving control actions, two basic

approaches have been reported to describe the movement time: (i) the simplified pure time delay; and (ii) the dynamic responses of the limbs. The first approach describes the muscle movement dynamic as a pure time delay which can be added to the perception-processing time to obtain an overall reaction time of the human driver [1,100-108]. Only a few studies have attempted to measure the perception-processing and movement times of human drivers. These have reported widely varying perception-processing times, ranging from 0.1 to 2.8 s, and movement times, ranging from 0.16 to 0.76 s. The differences are attributable to widely different stimuli considered in the reported studies, as seen in Table 1.6. Owing to complexities associated with measurements of reaction times, the vast majority of reported driver models identify the driver reaction time indirectly by minimizing the error between a response quantity and corresponding measured data. Table 1.5 summarizes the studies reporting the perception-processing and movement times or the overall reaction time, which are identified by the lead author alone. In the second approach, the movement time is identified from the muscle/limb reaction times considering different muscles dynamic models coupled with steering system dynamic, which are summarized in the following subsection.

Table 1.5**:** Studies reporting indirectly identified reaction times

Author	Perception-processing time (s)	Movement time (s)	Overall reaction time (s)
McRuer (1965)	-	-	0. 1 - 0.55
Weir (1968)	0.2	0.1	-
Yoshimoto (1969)	-	-	0.3
Donges (1978)	-	-	0.4 - 0.8
Hess (1981)	0.15	0.2 to 0.4	-
Reid (1981)	-	-	0.2 - 0.5
MacAdam (1981)	-	-	0.2
Mojtahedzadeh (1993)	0.15	0.4	-
Horiuchi (2000)	0.1	0.1	-
Yang (2002)	-	-	0.1 - 0.25 - 0.35
Guo (2004)	0.4	0.2	-
Edelmann (2007)	-	-	0.2
Pick (2008)	-	-	0.16

Table 1.6**:** Summary of studies reported measured reaction times of human drivers

Author	Response	Method of measurement	Velocity (m/s)	Perception-response time (s)	Movment time (s)	Number of subjects†	Stimulus	Major finding(s)
Barrett (1968)	Braking	Driving simulator	~11	0.8 - 1.1†		11	Appearance of pedestrian	Dominant braking response compared to steering
Davies (1969)	Braking	Driving simulator	-	0.15† (leveled brake and gas pedals) 0.31† (unleveled brake and gas pedals)		10	visual stimulus (light)	50% improvement of the movement time for the pedals at equal level
Olson (1986)	Braking	Automobile	12 - 14	(Y) [1] > 1.0 (O) [1] > 1.0	(Y) [1] > 0.7 (O) [1] > 0.5	49 (Y) [1] 15 (O) [1]	Obstacle avoidanc	The perception-response time is 1.6 s for 95th precentile
Hancock (1999)	Braking	Driving simulator	9, 13.5	0.61[2†] 0.93(d)[2†]		10	Traffic light	Response time increases in the presence of distraction
Lenne (1999)	Braking	Driving simulator	22	Alcohol: 0.86 - 0.93† Non alcohol: 0.80 - 0.86†		14 (M) 14 (F)	Visual sign	Response time under 0.7 ml/kg alcohol impairment
Warshawsky-Livne (2002)	Braking	Driving simulator	25	0.32(a) [3] 0.42(ua) [3] 0.35(Y) [1] 0.43(O) [1]	0.19 (M) 0.16 (F)	36 (M) 36 (F)	visual stimulus (light)	Perception-processing time increase by age but decrease with alertness
Young (2007)	Braking	Driving simulator	30	(NO)[4] 2.10-2.74 (EX)[4] 2.24-2.76	(NO) [4] 0.58-0.74 (EX) [4] 0.71-0.76	26 (M) 18 (F)	Lead car failure	Reaction response time of driver to decceleration of the lead vehicle
Mehmood (2009)	Braking	Driving simulator	25	1.32 (a) [3†] 0.78 (ua) [3†]		31 (M)	Brake light of the lead car	Reaction response time of driver to decceleration of the lead vehicle
				1.39 (a) [3†] 0.85 (ua) [3†]		29 (F)		
Summala (1981)	Steering	Automobile	16.5	1.5†		1326	Sudden appearence of an obstacle on the roadside	Inititation of the vehicle lateral movement used to determine the response time including the vehilce response delay
Summala (1981)	Steering	Automobile	16.5	2†		815	visual stimulus	Steering response to onset of a visual stimuli on a dark road
McGehee (2000)	Steering	Automobile	20	1.67†		192	intersection-incursion	statistical equivalence between driver's reaction time in both studies
		Driving simulator	20-25	1.64†		60 (M) 60 (F)	intersection-incursion	

† Overall reaction time; (M) male subject; (F) female subjects

1. Young (Y) and old drivers (O); 2. Driving under a distraction (d); 3. Aware (a) and Unaware (ua) of road stimuli; 4. Novice (NO) and Expert (EX) drivers

1.2.5 Limb Motion and Steering Dynamic

The driver's steering command transmitted to the vehicle steering system through the limb motions in response to skeletal muscles activations, as indicated in Figure 1.1 [76,90,109]. The muscles are made up of muscle fibers and spindles, which are controlled by motor neurons whose cell bodies lie in the spinal cord [110]. The α-motoneurons and γ-motoneuron cause contractions of muscle fibers and spindles, respectively, through releasing of a chemical agent in the muscle fibers and spindles [75,109]. The force developed by contraction of the muscle spindles, however, is substantially smaller than that caused by the muscle fibers [90,111]. The γ-motoneurons, however, determine the desired length of the muscle. The muscle spindles thus serve as sensory receptors within the muscle to provide the position and velocity feedback and generate an error signal [90,112,113]. This error signal coupled with a transmission delay time subsequently activates α-motoneurons which results in contraction of muscle fibers and thus the activation force, as seen in Figure 1.9 [43,109,114].

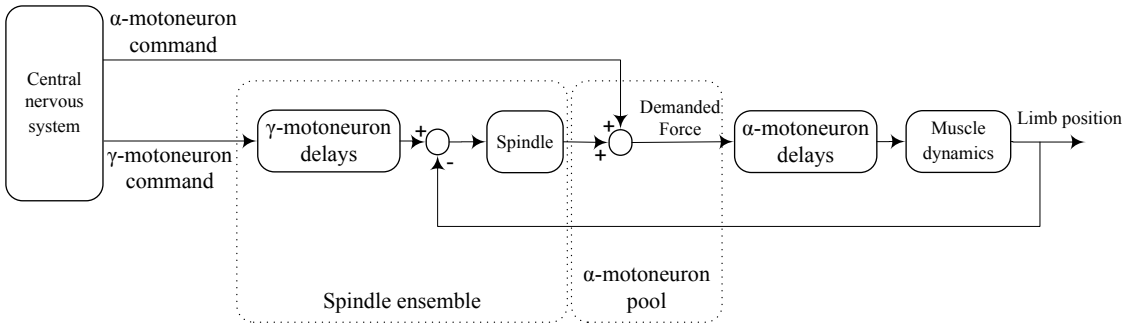

Figure 1.9: Basic components and schematic of neuromuscular system

Formulations of the human limb motions in a control task can be traced from early aircraft-pilot studies. These have established that during a compensatory tracking task, the pilot's muscle dynamics can be described by a linear second-order dynamic system

[10,27]. McRuer et al. [113] suggested that the muscular dynamic response of the combined limb and a manipulator system can be formulated by a third-order transfer function, denoted as the 'Precision Model'. This transfer function describes the combined manipulator/muscular dynamic from the α-motoneuron command signal to limb position in the following manner:

$$G_p(s) = \frac{\omega_n^2}{(T_{Nm}s + 1)(s^s + 2\zeta\omega_n s + \omega_n^2)} \tag{1.10}$$

where ζ and ω_n are the damping ratio and natural frequency of the combined manipulator and the limb muscles, while the first-order function describes the neuromuscular system lag (T_{Nm}). The above model is considered valid when the pilot operates a manipulator and may not be applicable for vehicle driving task [111,115-117].

A series of driving simulator studies have been conducted to simultaneously measure the muscle activity using surface electromyography (EMG) and the force applied to the steering wheel [115]. The measured data were used to characterize the limb motion response as a function of both the muscles and the steering system dynamic. The study proposed a limb motion model, as shown in Figure 1.10, considering the reference model $R_m(s)$, muscles reflex model $H_m(s)$, and active muscle stiffness function $K_m(s)$ [67,90].

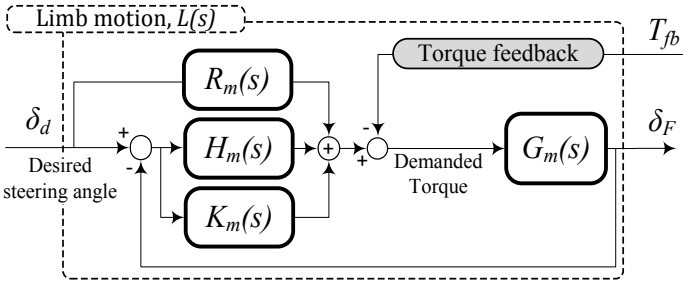

Figure 1.10: Limb motion dynamics coupled with the steering system dynamics proposed by Pick and Cole [67]

The coupled muscles and steering dynamics function, $G_m(s)$, is characterized considering second-order muscular dynamics of the human hand-arm and the steering system, as [67]:

$$G_m(s) = \frac{G_{st}}{(J_{dr} + J_{st})s^2 + (B_{dr} + B_{st})s + (K_{dr}+K_{st})} \tag{1.11}$$

where J_{dr}, B_{dr} and K_{dr} are the inertia, damping and stiffness of the drivers' hand-arm system, respectively, and J_{st}, B_{st}, K_{st} and G_{st} are inertia, damping, stiffness and steering ratio of the steering system, respectively. The steering action of the driver also involves estimation of the torque demand, which is estimated using the reference model function, $R_m(s)$, expressed as the steady-state inverse of $G_m(s)$ [67,118]:

$$R_m(s) = \frac{K_{dr}+K_{st}}{G_{st}} \tag{1.12}$$

The difference between the desired and the actual steering angle is subsequently sensed by muscle spindles [67,112]. A first-order lead-lag model is used to describe the muscles reflex property $H_m(s)$, which generates a corrective torque so as to maintain the spindle-sensed steering position as [110,115]:

$$H_m(s) = \frac{(sB_r + K_r)e^{-s\tau_r}}{s/\omega_c + 1} \tag{1.13}$$

where B_r and K_r are the damping and stiffness constants of the reflex system, respectively, ω_c is the cut-off frequency that describes the time delay between the muscle activation and generation of the muscle torque, and τ_r is the transport lag in sending messages to and from the spinal cord, which could range from 0.025 to 0.05 s [67]. It is also established that the muscle activation and co-contraction may imply greater stiffness of the driver's arms [118,119]. An additional gain constant K_{ma} is thus used to represent increase in the muscle stiffness, which is described by the active stiffness function $K_m(s)$

[67,90]. The overall transfer function *L(s)* relating the front-wheels steering δ_F to driver's steering command of δ_d, as shown in Figure 1.10, is described considering the torque feedback of the steering system, T_{fb}, as:

$$L(s) = \frac{\delta_F(s)}{\delta_d(s)} = \frac{R_m(s)G_m(s) + H_m(s)G_m(s) + K_m(s)G_m(s) - G_m(s)}{1 + H_m(s)G_m + K_m(s)G_m(s)} \qquad (1.14)$$

A number of studies have experimentally assessed the influence of steering torque feedback on path tracking performance of the vehicle driver, and concluded insignificant effect of the steering torque feedback [120-122]. It has been suggested that the dynamic behavior of the vehicle steering system can be effectively formulated considering the correlation between the vehicle response and the steering wheel angle, which may be taken as the steering gear ratio, G_{st} [67,120,123]. The majority of the reported studies thus neglect the torque feedback effect characteristics of steering dynamic. These studies either consider a constant gain as the steering ratio or characterize the steering system as a second-order system.

1.2.6 Performance Index and Identification of the Driver's Control Parameters

The directional control performance of road vehicles and thus the road safety are influenced by control actions of the human driver and directional responses of the vehicle such as lateral position and orientation errors. The control characteristics of the human driver have been mostly identified through minimization of a composite performance index of selected response measures. The selected measures for automobiles have been mostly limited to the lateral position error (Y_e) or orientation error (Ψ_e) or a combination of the two [7,17,40,78]. This approach of identifying the driver control properties may thus yield an idealized driver model, particularly when the control limits of the human

driver are not considered in the performance index minimization. The vast majority of the driver models, with only few exceptions, do not consider the driver control limits in the control parameters identification process. The reported driver models thus suggest widely different driver control characteristics that may be considered applicable for particular driving condition considered in individual studies. Table 1.7 summarizes the ranges of commonly used driver control parameters such as preview time, lead and lag time constant, and lateral position and orientation error compensatory gains [8,11,14,17,45]. These clearly show wide ranges of control parameters used in different studies. Only a few studies have reported solution of the minimization problem subject to limit constraints defining the practiced ranges of driver control characteristics [11].

Table 1.7**:** Range of human driver's control variables

Control variables	Unit	Range
Preview time, T_p	s	0.10 – 2.50
Lead time constant, T_L	s	0.05 – 3.00
Lag time constant, T_I	s	0.02 – 0.80
Lateral position error compensatory gain, K_y	rad/m	1e-5 – 1.80
Orientation error compensatory gain , K_Ψ	rad/rad	0.10 – 1.85

The reported vehicle driver models employ widely different control characteristics and performance indices comprising the vehicle path and directional responses together with some measures of demands imposed on drivers' effort. These include the maximum steering angle and its rate, which has been related to the driving effort and drivers' comfort [9,15,17]. Since the majority of the studies have focused on driver models applicable to automobiles or two-axle vehicles, the widely used performance index of lateral position and orientation errors alone would be justifiable. Such a performance index, however, would be inadequate for heavy articulated vehicle combinations where

the driver perceives additional cues from the vehicle responses. Only few studies have explored driver models for articulated vehicle combinations, which have suggested significance of many additional vehicle responses [9,25]. These employ performance indices comprising weighted function of lateral accelerations, yaw rates and roll angles of the articulated vehicle units; articulation angle and articulation rate; and steer angle and its rate. Yang et al. [16] proposed such a performance index, which was minimized upon consideration of ranges of reported control limits of the human driver including preview time, lead and lag time constants and compensation gains.

1.3 Scope and Objective of the Dissertation

From the literature review, it is apparent that the reported human driver models generally consider the driver as an ideal controller that can readily adjust its driving strategy to adapt to a desired vehicle path with little or no considerations of control limits of the human driver. Furthermore, the vast majority of the reported studies on driver-vehicle interactions focus on automobile drivers. The human driver's control performance is perhaps of greater concern for articulated vehicle combinations, which exhibit significantly lower control limits and may pose relatively greater highway safety risks compared to automobiles. The directional dynamic analyses of such vehicles have been limited either to open-loop steering and braking inputs or simplified path-following driver models.

In the context of interactions between the human driver and articulated vehicles, only a few studies have investigated the coupled driver-vehicle system responses. These generally focus on characterization of driving control requirements through minimization of lateral position error between center of mass (cg) of the tractor and the desired path

using a single-point preview strategy. A single point preview strategy, however, may lead to unsatisfactory path tracking performance and instability, particularly under high speed directional maneuvers coupled with a relatively short preview distance. Furthermore, the assessments of active safety devices in the vast majority of the studies have been limited to either open-loop simulations or in a closed loop simulations using simple driver models. The contributions of the human driver's control limits to the vehicle stability have been mostly ignored. It is thus desirable to develop more effective driver models for articulated vehicles considering feasible ranges of human driver control limits and multiple-point preview. Such a model could serve as an effective simulations tool for assessing safety dynamics of the coupled driver-vehicle system and provide essential guidance toward developments in driver-assist systems (DAS).

This dissertation research thus aims to develop a two-stage preview strategy, involving a near- and a far-point preview simultaneously, to characterize steering control properties of commercial vehicle drivers. The strategy includes a near and a far preview point targets to describe the driver control of lateral path deviation and vehicle orientation. A human driver model comprising path error compensation and dynamic motions of the limb is subsequently formulated and integrated to a yaw-plane model of an articulated vehicle. The coupled driver-vehicle model is analyzed under an evasive steering maneuver to identify limiting values of the driver control parameters through minimization of a generalized performance index comprising driver’s steering effort, path deviations and selected vehicle states. The performance index is further analyzed to identify relative contributions of different sensory feedbacks, which may provide important guidance for designs of driver-assist systems (DAS).

1.3.1 Objectives of the Dissertation Research

This dissertation research aims to characterize human driving behavior when coupled with an articulated commercial vehicle and development of a comprehensive closed-loop driver/vehicle model for identifications of control performance limits of heavy vehicle drivers. The specific goals of the proposed research are summarized below:

1. Characterize essential control properties of the human drivers through measurement on a vehicle simulator;

2. Develop a two-stage preview driver model and integrate the model to an articulated vehicle model for analysis of coupled driver-vehicle system responses as functions of vehicle drivers and operating factors;

3. Identify the ranges of driver model parameters, more specifically the driver control performance limits, through formulation and minimization of a composite performance index;

4. Identify the relative significance of difference motion and visual cues and formulate a concept in driver-assist system (DAS) as additional sensory feedbacks in order to enhance path tracking performance of the coupled driver-vehicle system.

1.3.2 Organization of the Dissertation

This dissertation research is organized into six chapters, including a literature review chapter (Chapter 1). In the initial chapter, the reported studies relevant to human driving cognitive behaviors, sensory feedbacks and driver model structures, are reviewed to build essential knowledge on methodologies for characterization of human driver and for developing directional pursuit-compensatory driver model. The scope and objectives of the dissertation research are also summarized.

In the second chapter, a number of reported driver models are selected and integrated with a single-unit vehicle model. These models are then evaluated based upon their directional responses and performance measures under a critical steering maneuver. The

relative significance of different control strategies, sensory cues and prediction strategies are then assessed considering variations of driving factors and vehicle design parameters.

The third chapter describes objective measurement of the human driver control properties, e.g., braking and steering reaction times and compensation abilities on a limited-motion driving simulator. An experiment design is formulated to characterize the human driver factors considering variations in the forward speed of vehicle. Further, this study aims to identify the influence of driving experience on control characteristics of the vehicle driver and extract certain patterns to quantitatively determine the driver's skill in a categorical (i.e., skilled, average and novice) form by examining the driver control actions.

In chapter four, a two-stage preview driver model, denoted as the baseline model, incorporating essential motion feedback variables is formulated. This model employs only the lateral position and orientation errors of the vehicle. The baseline driver model is then integrated with two different vehicle models: (i) a yaw-plane model of a single-unit vehicle; and (ii) a 18-wheels yaw-plane model of an articulated vehicle. Simulations are performed to determine directional responses of the coupled driver-vehicle system. In order to validate the proposed driver model, the directional responses of the coupled driver-single unit vehicle model is compared with the simulator-measured steering and path tracking responses, considering variations in vehicle forward speed and preview distance of the driver.

In the subsequent chapter, the proposed baseline driver model is then applied to assess control characteristics of the vehicle driver subject to variations of design parameters and forward speed of the vehicle. In particular, the coupled driver-vehicle model is analyzed

under an evasive steering maneuver to identify limiting values of the driver control parameters through assessment of the driver's control parameters, path deviations and peak values of the selected vehicle states.

It is hypothesized that a qualitative perception of vehicle states could help the driver to enhance its path tracking performance. Relative significance of additional sensory feedbacks on the path tracking performance and directional dynamic measures of the vehicle are thus investigated by integrating different motion perceptions to the driver model structure. A total of ten model structures are formulated involving different motion cues of the vehicle. Most effective motion feedback cues could thus be served as secondary cues to enhance the path tracking performance of the driver in emergency driving situations.

CHAPTER 2

RELATIVE PERFORMANCE ANALYSIS OF DRIVER MODELS

2.1 Introduction

A number of driver models with widely different control strategies have been reported in the literature. These models invariably employ different control structures, feedback cues, preview and prediction strategies that are selected to meet specific objectives subject to selected vehicle design parameters and driving conditions. The variations in vehicle design parameters or driving conditions may thus affect the performance measures of these coupled driver-vehicle models. Furthermore, the control parameters of majority of these models are determined considering an ideal vehicle driver that can readily adjust its driving strategy to perform desired control actions with little or no considerations of control limits of the human driver.

In this chapter, the reported driver models are reviewed and classified on the basis of the preview and control strategies. The relative performance characteristics of the selected models are subsequently evaluated considering a common single-unit vehicle subject to a double lane-change maneuver. Seven driver models employing widely different control strategies and sensory cues are selected and coupled with the yaw-plane model of a two-axle vehicle. The required compensatory gain constants of the models are determined using their respective control strategies. A generalized performance index is then formulated comprising the path tracking performance and steering effort of the driver to assess different performance measures of the selected models. The influences of

variations in vehicle design parameters and operating speeds on the path tracking performance, steering control action of the driver and the compensatory gain constants are further evaluated, so as to examine the applicability of the selected driver models over a range of operating conditions.

2.2 Yaw-Plane Vehicle Model

A two-degree of freedom (DoF) constant velocity linear yaw-plane model of a single-unit vehicle (Figure 2.1) is used for relative evaluations of selected driver models. The model is formulated assuming small side-slip and steering angles, and negligible contributions due to vehicle roll and pitch motions, as described in many earlier studies [124,125]. The equations of motion for the yaw-plane model of the vehicle are obtained in the following manner:

$$m(\dot{v}_y + r v_x) = F_{yf}\ cos\ \delta_F\ + F_{yr} \tag{2.1}$$
$$I_{zz}\dot{r} = F_{yf}\ a\ cos\ \delta_F + F_{yr}\ b + M_{yf} + M_{yr}$$

where v_y is the lateral velocity, r is yaw rate of the vehicle, m and I_{zz} are the mass and yaw moment of inertia of the vehicle, respectively, v_x is the longitudinal velocity of the vehicle, and F_{yi} and M_i are the cornering force and aligning moment of tire i (i=f,r where f and r refer to front and rear tires, respectively). In the above equations, a and b are the longitudinal distances of the front and rear tires from the cg of the vehicle, respectively, and δ_F is the front wheel steer angle. The well-known Magic Formula is used to derive cornering forces and aligning moments due to tire-road interactions as nonlinear functions of the side-slip angle and vertical load [125].

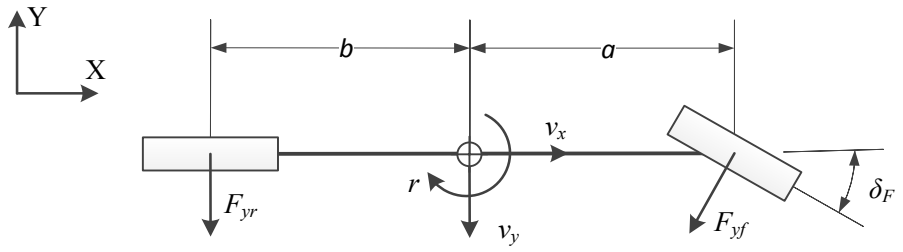

Figure 2.1: Two DoF yaw-plane model of a single-unit vehicle.

The vehicle parameters used in simulations are summarized in Table 2.1. The validity of the vehicle model was examined by comparing its directional responses to a steering input with the responses measured on a limited-motion driving simulator. The vehicle parameters are thus selected to match the vehicle data that are provided by the simulator manufacturer [126]. The measured responses were obtained on a driving-simulator considering a number of subjects, who were asked to perform a standardized double lane-change maneuver [127] at three different forward speeds. The experimental methods and data analyses are described in detail in chapter 3. The steer angle history obtained with one of the participants is used as the steering input to the vehicle model in an open-loop manner. The model responses in terms of vehicle path, lateral acceleration (a_y), yaw angle (Ψ) and yaw rate (r) are compared with the measured responses, as shown in Figures 2.2 to 2.4 for three different forward speeds (30, 50 and 70 km/h) considered in the study.

Table 2.1**:** Simulation parameters of the single-unit vehicle model

Vehicle design parameters	Value
Mass, m (kg)	1330
Yaw moment of inertia of the mass, I_{zz} (kg.m/sec^2)	1200
Horizontal distance from vehicle cg to front axle, a (m)	1.00
Horizontal distance from vehicle cg to rear axle, b (m)	1.50

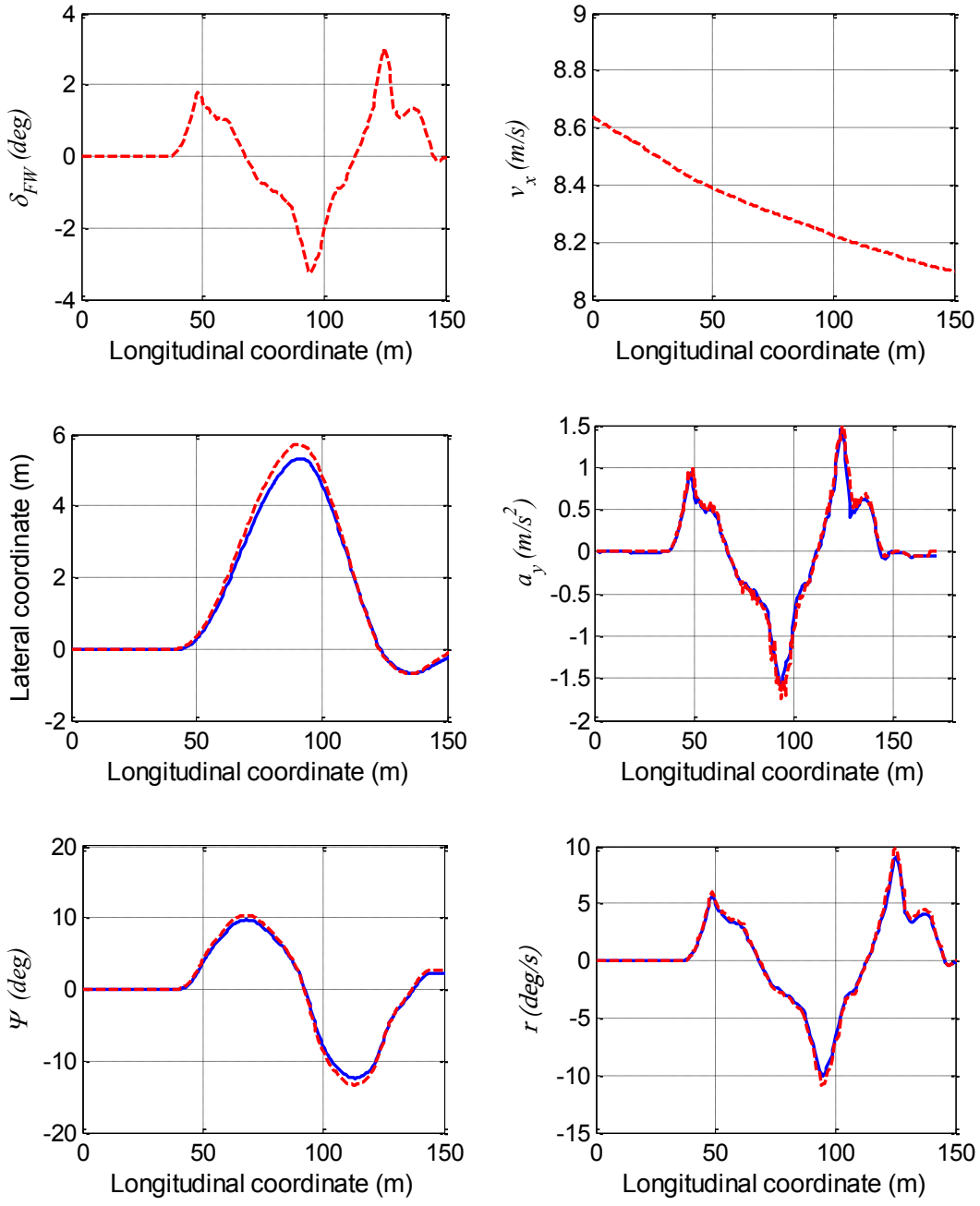

Figure 2.2: Comparisons of directional responses of the yaw plane vehicle model (solid line) with the simulator measured data (dashed line) under a double lane-change maneuver at 30 km/h

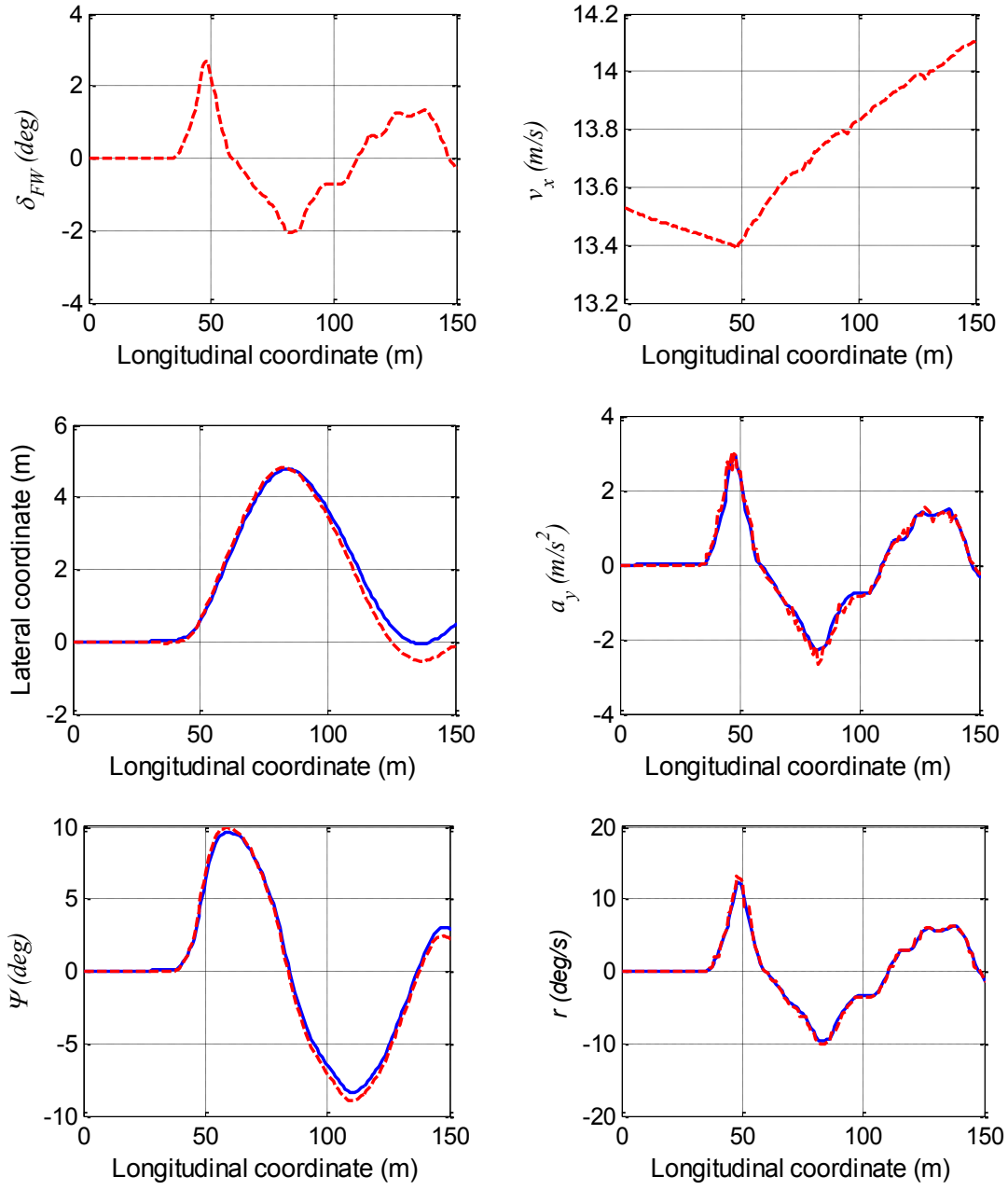

Figure 2.3: Comparisons of directional responses of the yaw plane vehicle model (solid line) with the simulator measured data (dashed line) under a double lane-change maneuver at 50 km/h

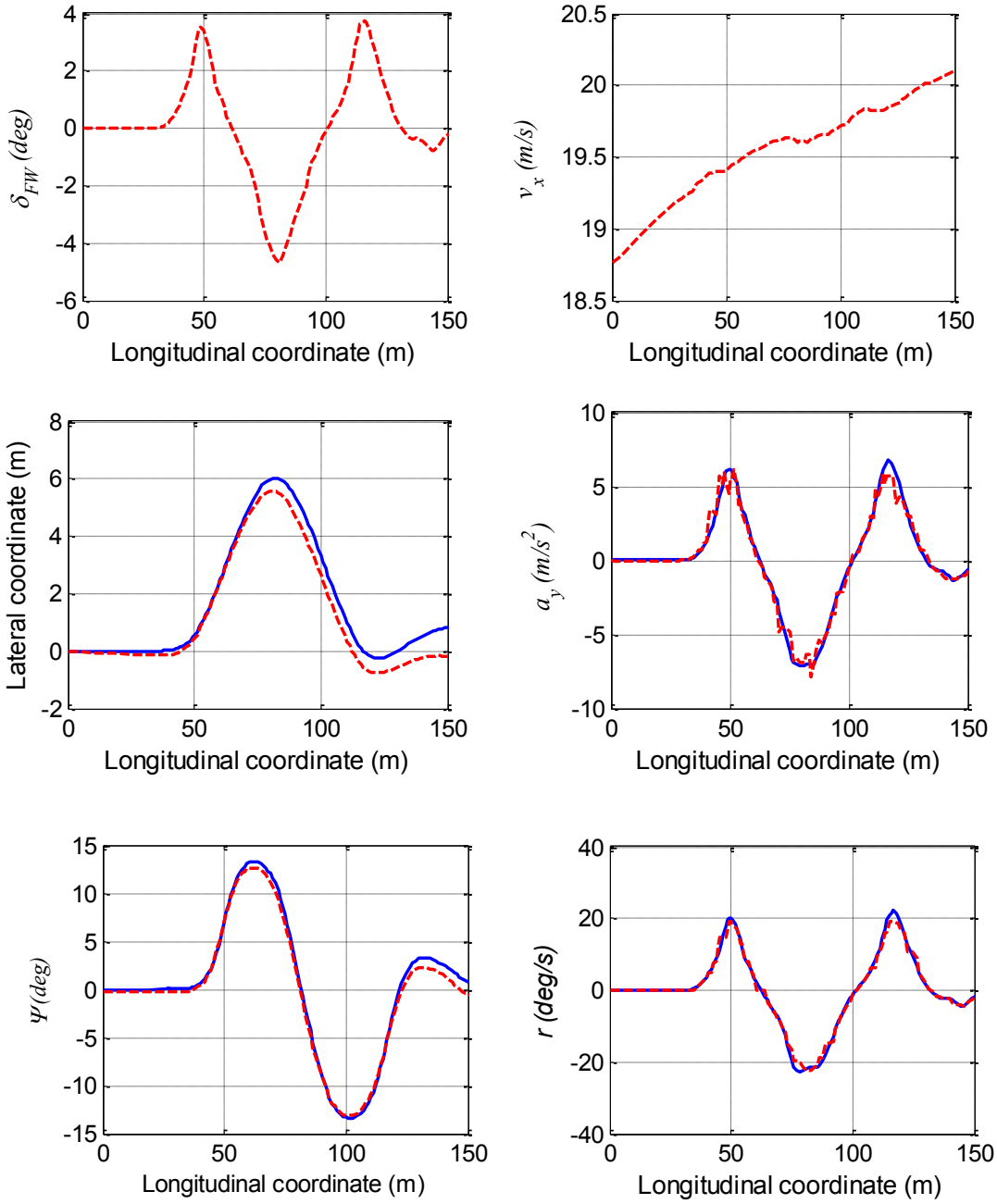

Figure 2.4: Comparisons of directional responses of the yaw plane vehicle model (solid line) with the simulator measured data (dashed line) under a double lane-change maneuver at 70 km/h

It should be noted that the driving simulator could provide measures of the steering angle, path coordinates and the heading angle of the vehicle, while the sampling rate was nearly constant. The lateral acceleration of the vehicle in the fixed global coordinate system (X,Y) was obtained from second derivative of the measured vehicle trajectory. Although a moving average approach is employed to smooth lateral acceleration response, the resulting curve revealed considerable oscillations which were attributed to time differentiation and slight variations in sampling rate. Comparisons of the directional responses of the model with the measured response quantities suggest that the yaw-plane vehicle model can provide reasonably good predictions of yaw and lateral responses of the vehicle to a steering input over the range of speeds considered. The observed deviations between the measured and model responses were mostly attributed to the simplifying assumptions and lack of precise parameters of the vehicle model that is used in the driving simulator.

2.3 Mathematical Formulations of the Selected Driver Control Strategies

The reported driver control models may be classified in three categories based upon their preview and control strategy, as discussed in section 1.2.3. A few models within each category are selected to study the relative performance characteristics of different control strategies. The selected models employ different preview and control strategies, and may thus yield different performance of the coupled driver-vehicle system.

The selected driver models are re-formulated in conjunction with the yaw-plane vehicle model, presented in section 2.2, while the performance evaluations are conducted for a constant speed double lane-change steering maneuver [127]. The parameters of each driver model are determined by minimizing the performance index defined in the

reporting study. Variations in the control characteristics of each model are also examined under variations in the forward speed, mass and understeer coefficient of the vehicle. The performance characteristics of the selected models are further investigated to examine their applicability under varying vehicle design parameters and operating conditions. Table 2.2 summarizes the sensory cues and ranges of control parameters of the selected models, where the studies are identified by the lead author alone.

2.3.1 Compensatory Driver Model

Ishio et al. [17] and Horiuchi and Yuhara [78] have proposed driver models considering the compensatory control approach, which are referred to as "Model 1" and "Model 2", respectively. The compensatory control approach aims to minimize the instantaneous path deviation (Y_e) between the desired road coordinate (Y_d) and instantaneous vehicle cg coordinate (Y). While the preview and prediction capabilities of the human driver are neglected, these models employ a lead time constant (T_L) to describe predictive control action of the driver [17,128].

The driver model proposed by Ishio et al. [17] tracks the desired path and maintains instantaneous central lane position by considering a first-order lead-lag controller based on the lateral position feedback alone (Figure 2.5). The driver describing function *H(s)* relating lateral path error (Y_e) to the front wheel steer angle, δ_F, can be expressed as:

$$H(s) = \frac{Y_e}{\delta_F} = K_y \frac{T_{Ly}s + 1}{T_{Iy}s + 1} \tag{2.2}$$

where T_{Ly}, T_{Iy} and K_y are the lead and lag time constants, and compensatory gain of the driver model corresponding to the lateral position error of the vehicle.

Table 2.2**:** Summary of selected driver models

Control strategy		Compensatory driver models		Preview compensatory driver models				Anticipatory-compensatory driver models
Model		Model 1	Model 2	Model 3	Model 4	Model 5	Model 6	Model 7
Reference		Ishio [17]	Horiuchi [78]	Guo [30]	Macadam [40]	Sharp [68]	Pick [67]	Donges [45]
Preview strategy		Single-point	Single-point	Single-point	Single-point	Multi-point	Multi-point	Two-point
Sensory feedback cues	Lateral deviation, Y_e	■	■	■	■	■	■	■
	Heading error, Ψ_e		■			■	■	■
	Lateral velocity, v_y					■	■	
	Yaw rate, r					■	■	
	Path curvature, C_d							■
Operating condition	Forward speed, v_x (km/h)	30	60	72	100	36,72,108	140	30 - 60
Driver model parameters	Preview time, T_p (s)			1.2	0.5 - 1.5	1 - 1.5	1.0 - 1.5	0.9 - 1.5
	Lead time, T_L (s)	0.2 - 1.4	0.05 - 0.2	0.80				
	Lateral position gain, K_y (rad/m)	0.1 - 1.4	0.1 - 0.1					0.002 - 0.07
	Orientation gain, K_ψ (rad/rad)		0.1 - 0.3					0.4 - 1.85
	Path curvature gain, K_C (rad.m)							0.17 - 13.9
	Anticipatory curvature, gain, K_a (rad.m)							0.1 – 8.7
Response time	Perception-processing time, $\tau_{pd} + \tau_p$ (s)		0.1	0.28			0.16	
	Movement time, τ_m (s)		0.1	0.2				
	Steering response time, τ_s (s)	0.02 - 0.3	0.2	0.48	0.2			0.1 - 0.8
Performance index components		Y_e, $\dot{Y}$, δ_F, $\dot{\delta}_F$	Y_e, δ_F, T_{LY}, $T_{L\Psi}$	Y_e, a_y, δ_F	Y_e	Y_e, Ψ_e, δ_F	Y_e, Ψ_e, δ_F	Y_e, Ψ_e, C_e

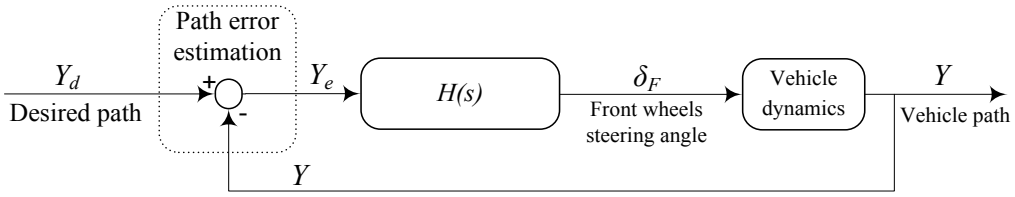

Figure 2.5: The compensatory driver model employing only lateral position feedback

The compensatory model proposed by Horiuchi and Yuhara [78] (model 2) employs feedback from the vehicle heading angle in addition to the lateral position error (Figure 2.6). This model thus aims to compensate for both the instantaneous path deviation and the heading error of the vehicle considering two lead compensators. The driver function *H(s)* has been derived as:

$$H(s) = K_\Psi \frac{T_{L\Psi}s + 1}{T_{I\Psi}s + 1}\left(Y_e\left(K_y T_{Ly}s + 1\right) - \Psi\right)\mathrm{e}^{-\tau_p s} \tag{2.3}$$

where $T_{L\Psi}$, $T_{I\Psi}$ and K_Ψ are the lead and lag time constants, and compensatory gain of the driver model corresponding to the orientation error of the vehicle, respectively. The summation of the two lead time constants, $T_{L\Psi}$ and T_{Ly}, associated with orientation and lateral path deviation may be considered as the overall lead time constant, T_L.

The first-order lag time constant, T_I, in both the models represents driver's response delay due to its muscular dynamics, while the pure time delay τ_p, considered in model 2, represents the processing time delay of the driver. This additional processing time delay affects the performance measures of the driver model and increases the path deviation of the vehicle, which will be discussed in section 2.5.1. Evaluations of these two models would provide guidance on the influences of the orientation feedback cue in addition to the lateral position error feedback and the processing time delay on the driver model performance.

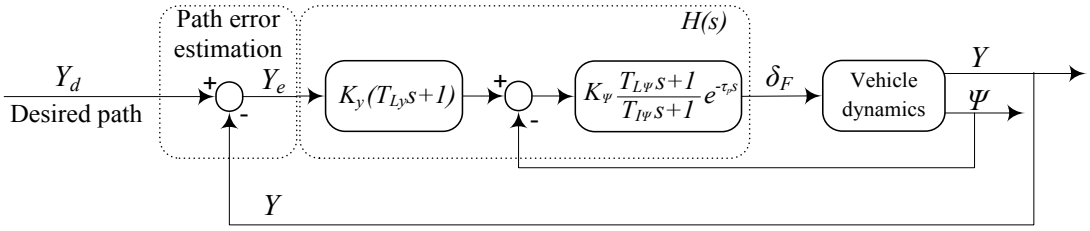

Figure 2.6: The compensatory driver model employing lateral position and orientation feedbacks

2.3.2 Preview Compensatory Driver Model

The preview compensatory control strategy aims to minimize the predicted lateral position error ($Y_{e,Tp}$) between the previewed target point(s) coordinate ($Y_{d,Tp}$) and the predicted coordinate of the vehicle (Y_{Tp}) at a future instant T_p. The preview-follower controller strategy proposed by Guo and Guan [8,30,129] is referred to as "Model 3" and is shown in Figure 2.7. The model employs a single-point preview and a 'second-order path prediction' strategy, described in Eq. (1.4) in section 1.2.1, to predict the vehicle motion within the preview interval T_p. For the single-target point, the preview function *P(s)* can be expressed as:

$$P(s) = \frac{Y_{d,Tp}}{Y_d} = e^{T_p s} \tag{2.4}$$

where T_p is the driver's preview time. The describing function of the driver, *H(s)*, relating the predicted lateral position error $Y_{e,Tp}$ and δ_F is given by:

$$H(s) = \frac{Y_{e,Tp}}{\delta_F} = K_y \frac{T_{Ly}s + 1}{T_{Iy}s + 1} e^{-\tau_p s} \tag{2.5}$$

In this model, the required model parameters are identified through minimization of a performance index comprising instantaneous lateral position error (Y_e), lateral acceleration (a_y) and magnitude of steer angle (δ_F) [23,129]. The summation of the lead

time constant (T_{Ly}) and the preview time (T_p) is considered as the overall lead time constant (T_L) of the model.

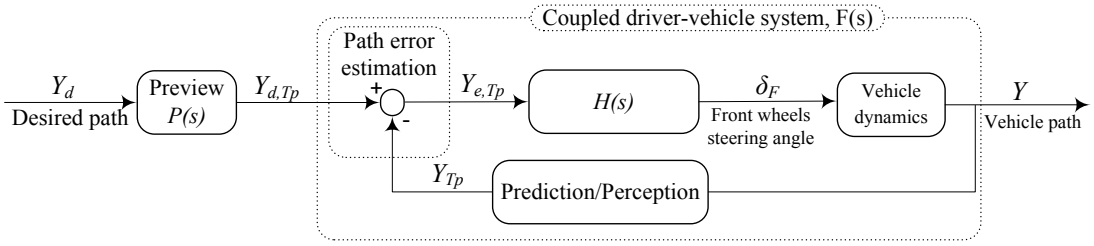

Figure 2.7: The preview compensatory model employing second-order path prediction

The model proposed by MacAdam [40] based on an optimal preview control strategy also falls within the category of preview compensatory models. The model referred to as "Model 4", is presented in Figure 2.8. The proposed model employs an 'internal vehicle model' strategy to predict the future trajectory of the vehicle, and aims to minimize the perceived lateral position error ($Y_{e,Tp}$) between a single target point on the roadway ahead ($Y_{d,Tp}$) and the predicted coordinate of the vehicle at a future instant (Y_{Tp}) [40,63]. The path prediction process through the 'internal vehicle model' has been described in Eq. (1.8) in section 1.2.1. The describing function of the driver model, *H(s)*, can be derived as:

$$H(s) = \frac{Y_{e,Tp}}{\delta_F} = K_y e^{-\tau_p s} \tag{2.6}$$

where K_y is the compensatory gain. The required model parameters are identified through minimization of a performance index comprising the perceived lateral position error between the previewed roadway and predicted vehicle trajectory, $Y_{e,Tp}$.

Driver steering effort and path tracking performance of the two single-point preview models (models 3 and 4) are evaluated to study effectiveness of different prediction

strategies. Furthermore, the performance analysis of the first two groups of models will provide the effectiveness of the preview feature of the human driver.

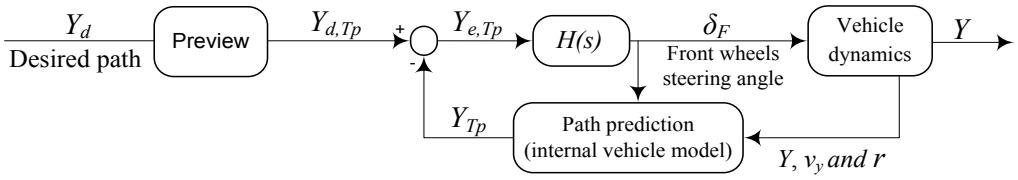

Figure 2.8: The preview compensatory driver model employing 'internal vehicle model' path prediction strategy

The above preview compensatory models, models 3 and 4, employ single-point preview strategy to obtain coordinates of the desired roadway. It has been suggested that a single-point preview may lead to unsatisfactory path tracking performance and instability, particularly under high speed directional maneuvers coupled with a relatively short preview distance [18,66]. A human driver would exhibit superior control performance when a preview of the entire roadway is available. A few studies have proposed multi-point preview strategy for enhanced directional control performance of the driver [20,67,68]. Considering a constant forward speed and preview time T_P, Sharp and Valtetsiotis [68] proposed a multi-point preview model, referred to as the "Model 5". The proposed model aims to minimize the lateral deviation between the predicted vehicle trajectory and a number of equally-spaced target points (Figure 2.9) [15,68]. The time interval ΔT between the N equally-spaced preview points is determined from the overall preview time, as $\Delta T = \frac{T_P}{N}$. The steering input of the driver model is subsequently formulated in the following manner:

$$\delta_F = K_{y0}\left(Y_{d,0} - Y\right) + K_{yi}\left(Y_{d,\Delta Ti} - Y_{\Delta Ti}\right) \quad i = 1\text{:N} \tag{2.7}$$

where $Y_{d,\Delta Ti}$ and $Y_{\Delta Ti}$ are the coordinates of the previewed target point on the roadway and predicted coordinate of the vehicle cg corresponding to the i^{th} preview point ($i = 1, \ldots, \text{N}$), respectively, and $Y_{d,0}$ is the path coordinate in the immediate vicinity of the vehicle cg. K_{yi} is the corresponding lateral position compensatory gain.

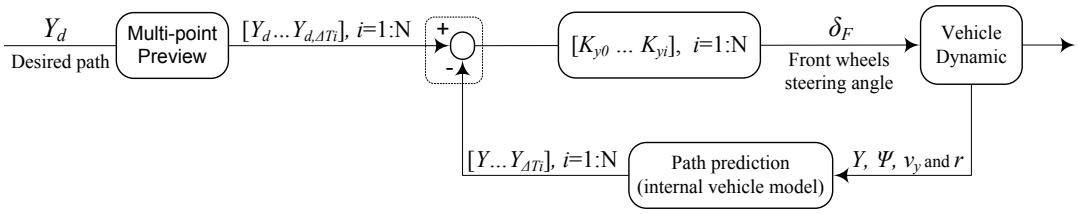

Figure 2.9: The preview compensatory driver model employing multi-point preview strategy

The driver's compensatory command is transmitted to the vehicle steering system through the limb motions. The limb and muscular dynamics, however, are mostly neglected in majority of the reported studies. These studies generally employ a pure time delay or a first-order lag time constant to formulate driver's response time and hand-arm dynamics. Some of the reported studies, however, have employed a mathematical formulation of the muscular dynamics [7,9,20] Pick and Cole [67] proposed a driver model, referred to as "Model 6", that integrates the limb dynamics with the multi-point preview control strategy proposed by Sharp and Valtetsiotis [68]. The model is shown in Figure 2.10, where the hand-arm dynamic system, *L(s)*, has been described in Eq. (1.15) in section 1.2.5.

2.3.3 Anticipatory/Compensatory Driver Model

A few experimental studies have suggested that a human driver exhibits superior control performance when preview of the entire roadway is available [46,51,130].

Measurements performed under restricted visual situations, however, have shown that human drivers observing only two segments of the roadway achieve can improved path tracking performance similar to that realized with preview of the entire roadway [70].

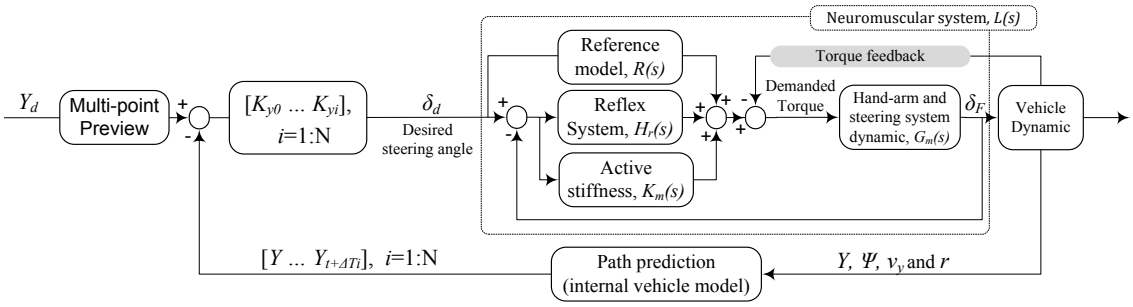

Figure 2.10: The preview compensatory driver model employing multi-point preview strategy together with the muscular dynamic

A two-point preview strategy may thus be considered adequate for describing the driver preview opposed to more complex multi-point preview strategy [45,65,73]. A two-point preview model proposed by Donges [45] referred to as "Model 7" is formulated to investigate the relative performance characteristics of the two-point preview strategy in terms of path tracking performance of the coupled driver-vehicle system. The model describes a two-level control strategy; an open-loop anticipatory and a closed-loop compensatory control strategy, as shown in Figure 2.11. The anticipatory open-loop strategy, attained through a learning process, is related to predictive steering action of the driver, δ_a, that involves driver's perception of the curvature of the future path, C_{d,T_p}. The closed-loop compensatory steering, δ_c, is evolved to enhance the path tracking performance of the coupled vehicle-driver system by maintaining the central lane position. The steering input of the driver model is described as summation of both the anticipatory and compensatory steering angles, such that:

$$\delta_F = \delta_a + \delta_c \tag{2.8}$$

where

$$\delta_a = K_a\, C_{d,T_p}$$
$$\delta_c = \left(K_c(C_d - C) + K_y(Y_d - Y) + K_\Psi(\Psi_d - \Psi)\right) \mathrm{e}^{-\tau_p \mathrm{s}} \tag{2.9}$$

where K_a and K_c are the anticipatory and compensatory gain constants associated with the roadway curvature, respectively. In the above equation C_d and C are the instantaneous curvatures of the roadway and the predicted coordinate of the vehicle trajectory, respectively. The difference, $C_d - C$, is referred to as the instantaneous path curvature error, C_e, in Table 2.2. Ψ_d is the desired vehicle heading angle, and C_{d,T_p} denotes the roadway curvature corresponding to the preview time T_p.

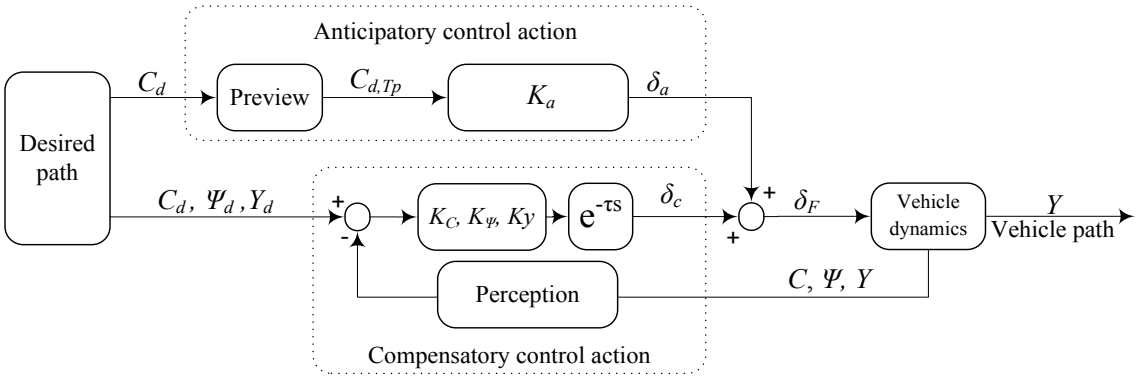

Figure 2.11: The anticipatory/compensatory driver model structure proposed by Donges [45]

2.4 Identification of Driver Models Control Parameters

The selected driver models are integrated with the yaw-plane model of the vehicle described in section 2.2 to obtain the coupled driver-vehicle models. A common vehicle model is used so as to perform relative assessments of different control strategies. The control parameters of each driver model are initially determined through minimization of the original performance index defined in the reporting study. These include the lateral position gain K_y, orientation gain K_Ψ, path curvature gain K_C, anticipatory curvature gain

K_a, preview time T_p, lead time constants (T_{Ly} and $T_{L\psi}$) and the lag time constant T_I. The reported studies generally employ unconstrained minimization of the performance index. The control limits of the human driver are thus not considered. In this study, the resulting model parameters, however, are examined in view of known ranges of human driver control characteristics. For this purpose, the studies reporting steering characteristics of the human driver were reviewed to identify practical ranges of driver's control limits. A set of limit constraints were subsequently established from the feasible ranges of driver control parameters in terms of preview time, lead-lag time constants and human driver's compensatory gains. The ranges summarized in Table 1.7 were subsequently applied as limit constraints for solution of the minimization problem.

A relative assessment of the reported control approaches involving perception and prediction, preview and limb motion dynamics, necessitated the formulation of a generalized performance index comprising lateral deviation, orientation error, magnitude and rate of steering angle, such that:

$$J_t = J_Y + J_\Psi + J_\delta + J_{\dot{\delta}} \tag{2.10}$$

Nearly equal weighting of each of the component is considered by normalizing each individual component. In the above equation, J_Y and J_Ψ are the normalized lateral position and orientation errors, respectively, described by the respective mean squared values:

$$J_Y = \frac{1}{T}\int_0^T \left[\frac{Y_e(t)}{Y_{e,max}}\right]^2 dt \quad ; \quad J_\Psi = \frac{1}{T}\int_0^T \left[\frac{\Psi_e(t)}{\Psi_{e,max}}\right]^2 dt \tag{2.11}$$

where $Y_e(t)$ and $\Psi_e(t)$ are, respectively, the instantaneous lateral deviation and orientation errors of the vehicle c.g. with respect to the desired roadway. $Y_{e,max}$ and $\Psi_{e,max}$ are the normalizing factors, defined as the maximum allowable deviations in the lateral displacement and orientation errors, respectively. The maximum allowable

deviations are considered as; $Y_{e,max} = 0.3$ m and $\Psi_{e,max} = 10^{\circ}$, on the basis of typical roadway geometry and vehicle track width. In the above formulation, *T* is the simulation time.

The components J_δ and $J_{\dot{\delta}}$ in equation (2.10) describe the weighted mean squared steering angle and its rate, which relate to driver's steering effort [9,78,131]:

$$J_\delta = \frac{1}{\mathrm{T}}\int_0^{\mathrm{T}} \left[\frac{\delta_F(t)*G_{st}}{\Delta\delta_F}\right]^2 \mathrm{dt} \;;\; J_{\dot{\delta}} = \frac{1}{\mathrm{T}}\int_0^{\mathrm{T}} \left[\frac{\dot{\delta}_F(t)*G_{st}}{\Delta\dot{\delta}_F}\right]^2 \mathrm{dt} \tag{2.12}$$

where G_{st}, δ_F and $\dot{\delta}_F$ are the steering ratio of the vehicle steering system, and the magnitude and rate of steering input. $\Delta\delta_F$ and $\Delta\dot{\delta}_F$ represent the corresponding maximum values in accordance with the known drivers' limits. On the basis of reported studies, these normalizing factors are selected as: $\Delta\delta_F = 187$ deg and $\Delta\dot{\delta}_F = 746$ deg/s [132,133].

2.5 Sensitivity Analysis

For a given driver-vehicle system, the directional control performance of the vehicle is generally dependent on a number of vehicle design parameters and situational conditions. The forward speed, mass and understeer coefficient of the vehicle are the key design parameters affecting the vehicle performance. Contributions of these parameters to the vehicle performance measures may differ considerably depending upon the driver control approach and vehicle dynamic characteristics. A sensitivity analysis of the path tracking performance of the selected driver-vehicle models and the corresponding driver model parameters is thus undertaken with respect to variations in the vehicle design and operating parameters. For this purpose, the forward speed, mass and understeer coefficient of the vehicle are varied about their nominal values. Variations in the vehicle

directional responses are evaluated in terms of: (i) peak steer angel; (ii) peak rate of steering; (iii) peak lateral position error; (iv) peak lateral acceleration; and (v) the total performance index J_t and its constituents. Table 2.3 summarizes the variations in the vehicle design and operating parameters considered in the sensitivity analysis. In each case, only one of the parameters was varied while the others were held at their respective nominal values.

Table 2.3**:** Range of vehicle parameters and the nominal values employed in sensitivity analysis

	Nominal value	Parameter values
Forward speed, v_x (m/s)	20	10 20 30
Mass, m (kg)	1330	997.5 1330 1662.5
Understeer coefficient, K_{us}	+0.004	-0.004 +0.004 0

Considering the yaw-plane vehicle model, described in section 2.2.1, as a time-invariant system, the response vector can be expressed as:

$$\dot{\vec{x}} = f(\vec{x}, \vec{p}, t) \tag{2.13}$$

where $\vec{x} = (v_y, r)$ is the state vector and $\vec{p} = (p_1, p_2, \dots, p_r)$ is the r-dimensional vector of vehicle design parameters and forward speed. The influences of parameters variations on the coupled driver-vehicle system responses are investigated by considering:

$$\vec{p} = \overrightarrow{p_0} + \overrightarrow{\Delta p} \tag{2.14}$$

where $\overrightarrow{\Delta p}$ is the variation about the nominal vector $\overrightarrow{p_0}$, while the parameter vector for the single-unit vehicle model is given by:

$$\vec{p} = (v_x, m, K_{us}) \tag{2.15}$$

where K_{us} is understeer coefficient of the vehicle model. The sensitivity of a response $\vec{S}_x$ to variations in the parameters is described by the percentage change with respect to its nominal value where $\vec{x} = g(\vec{p}, t)$:

$$\vec{S}_x = \frac{\mathrm{g}\left(\vec{p}_0 + \overrightarrow{\Delta p}, t\right) - \mathrm{g}(\vec{p}_0, t)}{\mathrm{g}(\vec{p}_0, t)} * 100\% \tag{2.16}$$

The sensitivity of the performance index and its components, described in Eq. (2.10), to variations in the parameters are also evaluated in a similar manner. The relative significance of different control strategies could thus be investigated by incrementally varying the vehicle speed, vehicle mass and understeer coefficient.

2.6 Results and Discussions

2.6.1 Influences of Variations in Vehicle Speed

The relative performance characteristics of the selected driver models are investigated under a double lane-change steering maneuver [127] at three different forward speeds (10, 20 and 30 m/s). Considering that the human driver exhibits limited control performance, a constrained minimization of each reported performance index was conducted considering the limit constraints summarized in Table 1.7, such that:

$$\begin{array}{lllll}
\text{Lateral position compensatory gain (rad/m)} & \text{1e-5} & \leq K_y \leq & 1.80 & \\
\text{Orientation compensatory gain (rad/rad)} & 0.10 & \leq K_\Psi \leq & 1.85 & \\
\text{Curvature compensatory gain (rad.m)} & 0.10 & \leq K_C \leq & 14.00 & \\
\text{Curvature anticipatory gain (rad.m)} & 0.05 & \leq K_a \leq & 1.00 & (2.17) \\
\text{Lead time constant (s)} & 0.05 & \leq T_L \leq & 3.00 & \\
\text{Lag time constant (s)} & 0.02 & \leq T_I \leq & 0.80 & \\
\text{Preview time (s)} & 0.10 & \leq T_P \leq & 2.50 &
\end{array}$$

The model parameters identified through solutions of the minimization problem together with the performance measures of the selected models are summarized in Table 2.4. Figure 2.12 further illustrate the variations in the model parameters with variations in

the forward speed. The model under the specified maneuver is judged to either "Pass" or "Fail" depending upon its path deviation. The model is judged to fail when the peak lateral position error exceeds the threshold value of 0.3 m.

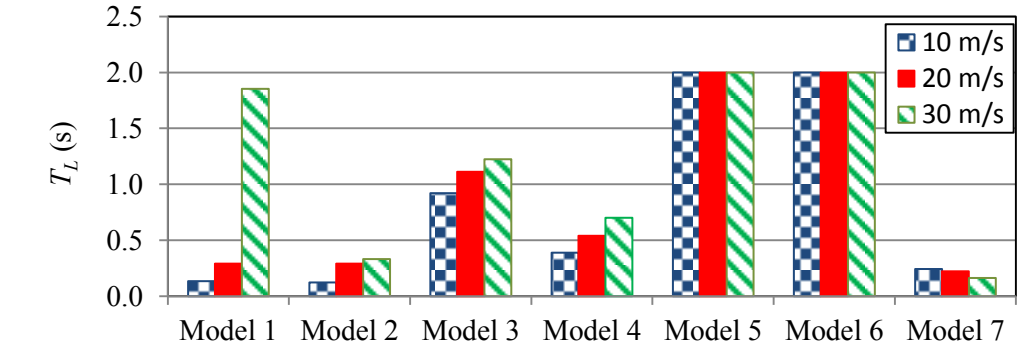

(a)

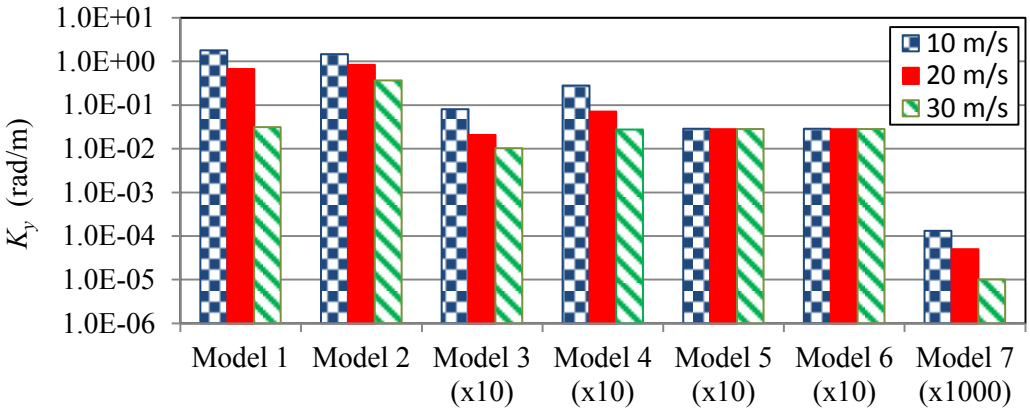

(b)

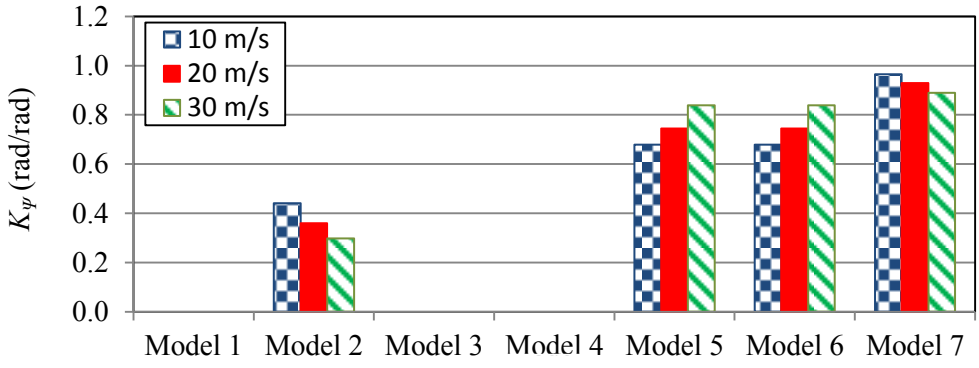

(c)

Figure 2.12: Comparisons of (a) the lead time constant; (b) lateral position gain constant (log scale); and (c) orientation gain constant of the selected driver models during a double lane-change maneuver at three different speeds (10, 20 and 30 m/s)

Table 2.4**:** Influences of variations in vehicle speed on the identified driver model parameters and corresponding performance measures of the selected driver-vehicle models

	Driver Model	Velocity (m/s)	Test Result	K_y[†] (rad/m)	K_Ψ (rad/rad)	K_C (rad.m)	K_a (rad.m)	T_L[‡] (s)	T_I[*] (s)	J_t	J_Y	J_Ψ	J_δ	$J_{\dot{\delta}}$
Compensatory models	Model 1	10	Pass	1.780	-	-	-	0.133	0.047	0.203	0.009	0.022	0.107	0.065
		20	Pass	0.669	-	-	-	0.291	0.045	0.613	0.093	0.028	0.145	0.347
		30	Fail	0.031	-	-	-	1.854	0.032	3.752	2.475	0.202	0.260	0.816
	Model 2	10	Pass	1.454	0.440	-	-	0.123	0.200	1.060	0.518	0.102	0.201	0.240
		20	Pass	0.840	0.360	-	-	0.292	0.200	1.933	0.960	0.103	0.240	0.631
		30	Fail	0.366	0.297	-	-	0.333	0.200	8.987	6.689	0.684	0.484	1.130
Preview compensatory models	Model 3	10	Pass	0.080	-	-	-	0.922	0.300	0.226	0.110	0.038	0.071	0.007
		20	Pass	0.021	-	-	-	1.112	0.300	1.503	1.404	0.058	0.034	0.007
		30	Fail	0.010	-	-	-	1.223	0.300	5.477	5.325	0.123	0.022	0.007
	Model 4	10	Pass	0.278	-	-	-	0.390	0.200	0.164	0.014	0.019	0.101	0.030
		20	Pass	0.071	-	-	-	0.540	0.200	0.301	0.153	0.031	0.087	0.029
		30	Pass	0.027	-	-	-	0.701	0.200	0.592	0.472	0.032	0.059	0.029
	Model 5	10	Pass	0.029	0.678	-	-	2.000	-	0.531	0.465	0.021	0.044	0.001
		20	Pass	0.028	0.745	-	-	2.000	-	0.935	0.861	0.033	0.038	0.002
		30	Pass	0.028	0.839	-	-	2.000	-	1.847	1.773	0.036	0.036	0.003
	Model 6	10	Pass	0.029	0.678	-	-	2.000	-	0.678	0.552	0.051	0.074	0.001
		20	Pass	0.028	0.745	-	-	2.000	-	1.100	0.978	0.047	0.073	0.003
		30	Fail	0.028	0.839	-	-	2.000	-	1.679	1.563	0.041	0.071	0.005
Compensatory Anticipatory	Model 7	10	Pass	1.3E-04	0.964	0.304	0.575	0.242	0.121	0.105	0.003	0.002	0.069	0.031
		20	Pass	5.0E-05	0.930	0.260	1.488	0.224	0.121	0.222	0.041	0.009	0.070	0.101
		30	Pass	1.0E-05	0.889	0.206	2.965	0.162	0.142	0.416	0.086	0.024	0.080	0.226

[†] K_y, the compensatory gain, for the multi-point preview models (models 5 and 6) is reported corresponding to the first preview point.

[‡] T_L represents the lead time constant (model 1) and summation of individual lead times (model 2), preview time in models employing only preview (models 4, 5, 6 and 7), and lead and preview time (model 3)

[*] The lag time, T_I, in models 2, 3 and 4 is the sum of first-order lag time and processing delay time τ_p, both being constant.

The results in general show wide variations in the control parameters of driver models employing different control strategies. Furthermore, the control parameters vary considerably with variations in the forward speed. The results show that the compensatory gains corresponding to lateral position error K_y decrease with the speed, irrespective of the control strategy, as shown in Figure 2.12(b). The result obtained for models based on multi-point preview (models 5 and 6), however, show negligible variation in K_y with increasing speed, which was observed only for the first preview point (as reported in Table 2.4). The gains corresponding to subsequent preview points revealed decreasing K_y with increasing speed. These suggest that the driver is required to undertake greater compensation to minimize lateral position error at lower speeds. Such a trend has also been reported in a few experimental and analytical studies [45,65,128]. It has been suggested that the human driver focuses on lateral position control at lower speed and vehicle heading errors at higher speeds. The models results, however, do not show a definite trend in K_ψ with increasing speed, Figure 2.12(c). The models employing a constant driver preview (models 5 and 6) suggest increase in K_ψ with increasing vehicle speed, while the compensatory model in the absence of driver preview (model 2) suggests an opposite trend. An opposite trend is also observed with anticipatory/compensatory model (model 7). The anticipatory gain K_a in this model, however, increases substantially (Table 2.4), which also emphasizes the heading error control.

Irrespective of the modeling strategy, an increase in the vehicle speed poses a higher demand for the lead time of the driver (T_L), which also suggests higher preview distance (D_p), Figure 2.12(a). The multi-point preview models (models 5 and 6), however, form an exception since these assume a constant preview time, irrespective of the speed. The two-

level anticipatory/compensatory control strategy (model 7) also suggests slightly lower T_L (=T_p) at higher speeds, while the preview distance increases with speed (Table 2.4). Furthermore, while all the compensatory gains of model 7 (K_y, K_Ψ and K_C) decrease with increase in vehicle speed, the open-loop anticipatory gain K_a increases with the forward speed. This further suggests lower compensatory demand but greater anticipatory demand on the driver at higher speeds. The results thus suggest that the human driver is required to employ a higher level of prediction at higher speeds. Such trends have also been reported in a few studies [23,134,135]. The two-level driver model proposed by Donges [45], however, requires relatively lower value of T_L. Despite decrease in the lead time constant at higher speeds, the preview distance, D_P, increases with the speed.

The results clearly show that the compensatory driver model, proposed by Ishio [17] (model 1), which considers only the instantaneous lateral position error of the vehicle, is highly sensitive to variations in the vehicle speed. This suggests that considering the orientation error and employing the driver's preview would help to attain more effective and consistent driver parameters. Furthermore, a higher lead time is essential for achieving desired position and orientation control of the vehicle at higher speeds. The multi-point preview models, employing constant preview time, achieve the position and orientation control by employing upper limit of the preview time.

The above results are obtained considering widely different performance indices. The models are thus further evaluated considering the identical performance index, defined in Eq. (2.10). Table 2.4 also presents the values of total performance index and its constituents of the selected models. The results show an increase in the total performance index J_t with increase in vehicle speed, irrespective of the modeling strategy. The models

employing anticipatory steering control (model 7) and enhanced prediction strategy based on the internal vehicle model (model 4) yield substantially lower values of J_t and show relatively less sensitivity to variations in vehicle speed. The model 1 [17], which neglects the driver preview and time delays, can effectively track the desired path at low speed, but fails the path tracking at 30 m/s. While consideration of the vehicle orientation feedback enhances the path tracking performance of the vehicle, the driver's delay associated with processing and muscular dynamics deteriorates the path tracking ability, as seen for models 2 and 3.

The compensatory driver models in the absence of driver preview (models 1 and 2) yield greatest path deviation and substantially higher performance indices corresponding to lateral position error (J_Y), orientation error (J_Ψ) and driver steering effort (J_δ, $J_{\dot{\delta}}$) at higher driving speeds. These models, however, can effectively track the desired path at the lower speed of 10 m/s. The compensatory model 1 in the absence of driver preview and vehicle orientation feedback provides superior path tracking performance by converging to lower time lag and higher compensation gain (K_y) that approaches the upper limit of control. Addition of the processing delay time to the compensatory model (model 2) results in substantially higher path deviation and corresponding performance measures (J_t, J_Y, J_Ψ, J_δ, $J_{\dot{\delta}}$) together with relatively higher lateral position compensatory gain (K_y). This is mostly attributed to lack of preview ability of the human driver.

Consideration of the human preview ability dramatically lowers the steering effort demand on the human driver in addition to the lower lateral position error compensatory gain, particularly at higher speeds, as seen in the results obtained for models 3 to 7. The results obtained for model 3 also suggest using the second-order path prediction yields

relatively greater path deviation compared to the other models employing internal vehicle model path predictions (models 4, 5, 6). The single-point preview coupled with internal vehicle model path predictor (model 4), however, achieves enhanced path tracking performance at the expense of higher steering effort, J_δ and $J_{\dot{\delta}}$. The greater demand for driver's steering control action is attributable to single-point preview strategy. The use of multi-point preview strategy coupled with internal vehicle model path predictor results in least demand on the driver's steering effort. The two multi-point preview models (models 5 and 6), however, employ a constant preview interval, which can cause higher path deviations at low and moderate forward speeds. While introducing the muscular dynamic in model 6 increases the path deviation compared to model 5, a more realistic representation of the driver steering control actions can be achieved through this model. Model 7 [45] employed the two-point preview concept but neglected the hand-arm dynamics. This model yields the lowest path deviation and thus the best path tracking performance in the entire speed range considered in the study. This is evident from substantially lower values of J_Y and J_Ψ for this model. As expected, the accurate path tracking imposes greater demand on the drivers' steering and control actions when compared to the driver models employing single- and multi-point preview strategies (models 3 to 6).

Using Eq. (2.16), the influence of variations in vehicle forward speed v_x on peak values of directional responses of vehicle, $\vec{Z}_1 = (\delta_F, \dot{\delta}_F, Y_e, a_y)$ and the corresponding performance measures, $\vec{Z}_2 = (J_Y, J_\Psi, J_\delta, J_{\dot{\delta}})$ are evaluated from:

$$\overrightarrow{S_Z} = \frac{\vec{Z}_i\big|_{v_x} - \vec{Z}_i\big|_{v_{x0}}}{\vec{Z}_i\big|_{v_{x0}}} * 100\% \quad i = 1, 2 \tag{2.18}$$

where v_{x0} is the nominal forward speed, considered as 20 m/s, and $\overrightarrow{S_Z}$ is the sensitivity in percent. Table 2.5 summarizes the influences of variations in forward speed on peak directional responses of the vehicle and driver's steering effort in terms of peak steer angle and peak rate of steering. Table 2.6 summarizes the variations in the total performance index and its various constituents. The positive percentage value represents increase in a response quantity with respect to the nominal value corresponds to 20 m/s.

Table 2.5**:** Sensitivity of directional responses and steering effort of selected driver-vehicle models to variations in forward speed

Driver Model	Speed (m/s)	Sensitivity of the peak values of directional responses (%)			
		δ_F (deg)	$\dot{\delta}_F$ (deg/s)	Y_e (m)	a_y (m/s^2)
Model 1	10	-53.2	-61.8	-77.9	-78.6
	30	48.4	58.5	663.7	131.4
Model 2	10	-29.0	-51.1	-49.4	-70.5
	30	37.9	45.6	247.6	120.2
Model 3	10	-7.6	-38.3	-84.7	-64.3
	30	5.1	37.5	114.0	76.4
Model 4	10	7.0	-12.3	-73.2	-69.3
	30	-18.9	8.7	115.9	30.9
Model 5	10	-12.8	-48.0	-12.2	-71.9
	30	14.9	56.0	30.4	85.8
Model 6	10	-21.5	-54.7	-25.5	-71.9
	30	30.2	72.6	46.2	97.0
Model 7	10	-28.4	-61.3	-79.9	-76.8
	30	28.8	115.7	35.1	102.1

The results show that increasing the forward speed invariably yields higher peak values of lateral deviation (Y_e), lateral acceleration (a_y) and steering rate ($\dot{\delta}_F$), and the total performance index and its constituents. Simulation results show greater sensitivity of the directional responses to speed variations, when compensatory driver models (models 1 and 2) are used. These models, particularly, exhibit substantially higher path error and lateral acceleration at higher speeds, and the corresponding performance measures. Employing the human driver preview process (model 3 to 7) greatly reduces the driver-

vehicle model sensitivity to variations in the vehicle speed. All of the models, however, show considerable sensitivity to variations in the vehicle speed.

The results also suggest that the steering control demand (δ_F and $\dot{\delta}_F$) and lateral acceleration response of vehicle are least sensitive to variation in v_x, for the single-point preview compensatory driver models (models 3 and 4). This is evident from relatively lower percentage changes in peak of δ_F, $\dot{\delta}_F$ and a_y in Table 2.5. Two- and multi-point preview models (Models 5 to 7), however, show relatively higher sensitivity of the response measures to speed variations. The anticipatory steering control (model 7), in particular, reveals greatest sensitivity of steer rate to speed variations, suggesting greater steering effort demand on the driver at higher speeds. This is also evident from substantial changes in $J_{\dot{\delta}}$ at the higher speed and is attributable to anticipatory open-loop control based on the previewed path curvature. The two multi-point preview models, however, show least sensitivity of path deviation to speed variations. This is also evident from the relatively lower sensitivity of J_t and J_Y to variations in the speed (Table 2.6).

Table 2.6**:** Sensitivity of total performance index and its constituents of the selected driver-vehicle models to variations in forward speed

Driver Model	Speed (m/s)	Sensitivity of performance measures (%)				
		J_t	J_Y	J_Ψ	J_δ	$J_{\dot{\delta}}$
Model 1	10	-66.8	-90.0	-20.3	-26.3	-81.3
	30	512.4	2566.6	624.6	78.7	135.3
Model 2	10	-45.2	-46.0	-1.5	-16.4	-62.0
	30	364.8	597.0	560.5	102.0	79.2
Model 3	10	-85.0	-92.1	-34.3	107.1	-1.7
	30	264.5	279.3	114.1	-35.5	1.0
Model 4	10	-45.5	-90.7	-39.8	15.9	0.8
	30	96.8	07.9	4.0	-32.9	-0.3
Model 5	10	-43.2	-46.0	-36.4	14.3	-55.5
	30	97.7	105.8	8.3	-6.0	68.6
Model 6	10	-38.4	-43.5	9.7	1.8	-62.0
	30	52.6	59.9	-13.1	-2.8	78.7
Model 7	10	-52.7	-92.9	-76.3	-1.9	-69.6
	30	87.7	108.4	186.0	13.8	122.4

2.6.2 Influence of Variations in Vehicle Mass

The sensitivity of the vehicle responses and driver-vehicle model performance indices to variations in the vehicle mass are evaluated considering ±25% variations about the nominal mass (1330 kg). Owing to sensitivity of the driver models to variations in vehicle parameters, the parameters of each driver model are identified through minimization of the respective performance index, defined in the reporting study. The limit constraints, defined in Eq. (2.17), however, are introduced for solution of the minimization problem at speed of 20 m/s. Table 2.7 lists the identified model parameters together with the performance indices described in Eq. (2.10). The table also lists the success of the model in satisfying path deviation threshold (0.3 m). The variations in the lead time and compensatory gains are also presented in Figure 2.13.

The results in general suggest that the control parameters of selected driver models vary with variations in the vehicle mass, although the changes are considerably small compared to those observed with speed variations. The results show that only the compensatory driver models, proposed by Ishio [17] (model 1) and Horiuchi [78] (model 2), which neglect the preview process, are relatively more sensitive to variations in vehicle mass. This suggests that employing the driver's preview process would help to attain more effective and consistent driver parameters. Irrespective of the modeling strategy, an increase in the vehicle mass affects the lead time of the driver (T_L) only slightly (Figure 2.13a). The compensatory model based on the lateral position feedback alone (model 1), however, forms an exception since increasing the vehicle mass poses relatively greater demand on T_L (Table 2.7). Further, the driver models that consider variable lag time constant (models 1 and 7) show slightly greater T_I for heavier vehicles.

Table 2.7**:** Influences of variations in vehicle mass on the identified driver model parameters and corresponding performance measures

	Driver Model	Mass (kg)	Test Result	K_y † (rad/m)	K_Ψ (rad/rad)	K_C (rad.m)	K_a (rad.m)	T_L ‡ (s)	T_I * (s)	J_t	J_Y	J_Ψ	J_δ	$J_{\dot{\delta}}$
Compensatory models	Model 1	997.5	Pass	0.698	-	-		0.210	0.043	0.490	0.064	0.023	0.121	0.283
		1330	Pass	0.669	-	-		0.291	0.045	0.613	0.093	0.028	0.145	0.347
		1662.5	Pass	0.442	-	-		0.376	0.047	0.748	0.123	0.036	0.172	0.417
	Model 2	997.5	Pass	1.068	0.272	-	-	0.288	0.200	1.544	0.698	0.097	0.206	0.544
		1330	Pass	0.840	0.360	-	-	0.292	0.200	1.933	0.960	0.103	0.240	0.631
		1662.5	Pass	0.684	0.494	-	-	0.274	0.200	2.439	1.301	0.118	0.282	0.738
Preview compensatory models	Model 3	997.5	Pass	0.019	-	-	-	1.098	0.300	1.436	1.338	0.062	0.030	0.006
		1330	Pass	0.021	-	-	-	1.112	0.300	1.503	1.404	0.058	0.034	0.007
		1662.5	Pass	0.022	-	-	-	1.132	0.300	1.550	1.446	0.057	0.039	0.008
	Model 4	997.5	Pass	0.067	-	-	-	0.529	0.200	0.280	0.151	0.030	0.075	0.024
		1330	Pass	0.071	-	-	-	0.540	0.200	0.301	0.153	0.031	0.087	0.029
		1662.5	Pass	0.075	-	-	-	0.550	0.200	0.346	0.155	0.033	0.099	0.059
	Model 5	997.5	Pass	0.028	0.727	-	-	2.000	-	0.821	0.755	0.029	0.035	0.002
		1330	Pass	0.028	0.745	-	-	2.000	-	0.935	0.861	0.033	0.038	0.002
		1662.5	Pass	0.028	0.763	-	-	2.000	-	1.141	1.060	0.037	0.041	0.002
	Model 6	997.5	Pass	0.028	0.727	-	-	2.000	-	0.660	0.570	0.030	0.057	0.003
		1330	Pass	0.028	0.745	-	-	2.000	-	1.100	0.978	0.047	0.073	0.003
		1662.5	Fail	0.028	0.763	-	-	2.000	-	1.717	1.598	0.043	0.074	0.003
Compensatory Anticipatory	Model 7	997.5	Pass	1.3E-05	0.907	0.386	1.137	0.229	0.109	0.196	0.028	0.009	0.063	0.096
		1330	Pass	5.0E-05	0.930	0.260	1.488	0.224	0.121	0.222	0.041	0.009	0.070	0.101
		1662.5	Pass	5.3E-05	1.033	0.210	1.627	0.224	0.137	0.261	0.047	0.010	0.084	0.120

† K_y, the compensatory gain, for the multi-point preview models (models 5 and 6) is reported corresponding to the first preview point.

‡ T_L represents the lead time constant (model 1) and summation of individual lead times (model 2), preview time in models employing only preview (models 4, 5, 6 and 7), and lead and preview time (model 3)

* The lag time, T_I, in models 2, 3 and 4 is the sum of first-order lag time and processing delay time τ_p, both being constant.

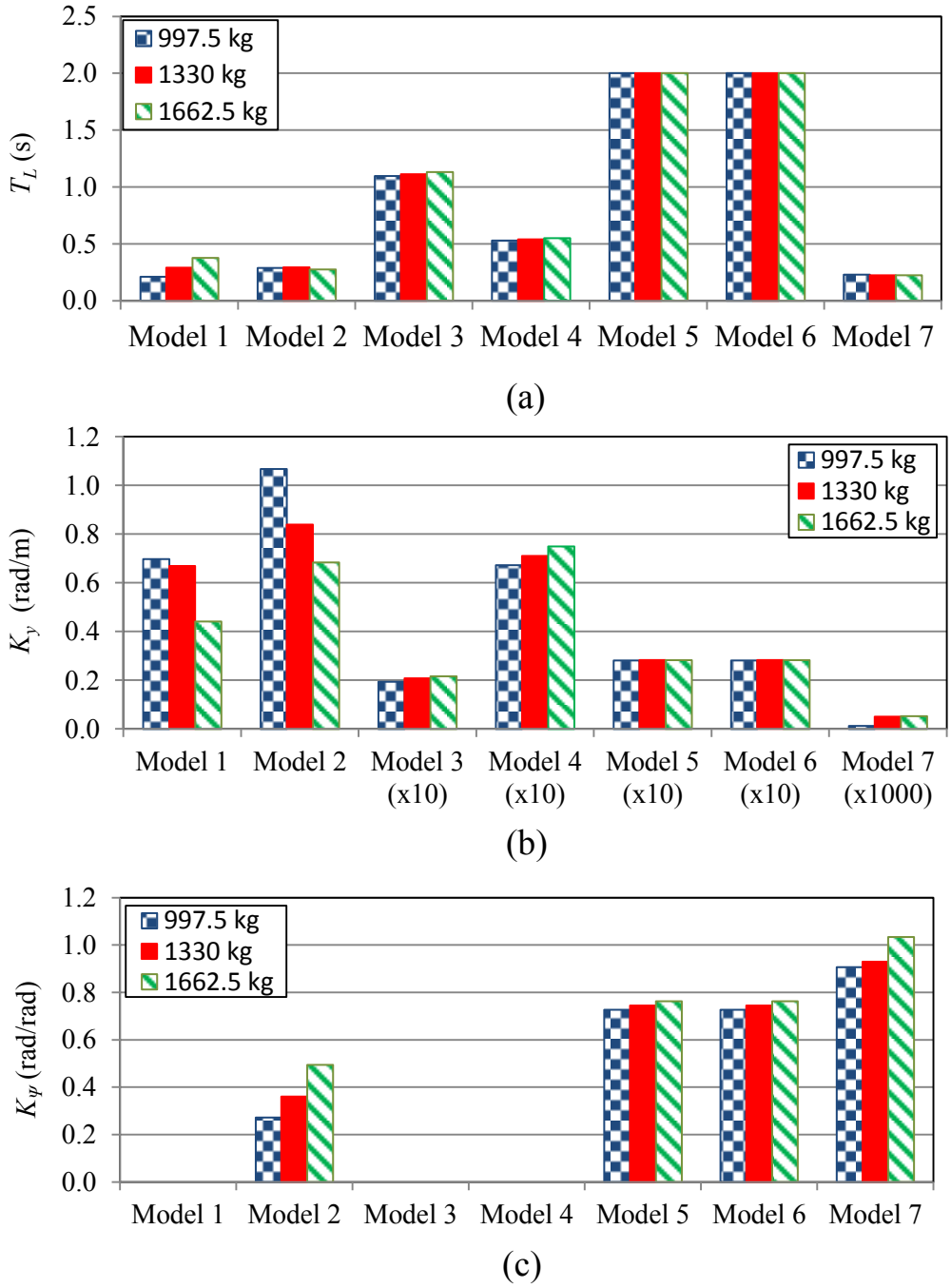

Figure 2.13: Comparison of (a) the lead time constant; (b) lateral position gain constant; and (c) orientation gain constant of selected driver models during a double lane-change maneuver subject to variations in the vehicle mass (speed= 20 m/s)

The results also suggest that the driver is required to undertake greater compensation to minimize the heading angle error with greater vehicle mass, as shown in Figure

2.13(c). In addition, the anticipatory gain K_a in the model based on the two-point preview strategy (model 7), increases with vehicle mass, leading to greater heading error. This further suggests greater anticipatory demands on the driver with increase in the vehicle mass. The results, however, do not show a definite trend in K_y with increasing mass (Figure 2.13b). The compensatory driver models in the absence of the preview (models 1 and 2), however, show that the compensatory gains K_y decreases with the vehicle mass, while the single- and two-point preview strategies (models 3, 4 and 7) suggest an opposite trend. The result obtained for the models based on multi-point preview (models 5 and 6), however, show negligible effect on K_y which was observed only for the first preview point. The same trend was also observed for the gains corresponding to subsequent preview points.

The above results are obtained considering widely different performance indices. The models are thus further evaluated considering the identical performance index, defined in Eq. (2.10). Table 2.7 also presents the values of total performance index and its constituents of the selected models. The results show an increase in the total performance index J_t and the path tracking performance J_Y with increase in vehicle mass, irrespective of the modeling strategy. The models employing anticipatory steering control (model 7) and enhanced prediction strategy based on the internal vehicle model (model 4) yield the lowest values of J_t. The model 1 [17], which neglects the driver preview and time delays, can effectively track the desired path by converging to lower lag time constant at the expense of substantially higher performance indices corresponding to driver steering effort (J_δ and $J_{\dot{\delta}}$). While consideration of the vehicle orientation feedback (model 2) enhances the path tracking performance, the driver's delay associated with processing

and muscular dynamics (model 2) deteriorate the path tracking ability (Table 2.7). Consideration of human preview ability dramatically lowers the steering effort of the driver in addition to a lower demand for the lateral position error compensatory gain, as seen in the results obtained for model 3 to 7. The results obtained for model 3 also suggest that using the second-order path prediction strategy yields relatively greater path deviation compared to the models employing the internal vehicle model path predictor (models 4, 5, 6). The single-point preview coupled with internal vehicle model predictor (model 4), however, achieves enhanced path tracking performance at the expense of higher steering effort, J_δ and $J_{\dot{\delta}}$. The greater demand for driver's steering effort for models 3 and 4 is attributable to the single-point preview strategy.

The use of the multi-point preview strategy coupled with internal vehicle model path prediction strategy results in the least demand on the driver's steering effort. The constant preview interval used in the multi-point preview models (models 5 and 6), however, may cause greater path deviations. Although consideration of muscular dynamics also yields greater path deviation, it represents driver steering control actions more realistically. The results obtained for the model based on compensatory/anticipatory control strategy [45] (model 7) exhibit the lowest path deviation and thus the best path tracking performance in the entire range of the vehicle mass considered in the study. This is evident from substantially lower values of J_Y and J_Ψ. As expected, the accurate path tracking imposes greater demand on the drivers' steering and control actions in comparison with the models employing the preview process (models 3 to 6).

The sensitivity of the responses and control parameters with respect to changes in mass are also evaluated using Eq. (2.16), where the nominal mass is m_0=1330 kg. Tables

2.8 and 2.9 summarize the influences of variations in the vehicle mass on peak directional responses, driver's steering effort and performance indices. A positive percent value represents increase in a response quantity with respect to that obtained with the nominal vehicle mass.

Table 2.8**:** Variation in peak directional responses of the selected driver models to variations in the vehicle mass (speed=20 m/s)

Driver Model	Mass (kg)	Sensitivity of the peak values of directional responses (%)			
		δ_F (deg)	$\dot{\delta}_F$ (deg/s)	Y_e (m)	a_y (m/s^2)
Model 1	997.5	-9.9	-10.0	-13.6	0.8
	1662.5	10.6	9.0	12.1	-0.7
Model 2	997.5	-7.2	-5.9	-10.1	4.1
	1662.5	8.3	9.7	12.7	-3.1
Model 3	997.5	-7.8	-8.0	-1.7	-0.5
	1662.5	7.1	6.6	1.5	0.4
Model 4	997.5	-8.5	14.6	-1.0	1.2
	1662.5	5.9	32.8	-3.6	-2.8
Model 5	997.5	-3.3	0.7	-36.4	3.7
	1662.5	2.9	4.3	-20.7	-3.8
Model 6	997.5	-5.6	-4.9	-23.8	4.4
	1662.5	5.9	4.3	24.0	-3.3
Model 7	997.5	-5.9	-21.4	-3.7	-0.4
	1662.5	9.9	11.5	1.5	2.1

Table 2.9**:** Variation in total performance index and its constituents of the selected driver models to variations in the vehicle mass (speed=20 m/s)

Driver Model	Mass (kg)	Sensitivity of performance measures (%)				
		J_t	J_Y	J_Ψ	J_δ	$J_{\dot{\delta}}$
Model 1	997.5	-20.0	-31.2	-17.4	-16.8	-18.5
	1662.5	22.1	32.3	28.6	18.5	20.4
Model 2	997.5	-20.1	-27.3	-6.6	-14.0	-13.7
	1662.5	26.1	35.6	14.0	17.5	17.1
Model 3	997.5	-4.4	-4.7	8.1	-13.8	-16.5
	1662.5	3.2	3.0	-1.1	13.4	14.4
Model 4	997.5	-7.0	-1.7	-3.6	-14.5	-17.3
	1662.5	14.8	1.2	5.5	13.1	100.3
Model 5	997.5	-12.2	-12.4	-11.7	-8.6	-3.6
	1662.5	22.1	23.1	12.0	8.5	3.3
Model 6	997.5	-40.0	-41.7	-34.7	-21.3	-4.6
	1662.5	56.1	63.4	-8.1	2.0	4.3
Model 7	997.5	-11.5	-32.7	6.5	-10.1	-5.4
	1662.5	17.7	13.5	19.1	19.0	18.3

The results show that increasing the vehicle mass invariably yields higher peak values of the steering angle (δ_F) and steering rate ($\dot{\delta}_F$), and thus the corresponding performance indices (J_δ and $J_{\dot{\delta}}$). Simulation results show greater sensitivity of the directional responses of vehicle to mass variations, when multi-point preview strategy with constant preview interval (models 5 and 6) is used, while the peak $\dot{\delta}_F$ and $J_{\dot{\delta}}$ are only slightly affected by the mass variations. Employing the single-point preview strategy with variable preview time greatly reduces the sensitivity of the path tracking performance to variations in the vehicle mass. This is evident from relatively lower percentage change in peak values of Y_e, J_Y and J_Ψ. The two-level model [45] also yields considerably lower sensitivity of peak path deviation (Y_e) to variations in the vehicle mass. The path tracking performance of this model, however, show relatively great sensitivity to variations in the vehicle mass, despite considering the variable preview time.

2.6.3 Influence of Understeer Coefficient of the Vehicle

The sensitivity of the vehicle responses, driver control parameters and performance indices to variations in the understeer coefficient of the vehicle are evaluated considering an understeer, oversteer and a neutral steer vehicle. The variations in the understeer coefficient (Table 2.3) are attained by varying the cornering stiffness of the front and rear tires. The understeer coefficients (K_{us}) for the oversteer, neutral and nominal vehicle are taken as -0.004, 0 and +0.004, respectively. The driver model parameters are identified through minimization of the reported performance index subject to limit constraints, defined in Eq. (2.17), while the forward speed is considered as 20 m/s. The identified model parameters and performance indices are summarized in Table 2.10 together with

the success or failure of each model considering the three vehicle handling scenarios. The variations in the lead time and the compensatory gains are also presented in Figure 2.14.

The simulation results again illustrate considerable variations in control parameters of the selected driver models with variations in the handling characteristics of the vehicle. Both the compensatory and single-point preview models exhibit higher position and orientation compensatory gains (K_y and K_Ψ) with increase in understeer coefficient of the vehicle, as shown in Figures 2.14(b) and 2.14(c), and Table 2.10. This suggests greater compensatory action demand when driving an understeer vehicle. The driver model based on the compensatory/anticipatory control strategy (model 7), however, yields substantially lower lateral position compensatory gain K_y with increasing values of K_{us} (Figure 2.14b). The orientation gain also increases for the understeer vehicle but is nearly constant for the over and neutral steer vehicles. Further, this driver model exhibits greatest sensitivity to variations in the understeer coefficient that is evident from substantial variations in its compensatory and anticipatory gains (K_y, K_ψ, K_C and K_a). The models results, however, do not show a definite trend in T_L with variations in understeer coefficient, as seen in Figure 2.14(a). The results obtained for the compensatory models in the absence of preview (models 1 and 2) show that the lead time constant T_L increase with the understeer coefficient, while the single- and two point preview strategies (models 3, 4 and 7) suggest an opposite trend. The models based on multi-point preview (models 5 and 6), however, assume a constant T_L. The compensatory and two-point preview models (models 1 and 7) exhibit greater lag time constant T_I with increasing in the understeer coefficient.

Table 2.10**:** Influences of variations in understeer coefficient of the vehicle on the identified driver model parameters and corresponding performance measures

	Driver Model	Understeer coefficient	Test Result	K_y[†] (rad/m)	K_Ψ (rad/rad)	K_C (rad.m)	K_a (rad.m)	T_L[‡] (s)	T_I[*] (s)	J_t	J_Y	J_Ψ	J_δ	$J_{\dot{\delta}}$
Compensatory models	Model 1	Oversteer	Pass	0.360	-	-	-	0.149	0.033	0.361	0.051	0.033	0.069	0.188
		Neutral	Pass	0.530	-	-	-	0.198	0.040	0.374	0.063	0.030	0.081	0.206
		Understeer	Pass	0.669	-	-	-	0.291	0.045	0.613	0.093	0.028	0.145	0.347
	Model 2	Oversteer	Pass	0.563	0.174	-	-	0.274	0.200	1.274	0.744	0.121	0.109	0.300
		Neutral	Pass	0.823	0.284	-	-	0.282	0.200	1.555	0.972	0.099	0.134	0.351
		Understeer	Pass	0.840	0.360	-	-	0.292	0.200	1.933	0.960	0.103	0.240	0.631
Preview compensatory models	Model 3	Oversteer	Pass	0.013	-	-	-	1.144	0.300	1.442	1.370	0.055	0.014	0.003
		Neutral	Pass	0.016	-	-	-	1.122	0.300	1.456	1.375	0.058	0.020	0.004
		Understeer	Pass	0.021	-	-	-	1.112	0.300	1.503	1.404	0.058	0.034	0.007
	Model 4	Oversteer	Pass	0.038	-	-	-	0.601	0.200	0.235	0.148	0.043	0.026	0.017
		Neutral	Pass	0.052	-	-	-	0.545	0.200	0.265	0.149	0.039	0.047	0.028
		Understeer	Pass	0.071	-	-	-	0.540	0.200	0.301	0.153	0.031	0.087	0.029
	Model 5	Oversteer	Pass	0.028[†]	0.704	-	-	2.000	0.000	0.311	0.286	0.009	0.014	0.001
		Neutral	Pass	0.028[†]	0.705	-	-	2.000	0.000	0.404	0.360	0.017	0.025	0.001
		Understeer	Pass	0.028[†]	0.745	-	-	2.000	0.000	0.935	0.861	0.033	0.038	0.002
	Model 6	Oversteer	Pass	0.028[†]	0.763	-	-	2.000	0.000	0.330	0.295	0.008	0.025	0.002
		Neutral	Pass	0.028[†]	0.704	-	-	2.000	0.000	0.448	0.387	0.017	0.041	0.002
		Understeer	Pass	0.028[†]	0.705	-	-	2.000	0.000	1.100	0.978	0.047	0.073	0.003
Compensatory Anticipatory	Model 7	Oversteer	Pass	1.3E-03	0.737	0.465	1.025	0.230	0.101	0.141	0.030	0.013	0.025	0.074
		Neutral	Pass	8.6E-04	0.807	0.475	0.966	0.229	0.113	0.162	0.033	0.011	0.041	0.078
		Understeer	Pass	5.0E-05	0.930	0.260	1.488	0.224	0.121	0.222	0.041	0.009	0.070	0.101

[†] K_y, the compensatory gain, for the multi-point preview models (models 5 and 6) is reported corresponding to the first preview point.

[‡] T_L represents the lead time constant (model 1) and summation of individual lead times (model 2), preview time in models employing only preview (models 4, 5, 6 and 7), and lead and preview time (model 3)

[*] The lag time, T_I, in models 2, 3 and 4 is the sum of first-order lag time and processing delay time τ_p, both being constant.

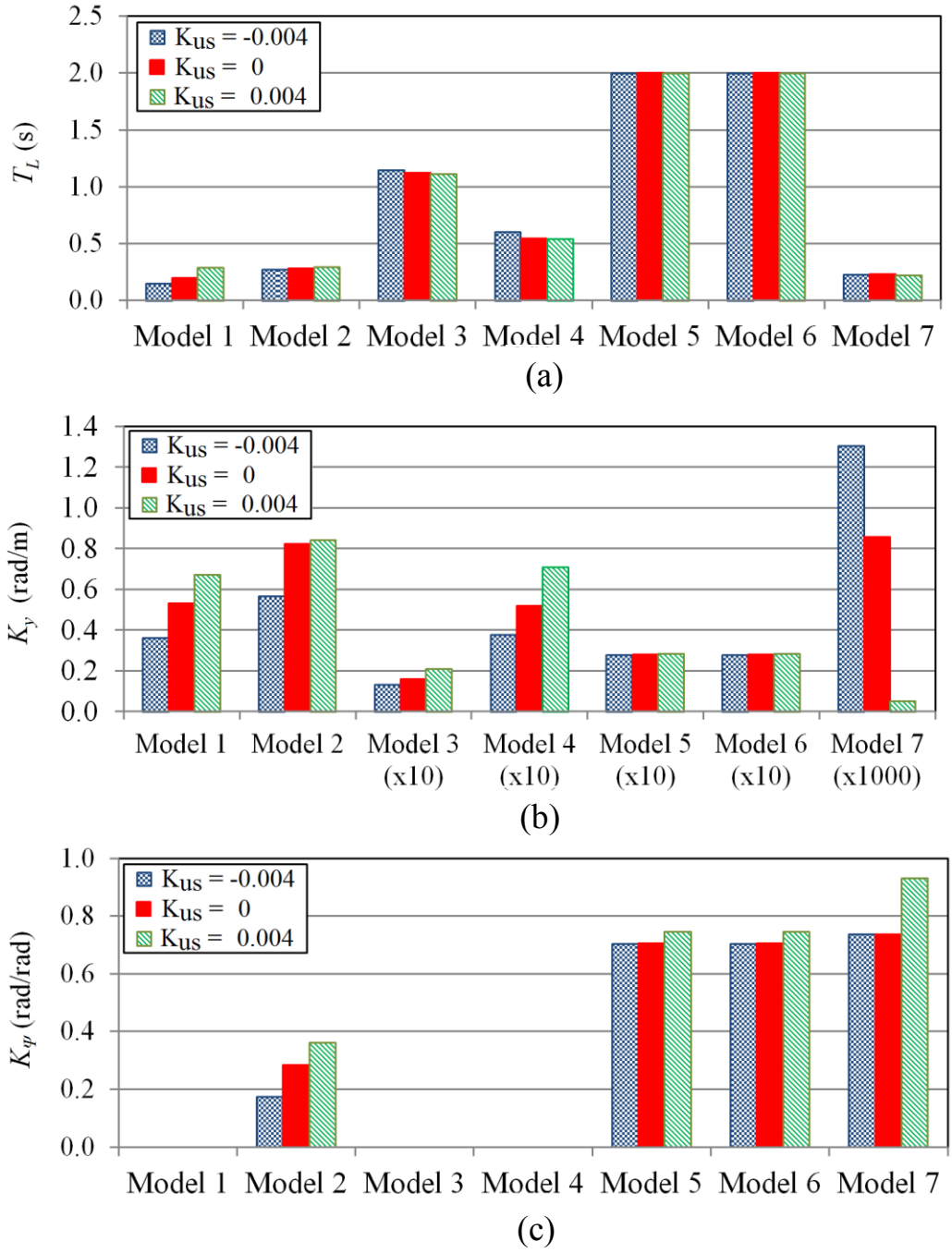

Figure 2.14: Comparison of (a) the lead time constant; (b) lateral position gain constant; and (c) orientation gain constant of selected driver models subject to variations of understeer coefficient (speed= 20 m/s)

The selected driver models are further evaluated considering the identical performance index, defined in Eq. (2.10). Table 2.10 also presents the values of total performance

index and its constituents. The results suggest that a vehicle with oversteer tendency yields lower total performance index J_t, path tracking performance J_Y, and steering effort indices (J_δ and $J_{\dot{\delta}}$), irrespective of the modeling strategy. The compensatory model 1 [17], without the driver preview and time delays can effectively track the desired path by converging to lower time lag at the selected forward speed (20 m/s). The compensatory models (models 1 and 2) in the absence of preview process, however, yield the greatest steering effort (J_δ and $J_{\dot{\delta}}$). The use of multi-point preview strategy (models 5 and 6), on the other hand, yields the lowest steering effort demands.

The simulation results suggest that employing the human driver preview process would help enhance the path tracking performance and reduce the steering effort demand, as observed for variations in the vehicle mass and vehicle speed. The path tracking performance and steering effort of the single-point preview control models (models 3 and 4) can be further enhanced through two- or multi-point preview strategies. The multi-point preview strategy coupled with internal vehicle model path prediction strategy yields least demand on the driver's steering effort. Consideration of a constant preview interval, however, yields a higher level of path deviation. The compensatory/anticipatory driver model [45] (Model 7) results in superior path tracking performance with over 50% lesser steering demand compared to the compensatory models. From the results, it is evident that two-point preview and internal vehicle model path prediction strategies yield most effective vehicle control with variations in its handling characteristics.

The sensitivity of the peak directional responses of the vehicle and driver's steering effort, and performance indices to variations in the K_{us} are evaluated using Eq. (2.16) and summarized in Tables 2.11 and 2.12, respectively. A positive percent value in the tables

represents an increase in a response quantity with respect to the nominal understeer vehicle (K_{us} = 0.004). As it would be expected, the results show that decreasing the understeer coefficient (approaching neutral and oversteer tendency) invariably lowers the peak steering angle (δ_F) and peak steering rate ($\dot{\delta}_F$), and the corresponding performance indices (J_δ and $J_{\dot{\delta}}$).

Table 2.11**:** Variation in the peak directional responses of the selected driver models to changes in the understeer coefficient (speed=20 m/s)

Driver Model	Under-steer coefficient	Sensitivity of the peak values of directional responses (%)			
		δ_F (deg)	$\dot{\delta}_F$ (deg/s)	Y_e (m)	a_y (m/s$_2$)
Model 1	Oversteer	-22.4	-18.5	-6.3	7.9
	Neutral	-19.6	-22.0	-8.2	6.3
Model 2	Oversteer	-33.6	-32.0	-15.6	-6.5
	Neutral	-25.3	-26.1	0.1	-0.6
Model 3	Oversteer	-34.5	-34.4	-1.3	0.8
	Neutral	-24.4	-24.3	-1.1	0.2
Model 4	Oversteer	-47.3	-29.4	-2.0	-7.9
	Neutral	-27.1	-8.2	-1.6	-3.6
Model 5	Oversteer	-33.4	-18.2	-55.3	19.1
	Neutral	-16.3	-6.6	-53.7	12.7
Model 6	Oversteer	-33.1	-15.1	-29.4	20.7
	Neutral	-17.4	-5.7	-35.4	14.2
Model 7	Oversteer	-39.9	-32.5	-15.3	0.9
	Neutral	-24.1	-31.7	-14.5	-0.8

The driver model employing single-point preview strategy (models 3 and 4) [30,40] yield substantially lower sensitivity of peak Y_e , J_t and J_Y, while the peak steering angle and steering rate and corresponding performance indices (J_δ and $J_{\dot{\delta}}$) vary substantially to satisfy the path tracking requirements. The simulation results further show that multi-point preview models [67,68] exhibit relatively greater sensitivity of peak path deviation Y_e, and the position and orientation performance indices (J_Y and J_Ψ) to variations in the understeer coefficient. This can be mostly attributed to the constant preview time assumption of the multi-point preview models.

Table 2.12**:** Variation in the total performance index and its constituents of the selected driver models to changes in the understeer coefficient (speed=20 m/s)

Driver Model	Understeer coefficient	Sensitivity of the performance indices (%)				
		J_t	J_Y	J_Ψ	J_δ	$J_{\dot{\delta}}$
Model 1	Oversteer	-41.1	-45.5	19.8	-52.6	-45.7
	Neutral	-38.9	-32.5	7.6	-43.9	-40.5
Model 2	Oversteer	-34.1	-22.5	17.0	-54.5	-52.5
	Neutral	-19.6	1.3	-4.8	-44.2	-44.4
Model 3	Oversteer	-4.0	-2.4	-5.0	-58.2	-55.7
	Neutral	-3.1	-2.1	0.4	-42.7	-42.7
Model 4	Oversteer	-21.9	-3.4	39.1	-70.0	-42.0
	Neutral	-11.9	-2.6	26.8	-46.0	-4.1
Model 5	Oversteer	-66.7	-66.8	-72.4	-63.0	-35.0
	Neutral	-56.8	-58.2	-49.0	-34.6	-15.3
Model 6	Oversteer	-70.0	-69.8	-81.9	-66.2	-31.9
	Neutral	-59.3	-60.4	-63.4	-43.0	-14.4
Model 7	Oversteer	-36.2	-27.5	49.1	-64.4	-27.3
	Neutral	-26.8	-21.3	24.5	-41.4	-23.1

2.7 Summary

Considering different driving conditions and vehicle design parameters, directional responses and performance measures of the selected models have been examined in terms of: (i) the preview process; (ii) prediction strategy; and (iii) the limb dynamics. The results can be summarized as below:

(i) The compensatory driver models in the absence of human preview (models 1 and 2) exhibit adverse path tracking performance and increase steering effort demand compared to the models that employ previewed path information, particularly at the higher driving speed of 70 m/s. Further, the directional responses and performance measures of these models are most significantly influenced by variations in the driving speed.

(ii) Integration of the path prediction and path preview strategies can substantially enhance the path tracking performance with reduced steering effort of the driver model. The path prediction using 'internal vehicle model' strategy (model 4) yields enhanced path tracking performance compared to the second-order path predictor (model 3).

(iii) A multi-point preview strategy (models 5 and 6) can significantly reduce the steering effort demand on the driver, while it yields greater path deviation compared to the models employing either single- and two-point preview strategy. This maybe in-part attributed to constant preview time considered in the model and in-part to large size of path coordinates array. Further, the peak path deviation

and directional responses of these models are most significantly affected by variations in the mass and understeer coefficient of the vehicle.

(iv) Considering a two-point preview strategy yields considerable improvement in the total performance index and its components related to path deviation and heading error (J_Y and J_Ψ) of the coupled driver-vehicle system in comparison with the compensatory and preview-compensatory models (model 1 to 6), for the ranges of maneuvers vehicle mass and understeer coefficient considered in this study.

(v) Consideration of limb dynamics (model 6) helps to improve the path tracking performance of the vehicle at the higher speed of 70 km/h and for the lighter vehicle. The muscle dynamics at lower driving speeds, however, tends to deteriorate the path tracking performance due to additional muscular delay.

2.8 Conclusion

Relative performance of different deriver models coupled with a two DoF yaw-plane vehicle model are evaluated for a range of operating speeds and vehicle parameters. The driver models based on different preview, prediction, control strategies and feedback cues were selected and re-formulated for analyses under a standardized double lane-change maneuver. Directional responses and different performance measures of the selected models are thoroughly examined so as to assess the contributions of different control strategies and to identify the most effective strategy for application to heavy vehicles. The results suggested that consideration of path preview/prediction by the human driver yields significant path tracking enhancement and reducing steering effort demand. The results further showed that the reported models exhibit their validity only in the vicinity of the conditions used to identify model parameters. The coupled driver-vehicle models are most significantly affected by the speed, vehicle mass and understeer coefficient.

A two-point preview strategy can provide most effective path tracking performance over a wide range of variations in speed and vehicle parameters. A two-point preview coupled with the ‘internal vehicle model’ path predictor will thus be considered in the

subsequent chapters to formulate the human driver model in conjunction with a heavy vehicle model.

CHAPTER 3

EXPERIMENTAL CHARACTERIZATION OF DRIVER CONTROL PROPERTIES

3.1 Introduction

A number of field-measurement and simulator-based studies have been conducted to objectively characterize human driving factors, which have been subsequently applied to driver control models [10,14,46,47,54,71,91,108,118]. These studies, however, report wide variations in the measured data, mostly due to variations in the experimental conditions, measurement methods and subject populations [9,54]. A review of reported ranges of the driver control measures, such as compensation gain, preview and response time, suggests that the identified ranges are too broad to be considered reliable. Additional experimental studies under carefully controlled but representative conditions are thus essential in order to accurately characterize the human driving control properties.

In an attempt to characterize driver control properties, this study aims to identify the influences of driving experience and vehicle forward speed on control characteristics of the vehicle driver using a limited-motion driving simulator. The measurements were performed for four different driving tasks, namely, a slalom maneuver [136,137], abrupt braking, obstacle avoidance and a standard double lane change maneuver [127] subject to incremental variations in driving speed. The data were analyzed to identify different control properties of the human drivers as functions of their driving experience and forward speed of the vehicle. These included the driver reaction time, and magnitude and rate of steering effort of the human driver. Although the main objective of this

dissertation research is to identify and characterize the human driver control actions in conjunction with an articulated heavy vehicle, the experiments were limited to an automobile driving simulator that was available for the study. It was thus assumed that the measured driving control actions, such as steering response time, would also be applicable for formulating a coupled driver-articulated vehicle model.

3.2 Driving Simulator

A limited-motion driving simulator has been used for objective measurements of driver's responses in conjunction with a single-unit vehicle under different selected maneuvers. The driving simulator, shown in Figure 3.1, designed to simulate the visual feedbacks and limited dynamic motions of an automobile, comprised: (i) an open cabin with the driver seat and center console of an actual car; (ii) three 52-inches LCD display arranged in a semi-circle formation in front of the driver's seat to provide essential visual cues; (iii) a three-axis motion system integrated within the driver's seat to provide acceleration cues and engine vibration and the road texture feedbacks as a function of the vehicle forward speed and road surface; and (iv) an automatic transmission. The steering wheel was equipped with a dynamic electrical load unit that provided a tactile sensory feedback simulating the steering torque feedback. Rear and side view mirrors were simulated through window inserts within the central and side screens.

Figure 3.1: Open cabin of the limited-motion driving simulator

3.2.1 Experiment Procedures

A total of 16 subjects (12 male; 4 female) participated in the driving simulator experiment, ranging in age from 22 to 38 years (mean=29.5 yrs; standard deviation=3.6 yrs) with different levels of driving experience ranging from less than 1 year to more than 15 years (mean=7 yrs; standard deviation=4.7 yrs). Table 3.1 summarizes the driving experience of the participants.

Table 3.1: List of subject information

Subject	Gender	Age	Years of driving	Description
1	Male	33	4	Experience in working with driving simulator
2	Male	32	15	Everyday driver
3	Male	26	7	Never drove with an automatic transmission
4	Male	27	3	Tended to drive very fast
5	Male	29	5	Occasional driver
6	Female	24	2.5	Everyday driver
7	Male	30	8	Occasional driver
8	Female	33	6	Occasional driver
9	Male	39	15	Discontinued the third trial due to simulator sickness
10	Male	29	10	Occasional driver
11	Male	31	12	Everyday driver
12	Male	29	9	Everyday driver
13	Female	26	2	Occasional driver
14	Male	27	0.5	Experienced in monitor-based games
15	Male	29	11	Experience in working with driving simulator
16	Female	28	2	Every day driver

The experiments were performed in four different phases, which were conducted in a sequential manner. The initial phase involved familiarization with the simulator and controls, where each participant was advised to perform random driving trials for a period of 10 minutes. During the familiarization process, each participant was asked if he/she felt symptoms of simulator sickness [138]. The participants, who felt such symptoms, were not permitted to continue with the experiment. In the second phase, each participant was asked to perform a slalom maneuver at three different driving speeds (30, 50 and 70 km/h). The data acquired in this phase was used to classify relative driving skills of the

participants. Each participant in the subsequent phase was asked to perform vehicle driving at the same 3 speeds, while sudden obstacles were displayed in a random manner. The participants were required to perform sudden braking and path-change maneuvers, and the braking and steering actions were recording to determine their reaction times. In the final phase, the participants performed a double-lane change maneuver at the same 3 speeds in clear and foggy road conditions. The steering profile and the path coordinates were recorded to determine path deviation, and the magnitude of steer angle and the steering rate. Participants were instructed to drive normally while maintaining a pre-defined steady speed throughout the selected maneuver. In order to investigate variability and repeatability of the experiments, each driving test was repeated three times. The test sessions were scheduled to permit the participants to take a short break between successive trials.

During each driving task, several vehicle states (i.e., forward speed, longitudinal and lateral path coordinates, and vehicle orientation) together with time-history of the steering input were measured. The data were subsequently analyzed to derive following dependent variables:

(1) steering and braking response times;
(2) peak steering angle and steering rate;
(3) crest factors of steer angle and steering rate;
(4) steering profile area;
(5) peak deviation in speed from the pre-defined forward speed; and
(6) peak deviation in speed from the average forward speed

The measured data were examined to identify influences of the driver's experience and vehicle forward speed on different control and performance measures. The variability in the measured data were also evaluated in terms of intra-subject variability, inter-subject variability, and the standard error. The standard error was estimated from:

$$\sigma_{\bar{x}} = \frac{\sigma}{\sqrt{n}} \tag{3.1}$$

where σ is the standard deviation (SD) of the data acquired for the sample group and n is the number of participants in the sample group.

A single-factor analysis of variance (ANOVA) was also performed to evaluate statistical significance of the main factors (driver's experience and forward speed) on the measured responses. A factor was considered significant when $p<0.05$.

3.2.2 Identification of Outliers

The data acquired with different participants revealed large variations in the path coordinates, steering and braking reaction times, and path deviations. These were attributed to wide variations in driving experiences and skills of the selected participants. The degree of attention of the participants and variations in the lead times associated with obstacles displays also contributed to the variability. While the variations were considered similar to those reported in other experimental studies [14,54,91,94,97], attempts were made to identify and remove the outliers during the data analysis. The outliers were determined on the basis of the data dispersion with respect to the average value. Owing to different roles of various contributory factors, the data outliers in each driving test were identified using different methods. The majority of the response measures revealed good correlations with the forward speed and the participant's driving experience. In these cases, a data was considered an outlier, when its removal resulted in notable gain in the correlation coefficient (r^2). In the case of braking and steering response times, which primarily depended upon the vehicle speed, a data beyond one standard deviation of the mean was considered an outlier.

The measured data acquired under the double-lane change maneuver, invariably, revealed considerably less deviations in peak steer angle and steer rate during the second and third repeated trials compared to those observed during the initial trial. This was in-part attributed to enhanced familiarity and predictive control of the driver in response to the expected visual cues in a simulator setting. In this case, the data acquired during the final trial were thus excluded from the analysis.

3.3 Skill Classification

During a normal driving task, the vehicle drivers are required to perform a number of simultaneous control actions such as path planning, path tracking and speed control [139]. Such actions are in-part related to human driving skill and experience [14,140,141]. In the context of a driving task, the skill is defined as the driver's ability to track a desired path at or near a pre-determined forward speed, while rejecting various environmental disturbances [14,139]. It is suggested that drivers with different levels of driving skill may perform the same maneuver with different path tracking performance and steering control actions [140,141]. Classifying the driving skill of individual drivers, however, is a highly challenging task. A methodology to classify drivers in a categorical form (i.e., experienced, typical, and novice) is proposed on the basis of the measured steering and path-following performance during the slalom maneuvers. The method may yield important guidance on considerations of the driving skill in the design process of driver assistance systems.

The driving skill may be described by five performance measures during a slalom maneuver: (i) maneuver accomplishment, which is assessed by the number of cones ‘hit’ or ‘missed’ by the participant during the maneuver [14]; (ii) peak steering angle and its

rate during the maneuver [131]; (iii) crest factors of steering angle and its rate during the maneuver; (iv) steering profile area during the maneuver; and (v) the peak deviation in speed from both the target speed and the average speed [140]. The simulator was programmed to generate a standard slalom course, as shown in Figure 3.2 [136,137]. Each participant was asked to perform the maneuver at three steady speeds (30, 50 and 70 km/h). The path coordinates and steer angle time-history was recorded during each trial. The path-coordinates data were analyzed to identify the number of 'hit' or 'missed' cones during the maneuver. It was noted that a number of subjects could not maintain the higher target speed of 70 km/h. These subjects opted to complete the maneuver at a relatively lower speed. In this case, the speed deviation from the chosen mean speed and the target speed was considered for the purpose of skill classification.

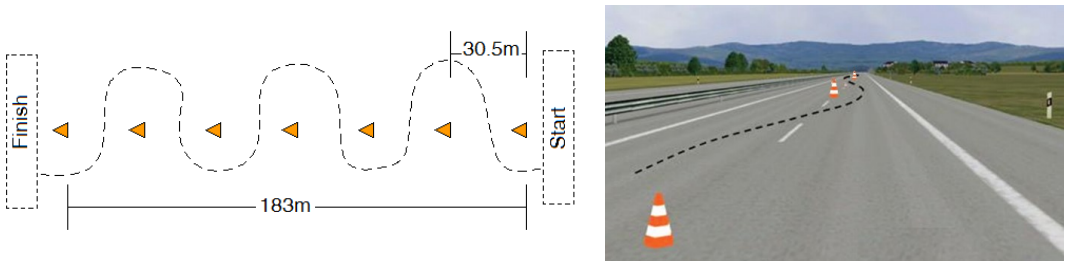

Figure 3.2: The standard slalom course used in the experiments (◀ - cones)

3.3.1 Maneuver Accomplishment

Table 3.2 summarizes the total number of cones 'hit' or 'missed' by each participant during all the three slalom course trials corresponding to each target forward speed. The data show that nearly all the participants successfully performed the maneuver at 30 and 50 km/h. The data obtained at these speeds, therefore, cannot provide a sound basis for classifying the driving skill. The number of 'hit' or 'missed' cones at the higher forward speed of 70 km/h, however, revealed some correlations with the driving experience, as shown in Figure 3.3. The results suggest that the participants with higher driving

experience ‘hit’ or ‘missed’ relatively fewer cones at 70 km/h. In the figure, the identified outliers are presented with black dots together with corresponding subject numbers. The data obtained for subject #14 (0.5 years of driving experience) was considered an outlier. The superior performance of this subject was attributed to his extensive experience with monitor-based games. This data was thus excluded from the subsequent analyses.

The number of ‘hit’ or ‘missed’ cones in a slalom maneuver at the higher speed of 70 km/h may thus be employed to classify the participants’ driving skill. A classification system was designed to categorize the skill as novice, when 3 or more cones are ‘hit’ or ‘missed’, average with 1 to 3 cones ‘hit’ or ‘missed’, and experienced when none of the cones are ‘hit’ or ‘missed’.

Table 3.2: Total number of ‘hit’ or ‘missed’ cones during all trials of slalom maneuvers

Subject ID	Driving experience (yrs)	Speed (km/h)		
		30	50	70
1	4	0	0	2
2	15	0	0	0
3	7	0	0	2
4	3	0	1	3
5	5	0	0	2
6	2.5	0	0	4
7	8	0	0	0
8	6	0	0	0
9	15	0	0	0
10	10	0	0	0
11	12	0	0	0
12	9	0	0	0
13	2	0	0	0
14	0.5	0	0	1
15	11	0	0	0
16	2	0	0	2

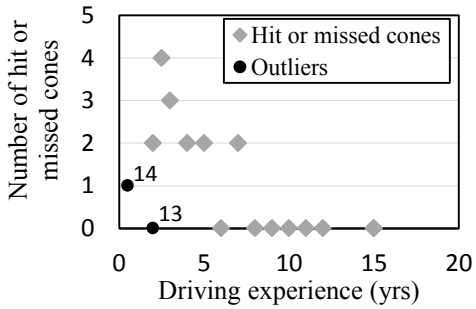

Figure 3.3: Correlations of number of hit or missed cones with the driving experience during slalom maneuvers at 70 km/h

3.3.2 Peak Steer Angle and Steer Rate

Steering input is the primary control action of the driver to track the desired path, maintain central lane position and to avoid road obstacles. It has been suggested that the magnitude and rate of steering input correlate with the driver's imposed physical and mental workload [16,17,78,131,142]. The reported studies have shown that experienced drivers generally perform the driving task with relatively less steering effort than the novice drivers [131]. The lower value of the physical and mental workloads, however, do not necessarily yield lower path tracking performance or responsiveness to the driving task. Conversely, this implies an effective level of directional control of the vehicle and driver's compensation with lesser driving effort [131,143]. Tables 3.3 and 3.4 summarize the peak values of front wheels steer angles ($\delta_{F,max}$) and the steering rates ($\dot{\delta}_{F,max}$), respectively, measured during the slalom maneuvers at three different forward speeds. The tables also present the mean peak values for the maneuver conducted at each speed.

Table 3.3: Peak front wheels steer angle measured during constant speed slalom maneuvers

Subject	Driving experience (yrs)	Peak steer angle (deg)											
		30 km/h				50 km/h				70 km/h			
		Trial 1	Trial 2	Trial 3	mean	Trial 1	Trial 2	Trial 3	mean	Trial 1	Trial 2	Trial 3	Mean
1	4	6.46	6.70	-	6.58	-	7.57	-	7.57	11.53	19.90	-	15.72
2	15	4.32	4.02	-	4.17	4.39	5.32	-	4.86	10.41	7.96	-	9.18
3	7	6.70	5.46	-	6.08	5.65	5.21	-	5.43	24.01	7.08	-	15.54
4	3	7.20	6.34	-	6.77	-	9.64	-	9.64	27.78	17.45	-	22.61
5	5	8.83	6.32	-	7.58	9.64	6.96	-	8.30	28.00	8.21	-	18.11
6	2.5	12.09	6.39	-	9.24	11.84	8.77	-	10.30	19.25	27.78	-	23.52
7	8	6.45	6.51	-	6.48	9.34	6.26	-	7.80	-	14.16	-	14.16
8	6	6.84	8.09	-	7.46	10.83	6.46	-	8.65	28.00	9.14	-	18.57
9	15	5.90	4.58	-	5.24	7.46	4.02	-	5.74	6.34	6.96	-	6.65
10	10	6.21	5.02	4.83	5.35	6.71	6.01	4.27	5.66	-	6.15	5.90	6.02
11	12	5.46	4.01	5.15	4.87	7.90	3.70	4.19	5.27	-	5.33	5.88	5.61
12	9	7.83	6.84	6.51	7.06	9.58	8.34	7.64	8.52	11.85	13.40	15.31	13.52
13	2	6.71	5.15	6.21	6.02	10.27	4.63	6.26	7.05	7.95	5.46	10.41	7.94
14	0.5	5.33	5.27	-	5.30	5.15	6.01	-	5.58	10.72	11.21	-	10.96
15	11	5.70	4.38	4.69	4.92	7.14	7.15	5.40	6.56	9.58	7.45	8.15	8.39
16	2	6.26	7.26	5.96	6.49	6.96	7.40	6.32	6.89	12.10	19.47	12.10	14.55

- : subjects did not successfully complete or perform the trial

Table 3.4: Peak rate of steering input measured during constant speed slalom maneuvers

Subject	Driving experience (yrs)	Peak rate of steering input (deg/s)											
		30 km/h				50 km/h				70 km/h			
		Trial 1	Trial 2	Trial 3	mean	Trial 1	Trial 2	Trial 3	Mean	Trial 1	Trial 2	Trial 3	Mean
1	4	7.74	8.91	-	8.32	-	12.31	-	12.31	14.75	16.19	-	15.47
2	15	6.27	6.93	-	6.60	8.22	9.88	-	9.05	13.73	12.75	-	13.24
3	7	9.65	7.61	-	8.63	12.00	8.46	-	10.23	15.18	12.18	-	13.68
4	3	10.20	8.07	-	9.13		14.37	-	14.37	25.00	19.36	-	22.18
5	5	11.48	7.21	-	9.35	14.56	10.41	-	12.48	17.19	11.71	-	14.45
6	2.5	15.12	8.74	-	11.93	17.01	15.25	-	16.13	23.71	31.10	-	27.41
7	8	8.69	7.70	-	8.19	14.32	10.24	-	12.28	-	16.00	-	16.00
8	6	9.84	10.73	-	10.28	16.04	11.07	-	13.55	26.42	13.11	-	19.77
9	15	8.75	6.88	-	7.81	9.60	7.94	-	8.77	12.12	10.44	-	11.28
10	10	8.50	7.35	6.43	7.43	13.05	11.09	8.63	10.92	-	11.47	10.14	10.80
11	12	8.85	4.74	4.63	6.08	12.27	5.80	6.50	8.19	-	10.03	8.84	9.43
12	9	10.62	8.27	7.75	8.88	15.22	11.42	10.66	12.43	13.81	16.23	14.18	14.74
13	2	9.11	7.47	9.79	8.79	17.24	8.99	10.30	12.18	13.14	10.67	12.91	12.24
14	0.5	7.18	8.04	-	7.61	11.14	9.37	-	10.26	15.38	14.21	-	14.80
15	11	7.26	6.37	6.04	6.56	10.77	11.81	9.44	10.68	13.08	11.18	10.89	11.72
16	2	8.93	9.12	8.49	8.85	11.94	11.87	10.73	11.51	17.09	20.55	11.66	16.43

- : subjects did not successfully complete or perform the trial

Figures 3.4 and 3.5 show the variations in mean peak steering angle and the steering rate with the driving experience of the participants for the three selected target speeds. In order to identify the outlier data, Figure 3.4 shows variations in coefficient of variances (CoV) and correlation coefficient (r^2) of peak steering angle, when data corresponding to a certain subject was removed, presented with black dots together with corresponding subject numbers in the figure. A data was considered an outlier, when its removal resulted in notable gain in the r^2, as shown in these figures. Analyses of the data for peak steering angle suggested that exclusion of the data acquired for subjects #13, 14 and 16 considerably improved the correlation coefficient, while r^2 enhanced slightly or reduced by removing data for a subject in addition to the previous outliers (subject #6 at 30 km/h, subject #12 at 50 km/h and subject #1 at 70 km/h). Based upon examinations of all the data during slalom maneuvers, the recorded data for subjects #13, 14 and 16 are identified as outliers and excluded from subsequent analyses.

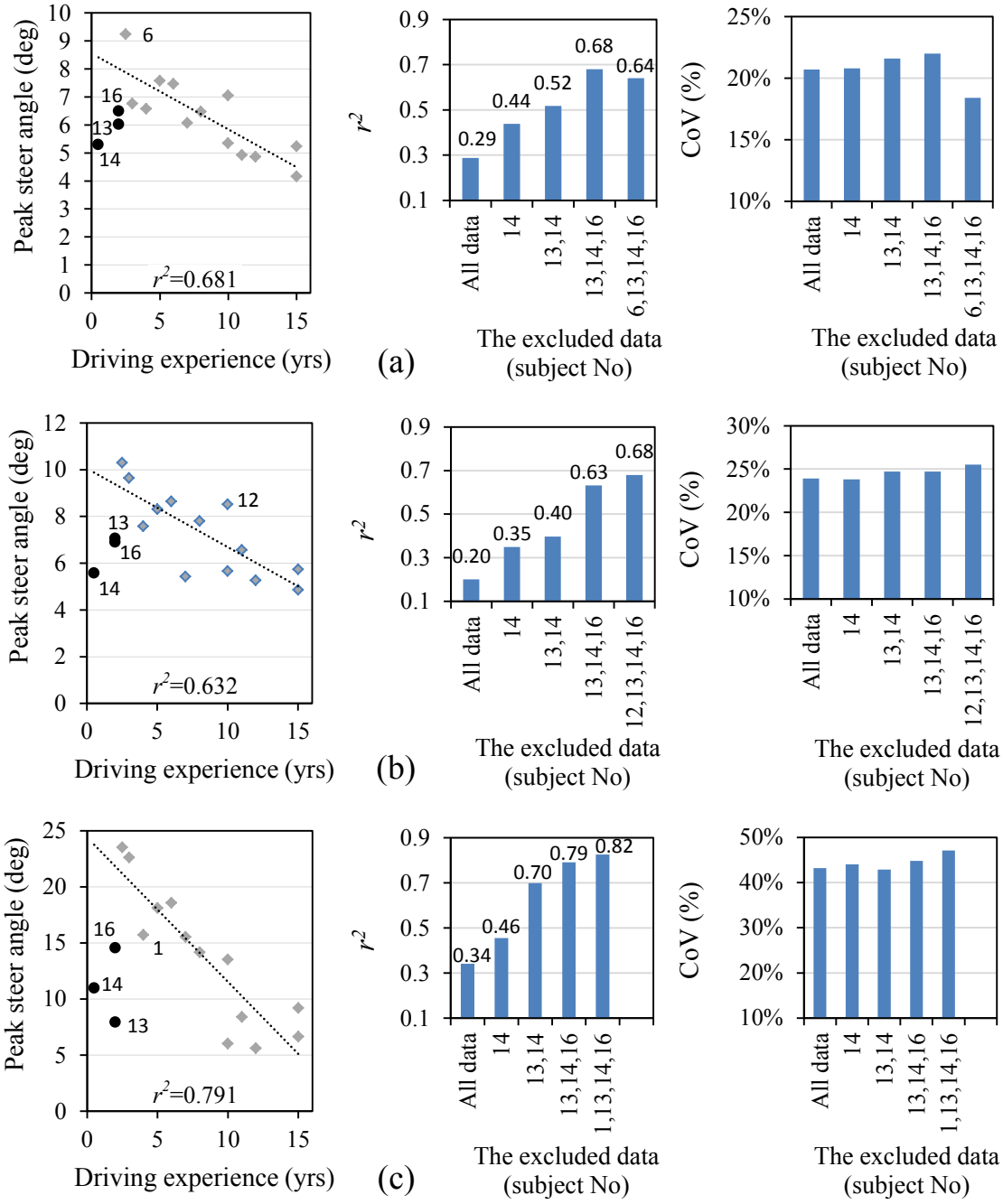

Figure 3.4: Correlations of mean peak steer angle, and r^2 values and variations in CoV when data corresponding to a certain subject was removed during slalom maneuver slalom at: (a) 30 km/h, (b) 50 km/h, and (c) 70 km/h

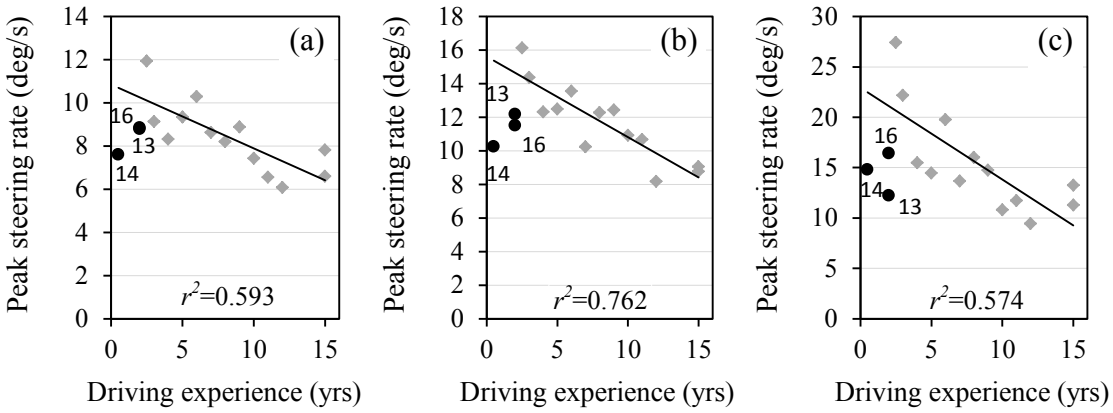

Figure 3.5: Correlations of mean peak steer rate during slalom maneuvers at: (a) 30 km/h, (b) 50 km/h, and (c) 70 km/h; r^2 values are shown upon removal of outliers

The measured data excluding the identified outliers suggest definite correlations between the peak steer angle and its rate with the driving experience. Furthermore, the mean peak steer angle and rate increase substantially when forward speed is increased to 70 km/h, while the increase is relatively small when speed is increased from 30 to 50 km/h. This suggests higher steering effort and mental workload demand for the drivers at higher speeds, as it would be expected. It is shown that the peak steer angle and rate decrease with increasing driving experience of the participants suggesting lower physical workload of experienced drivers compared with novice drivers for the same driving task. The measured data generally show improved steering performance of the participants during repetitive driving tasks. The peak values during the second and third trials thus tend to be lower than those measured during the initial trial

The peak steering angles and rates measured during the 70 km/h maneuver are applied to classify the driving skills as: 'novice' ($\delta_{F,max} > 15^{\circ}; \dot{\delta}_{F,max} > 20^{\circ}/s$), 'average' ($10^{\circ} \leq \delta_{F,max} \leq 15^{\circ}; 14^{\circ}/s \leq \dot{\delta}_{F,max} \leq 20^{\circ}/s$) and 'experienced' ($\delta_{F,max} < 10^{\circ};\ \dot{\delta}_{F,max} < 14^{\circ}/s$). These classifications were found to be consistent with those defined on the basis of number of 'missed' cones during the slalom maneuvers, as discussed in section 3.3.1.

3.3.3 Steer Angle and Steer Rate Crest Factors

Investigation of the peak steer angle and its rate can stress only a critical instant in steering response of the driver, while steering input is a continuous control action. This emphasizes introducing a response measure that helps to examine variation of the driver's steering responses throughout the desired driving task. The crest factors of the steering angle C_δ and rate of steering input $C_{\dot{\delta}}$ have thus employed in this study. The crest factor is a non-dimensional parameter and defines as the peak value divided by RMS value of a response measure. Tables 3.5 and 3.6 summarize the mean crest factors of the magnitudes and rates of steering input during the constant speed slalom maneuvers together with the mean values for all trials, respectively. The tables also summarize the RMS and peak values of the steer angle and steering rate for the three selected speeds. Figure 3.7 show the variations in crest factors of steering angle and the steering rate with the driving experience of the participants for the three selected target speeds (30, 50 and 70 km/h). In order to identify the outlier data, these figures show variations in r^2 when data corresponding to a certain subject was removed. In the figures, the identified outliers, whose removal resulted in notable gain, are presented with black dots together with corresponding subject numbers.

The measured data excluding the identified outliers suggest that crest factors of steer angle C_δ notably increase with driving experience at 50 and 70 km/h, while the increase is relatively small at lower speed of 30 km/h. Furthermore, the steer angle crest factors are substantially lower at 70 km/h compared to those at lower speeds. Almost same results can be seen for the steering rate crest factors $C_{\dot{\delta}}$. Furthermore, the result acquired during the slalom maneuvers suggest that both the RMS and peak values of the steer

angle and steering rate are decreased with increasing driving experience of the participants. This again suggests higher steering effort of the drivers at higher speeds and lower physical and mental workload demands of experienced drivers compared with novice drivers for the same driving task. Since both the peak values and RMS value and parameters present the almost same trend for variations in driving experience, a strong correlation between the crest factor and driving experience cannot be provided.

The experimental result thus suggest that the crest factors of steer angle and its rate during the slalom maneuver at 70 km/h alone may be applied to classify driving skill as: 'novice' $(C_\delta < 0.3; C_{\dot{\delta}} < 0.17)$, 'average' $(0.3 \leq C_\delta \leq 0.5;\ 0.17/s \leq C_{\dot{\delta}} \leq 0.22)$ and 'experienced' $(C_\delta > 0.5;\ C_{\dot{\delta}} > 0.22)$. These classifications were found to be consistent with those defined on the basis of peak values of the steer angle and steering rate even though the two measures exhibit opposing trends.

Table 3.5: Crest factor of the steer angle measured during slalom maneuvers

Subject	Driving experience (yrs)	Crest factor of steering angle								
		30 km/h			50 km/h			70 km/h		
		Peak	RMS	Mean crest factor	Peak	RMS	Mean crest factor	Peak	RMS	Mean crest factor
1	4	6.58	10.32	0.64	7.57	12.37	0.61	15.72	75.16	0.21
2	15	4.17	4.85	0.86	4.86	5.63	0.86	9.18	25.30	0.36
3	7	6.08	6.15	0.99	5.43	7.47	0.73	15.54	52.93	0.29
4	3	6.77	8.36	0.81	9.64	15.26	0.63	22.61	149.5	0.15
5	5	7.58	10.76	0.70	8.30	13.25	0.63	18.11	44.28	0.41
6	2.5	9.24	12.17	0.76	10.30	19.76	0.52	23.52	161.9	0.15
7	8	6.48	7.25	0.89	7.80	10.42	0.75	14.16	42.73	0.33
8	6	7.46	9.71	0.77	8.65	17.03	0.51	18.57	78.43	0.24
9	15	5.24	5.37	0.98	5.74	5.87	0.98	6.65	10.81	0.62
10	10	5.35	6.97	0.77	5.66	8.79	0.64	6.02	11.24	0.54
11	12	4.87	3.08	1.58	5.27	4.91	1.07	5.61	8.03	0.70
12	9	7.06	9.21	0.77	8.52	15.50	0.55	13.52	47.00	0.29
13	2	6.02	6.64	0.91	7.05	10.39	0.68	7.94	16.56	0.48
14	0.5	5.30	7.05	0.75	5.58	7.56	0.74	10.96	41.03	0.27
15	11	4.92	4.84	1.02	6.56	7.67	0.86	8.39	17.12	0.49
16	2	6.49	8.33	0.78	6.89	9.64	0.72	14.55	35.00	0.42

- : subjects did not successfully complete or perform the trial

Table 3.6: Crest factor of rate of steering input measured during slalom maneuvers

Subject	Driving experience (yrs)	Crest factor of rate of steering input								
		30 km/h			50 km/h			70 km/h		
		Peak	RMS	Crest factor	Peak	RMS	Crest factor	Peak	RMS	Crest factor
1	4	8.32	20.85	0.40	11.13	43.17	0.26	15.47	110.7	0.14
2	15	6.60	14.85	0.44	9.05	28.36	0.32	13.24	70.13	0.19
3	7	8.63	16.98	0.51	10.23	34.58	0.30	13.68	88.46	0.15
4	3	9.13	19.80	0.46	14.37	44.41	0.32	22.18	153.2	0.14
5	5	9.35	23.84	0.39	12.48	48.86	0.26	14.45	81.85	0.18
6	2.5	11.93	23.79	0.50	16.13	73.43	0.22	27.41	165.8	0.17
7	8	8.19	15.68	0.52	12.28	37.16	0.33	16.00	88.96	0.18
8	6	10.28	21.24	0.48	13.55	56.78	0.24	19.77	131.3	0.15
9	15	7.81	13.35	0.59	8.77	23.22	0.38	11.28	50.19	0.22
10	10	7.43	16.48	0.45	10.92	41.63	0.26	10.80	51.27	0.21
11	12	6.08	7.70	0.79	8.19	19.84	0.41	9.43	32.24	0.29
12	9	8.88	21.51	0.41	12.43	50.68	0.25	14.74	80.19	0.18
13	2	8.79	16.97	0.52	12.18	39.03	0.31	12.24	50.22	0.24
14	0.5	7.61	17.02	0.45	10.26	34.72	0.30	14.80	90.39	0.16
15	11	6.56	11.51	0.57	10.68	31.89	0.33	11.72	55.91	0.21
16	2	8.85	19.09	0.46	11.51	40.77	0.28	16.43	76.79	0.21

- : subjects did not successfully complete or perform the trial

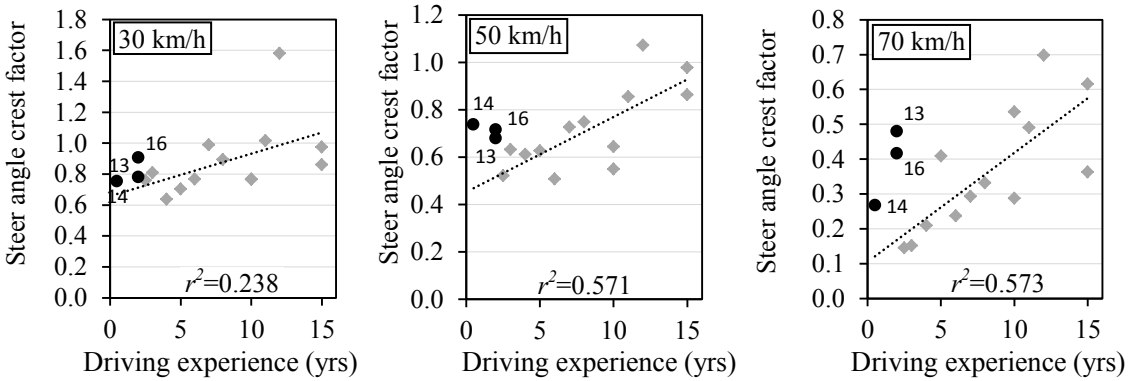

Figure 3.6: Correlations of: (a) mean steer angle crest factor; (b) mean steering rate crest factor with the driving experience during slalom maneuvers at three selected target speed (30, 50 and 70 km/h; r^2 values are shown upon removal of outliers

3.3.4 Steering Profile Area

An additional response measure, defined as the steering profile area, is introduced to investigate variations in participants' steering response during the slalom maneuver. Steering profile area be related to the effort or work done by the driver, and is indicated by the grey-shaded area in Figure 3.7. Table 3.7 summarizes the steering profile area for each participant during slalom maneuvers together with the mean of the trials conducted at three target speeds (30, 50 and 70 km/h). Figure 3.8 show variations in the mean steering profile area with the driving experience of the participants for the three selected forward speeds. The figures also show variation in r^2 and the identified outliers, which are presented with black dots together with corresponding subject numbers.

The measured data excluding the identified outliers suggest that the steering profile area substantially increases with increasing forward speed. This increase, however, is relatively small when speed is increased from 30 to 50 km/h but substantially higher at 70 km/h. This suggests higher steering effort and mental workload demand for the drivers at higher speeds. Further, it is shown that the steering profile area decreases considerably with increasing participants' driving experience suggesting lower physical workload of experienced drivers compared with novice drivers for the same driving task, as seen in the results obtained for peak steer angle and rate of steering.

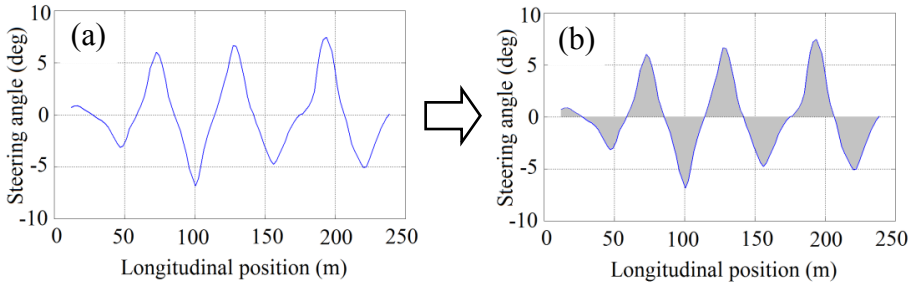

Figure 3.7: (a) Steering profile of the driver; (b) steering profile area, indicated by the grey-shaded area

The results suggest that the steering profile area during the slalom maneuver can be applied to classify drivers based upon their driving skill as: 'novice' more than 450 at 30 km/h, more than 550 at 50 km/h, and more than 1400 at 70 km/h; 'average' between 350 and 450 at 30 km/h, between 450 and 550 at 50 km/h, and between 900 and 1400 at 70 km/h; and 'experienced' less than 350 at 30 km/h, less than 450 at 50 km/h, and less than 900 at 70 km/h. The proposed classifications are consistent with those defined on the basis of the peak values and crest factors of the steer angle and steering rate and also with the maneuver accomplishment, as discussed in sections 3.3.1 to 3.3.3.

Table 3.7: Steering profile area during slalom maneuvers

Subject	Driving experience (yrs)	Steering profile area (deg.m)											
		30 km/h				50 km/h				70 km/h			
		Trial 1	Trial 2	Trial 3	mean	Trial 1	Trial 2	Trial 3	mean	Trial 1	Trial 2	Trial 3	Mean
1	4	471.9	555.8	-	513.9	-	502.5	-	502.5	1055.8	1937.5	-	1496.7
2	15	346.5	376.8	-	361.6	333.6	425.9	-	379.7	1063.7	672.0	-	867.9
3	7	443.2	324.7	-	384.0	584.1	368.0	-	476.0	1719.4	716.9	-	1218.1
4	3	580.6	351.3	-	466.0		619.3	-	619.3	2948.6	1431.1	-	2189.9
5	5	617.9	459.6	-	538.7	664.2	452.6	-	558.4	2363.8	553.8	-	1458.8
6	2.5	528.7	505.0	-	516.8	746.7	624.3	-	685.5	1782.2	2106.7	-	1944.4
7	8	473.8	363.8	-	418.8	678.3	394.1	-	536.2	-	1025.5	-	1025.5
8	6	476.7	444.0	-	460.3	758.6	538.0	-	648.3	3162.6	781.4	-	1972.0
9	15	407.9	320.0	-	363.9	469.6	327.9	-	398.7	567.7	519.9	-	543.8
10	10	475.0	431.2	343.6	416.6	679.3	455.4	400.1	511.6	-	582.3	522.7	552.5
11	12	331.6	206.4	204.9	247.6	487.0	268.9	290.7	348.9	-	507.1	408.1	457.6
12	9	498.6	424.8	385.6	436.4	667.1	619.6	576.8	621.2	920.6	1216.4	1205.6	1114.2
13	2	478.7	329.4	406.5	404.9	1008.8	371.0	392.3	590.7	712.0	453.1	874.6	679.9
14	0.5	382.4	471.7	-	427.0	473.6	423.5	-	448.5	1066.4	1039.5	-	1053.0
15	11	387.7	333.4	333.2	351.4	433.4	441.8	421.7	432.3	750.0	600.2	656.5	668.9
16	2	473.9	393.0	493.6	453.5	490.5	536.5	478.6	501.9	970.6	1576.1	598.0	1048.3

- : subjects did not successfully complete or perform the trial

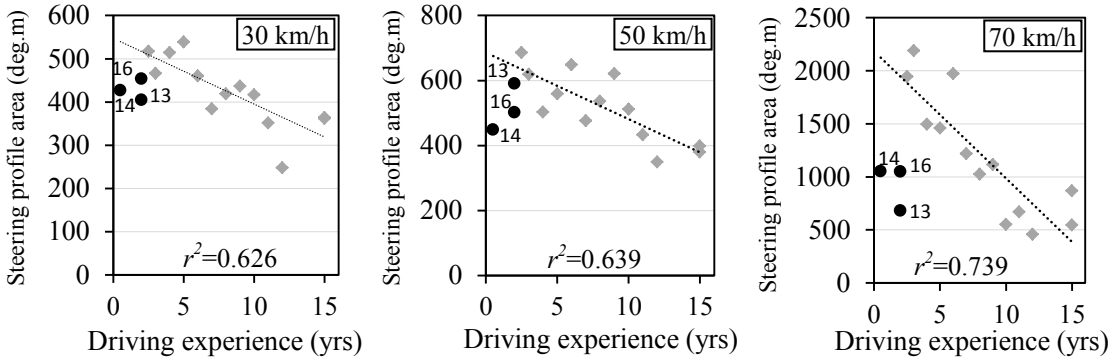

Figure 3.8: Correlations of mean steering profile area with the driving experience during slalom maneuvers at three target speeds; r^2 values are shown upon removal of outliers

3.3.5 Mean and Peak Speed Deviations from the Target Speed

Although the participants were instructed to maintain a constant forward speed during a trial, considerable variations in the speed were observed. The driver's ability to maintain a given speed was evaluated considering: (i) deviation of the average speed from the target speed, termed as 'mean speed deviation ($\Delta v_{x,mean}$)'; and (ii) peak difference between the instantaneous speed from the average speed, termed as the 'peak speed deviation ($\Delta v_{x,peak}$)'. The mean speed deviation indicates participants' capability to drive at a pre-defined target speed, while the peak speed deviation represents drivers' ability to maintain a steady speed. Table 3.8 summarizes the mean of 'mean' and 'peak' speed deviations observed over all the three trials corresponding to each target speed.

The results suggest only small 'mean' speed deviations for 30 and 50 km/h maneuvers, which revealed poor correlations with the driving experience. The 'mean' speed deviation, however, is substantially larger at 70 km/h, and shows a negative correlation with the driving experience, as seen in Figure 3.9(a). The r^2 was obtained as 0.44 when outliers data (subjects #13, 14 and 16) were removed. The 'peak' speed deviations are also relatively small at the lower speeds, with a few exceptions, but significantly higher at 70 km/h. The data also showed negative correlation with the driving experience, as shown in Figure 3.9(b). Despite the relatively low r^2 values, the results show substantially lower 'mean' and 'peak' speed deviations for the drivers with higher driving experience. A driving skill classification was thus attempted on the basis of 'mean' and 'peak' speed deviations at 70 km/h: novice' ($\Delta v_{x,mean} > 3\ km/h; \Delta v_{x,peak} > 8\ km/h$), 'average' ($1\ km/h \leq \Delta v_{x,mean} \leq 3\ km/h;\ 4\ km/h \leq \Delta v_{x,peak} \leq 8\ km/h$) and 'experienced' ($\Delta v_{x,mean} < 1\ km/h; \Delta v_{x,peak} < 4\ km/h$).

Table 3.8: Mean of 'mean' and 'peak' speed deviations during slalom maneuvers

Subject	Years of driving	Mean speed deviation (km/h)			Peak speed deviation (km/h)		
		30 km/h	50 km/h	70 km/h	30 km/h	50 km/h	70 km/h
1	4	0.01	0.25	1.97	0.87	1.12	5.59
2	15	0.74	1.47	0.40	1.02	2.62	1.16
3	7	1.40	0.16	0.83	4.50	2.94	2.52
4	3	0.43	0.34	3.45	2.96	2.87	9.51
5	5	0.03	0.60	2.33	1.31	1.79	7.99
6	2.5	0.36	0.11	4.80	2.77	2.56	11.09
7	8	0.23	1.28	1.85	1.35	2.89	5.50
8	6	0.04	0.84	2.59	1.08	2.24	9.17
9	15	0.45	0.25	0.73	2.60	1.53	1.90
10	10	0.12	0.09	3.13	0.57	0.74	14.81
11	12	0.55	0.54	0.93	1.08	2.30	4.86
12	9	0.54	0.26	0.38	1.47	0.94	2.82
13	2	0.56	0.42	0.79	3.29	4.33	2.53
14	0.5	0.17	0.24	0.37	0.76	1.32	2.32
15	11	0.04	0.12	0.44	0.56	1.25	1.44
16	2	0.29	0.58	1.36	1.36	2.85	5.21

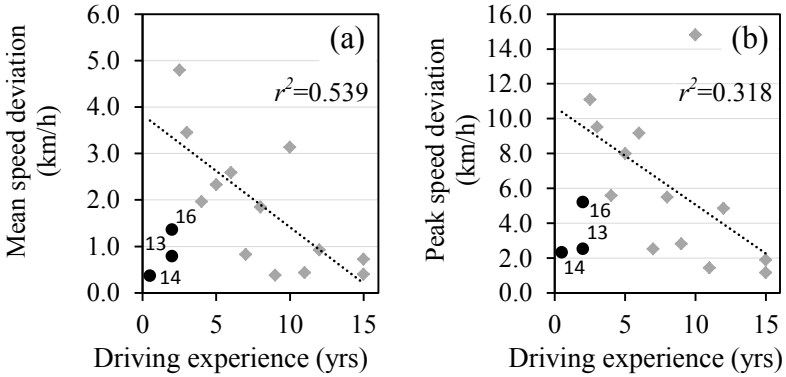

Figure 3.9: Correlations of: (a) mean speed deviations; and (b) peak speed deviations with the driving experience during slalom maneuvers at 70 km/h; r^2 values are shown upon removal of outliers

3.3.6 Summary of Skill Classifications

The results suggest good correlations of the driving experience with the five different measures acquired during slalom maneuvers at different speeds. These include: (i) maneuver accomplishment at the higher speed of 70 km/h; (ii) peak steer angle and rate of steering; (iii) crest factors of steer angle and its rate; (iv) steering profile area; and (v) the 'mean' and 'peak' speed variations at the higher speed of 70 km/h. The results also

suggest strong dependency on the forward speed, as evidenced from large standard deviations of the mean measures across the three speeds. Irrespective of such variations, all the five measures can be applied to obtain consistent objective skill classifications, as seen in Table 3.9.

Table 3.9: Summary of driving skill classification based upon the measures considered during a slalom maneuvers

Measure	Speed (km/h)	Driving skill		
		Novice	Average	Experienced
Maneuver accomplishment	70	> 3[†]	1 to 3[†]	< 1[†]
Peak steering angle (deg)	70	> 15	10 to 15	< 10
Peak steering rate (deg/s)	70	> 20	14 to 20	< 14
steer angle crest factor	70	< 0.3	0.3 to 0.5	> 0.5
steering rate crest factor	70	< 0.17	0.17 to 0.22	> 0.22
Steering profile area	30	> 450	350 to 450	< 350
	50	> 550	450 to 550	< 450
	70	> 1400	900 to 1400	< 900
Mean speed deviation (km/h)	70	> 3	1 to 3	< 1
Peak speed deviation (km/h)	70	> 8	4 to 8	< 4
# years of driving experience	-	< 4	4 to 9	> 9

[†] Number of cones 'hit' or 'missed'

3.4 Measurement of the Braking and Steering Response Times

In general, human reactions to external stimuli exhibit considerable time delays attributed to perception of the stimuli, neuromuscular dynamics, and decision-making ability. The driver response time defines the interval between initiation of the stimulus and initiations of the driver's action, which could be decomposed into two distinct components: (i) driver perception and processing time delay of the central nervous system; and (ii)

movement time of the muscle and the limbs. It is widely accepted that the human driver exhibits time delay in perceiving the information, which is denoted as the perception delay time, τ_{pd} [1,94,95]. Further, the human central nervous system involves an additional delay for analysis of the detected stimuli and subsequently send a control command to the muscles, which is generally denoted as the processing time delay, τ_p [1,95]. Movement time defines the interval to initiate the intended action in response to the actuation signal of the central nervous system, which mostly depends on muscles dynamic, age and fatigue [91-95]. In this section, the braking and steering response times of the participants are examined through three sequential trials of different simulator-based maneuvers, namely, abrupt braking and obstacle avoidance maneuvers.

3.4.1 Abrupt Braking Maneuver

Participants were asked to drive on a straight-line road segment at three different constant speeds (30, 50 and 70 km/h) and brake upon detecting a pre-designed visual stimulus (i.e., a visual stop sign). The driver's overall braking response time (τ_b) describes the time interval between display of the visual stimulus and the time at which the participant initiates braking. It thus represents the sum of perception and processing delays ($\tau_{pd} + \tau_p$) and the foot movement time (τ_m), the time interval between lifting off the foot from accelerator and initiating the brake pedal actuation. The time-history of brake and accelerator pedals position was thus recorded throughout the maneuvers to determine the braking response time of the driver, as shown in Figure 3.10, for one of the participants. The figure shows the instantaneous positions of the accelerator and brake pedals, normalized with respect to their total travel. The perception and processing delays are measured from the instant of the display of a stop sign until the initiation of the

accelerator pedal release, as indicated by 'A' in the figure. The movement time, τ_m, the time lapse between release of the accelerator and depression of the brake pedal, is indicated by 'B' in the figure.

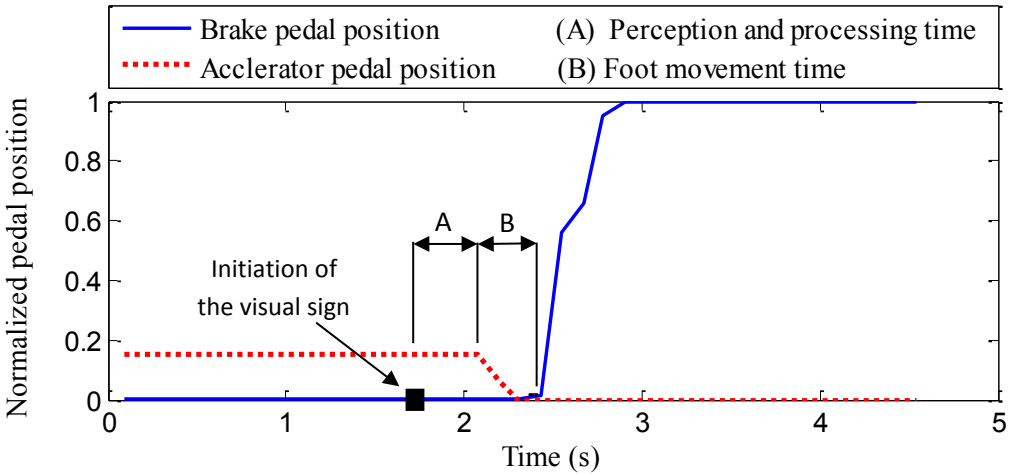

Figure 3.10: Braking response time in an abrupt braking maneuver

3.4.2 Obstacle Avoidance Maneuver

Participants were asked to drive the vehicle at the same three target speeds on a straight-line road and avoid an unexpected visual sign by steering only. The driver's overall steering response time (τ_s) describes the time interval between initiation of the visual signal and the time at which participant initiates steering, as indicated by duration 'C' in Figure 3.11. The overall steering response time is described as a summation of the perception-processing time ($\tau_{pd} + \tau_p$) and the arm's movement time (τ_m). The visual signal is designed as a warning road-sign which includes an unexpected direction to follow. The measured response time, thus, includes a higher level of decision making process compared with the straight-line braking response time, described in the previous section.

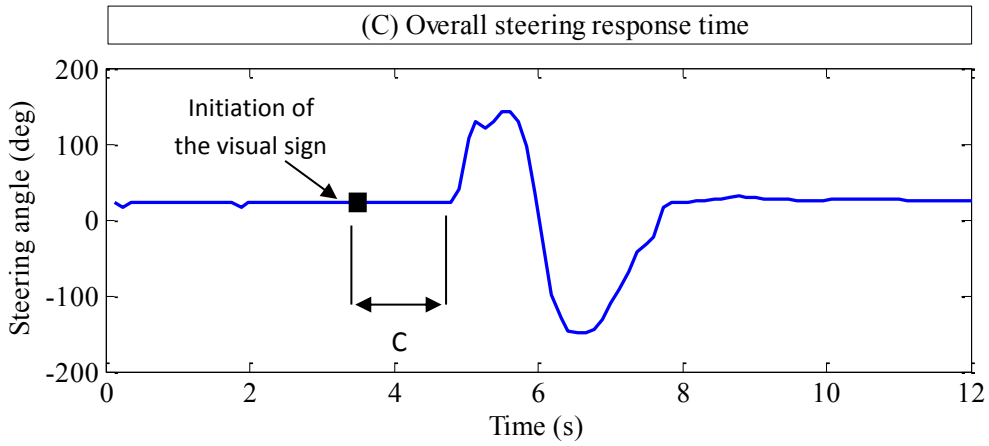

Figure 3.11: Steering response time observed during an obstacle avoidance maneuver

3.5 Results and Discussions

3.5.1 Braking Response Time

Table 3.10 summarizes the measured perception-processing and movement times of participants measured during the straight-line braking maneuvers at three target speeds. Considerable variations in the pedals positions were observed for many subjects who periodically decreased or increased the pressure on the accelerator to maintain the desired vehicle speed. The data for some of the trials thus did not provide clear indications of the accelerator pedal release following the display of the visual stimulus. Further, one of the participants (subject #3) did not follow the pre-defined experimental procedure for the braking maneuver; the data obtained for this participant was thus excluded from the analyses.

The measured data are analyzed to derive mean perception-processing, and movement times of all the subjects, corresponding to each speed, as shown in Figure 3.12 (a and b) together with the error bars (± standard deviation). The results illustrate that braking perception-processing time tends to decrease slightly with increase in vehicle speed, although this trend is not evident when speed is increase from 50 to 70 km/h. The general

trend of the lower perception-processing time can be attributed to enhanced drivers' attention at higher driving speeds [1,92]. The results further show only slight effect of vehicle speed on the foot movement time. The braking response time, obtained from summation of the perception-processing and movement times, tends to be nearly constant at all the speeds considered in the study, as seen in Figure 3.12(c). The results suggest that the drivers tend to compensate for higher perception-processing delay through faster foot movement. A few studies reporting measured braking times from road tests suggested decrease in braking time with speed [92,144,145]. The tests in these studies were mostly conducted at relatively higher speeds, which may be the cause of observed differences.

Table 3.10: Mean perception-processing and movement times of each participant performing a straight-line braking maneuver at three different speeds

Subject	Driving experience (yrs)	Perception-processing time (s)			Movement time (s)		
		30 km/h	50 km/h	70 km/h	30 km/h	50 km/h	70 km/h
1	4	0.385	0.271	0.344	0.391	0.479	0.391
2	15	0.343	0.235	0.360	0.344	0.469	0.469
3	7	-	-	-	-	-	-
4	3	-	0.234	0.235	0.359	0.414	0.414
5	5	0.437	0.251	0.250	0.469	0.500	0.438
6	2.5	0.344	0.234	0.344		0.469	0.368
7	8	0.360	-	-	0.352	-	0.469
8	6	-	0.266	0.344	0.469	0.453	0.415
9	15	0.359	0.349	0.360	0.415	0.469	0.414
10	10	0.343	0.276	0.354	0.407	0.469	0.391
11	12	-	0.359	0.234	0.468	0.360	0.422
12	9	0.383	-	0.282	0.430	-	0.453
13	2	0.390	0.235	0.344	0.407	0.532	0.485
14	0.5	0.360	0.234	0.352	0.399	-	0.360
15	11	0.386	0.343	0.307	0.352	0.453	0.360
16	2	0.328	0.344	0.290	0.468	0.453	0.427
Average	7	0.368	0.279	0.314	0.409	0.460	0.418
SD	4.66	0.030	0.050	0.047	0.047	0.042	0.040

- : The perception and movement times could not be identified since the subject did not follow the experiment protocol

The measured perception-processing and foot movement times were subsequently analyzed to examine correlations with the driving experience of participants. Owing to

relatively small effect of the speed, the correlations are examined considering the mean data obtained for all the three speeds. Figure 3.13 illustrates variations in the mean perception-processing and movement times with the participants' driving experience. The results show nearly constant perception-processing and foot movement times of the participants with varying driving experience, suggested insignificant effect of the driving experience.

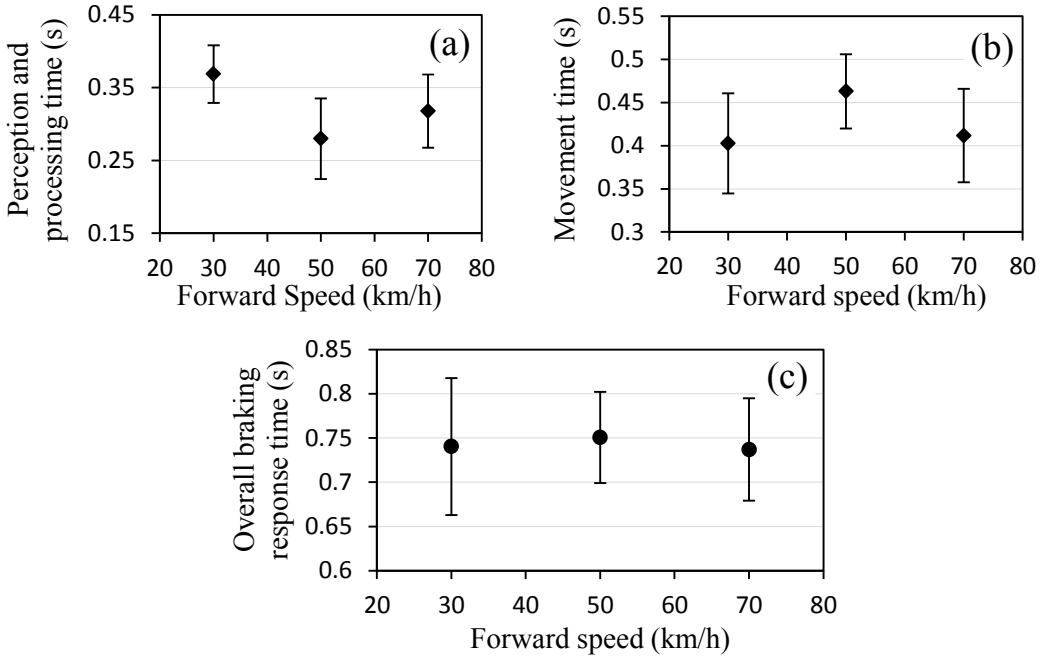

Figure 3.12: Variations in: (a) mean perception-processing times, (b) mean foot movement time, and (c) mean overall brake response time with forward speed.

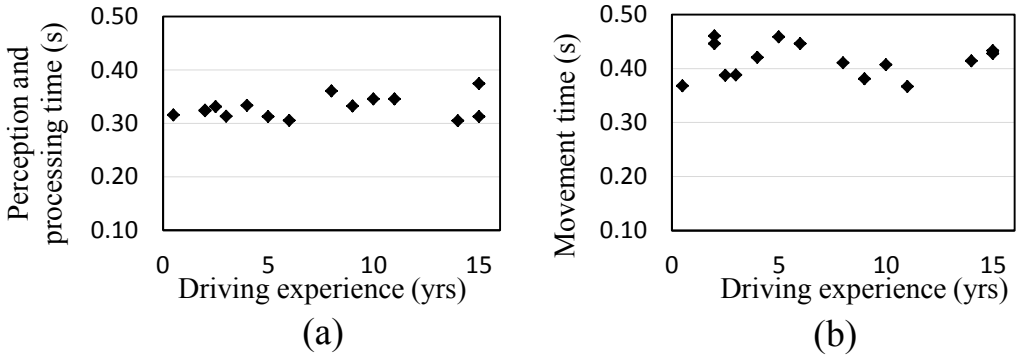

Figure 3.13: Variations in: (a) mean perception-processing, and (b) movement time with participants' driving experience

3.5.2 Steering Response Time

Table 3.11 summarizes mean steering response times (τ_s) of participants measured during the obstacle avoidance maneuver at three constant forward speeds. Figure 3.14(a) and 3.14(b) illustrate the mean steering response times of all the subjects together with the standard deviations as functions of the forward speed and driving experience, respectively. The results suggest that the mean steering response time decreases with increase in speed nearly linearly, while it remains nearly constant with the driving experiences. This suggests a higher level of driver's attention at higher speeds leading to lower steering response time, while driving experience does not significantly influence the steering response time of participants.

Table 3.11: Mean steering response time of each participant performing an obstacle avoidance maneuver at three different speeds

Subject	Driving experience (yrs)	Steering response time (s)		
		30 km/h	50 km/h	70 km/h
1	4	0.524	0.500	0.406
2	15	0.523	0.523	0.344
3	7	0.532	0.469	0.469
4	3	0.532	0.469	0.469
5	5	0.539	0.469	0.578
6	2.5	0.594	0.461	-
7	8	0.594	0.469	0.469
8	6	0.469	0.438	0.469
9	15	0.469	0.578	0.406
10	10	0.476	0.461	0.406
11	12	0.594	0.524	0.555
12	9	0.508	0.453	0.461
13	2	0.563	0.474	0.359
14	0.5	0.578	0.453	0.344
15	11	0.578	0.459	0.523
16	2	0.532	0.562	0.420
Mean	7	0.537	0.485	0.445
SD	4.66	0.043	0.040	0.071

- : subjects did not successfully perform the trial

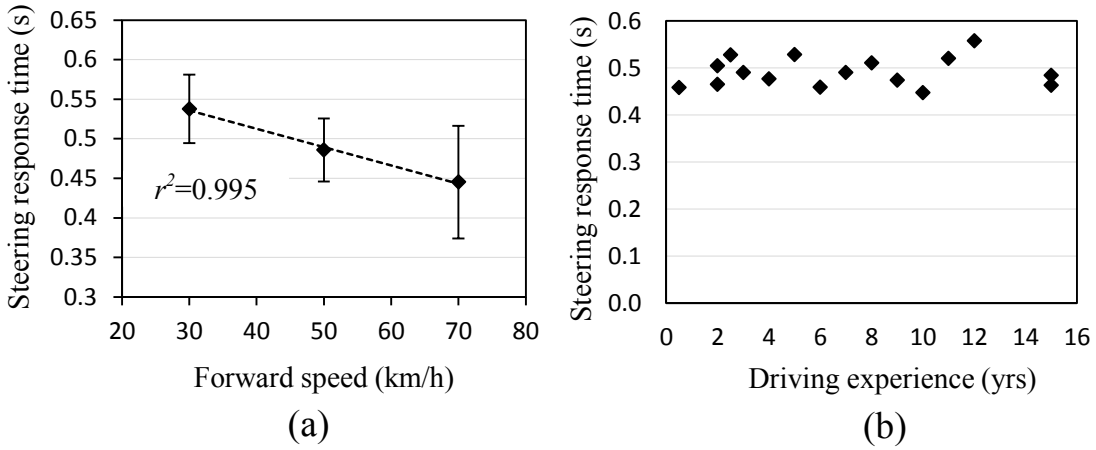

Figure 3.14: Variations in the steering response time due to variations in: (a) the forward speeds and (b) driving experience

The measured data suggest negligible variations in the overall steering response time across the participants, which was also evident from relatively small standard deviations of the mean at all three speeds (Table 3.11). Greater variations in the steering response time, however, were observed with speed for all the participants. The measured data are thus further analyzed to study the inter-subject variability and statistical significance of the vehicle speed using single-factor ANOVA and to formulate a regression model of steering response time as a function of the forward speed. For this purpose, the data corresponding to each trial was carefully examined to detect outliers. A trial was considered an outlier when the response time was observed beyond one standard deviation. A total of 19 out of 127 successful trials were found to exceed one standard deviation. The measured data revealed considerable inter-subject variability, ranging from 25% at 30 km/h to 32% at 70 km/h. This variability reduced to 11.2% and 18.2%, respectively, when the outlier trials were excluded from the analysis. The single-factor ANOVA and pairwise comparisons of the data revealed strongly significant effect of the forward speed (p<0.05) and negligible effect of the driving experience (p>0.3). Nearly

linear decrease in the steering response time with increase in vehicle speed is also evident from Figure 3.14(a) (r^2=0.981), suggesting the following relation:

$$\tau_s = 0.605 - 0.0023\, v_x \tag{3.2}$$

where v_x is the forward speed in km/h.

3.6 Characterization of Drivers' Control Properties

The analysis of measured data on human driving behavior during slalom and obstacle avoidance maneuvers, presented in sections 3.4 and 3.5, suggest that drivers' steering responses in terms of peak steer angle and its rate are strongly influenced by the driving experience and the forward speed of vehicle. It is thus desirable to seek relation of the driver response parameters with the speed and driving experience. For this purpose, subsequent experiments were conducted to measure driver responses in terms of peak steer angle and steer rate while negotiating a standard double-lane change maneuver [127], as shown in Figure 3.15. The measured data are used to obtain a regression model relating selected response parameters with the vehicle speed and driving experience. Owing to the considerable inter- and intra-subject variability observed in the measured data, analyses of variance (ANOVA) of the data is also performed to enhance understanding of the main factors that significantly affect driver's steering response, namely, (i) peak steer angle; and (ii) peak rate of steering input.

Variations in steering control actions and path tracking responses of participants during the selected maneuver are also investigated under poor visibility condition to study the effect of visibility on participants' perception and compensation ability. The participants with different level of driving experiences were thus asked to perform the

standardized double-lane change maneuvers at three steady speeds (30, 50 and 70 km/h) in clear as well as foggy road conditions.

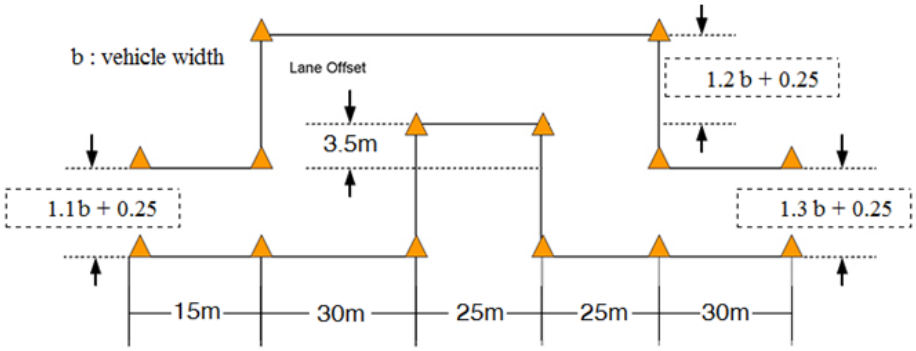

Figure 3.15: Standard course of the double-lane change maneuver [127]

3.6.1 Peak Steer Angle

Table 3.12 presents the peak steer angle, $\delta_{F,max}$, measured during the first two trials of the double-lane change maneuvers at each speed. The results suggest that the peak steering angle is strongly influenced by variations in the driving speed. This trend is consistent with that observed during the slalom maneuvers (Table 3.3). The results also show considerable variations in the peak steering angle across different participants leading to inter-subject variability of 25%, 24% and 29% at 30, 50 and 70 km/h, respectively. This variability is in-part attributed to variations in the participants' driving experience. Further, larger variations in the peak steer angle at the higher speed of 70 km/h suggest the effect of driving experience. The measured data are thus analyzed to examine the statistical significance of vehicle speed and participants' driving experience on peak steer angle using ANOVA. A regression model is subsequently formulated for peak steer angle as a function of forward speed and driving experience. Although the slalom test trials with subjects #13, 14 and 16 were considered outliers (section 3.3.2), the removals of these trials in this case resulted in only small changes in the inter-subject

variability. The data corresponding to all the subjects were thus retained for subsequent analyses.

Table 3.12: Peak steer angle measured during the first two trials of constant speed double-lane change maneuvers

Subject	Driving experience (yrs)	Peak steer angle (deg)								
		30 km/h			50 km/h			70 km/h		
		Trial 1	Trial 2	Mean	Trial 1	Trial 2	Mean	Trial 1	Trial 2	Mean
1	4	3.27	3.19	3.23	3.89	4.83	4.36	6.64	6.64	6.64
2	15	2.56	2.94	2.75	3.57	1.94	2.75	3.13	2.70	2.92
3	7	3.13	2.44	2.78	3.89	4.51	4.20	3.44	3.63	3.54
4	3	-	4.69	4.69	-	-	-	4.63	6.39	5.51
5	5	5.32	4.32	4.82	-	3.38	3.38	8.33	3.20	5.77
6	2.5	-	5.82	5.82	6.32	-	6.32	-	-	-
7	8	4.76	4.00	4.38	-	3.69	3.69	6.76	4.69	5.73
8	6	2.75	3.50	3.13	5.63	3.52	4.58	-	6.58	6.58
9	15	3.88	3.45	3.67	3.39	2.88	3.13	2.77	2.75	2.76
10	10	5.02	3.25	4.14	6.14	2.63	4.38	5.15	2.83	3.99
11	12	2.75	2.13	2.44	3.19	3.00	3.10	-	3.44	3.44
12	9	-	3.50	3.50	4.14	3.01	3.57	8.08	6.83	7.45
13	2	3.94	2.89	3.42	4.14	3.19	3.67	7.65	3.27	5.46
14	0.5	-	5.07	5.07	6.26	3.96	5.11	-	4.52	4.52
15	11	3.27	2.58	2.92	2.69	3.25	2.97	4.64	4.71	4.68
16	2	4.00	2.94	3.47	3.75	3.82	3.79	8.83	3.57	6.20
Mean	7			3.62			3.87			5.03
SD	4.66			0.96			1.12			1.94

- : subjects did not successfully complete or perform the trial

The measured data suggest a negative correlation of peak steer angle with the driving experience at 50 and 70 km/h, while the correlation is relatively small at lower speed of 30 km/h. Furthermore, the peak steer angles are substantially greater at 70 km/h compared to those at lower speeds, suggesting considerable effect of speed on peak steer angle, particularly at higher speeds. The single-factor ANOVA and pairwise comparisons of the data also revealed significant effect of the forward speed (p<0.005) on peak steer angle at 70 km/h. The effect of variations in vehicle speed on peak steer angle at 30 km/h, however, were observed to be negligible (p>0.7).

In order to investigate the influence of variations in driving experience on peak steer angle, the participants were grouped in three groups based upon their years of driving

experience as: novice, with less than 4 years of driving experience; average with 4 to 9 years of driving experience; and experienced with more than 9 years of driving experience. These classifications were found to correlate well with the measured data derived from the slalom maneuvers, as illustrated in Table 3.9. The results suggested significant differences in peak steer angle among all the three groups of drivers, while the difference between the novice and average, and average and experienced were smaller compared to those observed between the novice and experienced drivers. The variations in peak steer angle with varying vehicle speed and driving experience during a double-lane change maneuver suggest the following relation:

$$\delta_{F,max} = 1.662 + 1.342\,D + 0.057\,v_x - 0.012\,Dv_x - 0.370\,D^2 \qquad (3.3)$$

where v_x is the forward speed in km/h and D is an index related to the driving experience (D=1,2,3 for novice, average and experienced drivers, respectively). The above regression model resulted in very good fit with the measured data (r^2 =0.907), as shown in Figure 3.16(a).

3.6.2 Peak Steer Rate

Table 3.13 summarizes the peak steer rate, $\dot{\delta}_{F,max}$, measured during the first two trials of the double-lane change maneuvers performed at each speed. As it would be expected, the results suggest strong influence of the speed and participants' driving experience on the peak steer rate. The data suggest trends that are identical to those observed during the slalom maneuvers (Table 3.4). The efficient of variances of the data were observed to be nearly 23%, 21% and 19% corresponding to 30, 50 and 70 km/h maneuvers.

Table 3.13: Peak rate of steering input measured during the first two trials of constant speed double-lane change maneuvers

Subject	Driving experience (yrs)	Peak steer rate (deg/s)								
		30 km/h			50 km/h			70 km/h		
		Trial 1	Trial 2	Mean	Trial 1	Trial 2	Mean	Trial 1	Trial 2	Mean
1	4	5.44	4.68	5.06	7.92	6.36	7.14	10.13	9.92	10.02
2	15	3.30	3.69	3.49	5.29	3.96	4.63	6.32	5.79	6.05
3	7	4.24	3.56	3.90	6.18	5.09	5.63	6.68	8.14	7.41
4	3	-	7.02	7.02	-	-	-	5.73	9.13	7.43
5	5	4.82	4.99	4.90	-	5.36	5.36	11.14	7.82	9.48
6	2.5	-	6.92	6.92	7.89	-	7.89	-	-	-
7	8	5.17	4.40	4.79	-	5.47	5.47	9.80	7.54	8.67
8	6	4.24	4.28	4.26	8.99	6.53	7.76	-	10.71	10.71
9	15	5.30	5.08	5.19	5.22	5.54	5.38	5.71	5.61	5.66
10	10	5.05	4.09	4.57	8.69	5.11	6.90	8.22	7.31	7.77
11	12	3.84	3.47	3.66	4.76	4.74	4.75		7.89	7.89
12	9	-	4.48	4.48	8.27	8.02	8.15	7.30	8.33	7.81
13	2	6.09	4.78	-	6.91	4.89	-	11.98	7.27	-
14	0.5	-	5.24	-	7.51	7.03	-	-	9.99	-
15	11	4.63	3.85	4.24	4.55	5.65	5.10	9.33	9.47	9.40
16	2	4.25	3.10	-	5.71	5.56	-	8.72	5.80	-
Mean	7			4.81			6.18			8.19
SD	4.66			1.09			1.30			1.53

- : subjects did not successfully complete or perform the trial

The measured data suggest definite correlations of the peak steer rate with the driving experience and forward speed. The peak steer rate increased with increasing speed, while it shows negative correlations with the driving experience. The pairwise comparisons and single-factor ANOVA of the data revealed significant effect of the forward speed and driving experience (p<0.05) on the peak rate of steering input. Pairwise comparisons of the 30 and 70 km/h data with the data for 50 km/h revealed relatively lesser difference, although the effect was significant (p<0.05). The similar trend was also observed from pairwise comparison of the data for novice and experienced drivers with the 'average' drivers data. The variations in the peak steer rate with varying vehicle speed and driving experience for the double-lane change maneuvers also resulted in the following regression model in v_x and D, with r^2 =0.98, as shown in Figure 3.16(b):

$$\dot{\delta}_{F,max} = 4.637 - 0.001v_x + 0.188D - 0.004Dv_x - 0.187D^2 + 0.001{v_x}^2 \qquad (3.4)$$

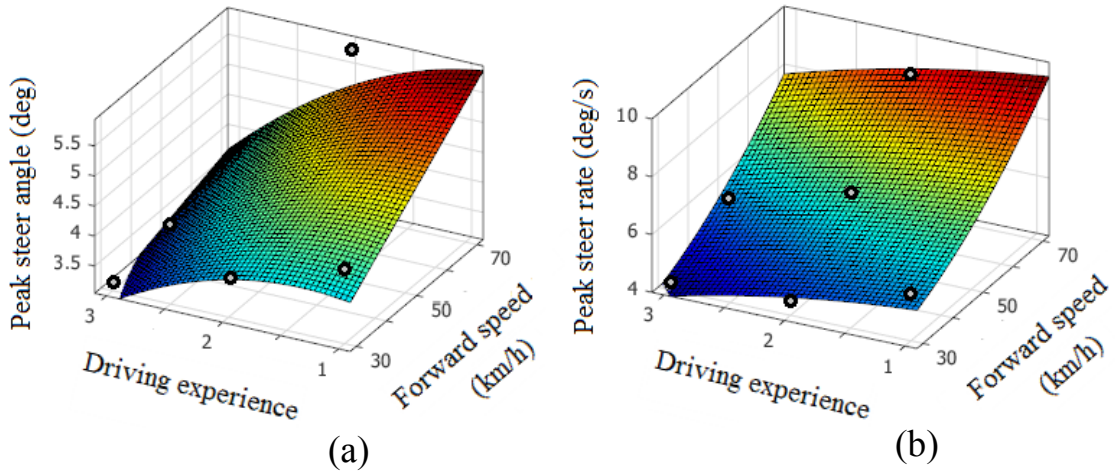

Figure 3.16: (a) Peak steer angle; and (b) peak steer rate as functions of the forward speed and driving experience during double-lane change maneuvers

3.6.3 Coupled Driver-Vehicle responses - Clear Visual Situation

The path tracking performance of the drivers undertaking the standardized double lane-change maneuvers was evaluated in terms of measured time histories of the lateral vehicle position and steer angle input. The recorded data shows that the majority of the 'novice' drivers revealed substantial path deviations and very high frequency of the steering input. These variations were even greater under the foggy road condition, which resulted in continuous steering oscillation or path hunting by the novice drivers. The data analyses were thus limited to those obtained for the 'average' and 'experienced' drivers. Figure 3.17 illustrate the time histories of the mean lateral path coordinate of the vehicle together with the mean steer angle input of the 'average' and 'experienced' drivers groups corresponding to the three selected speeds. The results suggest negligible differences in path tracking responses of the two groups, although drivers' data revealed substantially higher peak steer angle and steer rate compared to 'experienced' drivers, which is also observed in Tables 3.12 and 3.13. The observed trends are also identical to those obtained from the slalom maneuver data (Tables 3.3 and 3.4). The results suggest

considerably higher effort by the 'average' drivers' group to maintain central lane position, which can be attributed to higher compensation by the drivers to reduce the lateral position error. The greater compensation by the 'average' drivers to minimize the path deviation has also been reported in a number of simulations studies [7,18]. The results also suggest that the 'experienced' drivers employ a relatively larger preview distance to track a desired path. The smoother steering and path tracking responses of the 'experienced' drivers group also suggest the use of distant road information to track the desired trajectory.

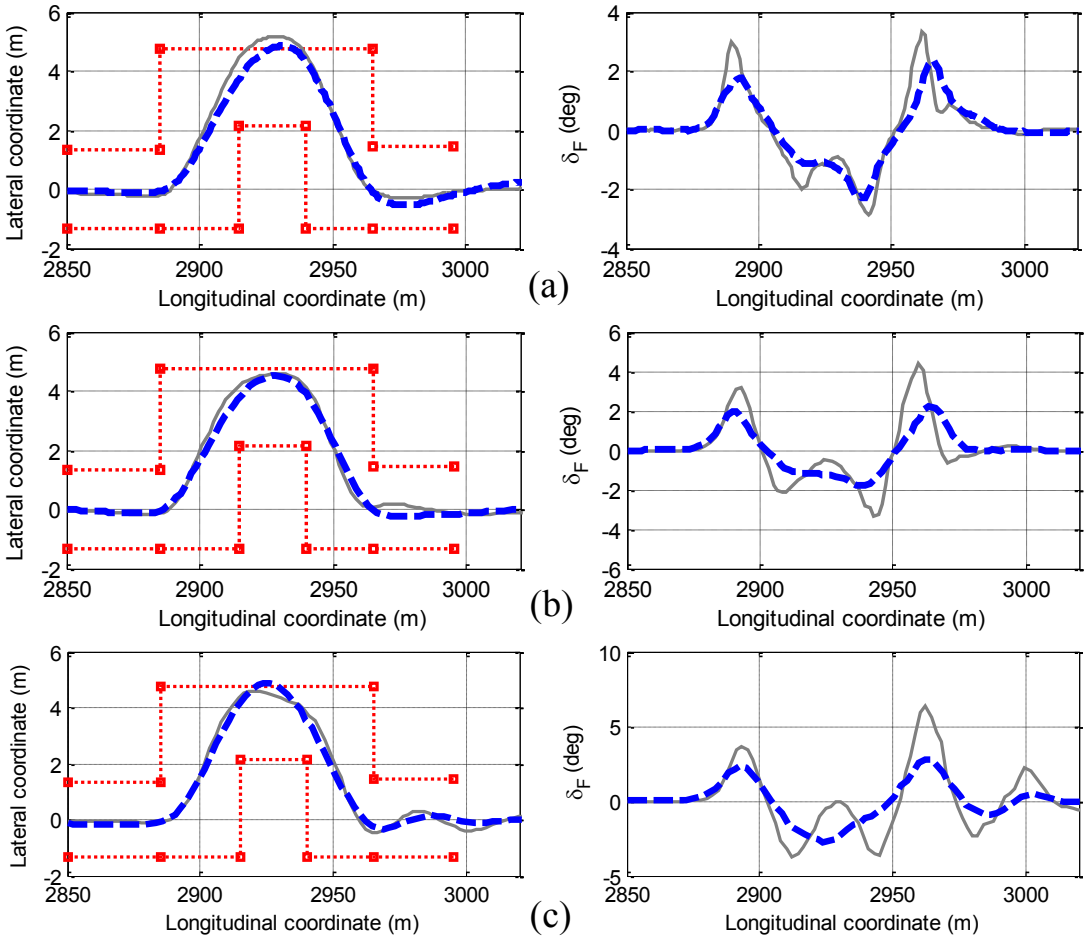

Figure 3.17: Comparisons of path tracking and steering responses of 'average' (solid line) and 'experience' (dashed line) drivers groups under a double lane-change maneuver at different speeds: (a) 30 km/h; (b) 50 km/h; and (c) 70 km/h (clear visual situation)

3.6.4 Coupled Driver-Vehicle responses - Restricted Visual Situation

Figure 3.18 illustrates the mean steering and path tracking responses of the 'average' and 'experienced' drivers group during a double lane-change maneuver in a limited visibility condition at the three target speeds. The simulator was programmed to limit the road visibility to a maximum of 20 m by introducing a foggy condition. The results suggest similar control actions by both the groups at 30 km/h, as observed for the clear road condition. The steer angle responses, however, exhibit larger oscillations at 50 and 70 km/h compared to those observed for the clear road conditions, for the experienced drivers. The steering control actions of the 'average' drivers group, however, are similar to those measuring for the clear road condition for all the three speeds. The greater steer input and path deviation of the 'experienced' driver in the foggy road situation can be primarily attributed to the reduced preview distance. The effect of limited visibility on the 'experienced' drivers is substantial since the 'experienced' drivers tend to rely on greater preview distances [9,18,46].. An 'average' driver, on the other hand, does not employ distance preview of the road. The limited visibility thus does not greatly alter the 'average' drivers' steering and path tracking performance under foggy road condition.

The greater reliance of the 'experienced' drivers on the far preview of the road also yields a delayed steering action of the 'experienced' drivers compared to the 'average' drivers, which is clearly evident at the higher speed of 70 km/h. This additional delay contributes to relatively higher path deviation at 70 km/h, and greater compensation by the 'experienced' drivers, which may suggest the use of a near preview in addition to the far preview for tracking the desired path in limited visibility situation.

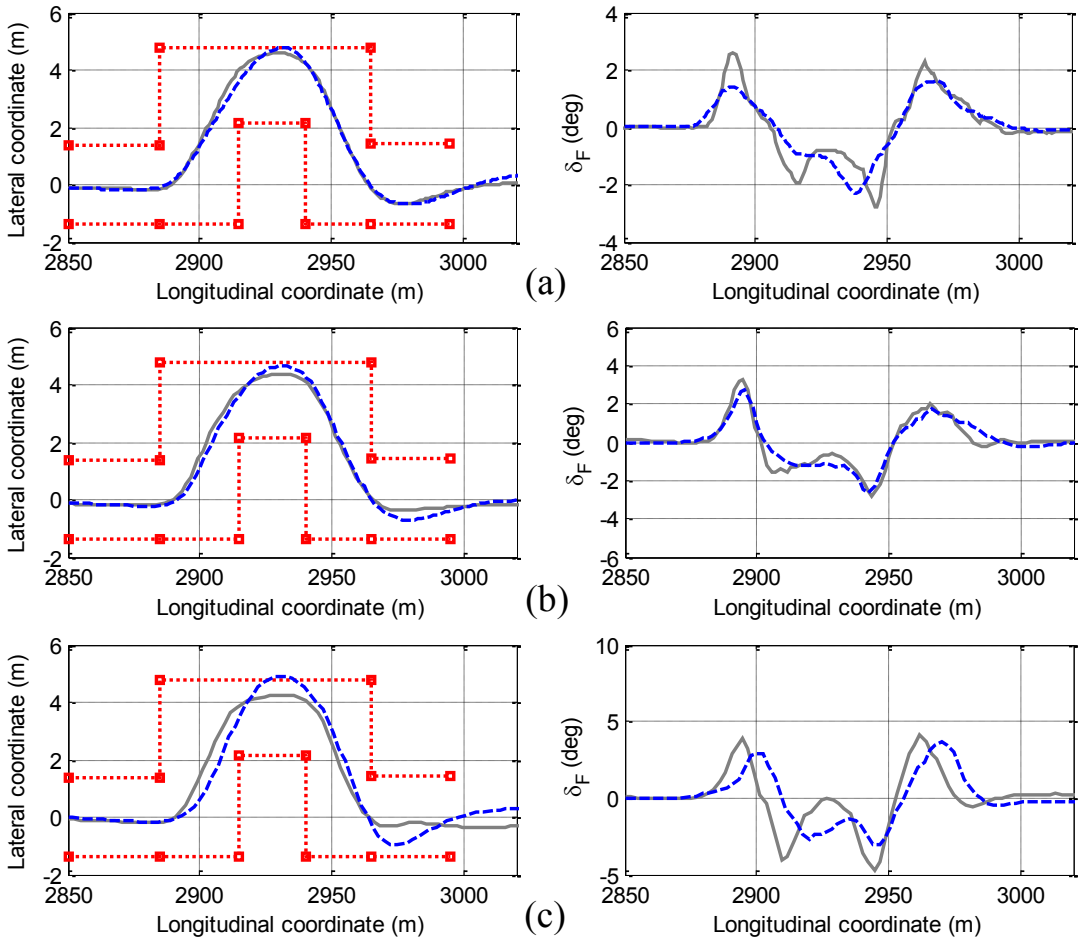

Figure 3.18: Comparisons of mean path tracking and steering responses of average (solid line) and experience (dashed line) drivers groups under a double lane-change maneuver at different speeds: (a) 30 km/h; (b) 50 km/h; and (c) 70 km/h (limited visibility condition)

3.7 Summary

Experiments were performed on a limited motion-based driving simulator of a single-unit vehicle to measure the human drivers' reaction times under different steering and braking inputs, and steering responses and path tracking performance of the drivers at different forward speeds. Owing to observed dependence of the measured data on forward speeds and driving experience of the participants, single-factor ANOVA and pairwise comparisons of the data were performed to enhance understanding of significant factors that affect control actions of drivers. The results showed that the steering responses of

human drivers are significantly affected by the forward speed and the participants' driving experience. Subsequently, a regression model was defined to relate the drivers' steering response time with the forward speed. Regression models are also obtained to describe peak steer angle and peak steer rate of the human drivers during a double lane-change maneuver as function of the forward speed and drivers' experience. These regression models are applied in the following chapter for deriving a coupled driver-vehicle model based on two-stage preview strategy. The measured data are also used to examine the validity of the coupled driver-single-unit vehicle model. Furthermore, the path tracking and steering responses of 'average' and 'experienced' drivers groups were compared under two different road visibility conditions, which suggested considerably poor path tracking performance of 'experienced' drivers at 70 km/h due to reduced path preview distance.

CHAPTER 4

DEVELOPMENT OF THE COUPLED DRIVER-VEHICLE MODEL

4.1 Introduction

The human decision making process is a highly adaptive controller which is strongly influenced by a number of situational and environmental conditions in a very complex manner. It is suggested that formulations of driver-vehicle models that emulate human driving behaviour can help to identify driver performance limits and contribute to enhanced driver control performance through developments in effective driver-assist systems (DAS) and driver-adaptive vehicle designs [7-9]. Considerable efforts have thus been made to develop more reliable driver models applicable to automobiles. Such efforts, however, have been very limited to commercial articulated vehicles, where the control performance of the driver is more crucial. These studies have focused on control requirements of the driving task through minimization of the lateral displacement between the tractor cg and the desired path using a single preview point strategy [25,26]. A single preview point strategy, however, may lead to unsatisfactory path tracking performance and stability limits, particularly under high speed directional maneuvers coupled with a relatively short preview distance [18,66].

A human driver would exhibit superior control performance when a preview of the entire roadway is available. A few studies have thus proposed the multi-point preview strategy employing simultaneous preview of a number of equally spaced target points for mapping of the required path information [15]. Measurements performed under restricted visual situations have shown that human drivers observing only two segments of the

roadway achieve improved path tracking performance that is similar to that realized with the entire roadway being visible [70]. A two-preview point strategy is thus considered adequate to describe the driver preview as opposed to the more complex multi-point approach. A few studies have employed two-preview point strategy to develop coupled single-unit vehicle-driver models [45,65,72,73]. These have also suggested that the vehicle driver needs only two target points ahead of the vehicle to obtain the required roadway coordinates. While the human driver exhibits limited ability to estimate the path curvature, particularly on short-radius curves [80], these models, invariably, obtain the road information on the basis of the previewed path curvature. Considering automobile dynamics, these driver models thus aim to track the desired path with little or no considerations of the cognitive behavior and control limits of the human driver.

In this section, a modified two-stage preview strategy is proposed for identifying the coordinates of the preview points. The preview model involves simultaneous previews of a near- and a far-point on the road, and is applied to develop a driver model applicable to single as well as multiple unit articulated vehicles. The proposed driver-vehicle model involves essential elements of the human driver, such as perception, prediction, path preview, error estimation, decision making and hand-arm dynamics in conjunction with yaw-plane models of the single-unit and articulated vehicles. The path preview of the model is realized using near and far preview points, where the near preview helps maintain central lane position and the far preview helps control vehicle orientation. The driver model parameters are identified by minimizing a composite performance index subject to constraints imposed by the human driver's control and compensation limits.

4.2 Yaw-plane Vehicle Models

In this dissertation, yaw-plane models of two different vehicles are considered: (i) a two DoF single-unit vehicle model, as described in Chapter 2; and (ii) a three DoF articulated vehicle model. The single-unit vehicle model is integrated with the proposed two-stage preview driver model to examine the validity of the model using the simulator measured data (sections 3.6.3 and 3.6.4) under double lane-change maneuvers at different speeds and visibility conditions. A single-track yaw-plane model of the articulated vehicle is also derived to develop a linear state-space 'internal vehicle model' for predicting the future trajectory of the vehicle. The driver model employing the proposed two-stage preview strategy and the 'internal vehicle model' path predictor are subsequently applied to the articulated freight vehicle model to study its directional response characteristics, and performance and control limits, and steering control demands of the human driver during the double lane-change maneuvers at different speeds.

4.2.1 Yaw-Plane Model of the Articulated Vehicle

A number of in-plane and three-dimensional models of varying complexities have been developed to characterize lateral and longitudinal dynamics of articulated freight vehicles. These vary from simplified constant speed linear yaw-plane model to the several DoF multi-body dynamic models [147-151]. It has been shown that a simple yaw-plane model could yield accurate prediction of the lateral dynamics of the vehicle in a highly efficient manner [150]. A nonlinear yaw-plane is thus considered appropriate to study lateral dynamics of the articulated vehicle coupled with the driver model. A simple single-track model of the five-axle articulated vehicle is initially formulated assuming constant speed and linear cornering characteristics of tires. This model is applied as the

reference ‘internal vehicle model’ to simulate the driver's prediction process. Subsequently, a comprehensive yaw-plane model of the articulated vehicle is formulated incorporating the nonlinear tire cornering properties. The model incorporates two DoF of the three-axle tractor (lateral velocity, v_{y1}; and yaw velocity, r_1) and one DoF of the two-axle semi-trailer unit (yaw velocity, r_2), as presented in Figure 4.1. The yaw-plane model is formulated assuming constant speed (v_{x1}), small side-slip and steering angles, negligible contributions due to vehicle roll and pitch motions, and free relative yaw motions of the two units at the articulation joint, as described in a number of earlier studies [9,25,147, 151-152]. The equations of motion for the two yaw-plane models are presented in Appendix A. The well-known Magic Formula is used to derive cornering forces and aligning moments developed by the tires as nonlinear functions of the side-slip and vertical load [125,153-156].

The measured tire data reported by Ervin and Guy [148] was used to identify the model parameters of the magic formula, as illustrated in Appendix A. The validity of the two yaw-plane vehicle models was examined by comparing their directional responses with the reported measured responses of a five-axle tractor-semitrailer combination subject to a constant speed lane-change maneuver [149]. The measured front wheel steer angle time-history, shown in Figure 4.2, was applied to the vehicle model in an open-loop manner. The steering responses of the two yaw-plane models are compared with the reported measured data in Figure 4.2. From the comparison, it was deduced that both the models used in this study can provide reasonably good prediction of the yaw directional responses of the vehicle to driver’s steering inputs. The observed deviations between the measured and model responses were mostly attributed to simplifying assumptions and

lack of precise parameters of the vehicle used in the field-measurements. In Figure 4.2, a_{y1} and a_{y2} are lateral accelerations of the tractor and trailer units, respectively, and δ_F and γ are the front wheel steer angle and articulation angle, respectively.

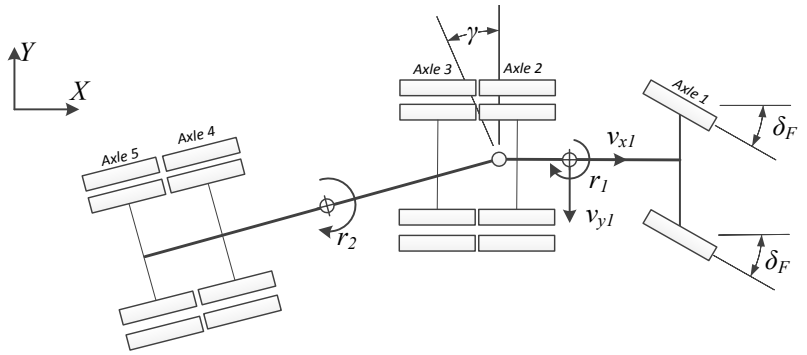

Figure 4.1: Three DoF yaw-plane model of the articulated vehicle

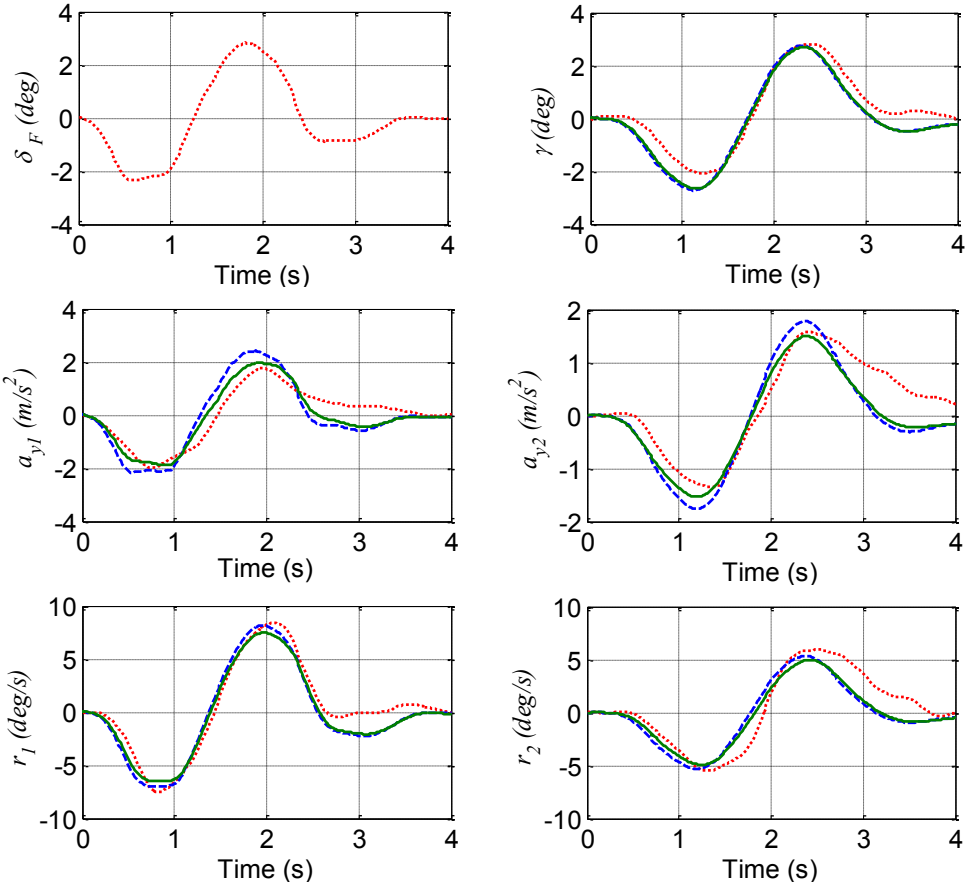

Figure 4.2: Comparisons of directional responses of the single-track yaw-plane vehicle model (dashed line) and the nonlinear yaw-plane vehicle model (solid line) with the measured data (dotted line) during a lane-change maneuver at 68.8 km/h [149]

4.3 Formulation of the Two-Stage Preview Driver Model

For the purpose of driver model formulation, the driver steering process is generalized by four essential elements: (i) perception; (ii) prediction; (ii) preview; (iii) decision making process; and (iv) limb motion, as shown in Figure 4.3. In the following subsections each element of the driving process is mathematically described. The element models are subsequently integrated to formulate the two-stage preview driver model. The proposed driver model is then coupled with the single-unit vehicle model as well as the articulated vehicle model.

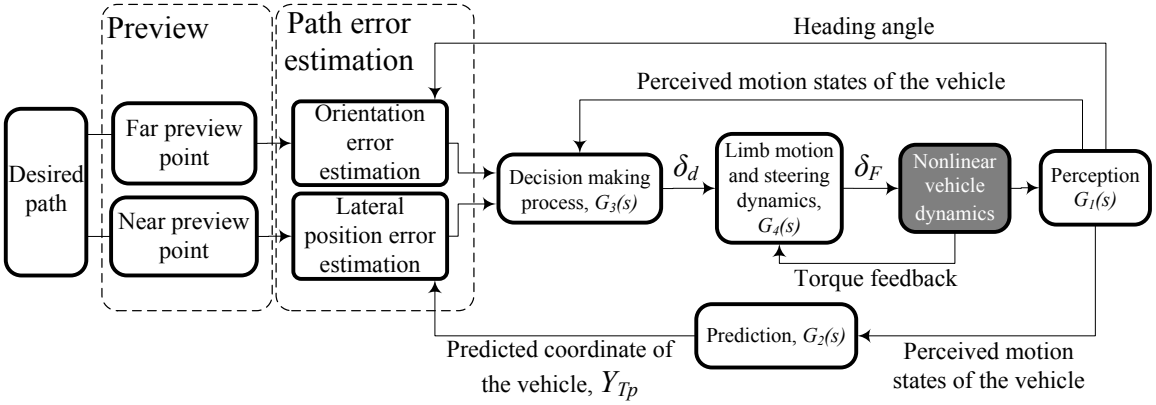

Figure 4.3: The structure of the proposed two-stage preview driver model

4.3.1 Driver's Perception and Prediction

The human perception of the vehicle states could be described considering two essential characteristics: (i) perception delay time [32]; and (ii) a perception threshold that relates to the minimum value of a state that can be sensed by the human driver [5]. The delay time to perceive vehicle states can be mathematically expressed as:

$$D(s) = e^{-s\tau_{pd}} \tag{4.1}$$

where τ_{pd} is the driver's perception delay time, which could vary depending upon the driver's sensory channels and environmental factors, and ranges from 0.1 to 0.2 s

[5,9,144]. The magnitude of a vehicle state, however, must exceed its threshold value to be detected by the human driver. The threshold values vary for different sensory channels [32]. The perception threshold of the human driver can be mathematically expressed by a dead-zone operator (Figure 1.2) such that [5]:

$$S_j(I_j, T_j) = \begin{cases} \max\{I_j - T_j\,, 0\} & ; \quad T_j > 0 \\ I_j & ; \quad T_j = 0 \\ \min\{I_j - T_j\,, 0\} & ; \quad T_j < 0 \end{cases} \tag{4.2}$$

where I_j and S_j are respectively, the instantaneous and perceived motion states, and T_j is the perceptive threshold of vehicle state j (j=1,…, n); n being the number of motion states to be perceived.

The transfer function describing the drivers' perception of vehicle states, $G_1(s)$, is formulated as a combination of perception time delay and perception threshold, such that:

$$G_1(s) = S_j(I_j, T_j)\; D(s) \tag{4.3}$$

Apart from the path perception, a human driver continually predicts vehicle coordinates at a future instant in a qualitative sense on the basis of the perceived information related to primary and secondary cues such as heading angle, forward speed and lateral coordinates of the vehicle [8,40]. It is suggested that the human drivers may employ a previously learnt pattern of vehicle response to predict the vehicle coordinates at a future instant [18,22,28]. This prediction process is mathematically described using the linear state-space model of the vehicle, also referred to as the 'internal vehicle model' [40]. Assuming the vehicle driver can perceive the necessary motion states of the vehicle, in this study, the single-unit vehicle model and the simplified single-track articulated vehicle model are used to predict the future coordinates of the vehicle cg and the tractor cg, respectively. The vehicle model is expressed by the following stat-space equation:

$$\dot{\vec{x}}(t) = [A_l]\vec{x}(t) + [B_l]\vec{u}(t) \tag{4.4}$$

where $\vec{x}$ and $\vec{u}$ are the state and input vectors of the state-space model of vehicle, and A_l and B_l (l=1 for the single-unit vehicle model, and l=2 for the single-track articulated vehicle model) are respectively the state and input matrices of the vehicle model. The homogenous and non-homogenous solutions of the vehicle motion can be obtained from:

$$\vec{x}(t) = [\emptyset(t - t_0)]\vec{x}(t_0) + \int_{t_0}^{t} [\emptyset(t - \tau)][B_l]\vec{u}(\tau)d\tau \tag{4.5}$$

where t_0 is the initial time. Assuming time invariant vehicle parameters, the state transition matrix $[\emptyset(t)] = e^{[A_l]t}$ is estimated using the Taylor series approximation:

$$e^{[A_l]t} = \sum_{n=0}^{\infty} \frac{([A_l]t)^n}{n!} \tag{4.6}$$

Considering Eq. (4.5) and (4.6), the predicted motion states of the vehicle at a future instant T_p are obtained as follow:

$$\vec{x}(t + T_p) = \left(\sum_{n=0}^{\infty} \frac{([A_l]T_p)^n}{n!}\right)\vec{x}(t) + T_p\left(\sum_{n=0}^{\infty} \frac{([A_l]T_p)^n}{(n+1)!}\right)[B_l]\vec{\mathrm{u}}(\mathrm{t}) \tag{4.7}$$

Using the above equation the predicted vehicle cg coordinates (X_P, Y_P) at a future instance T_p can be determined, as indicated by point '*P*' in Figure 4.4(b).

4.3.2 Two-Stage Preview and Parameters Estimations

A two-stage strategy is used to describe the human drivers' path preview process, which involves simultaneous previews of a near- and far-point on the roadway. The human driver previews path coordinates in the near visual field to minimize the lateral position error between the vehicle trajectory and the desired roadway. The preview of a distant location, on the other hand, is used to control the relative orientation error between the

direction of motion of the vehicle and the far preview point on the roadway. The two-stage preview strategy is formulated to identify locations of the near and far preview points, in three sequential steps involving: (i) identifications of the near and far visual fields; (ii) locating the near preview point with respect to driver's position; and (iii) locating the point of tangency and far preview point with respect to driver's position. These are described below considering the path geometry.

The majority of the reported studies have defined path coordinates with respect to the vehicle cg, assuming that the driver is located at or near the vehicle cg. This, however, may lead to substantial errors, particularly for articulated vehicles. The coordinates of the driver's seat (point *D* in Figure 4.4) can be determined from the lateral (W_D) and longitudinal (L_D) position of the seat with respect to the tractor cg:

$$\begin{aligned} X_D &= X_g + L_D \cos\psi_1 - W_D \sin\psi_1 \\ Y_D &= Y_g + L_D \sin\psi_1 + W_D \cos\psi_1 \end{aligned} \tag{4.8}$$

where ψ_1 is the tractor heading angle, and (X_g, Y_g) and (X_D, Y_D) are, respectively, the coordinates of the vehicle cg and the driver's seat in the global axis system (OXY).

Referring to Figure 4.4(a), the driver's overall visual field is described as a circular sector centered at the driver's seat position. The overall visual field is defined by the field angle Φ and its radius, which is determined through minimization of a performance index, as described in the following sections. In the two-stage preview strategy, it is hypothesized that the driver determines the coordinates of the roadway at two target points within the overall visual field in consideration of the road curvature. These include a near preview point and a far preview point. The overall visual field is thus represented by near and far visual fields, indicated by radii L_N and L_F, respectively, in Figure 4.4(a).

Through measurements, it has been shown that the visual field angle of human drivers is in the order of 120˚, while the temporal field of vision describing the left/right rotation of the driver's head is approximately 35˚ [157].

A methodology is developed for locating the near and far preview points considering straight-line and curved roadways. For a straight-line road segment, the driver aims to maintain a central lane position, while compensating for the environmental disturbances. In this situation, the near and far preview points are located at the intersection of the boundaries of the near and far visual fields with the centerline of the road, respectively, as shown in Figure 4.4(a). The near and far preview distances are thus obtained equal to the visual field radii, $D_{PN}=L_N$ and $D_{PF}=L_F$, respectively. Assuming constant driving speed within the preview interval, the preview distance is generally expressed in terms of preview time T_P, where $T_P = D_p/v_x$ and D_p is the preview distance.

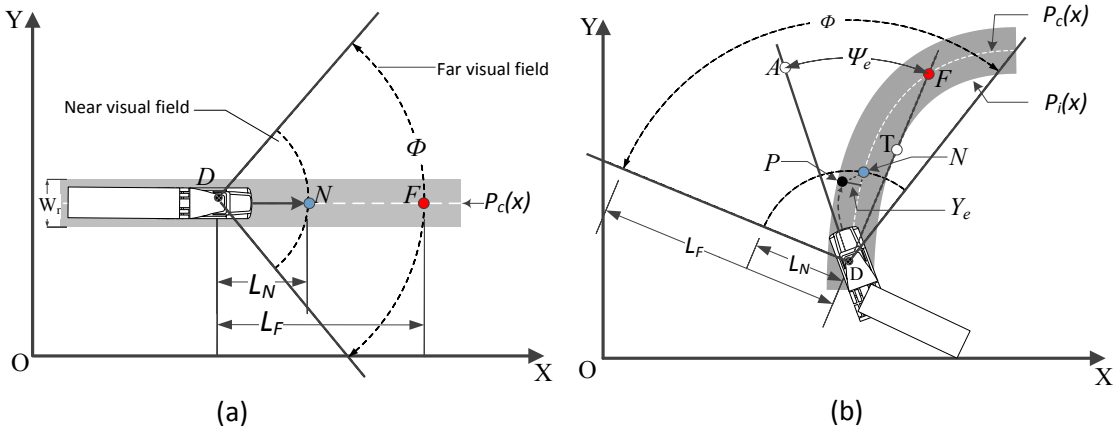

Figure 4.4: Estimation of the near and far preview points on: (a) a straight-line roadway; and (b) a curved path

During curve negotiation, the driver aims at near and far preview points within the overall visual field so as to minimize the lateral position and orientation errors of the vehicle, while maintaining a central lane position. The near preview point '*N*', located at

the near visual field boundary, is described by a function $P_c(x)$, such that $D_{PN} = L_N$. The driver's preview process to locate the near preview point on the centerline of the road $P_c(x)$ as a function of driver's seat coordinate (X_D, Y_D) and the near preview distance L_N, can be mathematically expressed as:

$$P_c(X_N) = min\left\{L_N - \left(\sqrt{(x - X_D)^2 + (P_c(x) - Y_D)^2}\right)\Big|_{x=X_N}\right\} \tag{4.9}$$

where $(X_N,\ P_c(X_N))$ are coordinates of the near preview point on the centerline of the desired path. In the above equation, $P_c(x)$, may be described a function or by a look-up table.

For a given forward speed, the near preview distance is assumed to be a constant for both the straight-line and the curved paths, while the far preview distance varies substantially with the path curvature. The driver locates the far preview point by projecting a tangent line to the inside edge of the previewed path (line *DF*), as shown in Figure 4.4(b). The coordinates of the tangent point *T* on the inside edge of a curved roadway $P_i(x)$, can be related to the driver's seat coordinate (X_D, Y_D) in the following manner:

$$P_i(X_T) = min\left\{\left(\frac{P_i(x) - Y_D}{x - X_D} - \frac{dP_i(x)}{dx}\right)\Big|_{x=X_T}\right\} \tag{4.10}$$

where $(X_T, P_i(X_T))$ are coordinates of the tangent point *T*, and $P_i(x)$ describes the inside edge of the roadway, which is parallel to $P_c(x)$ but shifted laterally by 1.85 m for a standard lane width of the high-speed divided highways [159].

The intersection of the tangent line with $P_c(x)$ within the far preview field is considered as the far preview point *F*, as shown in Figure 4.4(b). During curve negotiation, the far preview distance, D_{PF}, is generally less than L_F, but approaches L_F on

straight-line segments. The point F may also lie beyond the far visual field for relatively large curve radius. In this case, the far preview point is considered to lie on the boundary of the far visual field, leading to $D_{PF} = L_F$. The temporal field of vision is employed when the driver fails to identify the preview points on the road surface within the overall visual field of 120˚ due to possibly excessive road curvature or vehicle orientation [157].

The instantaneous lateral position error of the vehicle, Y_e, is assessed by the driver from the predicted tractor path, shown as point P in Figure 4.5, with respect to the near preview point N. The coordinates of point P, (X_P, Y_P), are obtained using the 'internal vehicle model', described in section 4.3.1, considering the near preview interval $T_{PN}=L_N/v_x$. This position error is normal to line (DN), and is given by (Figure 4.5):

$$Y_e = \left(\sqrt{(X_N - X_P)^2 + (Y_N - Y_P)^2}\right) sin\,\theta_n \tag{4.11}$$

where:

$$\theta_n = tan^{-1}\left(\frac{Y_N - Y_D}{X_N - X_D}\right) + tan^{-1}\left(\frac{Y_N - Y_P}{X_N - X_P}\right) \tag{4.12}$$

The far preview point is also applied to determine the instantaneous orientation error of the vehicle, Ψ_e, defined as the angle between the vehicle longitudinal axis passing through point D (AD) and the far preview distance line (FD), as seen in Figure 4.4(b).

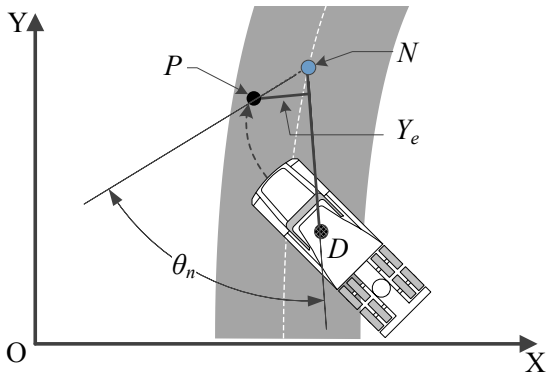

Figure 4.5: Estimation of the lateral position error

4.3.3 Decision Making Process

The decision making process involves the driver's strategy to simultaneously compensate for both the estimated lateral position and orientation errors, which have been described by a first-order lead-lag and a proportional gain function, respectively [72]. The compensation functions corresponding to the lateral position and orientation errors have been widely expressed by the well-known crossover model [29], which implies that the driver undertakes compensations so as to realize a stable and well-damped non-oscillatory vehicle response in the vicinity of the crossover frequency. The crossover model, however, may lead to substantial tracking errors and a directional instability at frequencies distant from the crossover frequency, which are mostly attributed to the lead-lag compensation strategy [9,32]. The decision making process of the human driver, $G_3(s)$, as shown in Figure 4.3, may thus be expressed as a function of the position and orientation errors together with the perception of vehicle states Z_j:

$$G_3(s) = \left(K_1 \frac{T_L S + 1}{T_I S + 1} Y_e + K_2 \Psi_e + \sum_{j=3}^{7} K_j Z_j \right) \mathrm{e}^{-\tau_p \mathrm{s}} \tag{4.13}$$

where K_j (j=1 to 7) represent proportional compensatory actions of the driver with respect to the estimated lateral deviation and orientation errors of the tractor unit, and the selected perceived motion states of both the tractor and semi-trailer units, Z_j (j=3 to 7).

Under medium- and low-speed steering maneuvers, it is hypothesized that driver is able to track the desired path by considering only the lateral position and orientation errors of the vehicle that has been commonly employed in reported studies on two-axle vehicles [7,8,10,12-26]. The driver's perception of the lateral position and orientation errors alone, K_j=0 (j=3 to 7), is thus used to formulate the 'baseline driver model'. In the

case of articulated vehicles, it is suggested that a qualitative perception of additional vehicle states can help the driver to improve the path tracking performance during high speed emergency situations [11]. Considering only the lateral dynamics of the articulated vehicle using the yaw-plane vehicle model, the additional vehicle states in the above formulation are limited to lateral accelerations and yaw rates of the tractor and semi-trailer units (a_{y1}, a_{y2}, r_1 and r_2) and articulation rate ($\dot{\gamma}$). The effect of human driver's perception on the path-tracking performance are further investigated by considering combinations of nine different motion cues of the vehicle in Chapter 6. In Eq. (4.13), τ_p is the processing time delay of the human's central nervous system, which is determined using the regression model formulated on the basis of the simulator-measured data, Eq. (3.2). The compensation gains, K_1 to K_7, are identified through minimization of a composite performance index comprising the steering effort, path tracking and directional dynamic measures of the vehicle.

The driver's compensatory command is subsequently transmitted to the vehicle steering system through the limb motions. The limb and steering motion function, $G_4(s)$, is a coupled function of the muscles and steering dynamic $G_m(s)$, reference model $R_m(s)$, the muscles reflex model $H_m(s)$ and active muscle stiffness function $K_m(s)$ [67]. Each element of the limb and steering motion function is mathematically expressed in Eqs. (1.11) to (1.13), described in section 1.2.5. The coupled muscles and steering dynamic is characterized considering muscular dynamics of the human hand-arm and the steering system relating the front-wheels steering, δ_F, to driver's steering command, δ_d, as shown in Figure 4.3, is described in the following manner:

$$G_4(s) = \frac{\delta_F(s)}{\delta_d(s)} = \frac{R_m(s)G_m(s) + H_m(s)G_m(s) + K_m G_m(s) - G_m(s)}{1 + H_m(s)G_m + K_m G_m(s)} \tag{4.14}$$

4.4 Coupled Driver-Single-Unit Vehicle Model

It is hypothesized that the driver can effectively track a desired path by considering the lateral position and orientation errors of the vehicle. A 'baseline driver model' structure is thus initially formulated using the lateral position and orientation errors together with the proposed two-stage path preview strategy. The driver model coupled with the single-unit vehicle model, as shown in Figure 4.6, includes four essential elements of the driver steering process, $G_1(s)$, $G_2(s)$, $G_3(s)$ and $G_4(s)$, described in section 4.3. In the figure, Y and Y_{Tp} are the perceived lateral coordinates and the predicted position of the vehicle cg at a future instant, respectively. This initial model was limited to a two-axle vehicle so as to examine the validity of the proposed driver model using the simulator-measured data. The simulations are performed assuming a constant perception time τ_{pd}, selected as 0.1 s [5,144]. The minimum perceivable heading error and lateral position error of the driver, reported by Bigler and Cole [37], are set as 0.025 deg and 0.025 D_{pi} (i=N,F), respectively, where D_{pi} is the preview distances corresponding to the near and far target points. The baseline driver model parameters are identified through minimization of a performance index. A generalized performance index comprising different vehicle dynamic and driver characteristics has been formulated and solved subject to inequality constraints describing practical ranges of human control parameters (Table 1.7).

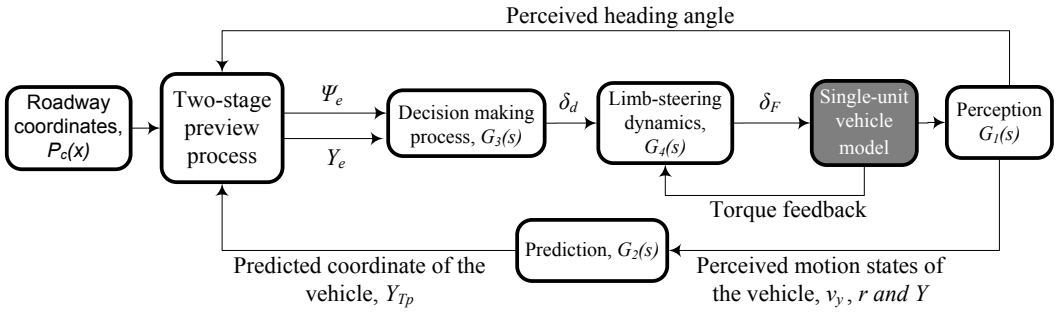

Figure 4.6: The two-stage preview driver coupled with the single-unit vehicle model

The validity of the identified human driver model is illustrated for the standardized double lane-change maneuvers for a range of operating and visual conditions at different forward speeds (30, 50 and 70 km/h). As it was discussed in section 3.6.3, the data obtained with majority of the 'novice' drivers revealed substantial path deviations and steering oscillations, particularly under the foggy road condition. For the purpose of model validation, the data obtained for only 'average' and 'experienced' drivers, were thus considered.

4.4.1 A Generalized Performance Index

A generalized performance index for a single-unit vehicle was formulated as a composite function of normalized lateral deviation, orientation error, magnitude and rate of steering angle, lateral acceleration and yaw rate of the vehicle, such that:

$$J_t = J_Y + J_\Psi + J_\delta + J_{\dot{\delta}} + J_{a_y} + J_r \tag{4.15}$$

where J_Y and J_Ψ are the weighted mean square lateral deviation and orientation error of vehicle cg, given by:

$$J_Y = \frac{1}{T}\int_0^T \left[\frac{Y_e(t)}{Y_{e,max}}\right]^2 dt;\; J_\Psi = \frac{1}{T}\int_0^T \left[\frac{\Psi_e(t)}{\Psi_{e,max}}\right]^2 dt \tag{4.16}$$

where T is the simulation time, and $Y_{e,max}$ and $\Psi_{e,max}$ are the maximum allowable deviations in the lateral displacement and orientation errors, selected as 0.5 m and 10 deg, respectively. These have been selected on the basis of the geometrical specification of the roadway and the vehicle track width.

The indices J_δ and $J_{\dot{\delta}}$ in Eq. (4.15) describe the weighted mean squared steering angle and its rate, which relate to the driver's steering effort:

$$J_\delta = \frac{1}{T}\int_0^T \left[\frac{\delta_F(t)}{\delta_{F,max}}\right]^2 dt \;;\; J_{\dot{\delta}} = \frac{1}{T}\int_0^T \left[\frac{\dot{\delta}_F(t)}{\dot{\delta}_{F,max}}\right]^2 dt \tag{4.17}$$

where $\delta_{F,max}$ and $\dot{\delta}_{F,max}$ represent the steer angle and steer rate corresponding to the front wheels of the vehicle, which are established from the regression models, Eqs. (3.3) and (3.4), in forward speed and driving experience, ranging from 3.2 deg for 'experienced' at 30 km/h to 5.7 deg for 'novice' at 70 km/h, and 4.2 deg/s for 'experienced' at 30 km/h to 9.1 deg/s for 'novice' at 70 km/h. The reported studies, however, observed wider ranges of the drivers' peak steer angles and peak steer rates that are invariably measured on the steering wheel. Considering the steering ratio equal to 15 for the single-unit vehicle considered in this study, the peak steer angle and peak steer rate could range from 5.3 to 12.5 deg, and 10.7 to 49.7 deg/s, respectively [132]. The wide ranges of observation are mostly attributed to variations in the forward speed, driver skill and objective of the experiment. For instance, the peak steer rate of 49.7 deg/s is acquired during a high speed double lane-change maneuver performed by experienced drivers to examine the active safety features of the vehicle.

The indices J_{a_y} and J_r are the weighted mean squared lateral acceleration and yaw rate of the vehicle, given by:

$$J_{a_y} = \frac{1}{T}\int_0^T \left[\frac{a_y(t)}{a_{y,max1}}\right]^2 dt \; ; \; J_r = \frac{1}{T}\int_0^T \left[\frac{r(t)}{r_{max1}}\right]^2 dt \tag{4.18}$$

where $a_{y,max1}$ and r_{max1} are the maximum lateral acceleration and yaw rate of the vehicle, which are selected as 0.7g and 10 deg/s. These values are determined based upon the measured responses acquired through the driving simulator experiment, described in section 3.6, which are considered similar to the reported studies [5,158].

4.4.2 Validation of the Coupled Driver-Vehicle Model - Clear Visual Field

The 'baseline driver model' based on the lateral position and orientation errors is integrated with the yaw-plane model of the single-unit vehicle, presented in section 2.2, to obtain the coupled driver-vehicle model. The control parameters of the driver model are determined through minimization of the generalized performance index, as described in Eq. (4.15). These include the compensatory gains corresponding to the lateral position and orientation errors, K_1 and K_2, lead and lag time constants, T_L and T_I, and near and far preview times, T_{PF} and T_{PN}. Variations in the peak steer angle and peak steer rate, Eqs. (3.3) and (3.4), in the generalized performance index relate to variations in the driving skill of the driver model. Figure 4.7 illustrates the driver model parameters obtained for the two-stage preview driver model corresponding to 'experienced' and 'average' drivers for the standardized double lane-change maneuvers at three selected forward speeds.

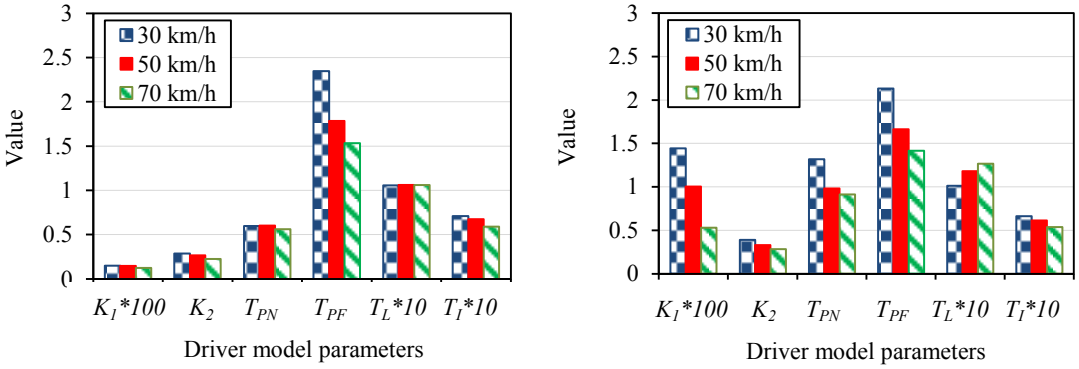

Figure 4.7: Variations in control parameters of the driver model during a double lane-change maneuver at different speeds: (a) 'experienced' driver; and (b) 'average' driver (clear visual field)

The results suggest that the 'average' driver requires notably greater lateral position (K_1) and relatively higher orientation errors compensatory gains (K_2) compared to the 'experienced' driver, suggesting greater effort by the 'average' driver to minimize the

path deviation and orientation error, irrespective of the forward speed. The results suggest that the near and far preview times, T_{PN} and T_{PF}, decrease with increase in speed, while the near and near preview distances (D_{PN} and D_{PF}) increase with speed for both the 'experienced' and the 'average' driver models. While the 'experienced' drivers employ greater far preview distances (D_{PF}=19.9, 25.2 and 29.4 m for 30, 50 and 70 km/h, respectively) compared to the 'average' driver (D_{PF}=17.1, 22.8 and 23.7 m for 30, 50 and 70 km/h, respectively), the 'experienced' drivers employ lower near preview times compared to the 'average' drivers in the entire range of the selected speeds. This suggests that 'average' drivers tend to employ a smaller segment of the previewed roadway to obtain the path information. The 'experienced' drivers, on the other hand, simultaneously look at both the distant and very near segments of the roadway.

The results also suggest that the lead time constant T_L increases and the lag time constant decreases with increase in speed for both the driver models, suggesting a higher level of prediction and faster steering responses at higher speeds. Furthermore, the results suggest relatively higher lead time constant of the 'average' driver compared to the 'experienced' driver, particularly at higher speeds that shows a higher level of predictive control and thus mental workload of 'average' drivers at higher speeds driving [78,131]. The results clearly show notable differences between the 'average' and 'experienced' drivers in terms of: (i) lateral position error compensatory gain; (ii) far and near preview times; and (iii) the lead time constant, which are primarily attributed to varying steering responses of drivers with different driving skills.

The time histories of the measured lateral vehicle position and steer angle were further examined to determine validity of the proposed driver model in view of the path tracking

and steering responses. Figures 4.8 and 4.9 compare the model responses with the measured data for the average and experimental drivers, respectively. The figures show mean measured data together with the error bars (ranges of measured data). Comparison of the simulation and measured responses suggest that the proposed two-stage driver model provides relatively good predictions of the drivers' steering response with varying driving skills.

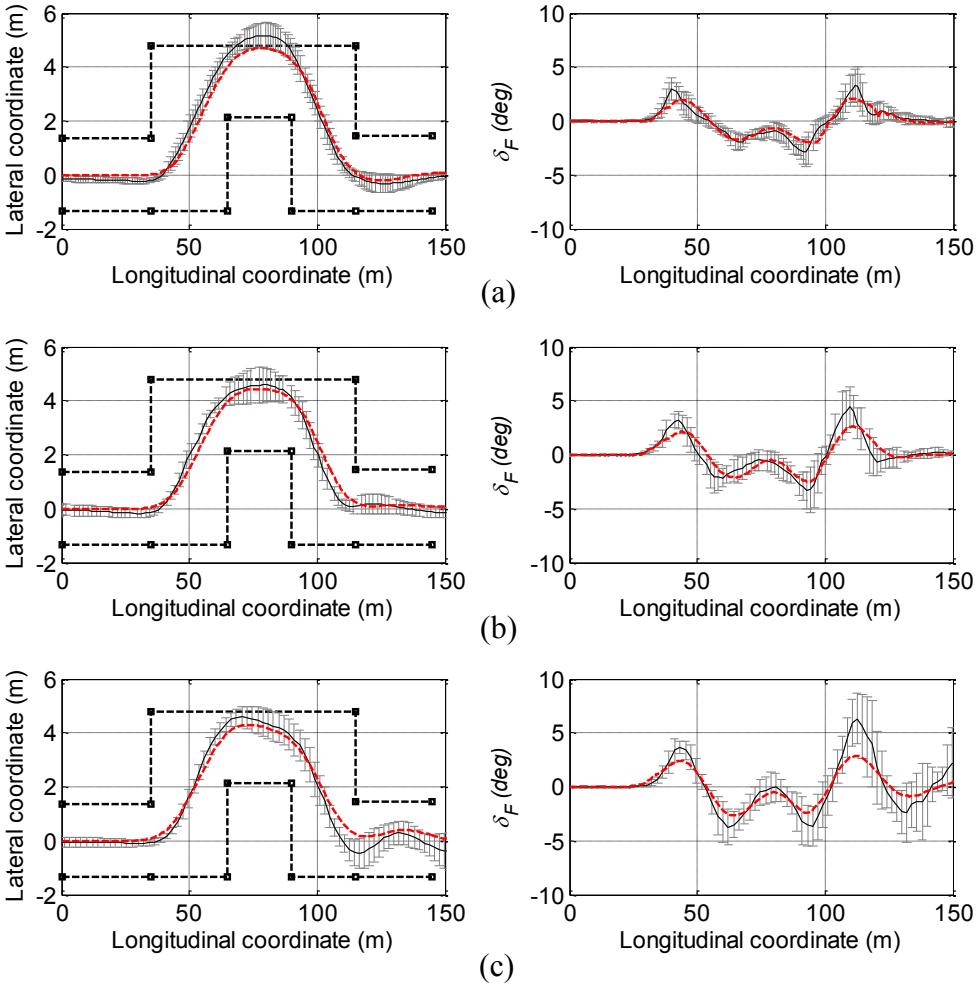

Figure 4.8: Comparisons of measured path tracking and steering responses (solid line) with the model responses (dashed line) for the 'average' driver group under a double lane-change maneuver at different speeds: (a) 30 km/h; (b) 50 km/h; and (c) 70 km/h (clear visual field)

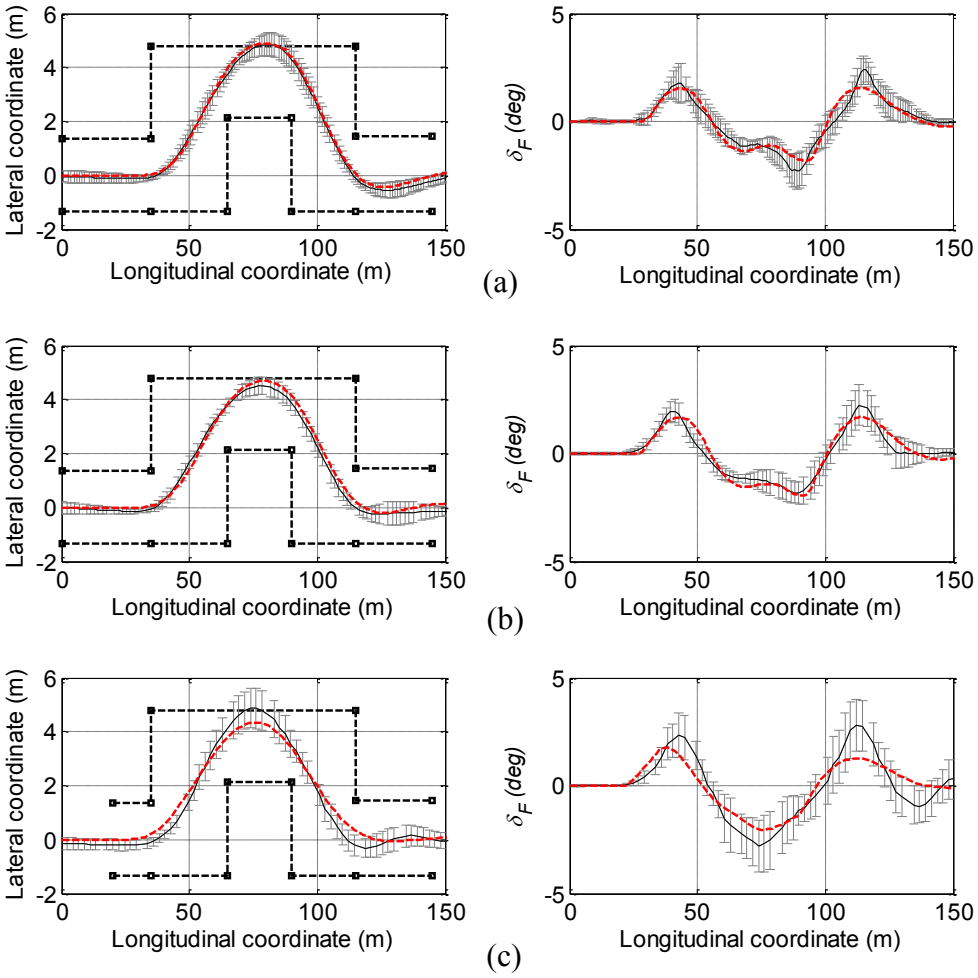

Figure 4.9: Comparisons of measured path tracking and steering responses (solid line) with the model responses (dashed line) for the 'experienced' driver group under a double lane-change maneuver at different speeds: (a) 30 km/h; (b) 50 km/h; and (c) 70 km/h (clear visual field)

4.4.3 Validation of the Coupled Driver-Vehicle Model - Limited Visual Field

The validity of the proposed driver model in the limited visibility condition was also examined by comparing the model responses with the measured responses for both driver groups. The control parameters of the two drivers groups were identified through minimization of the generalized performance index, described in Eq. (4.15). The limited visual field corresponding to the foggy condition was simulated by limiting the maximum

previewed distance to 20m. The far preview times were thus limited to 2.4, 1.4 and 1.0 s for the 30, 50 and 70 km/h speeds, respectively. The parameters obtained for two groups of driving skills (average and experienced) and three selected forward speeds are shown in Figure 4.10.

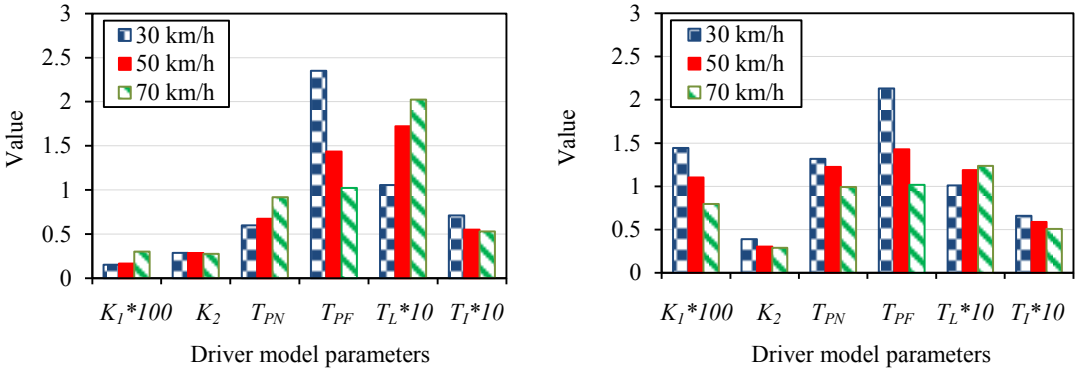

(a) (b)

Figure 4.10: Variations in control parameters of the driver models during a double lane-change maneuver at different speeds: (a) 'experienced' driver; and (b) 'average' driver (limited visibility field)

The results yield similar path tracking and steering responses of both drivers groups at 30 km/h, since the far preview distances were lower than the defined limit (20 m). The 'average' driver model revealed only minimum changes in the control parameters at 50 km/h, when compared to those obtained for clear visual field. At the higher speed of 70 km/h limiting the preview distance resulted in more than 50% increase in the lateral position compensatory gain. This suggests higher steering effort by the driver at the higher speed to track the desired roadway in limited visibility condition. Very similar preview times for both the far and near preview are also evident for the 'average' drivers, suggesting that the driver previews a smaller segment of the roadway to obtain the required path information. The variations in the all control parameters (K_1, K_2, T_{PN}, T_{PF},

T_L and T_I) with changing of the speed revealed trends comparable to those obtained in clear visibility condition (section 4.4.2).

While decrease in visible road distance yields only slight influence on the path tracking and steering responses of the ‘average’ driver model, the ‘experienced’ driver model shows considerable variations in all the control parameters, particularly at the higher speed of 70 km/h. Introducing the foggy road condition yields substantial increase in lateral position compensatory gain of the 'experienced' driver model at the higher speed of 70 km/h. The gain value is over 130% of that obtained for clear visibility condition. Further, in the absence of the far target point, owing to the limited far preview, the near preview time of the 'experienced' driver model increases with speed. Comparable near and far preview times are thus identified for the higher speeds, suggesting similar preview strategy of the ‘experienced’ as well as ‘average’ drivers under limited visual field. The lower lateral position error compensatory gain of the ‘experienced’ driver compared to the ‘average’ driver model at 50 and 70 km/h also results in notable increase in the lead time constant. This suggests that while the ‘experienced’ driver model tends to employ less steering effort to minimize the path deviation, the driver needs to employ considerably greater predictive control to achieve satisfactory path tracking performance.

The time histories of the measured lateral position and front wheel steer angle of the vehicle for the double lane-change maneuvers under foggy condition are compared with the responses of the ‘average’ and ‘experienced’ driver models in Figures 4.11 and 4.12, respectively. The error bars in the figures indicate the ranges of the measured data. From the comparisons, it is deduced that the proposed two-stage driver model can provide

reasonably good predictions of the human steering control actions under limited visibility conditions.

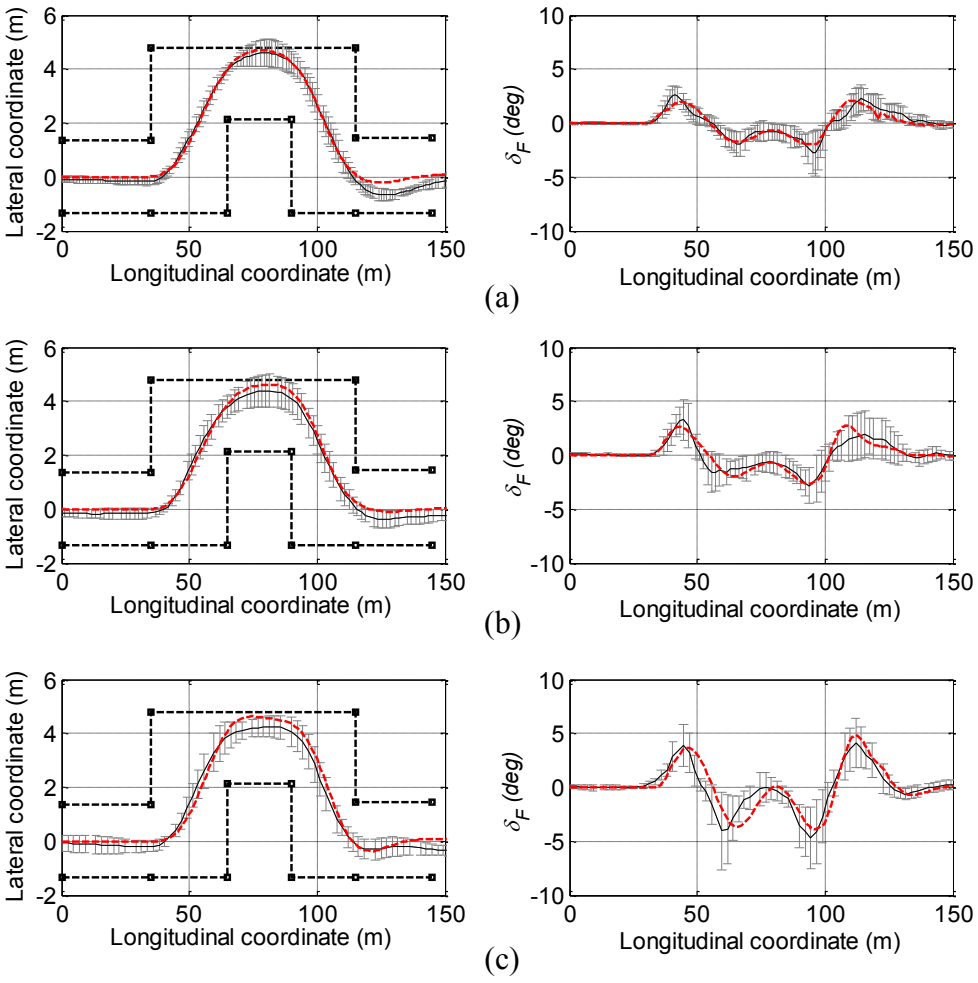

Figure 4.11: Comparisons of measured path tracking and steering responses (solid line) with the model responses (dashed line) for the 'average' driver group under a double lane-change maneuver at different speeds: (a) 30 km/h; (b) 50 km/h; and (c) 70 km/h (limited visual field)

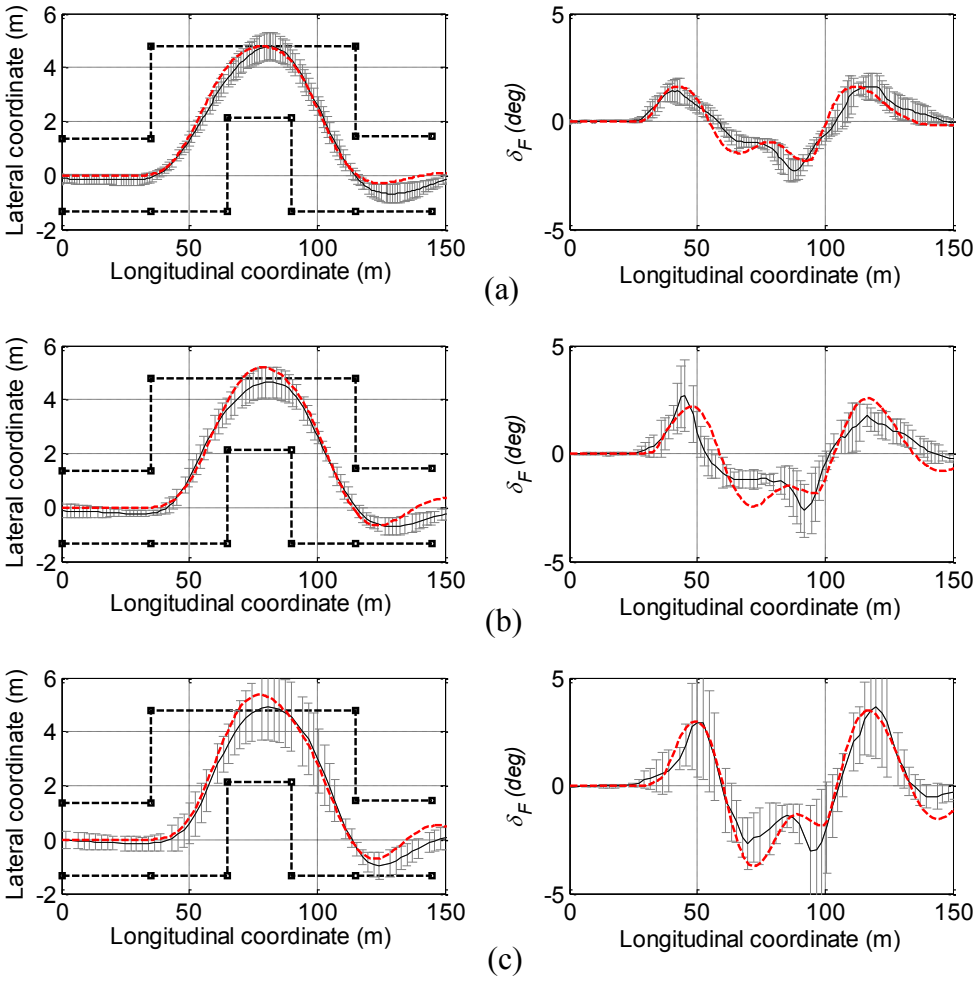

Figure 4.12: Comparisons of measured path tracking and steering responses (solid line) with the model responses (dashed line) for the 'experienced' driver group under a double lane-change maneuver at different speeds: (a) 30 km/h; (b) 50 km/h; and (c) 70 km/h (limited visual field)

4.5 Coupled Driver-Articulated Vehicle Model

The coupled driver-articulated vehicle model is developed by integrating the proposed two-stage preview baseline driver model, based on the lateral position and orientation errors, to the three DoF yaw-plane articulated vehicle model, described in section 4.2.1 (Figure 4.13). The coupled model is evaluated to study the path-tracking performance, steering responses and control limits of the vehicle driver in conjunction with a

commercial freight vehicle. In Figure 4.13, Y and Y_{Tp} are the perceived instantaneous lateral coordinates and the predicted position of the tractor cg at a future instant T_P, respectively.

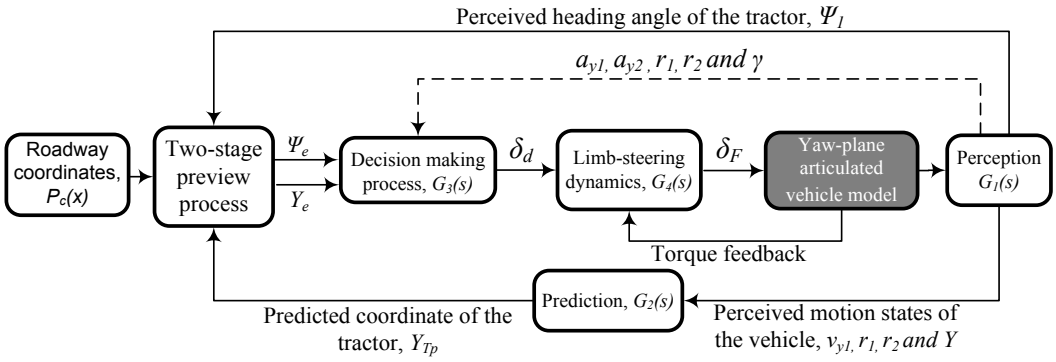

Figure 4.13: The baseline driver model coupled with an articulated vehicle model (solid line) and the additional perceived motion states of the vehicle (dashed line) corresponding to structures 2 to 10

The control parameters of the driver model are identified by minimizing a generalized performance index, subject to limit constraints on the driver control parameters (Table 1.7). The generalized performance index for the articulated vehicle system, however, may involve additional driver cues arising from directional responses of the units. The performance index is thus formulated considering the articulation rate, lateral accelerations and yaw rates of both the units in addition to the indices related to Y_e, Ψ_e, δ_F and $\dot{\delta}_F$, such that:

$$J_t = J_Y + J_\Psi + J_\delta + J_{\dot{\delta}} + J_{\dot{\gamma}} + J_{a_{y1}} + J_{a_{y2}} + J_{r_1} + J_{r_2} \tag{4.19}$$

where J_Y and J_Ψ refer to the weighted mean square lateral deviation and orientation error of the tractor cg. These are identical to those defined for the single-unit vehicle in Eq. (4.16). The J_δ and $J_{\dot{\delta}}$, indices describe the weighted mean squared steering angle and its rate, which relate to the driver's steering effort:

$$J_{\delta} = \frac{1}{T}\int_0^T \left[\frac{\delta_F(t)}{\Delta\delta_F}\right]^2 dt \; ; J_{\dot{\delta}} = \frac{1}{T}\int_0^T \left[\frac{\dot{\delta}_F(t)}{\Delta\dot{\delta}_F}\right]^2 dt \tag{4.20}$$

where δ_F and $\dot{\delta}_F$ are the steer angle and steer rate of the front wheels, respectively, and $\Delta\delta_F$ and $\Delta\dot{\delta}_F$ represent the corresponding maximum values as per the human driver's capabilities, which are obtained from the reported measured data ($\Delta\delta_F$=6.2 deg and $\Delta\dot{\delta}_F$=24.8 deg/s) [132]. The steering gear ratio is assumed to be 30 [149]. The terms $\Delta\delta_F$ and $\Delta\dot{\delta}_F$ differ from those measured in this study using the single-unit vehicle, which were denoted as simulator $\delta_{F,max}$ and $\dot{\delta}_{F,max}$ in Eq. (4.17). The differences are likely due to wide variations in the steering system design, steering dynamics of various vehicles and experiment conditions. Furthermore, measured data revealed considerable variations in $\delta_{F,max}$ and $\dot{\delta}_{F,max}$ with varying vehicle speed and drivers' skill. Consequently, the reported constant values of the peak steer angle and peak steer rate, $\Delta\delta_F$ and $\Delta\dot{\delta}_F$, are employed considered in the generalized performance index for the coupled driver-articulated vehicle system model.

The term $J_{\dot{\gamma}}$ in Equation (4.23) describes the weighted mean squared articulation rate $\dot{\gamma}$, given by:

$$J_{\dot{\gamma}} = \frac{1}{T}\int_0^T \left[\frac{\dot{\gamma}}{\dot{\gamma}_{max}}\right]^2 dt \tag{4.21}$$

where $\dot{\gamma}_{max}$ is the maximum allowable articulation rate, which is selected as 8 deg/s and is related to the jackknife limit of articulated vehicles [159]. The weighted mean squared lateral accelerations (a_{y1} and a_{y2}) and yaw rates (r_1 and r_2) of both the tractor and the semi-trailer units are also integrated within the proposed performance index, such that:

$$J_{a_{yj}} = \frac{1}{T}\int_0^T \left[\frac{a_{yj}(t)}{a_{y,max2}}\right]^2 dt \; ; J_{r_j} = \frac{1}{T}\int_0^T \left[\frac{r_j(t)}{r_{max2}}\right]^2 dt \qquad j = 1,2 \tag{4.22}$$

where $a_{y,max2}$ and r_{max2} are defined as the maximum allowable lateral acceleration and yaw rate of unit j (j=1 for tractor and 2 for the semi-trailer unit), which are selected as 0.3g and 10 deg/s. The quantity $a_{y,max2}$ is related to the rollover threshold limits for the five-axle tractor-semitrailer combinations, which could range from 0.25g to 0.5g depending upon the vehicle loading and height of the vehicle cg [16,160-162]. The quantity r_{max2} is also related to the maximum reported yaw rates for both the units of the tractor-semi trailer vehicle during [9,16,163]

Figure 4.14 illustrates the front wheel steer angle, δ_F, and the path coordinates of the tractor cg coupled with the proposed 'baseline' driver model during a lane-change maneuver at a steady speed of 80 km/h. The control parameters of the driver model are obtained through minimization of the performance index, Eq. (4.19). Further discussions on the 'baseline driver model', and the influences of variations in selecting design and operating parameters on the driver control parameters are evaluated and presented in chapters 5 and 6. In Figure 4.14(a), the dashed line represents the centerline of the roadway, while the solid line describes the trajectory of the tractor cg.

The proposed two-stage preview 'baseline driver model' in conjunction with the equations of motion for the nonlinear three DoF articulated vehicle, presented in section 4.2.1, are solved under a lane-change maneuver, shown in Figure 4.14(a), at a steady speed of 68.8 km/h. The resulting steering response is compared with the measured data, reported by Fancher et al. [149], as shown in Figure 4.14(b), to demonstrate the validity of the proposed model and the identified parameters. The generalized performance index, Eq. (4.19), is minimized for identifying the driver model parameters of the two-stage baseline driver model, namely, K_1, K_2, T_{PN}, T_{PF}, T_L and T_I. Table 4.1 summarizes the

identified driver model parameters as well as the constant limb, steering and driver model parameters. The results suggest a good agreement between the model responses and the measured data.

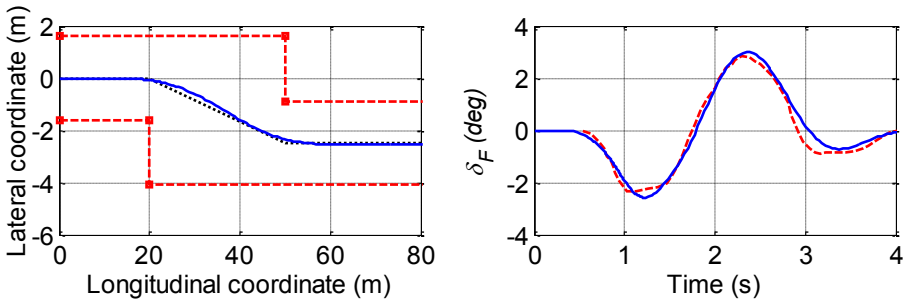

Figure 4.14: Comparisons of: (a) path tracking response; and (b) front wheel steer angle of the coupled driver-articulated vehicle model (solid line) with the measured data (dashed line) during a lane-change maneuver at a constant speed of 68.8 km/h [149] (Dotted line: centerline of the roadway)

Table 4.1**:** The steering system and the limb dynamic parameters, and the identified control parameters of the coupled driver-articulated model during a lane-change maneuver at 68.8 km/h

	Parameter	(unit)	Identified from	Value
Steering dynamics	J_{st}	(kg.m^2)	Ervin and Guy [148]	1.67
	K_{st}	(N.m/rad)	Ervin and Guy [148]	5.68
	B_{st}	(N.m.s/rad)	Ervin and Guy [148]	6.56
Driver limb dynamics	J_{dr}	(kg.m^2)	Pick and Cole [67]	0.064
	K_{dr}	(N.m/rad)	Pick and Cole [67]	3.8
	B_{dr}	(N.m.s/rad)	Pick and Cole [67]	0.56
	K_a	(kg.m^2)	Pick and Cole [67]	20
	B_r	(N.m.s/rad)	Pick and Cole [67]	1
	K_r	(N.m/rad)	Pick and Cole [67]	10
	ω_c	(rad/s)	Pick and Cole [67]	20
	τ_r	s	Pick and Cole [67]	0.04
	K_m	(kg.m^2)	Pick and Cole [67]	0.2
Perception delay time	τ_{pd}	s	Triggs and Harris [144]	0.1
Processing delay time	τ_p	s	Eq. (3.2)	0.285
Driver model parameters	K_1	m/rad	Minimization of Eq. (4.19)	0.016
	K_2	rad/rad	Minimization of Eq. (4.19)	0.651
	T_{PF}	s	Minimization of Eq. (4.19)	1.105
	T_{PN}	s	Minimization of Eq. (4.19)	1.727
	T_L	s	Minimization of Eq. (4.19)	0.131
	T_I	s	Minimization of Eq. (4.19)	0.091

4.6 Summary

The primary goal of this chapter was to formulate a two-stage preview driver model integrated with the single-unit vehicle model as well as the articulated vehicle model. The proposed model, referred to as the 'baseline driver model' aims to control the lateral position and orientation errors of the vehicle and involves four essential elements of the human driving process together with known control limits of the driver. Validity of the coupled driver and single-unit vehicle model was examined by comparing its path tracking and steering responses with the simulator-measured data under standardized double lane-change maneuvers at different selected speeds and two different visibility conditions. The results suggested reasonably good prediction of the human control actions using the proposed driver model. The baseline driver model was subsequently integrated to the articulated vehicle model. The steering responses of the coupled driver-articulated vehicle model during a steady speed lane-change maneuver were evaluated and compared to the reported measured data in order to examine the validity of the proposed two-stage preview driver model.

In the subsequent chapter, the two-stage preview baseline driver model is applied to investigate control characteristics of the human driver, and influences of variations in selected vehicle design parameters and the driving speed on the driver control characteristics. In chapter 6, a qualitative perception of additional vehicle states, namely, lateral accelerations and yaw rates of the tractor and semi-trailer units and articulation rate, are also integrated to the 'baseline driver model' to further investigation of relative contributions of different motion feedbacks to improve the path tracking performance of the vehicle during high speed steering maneuvers.

CHAPTER 5

IDENTIFICATION OF DRIVER'S CONTROL LIMITS

5.1 Introduction

The safety dynamic performance of a road vehicle is strongly influenced by the driving skill and control limits of the driver. The human driver is known to exhibit limited control capabilities in terms of reaction time and path error compensation, particularly in situations demanding critical steering maneuvers. These control limits have been associated with unsafe vehicle operations and may contribute to road accidents [1,9]. The reported studies related to human driving behavior mainly focus on formulation of steering control actions of the driver considering an ideal controller that can adjust its driving strategy to different operating conditions [7,9]. These ideal controllers, in general, perform specific steering maneuvers with little or no considerations of control limits of the human driver. A few studies have attempted to identify a range of driver control limits, although these have been mostly limited to single-unit vehicles [7,30,45,76]. The control of an articulated vehicle, however, may pose considerable demands on the drivers, due to their large dimensions and weight, and thus relatively lower stability limits compared to the light vehicles [26,151]. Further, the directional performance of an articulated vehicle is greatly influenced by its design parameters as well as the operating conditions. Considerable attempts are thus being made towards designs of active safety enhancement systems for such vehicles, while the contributions of the driver and its control limits are mostly ignored [25,26].

The human drivers, in general, have the capability to adapt to the vehicle through a qualitative assessment of the path tracking performance depending upon their driving skill and experience [16]. The vehicle driver can thus perform a steering maneuver within its control and performance limits, with varying vehicle design parameters and operating conditions. It is suggested that the directional and safety performance of the coupled driver-vehicle system can be improved by incorporating the control characteristics of the human driver in the vehicle design process [16]. Ideally, these parameters may be selected such that the driver can satisfy the path tracking and safety requirements under extreme conditions by minimum steering effort.

In this chapter, the proposed two-stage preview driver model structure, described as the 'baseline driver model' in chapter 4, is coupled with a yaw-plane articulated vehicle model. The two-stage preview is referred to as the driver's strategy to simultaneously compensate for both the estimated lateral position and orientation errors using two target points ahead of the vehicle. The coupled driver-articulated vehicle model is studied to investigate the control characteristics and steering effort demands of the human driver, and the influences of variations in selected vehicle design parameters and the driving speed on directional responses of the vehicle in clear visibility condition. The driver model parameters are identified through minimization of the generalized performance index, Eq. (4.19), considering variations in the vehicle parameters and the forward speed.

5.2 Identification of the Driver's Control Parameters

Assuming clear visibility condition, the performance characteristics of the coupled driver-articulated vehicle system are investigated under the standardized double lane-change steering maneuver [127] subject to different steady speeds and various vehicle

design parameters. The vehicle design parameters are lumped in two different groups: (i) geometry parameters (wheelbase, $L_{1,2}$, and tandem axle spread, $t_{1,2}$, of both the tractor and trailing units); and (ii) inertial parameters (the tractor and semi-trailer masses, $m_{1,2}$), as shown in Figure 5.1.

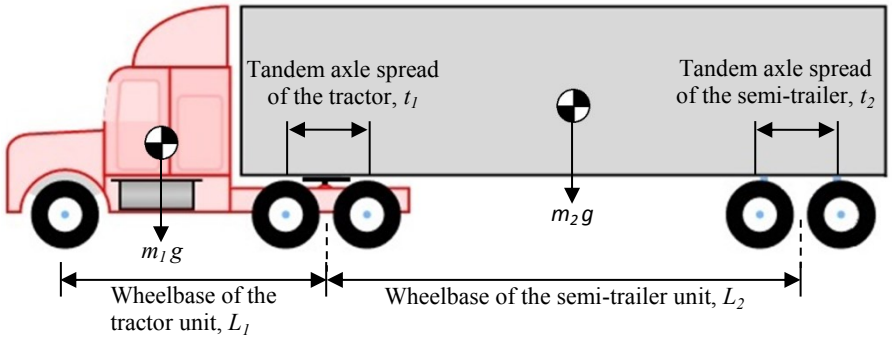

Figure 5.1: Schematic of a tractor and semi-trailer combination illustrating geometric and inertial parameters of interest

The 'baseline driver model' structure, formulated in section 4.3, is employed to study the control characteristics and performance limits of the driver in conjunction with the articulated vehicle model. The baseline driver model structure involves driver's estimations of the lateral position and orientation errors alone. Various control parameters of the driver model, namely, the lateral position and orientation error compensatory gains, near and far preview times, and the lead and lag time constants are identified through minimization of the generalized performance index, as described in Eq. (4.19), subject to limit constraints listed in Table 1.7. The peak values of a number of selected motion states of the coupled driver-articulated vehicle system and steering control action of the driver are then analyzed to identify threshold values of the human driver control measures under variations in the vehicle design parameters and operating conditions.

The performance index minimization process employs a constrained multi-variable optimization method with a set of 'initial values' of the driver model parameters. Due to the nonlinearity of the performance index function, which involves a number of local minimums, the accuracy of the minimization process depends upon the selection of the 'initial values'. Different initial values were thus considered in the parameter identification process. The model parameters were subsequently identified from different solutions of the minimization problem that resulted in lowest value of the performance index.

As an example, Figure 5.2 illustrates the solutions attained for three different sets of initial values, denoted as the 'estimated values'. The solutions were obtained for a double lane-change maneuver at a constant forward speed of 100 km/h. The results suggest that the compensatory gains associated with the lateral position and orientation errors, and near and far preview times of the driver model converge to nearly similar solutions. The estimated values of the lead and lag time constants, however, converge to somewhat different values for each set of initial values. A sensitivity analysis of the driver model parameters was thus undertaken to further investigate the relative contributions of the driver model parameters on the defined generalized performance index. The sensitivity analysis is also performed to study influences of variations in vehicle design parameters and forward speed on peak directional responses of the vehicle during a constant speed step-steer maneuver performed in an open-loop manner.

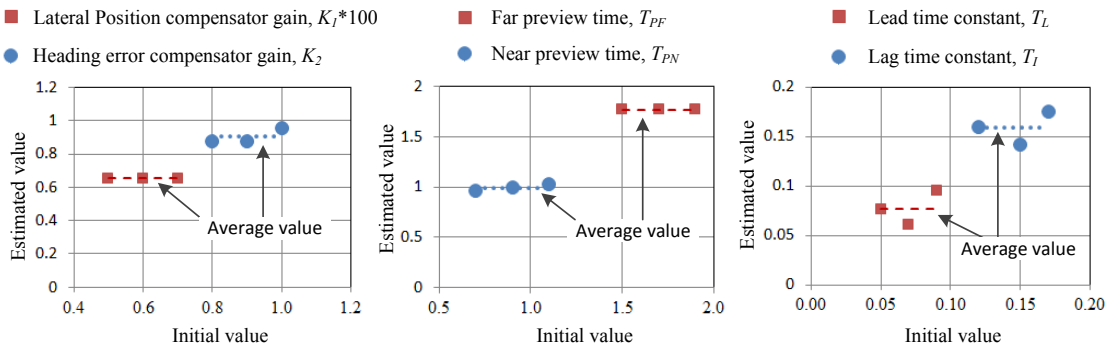

Figure 5.2: Variations in the optimization problem solutions corresponding to three different sets of initial values: (a) lateral position and orientation gains; (b) far and near preview times; and (c) lead and lag time constants

5.3 Sensitivity Analysis - Driver Model Parameters

In this section, influences of variations in the driver control parameters on various constituents of the generalized performance index are investigated. A set of driver model parameters is initially identified through minimization of the generalized performance index, referred to as the 'nominal driver model parameters'. The corresponding individual indices are referred as the 'nominal performance indices'. Subsequently, each of the driver model parameter is varied by ±20%, while all other parameters are held at their nominal values, and the resulting performance measures are determined. Percent variations in a performance index due to variations in a driver model parameter are determined from:

$$\vec{S}_{J_i} = \frac{J_i(\vec{p}_0 + \overrightarrow{\Delta p}) - J_i(\vec{p}_0)}{J_i(\vec{p}_0)} * 100\% \tag{5.1}$$

where $\vec{S}_{J_i}$ refers to the sensitivity of an index J_i ($J_t, J_Y, J_\Psi, J_{a_{y1}}, J_{a_{y2}}, J_{r_1}, J_{r_2}, J_{\dot{\gamma}}, J_\delta$ and $J_{\dot{\delta}}$) to variations $\overrightarrow{\Delta p}$ in the driver model parameter about the nominal values $\overrightarrow{p_0}$, while the parameter vector for the two-stage baseline driver model is given by:

$$\vec{p} = (K_1, K_2, T_{PN}, T_{PF}, T_L, T_I) \tag{5.2}$$

Table 5.1 summarizes the percentage variations in the total and individual performance indices with respect to their respective nominal values. A negative percentage value represents decrease and thus improvement in a performance measure with respect to its nominal value. The percentage variation in a performance measure could help determine the significance and influence of each driver model parameter on the coupled driver-vehicle system performance.

The results suggest that variations in each of the driver model parameter yield a higher value of the total performance index (J_t) suggesting the validity of the solution of the minimization problem. Increasing the lateral position and orientation compensatory gains (K_1 and K_2) help reduce the corresponding indices, J_Y and J_Ψ, by -1.7% and -9.1%, respectively. Enhanced path tracking performance, however, is achieved at the expense of greater steering effort of the driver, which can be seen from the substantially higher positive values of J_δ and $J_{\dot{\delta}}$. Employing more distant path information by increasing the near and far preview time (T_{PN} and T_{PF}) yields lower performance measures related to vehicle directional responses, namely, the articulation rate ($J_{\dot{\gamma}}$), lateral accelerations (J_{ay1} and J_{ay2}) and yaw rates (J_{r1} and J_{r2}) of both the units, while the path and orientation measures (J_Y and J_Ψ) tend to be substantially higher. The lower peak values of the motion states of the tractor and the trailing units suggest smoother steering input by the driver, which is also evident from lower value of J_δ. The rate of steering maneuver, $J_{\dot{\delta}}$, however, tends to be substantially higher. Increasing T_L and decreasing T_I by 20% yield only slight reductions in J_Y by 1.6% and 0.4%, respectively, the performance measures corresponding to steering effort of the driver (J_δ and $J_{\dot{\delta}}$) and motion variables of both units ($J_{\dot{\gamma}}, J_{ay1}, J_{ay2}, J_{r1}$ and J_{r2}), however, increased. These suggest greater steering effort

demands of the driver and relatively poor directional performance of the coupled driver-vehicle system.

Table 5.1: Percentage change of the total performance index and its constituents with variations in the driver model parameters

Control parameter	Variation (%)	Percentage change of the performance measures (%)									
		S_{Jt}	S_{JY}	$S_{J\Psi}$	S_{Jay1}	S_{Jay2}	S_{Jr1}	S_{Jr2}	$S_{J\dot{\gamma}}$	$S_{J\delta}$	$S_{J\dot{\delta}}$
K_1	-20	0.2	2.5	3.5	-2.8	-2.7	-3.1	-2.7	-4.5	-4.3	-17.7
	+20	0.3	-1.7	-1.1	2.4	2.3	3.0	2.3	5.4	4.9	25.7
K_2	-20	10.8	28.6	3.7	-7.6	-8.8	-10.3	-8.8	-19.1	-12.5	-17.7
	+20	8.2	8.8	-9.1	5.1	6.4	8.4	6.4	19.1	11.2	20.3
T_{PN}	-20	1.5	3.4	5.6	-1.8	-1.8	-1.1	-1.8	1.7	0.8	6.4
	+20	1.7	6.6	7.8	-5.3	-5.3	-4.9	-5.3	-3.0	-3.5	22.2
T_{PF}	-20	30.1	-24.9	-19.0	95.7	99.6	103.7	99.6	127.9	106.9	65.1
	+20	16.6	67.2	21.2	-45.9	-46.2	-43.3	-46.2	-32.0	-34.4	62.0
T_L	-20	0.1	2.3	1.9	-2.6	-2.6	-2.9	-2.6	-4.0	-3.5	-11.7
	+20	0.2	-1.6	-0.7	2.0	2.0	2.5	2.0	4.3	3.7	18.2
T_I	-20	0.1	-0.4	1.0	0.5	0.5	0.5	0.5	0.7	0.6	3.1
	+20	0.1	0.8	0.5	-0.9	-0.9	-0.9	-0.9	-0.8	-0.8	-1.2

The results also reveal that variations in the far preview time and orientation error compensatory gain yield the greatest effect on the performance measures of the coupled system and steering effort of the driver, while variations in the lead and lag time constants have the lowest influences on the total performance index J_t. The greater dependency of the estimated values of the T_L and T_I on their initial values, shown in Figure 5.2, is thus attributed to relatively lower influences of these two parameters on J_t. The lead and lag time constants, however, have greater effects on the path tracking performance (J_Y and J_Ψ) and steering effort of the driver (J_δ and $J_{\dot{\delta}}$) and thus cannot be excluded in formulation of the driver model (Table 5.1).

5.4 Sensitivity Analysis - Variations in Speed and Vehicle Design Parameters

The directional dynamic behavior of the vehicle is generally dependent on a number of design parameters and forward speed of the vehicle [135,159]. A sensitivity analysis of the selected motion states of the vehicle is thus undertaken with respect to variations in the vehicle design parameters and the driving speed. For this purpose, the forward speed, mass, wheelbase and tandem axle spread of both the units are increased by 20 percent with respect the nominal values, while the other parameters were held at their respective nominal values. Due to nearly linear variations in peak directional responses of the vehicle in the vicinity of the nominal design parameters, the sensitivity analyses in this section are limited to 20% increase in the vehicle parameters alone. Variations in the vehicle directional responses are evaluated in terms of (i) peak lateral accelerations of both units, $a_{y1}$and a_{y2}; (ii) peak yaw velocities of both units, $r_1$and r_2; and (iii) peak articulation rate, $\dot{\gamma}$. Table 5.2 summarizes the variations in the vehicle design and operating parameters considered in the sensitivity analysis.

It is suggested that variations in the wheelbase and mass of the tractor and the trailing units affect the yaw moment of inertia of the respective units [148]. Two empirical relations proposed by Ervin and Guy [148] are used to determine the yaw moment of inertia of the tractor and the semi-trailer units (I_{zz1} and I_{zz2}) with different wheelbases. The formulations are based on the load distributions of both the units, given by:

$$I_{zz1} = \left(\left(\frac{F_{z1}}{g} + 0.4 \frac{F_{z2} + F_{z3}}{g} \right) {a_1}^2 + 0.6 \left(\frac{F_{z2} + F_{z3}}{g} \right) \left(\frac{a_2 + a_3}{2} \right)^2 \right) \frac{1}{g} \qquad (5.3)$$

$$I_{zz2} = \frac{F_{z4} + F_{z5}}{F_{z4,0} + F_{z5,0}} \left(\frac{L_2}{L_{2,0}} \right)^2 I_{zz2,0} \qquad (5.4)$$

where a_k is the longitudinal distance from axle k (k=1,2 and 3) to the center of gravity of the tractor, F_{zk} is normal load on k^{th} axle (k=1,2,3,4,5) of the articulated vehicle combination and L_2 represents wheelbase of the semi-trailer. In the above formulation, the subscripts "0" refer to nominal values of the yaw moment of inertia, wheelbase and normal axle loads of the semi-trailer unit, respectively.

It should be noted that considering fixed distribution of the weights on different axles, variations in the wheelbases of both the units do not affect the cg position of the respective unit. Equations (5.3) and (5.4) further suggest that variations in the geometric parameters yield greater influences on yaw moment of inertia compared to variations in the inertial parameters. In this study variations in yaw moment of inertia of both the units are thus assumed to vary only due to considered changes in the geometric parameters.

Table 5.2: Range of vehicle parameters and the nominal values employed in sensitivity analysis

	Nominal value	Parameter values
Forward speed, v_x (km/h)	100	100 120
Mass of the tractor, m_1 (kg)	7269.6	7269.6 8723.5
Mass of the semi-trailer, m_2 (kg)	18416	18416 22099.2
Wheelbase of the tractor, L_1 (m)	3.6	3.6 4.3
Wheelbase of the semi-trailer, L_2 (m)	10.4	10.4 12.5
Tandem axle spread of the tractor, t_1 (m)	1.3	1.27 1.52
Tandem axle spread of the semi-trailer, t_2 (m)	1.3	1.27 1.52

Considering the yaw-plane articulated vehicle model, described in Appendix A, as a time-invariant system, the response vector of the vehicle can be expressed as:

$$\dot{\vec{x}} = f(\vec{x}, \vec{p}, t) \tag{5.5}$$

where $\vec{x} = (v_{y1}, r_1, r_2)$ is the state vector and $\vec{p} = (p_1, p_2, \dots, p_r)$ is the r-dimension vector of the vehicle design parameters and the forward speed. The influences of parameters variations on steering characteristics of the vehicle are investigated by considering:

$$\vec{p} = \overrightarrow{p_0} + \overrightarrow{\Delta p} \tag{5.6}$$

where $\overrightarrow{\Delta p}$ is the variation about the nominal vector $\overrightarrow{p_0}$, while the parameter vector for the articulated vehicle model is given by:

$$\vec{p} = (v_x, m_1, m_2, L_1, L_2, t_1, t_2) \tag{5.7}$$

The sensitivity of the peak response ($\vec{S}_{x,max}$) of the open-loop articulated vehicle to variations in vehicle parameters is described by the percentage change in a peak response, $\vec{x}_{max} = g(\vec{p})$, with respect to its nominal value, $\vec{x}_{0,max} = g(\vec{p}_0)$:

$$\vec{S}_{x,max} = \frac{\mathrm{g}(\vec{p}_0 + \overrightarrow{\Delta p}) - \mathrm{g}(\vec{p}_0)}{\mathrm{g}(\vec{p}_0)} * 100\% \tag{5.8}$$

Figure 5.3 illustrates the coordinates of the tractor cg during a step-steer input (δ_F = 1.0 deg) at a speed of 100 km/h subject to 20% increase in each of the vehicle design parameter, as listed in Table 5.2. The results suggest considerable variations in the steering characteristics of the vehicle. The results suggest that steering characteristics of the vehicle tend to vary from understeer to oversteer with increase in the semi-trailer mass. Increase in the tractor's mass and wheelbase, on other hand, increase the understeer tendency of the vehicle. Variations in wheelbase of the trailing unit and tandem axle spreads of both units, however, yield negligible changes in steering characteristics of the vehicle.

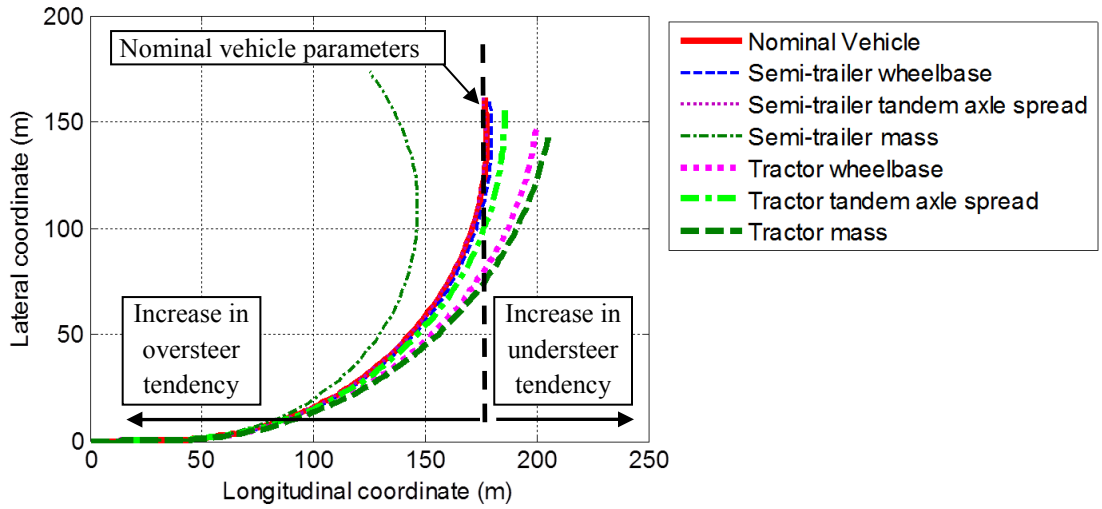

Figure 5.3: Path coordinates of the tractor cg during an open-loop step-steer maneuver at 100 km/h with 20% increase in selected geometric and inertial parameters

Table 5.3 summarizes the results from the sensitivity analysis of the vehicle model subject to 20 percent increase in selected vehicle design parameters. The percentage variations in the peak directional responses of the articulated vehicle are evaluated using Eq. (5.8). A positive and negative percentage value, respectively, represents an increase and decrease in the peak motion state with respect to that obtained for the nominal vehicle design parameters.

The results suggest that the peak directional responses of an articulated vehicle are primarily affected by variations in the forward speed and mass of the trailing unit, while increase in the wheelbase and tandem axle spread of the semi-trailer have the lowest effect. Increasing in mass, wheelbase and the tandem axle spread of the tractor unit resulted in decrease in all the peak directional responses of vehicle. This can be attributed to increasing understeer tendency of the vehicle. A 20 percent increase in the mass and tandem axle spread of the semi-trailer unit yields an increase in all the selected responses of the vehicle, although the influences of tandem axles spread are relatively small

compared to that of the semi-trailer mass. Further, an increase in the semi-trailer wheelbase yields slight reduction in lateral accelerations and yaw rates of both the tractor and semi-trailer units, while it increases the articulation rate of the vehicle. This suggests that an increase in the semi-trailer wheelbase may slightly improve the roll stability of the vehicle, the jackknife potential may increase with a longer trailing unit.

Table 5.3: Percent changes in peak directional responses of the articulated vehicle with 20% increase in the selected parameters

	Percentage change of the peak directional responses (%)				
	a_{y1}	r_1	a_{y2}	r_2	$\dot{\gamma}$
Forward speed, v_{x1}	61.1	39.8	67.1	39.1	25.5
Tractor mass, m_1	-18.2	-17.5	-18.0	-18.0	-9.9
Tractor wheelbase, L_1	-14.7	-14.7	-14.7	-14.7	-12.6
Tractor tandem axle spread, t_1	-5.5	-5.4	-5.5	-5.5	-4.5
Semi-trailer mass, m_2	32.5	33.0	33.1	33.0	16.1
Semi-trailer wheelbase, L_2	-0.2	-0.3	-0.2	-0.2	1.9
Semi-trailer tandem axle spread, t_2	0.4	0.4	0.4	0.4	0.1

5.5 Identification of Control Limits of the Driver

The identified driver model parameters and the peak directional response quantities of the coupled driver-articulated vehicle system are evaluated considering variations in the selected geometric and inertial parameters, and the forward speed. The model parameters and peak response measures are compared with those obtained using the nominal vehicle design parameters under the same maneuver and forward speed. The directional responses of the coupled driver-articulated vehicle model are further studied to determine a set of vehicle parameters that could improve the directional performance measures of the coupled driver-vehicle system.

The selected design parameters of the vehicle are permitted to vary within ranges specified in the weights and dimensional regulations. These regulations include geometric specifications and axles load limits of different combination vehicles [160,161]. Owing to variations in the provincial and territorial weights and dimensions regulations in Canada, a set of standards for the weight and dimension limits of trucks, which is generally referred as the 'Memorandum of Understanding (MOU)', is used to define the limiting values of geometric and inertial parameters [160].

The simulations are performed assuming a constant perception time (τ_{pd}) selected as 0.1 s [5,144], while the processing time delay (τ_p) of the human's central nervous system is determined from the regression model formulated in section 3.5.2, as a function of the vehicle forward speed. The driver's hand-arm parameters are taken as those reported in [67]. The peak steer angle and peak steer rate in the generalized performance index, Eq. (4.22), are limited to those reported by Breuer [132] on the basis of the measured data ($\Delta\delta_F$=6.2 deg and $\Delta\dot{\delta}_F$=24.8 deg/s) considering the steering ratio equal to 30 for the articulated vehicle, as described in section 4.5.

5.5.1 Variations in the Forward Speed

The performance characteristics of the coupled driver-vehicle system are investigated under a double lane-change steering maneuver at four different forward speeds (50, 80, 100 and 120 km/h). Figure 5.4 illustrates the driver model parameters obtained for these speeds, while the time histories of the front wheels steer angle, δ_F, and the tractor cg coordinates are shown in Figure 5.5. In Figure 5.5, the centerline of the desired roadway is shown by the thin solid line.

The results suggest that vehicle operation at higher forward speeds involves only slightly higher orientation error compensatory gain K_2, but a substantially lower lateral position compensatory gain, K_1. This suggests that the driver is required to undertake lower compensation to minimize the lateral position error and relatively higher compensation of the orientation error at higher speeds. Increasing the forward speed also implies slightly higher compensatory lead time constant of the human driver but considerably lower lag time constant. This suggests that the driver is required to respond faster and employ a higher level of prediction at higher speeds. Such trends in driver control characteristics have also been reported for single unit vehicles [9].

The results also suggested that considering the known ranges of the driver control limits (Table1.7), the coupled driver-vehicle system would not be able to track the desired roadway. The minimization problem failed to converge for the maneuver at 120 km/h. The limit constraints on the driver control parameters were thus relaxed in a sequential manner and the minimization problem was solved. The solutions revealed that slight relaxation in the lower limit of the lag time constant (T_I) could help realize the path tracking performance in a stable manner. The results thus suggest that the human driver is required to employ a lower lag time constant (T_I) to perform the desired steering maneuver at the higher speed of 120 km/h, when compared to the maneuvers at lower speeds. This lag time constant, however, is beyond the reported limits for the human driver, and suggests that the driver may not be able to perform the double lane-change maneuver at 120 km/h with acceptable path tracking performance.

The results also suggest that the near and far preview times, T_{PN} and T_{PF}, decrease with increase in the driving speed, although the resulting near and far preview distances,

D_{PN} and D_{PF}, generally increase with the speed. The near preview distance, however, formed an exception at 120 km/h; it was lower than that obtained at 100 km/h. This can be attributed to higher T_L and considerably lower T_I at this speed. The results also show that increasing the speed invariably yields greater path deviation and relatively lower peak steer angle (Figure 5.5), which is mostly attributed to employing the lateral accelerations perception of the human driver within the generalized performance index. At the higher driving speeds, the proposed driver model, thus, deviates considerably from the centerline of the desired roadway to minimize the lateral accelerations and yaw velocities of both the units.

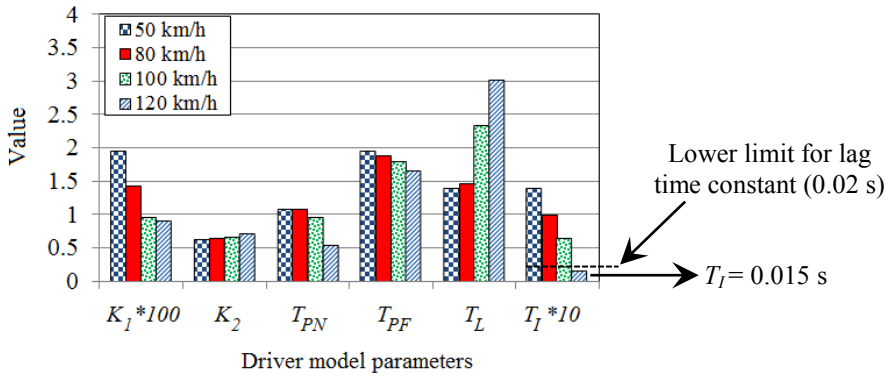

Figure 5.4: Influence of variations in the forward speed on the driver control parameters during a double lane-change maneuver (50, 80, 100 and 120 km/h)

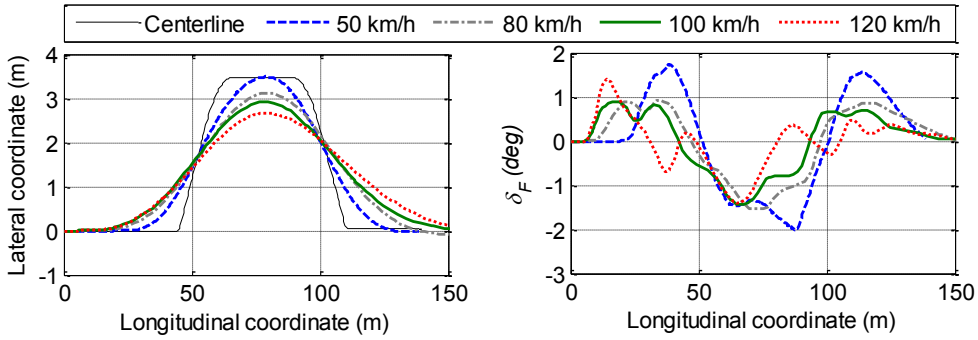

(a) (b)

Figure 5.5: Influence of variations in the forward speed on: (a) path tracking response; and (b) steer angle of the tractor unit during double lane-change maneuvers

Table 5.4 summarizes variations in the path tracking measures that can be described by: (i) peak lateral deviation between the desired path and tractor cg, Y_e; (ii) peak path deviation in the median segment, Y_{em}; and (iii) peak heading error, Ψ_e (Figure 5.6). The peak directional responses of the coupled driver-articulated vehicle system are also summarized in Table 5.5. The grey shaded areas in the tables indicate the peak directional responses in terms of path deviation and lateral accelerations of both the units beyond the selected threshold levels, presented in section 4.5.

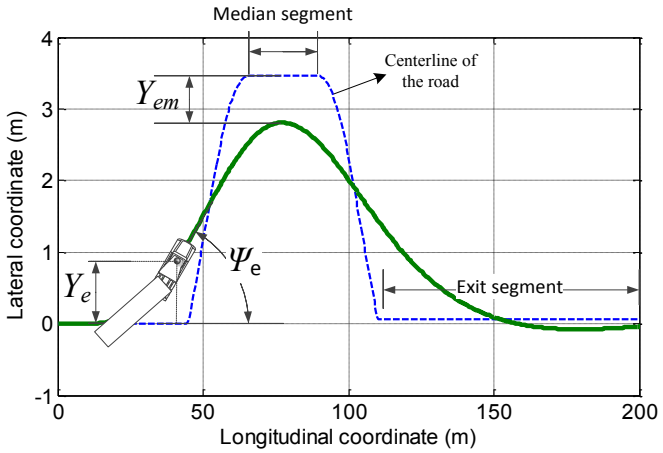

Figure 5.6: Path deviation and orientation error of the articulated vehicle

The peak errors in path tracking measures of the driver-vehicle system, as shown in Table 5.4, suggest that the vehicle driver can successfully perform the selected double lane-change maneuver for the given vehicle only at 50 and 80 km/h. The driver, however, exhibits limited control performance at the higher speeds of 100 and 120 km/h. At these speeds, the peak path deviation of the tractor cg during the median segment, Y_{em}, is greater than the maximum permissible path deviation (0.5 m, as described in section 4.5). At 100 and 120 km/h, the peak lateral acceleration of the trailing unit also approaches the permissible limit of 0.3g, as described in section 4.5. The control of the vehicle at these speeds would necessitate greater compensation by the driver beyond the known ranges of

the driver control limits listed in Table 1.7. The driver would thus be expected to reduce the speed to execute such a maneuver or relax the path tracking error requirements [14].

Further, the results suggest that the peak articulation rate, peak lateral accelerations and peak yaw rates of both the tractor and the semi-trailer units increase with increase in the forward speed. The similar trends were also observed in the open-loop step-steer responses, presented in section 5.3.2. The results also imply that the peak steer rate increases with speed, while the peak steer angle decreases with increase in the forward speed. This suggests that the human driver is required to perform faster steering actions at the higher driving speeds. It should be also noted that the nominal tractor unit is understeer (K_{us} = 0.003) and the semi-trailer unit is oversteer ($K_{us,t}$ = -0.007). In this case, the articulation angle of the vehicle remains finite for all the driving speeds considered [124].

Table 5.4: Influence of variations in the forward speed of the vehicle on peak errors in path tracking measures tracking responses of the driver-vehicle system

Forward speed (km/h)	Peak errors in path tracking measures		
	Y_{em} (m)	Y_e (m)	Ψ_e (deg)
50	0.08	0.81	7.39
80	0.27	1.07	7.93
100	0.54	1.22	8.67
120	0.80	1.44	9.71

Table 5.5: Influence of variations in the forward speed of the vehicle on peak directional responses of the driver-vehicle system

Forward speed (km/h)	Peak directional responses						
	a_{y1} (m/s^2)	r_1 (deg/s)	a_{y2} (m/s^2)	r_2 (deg/s)	$\dot{\gamma}$ (deg/s)	δ_F (deg)	$\dot{\delta}_F$ (deg/s)
50	1.50	6.16	1.26	5.20	4.70	60.40	115.38
80	2.86	8.10	2.70	6.98	4.85	52.44	138.57
100	3.39	8.85	3.71	7.65	4.87	46.96	142.71
120	3.88	9.80	5.12	8.80	5.36	42.52	269.55

5.5.2 Variations in Tractor Design Parameters

The influences of variations in the tractor design parameters on the driver control demands and directional responses are further evaluated. These include the variations in the wheelbase (L_1), mass (m_1) and tandem axle spread (t_1) of the tractor unit. The simulation results may help in identifying the parameters of a driver-adaptive design of a vehicle.

Tractor Mass

The nominal value of the tractor mass (m_1=7270 kg) is increased by 29 percent to 9376 kg, so that the load on the tractor steering axle reaches the maximum allowable load of 5500 kg [160]. The nominal value of the tractor mass is then decreased by 29 percent to obtain the lower value of 5162 kg. Figure 5.7 shows the driver model parameters obtained for three different tractor masses, while the time-histories of the front wheels steer angle (δ_F) and path coordinates of the tractor cg are shown in Figure 5.8.

The results show that a tractor unit with larger weight imposes relatively lower position compensatory action from the driver to maintain the central lane position (K_I), while a greater steering action is required to minimize the orientation error of the vehicle. Increasing the tractor mass m_1 also implies relatively lower near and far preview times T_{PN} and T_{PF}, suggesting longer near and far preview distances of the driver. The tractor's understeer coefficient tends to increase with increase in the tractor mass, when the articulation load is held constant, as seen in Figure 5.3. The results thus suggest that a driver with a longer preview distance would be more suited for control of the vehicle with relatively oversteer tractor. Such a trend has also been reported for articulated vehicles [16]. The results also show greater lead (T_L) and lower lag time constants (T_I) of

the vehicle driver, when driving a tractor with larger weight. This suggests that an articulated vehicle with heavier tractor requires a higher level of prediction and faster steering responses of the driver to effectively track the desired path.

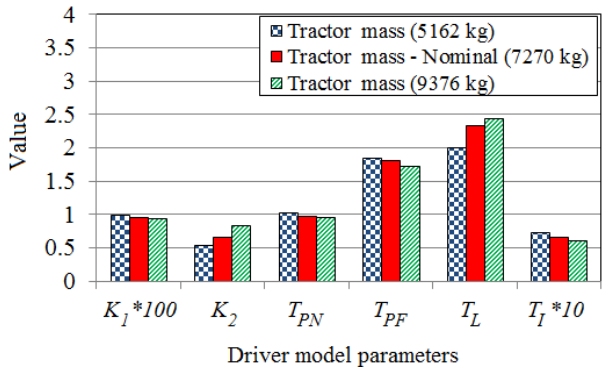

Figure 5.7: Influence of variations in the tractor mass on the driver control parameters during a double lane-change maneuver (speed=100 km/h)

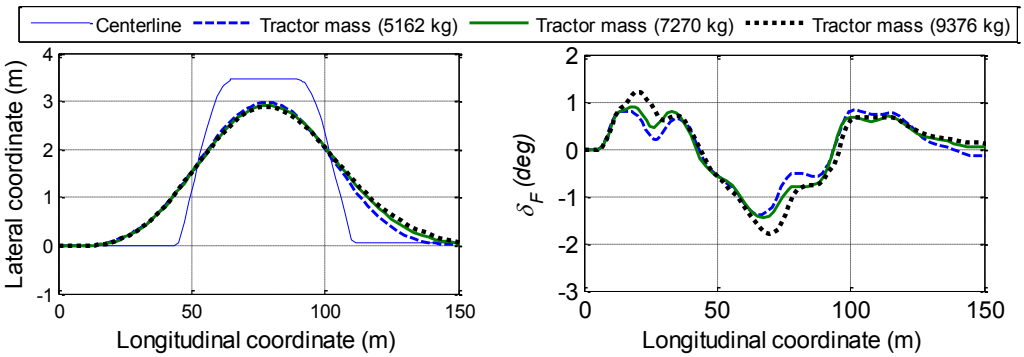

Figure 5.8: Influence of variations in the tractor mass on: (a) path tracking response; and (b) steer angle during a double lane-change maneuver (speed=100 km/h)

Tables 5.6 and 5.7 summarize the peak errors in path tracking measures and peak directional responses of the driver-articulated vehicle system, respectively. The grey shaded areas in the tables indicate the identified values that are beyond the selected threshold levels in terms of lateral deviation and lateral accelerations of both the units, presented in section 4.5. Considering the acceptable peak lateral deviation, Y_{em}= 0.5 m, the results suggest that the vehicle driver can successfully perform the given steering maneuver only with the lowest tractor mass (m_1=5162.5 kg). The results also suggest that

increasing the tractor mass increases the path deviation and orientation error of the vehicle with respect to the desired path (Table 5.6). Further, the peak steer angle increases with increase in the tractor mass, while the peak steer rate remains nearly constant, as indicated in Table 5.7. This suggests greater steering effort of the driver when driving a vehicle with a heavier tractor. The results also reveal decrease in the peak articulation rate, peak lateral accelerations and peak yaw rates of both the tractor and the semi-trailer units with increase in the tractor mass. The similar trends were also observed from the open-loop step-steer response of the vehicle (section 5.3.2).

Table 5.6: Influence of variations in the tractor mass on peak errors in path tracking measures of the driver-vehicle system (speed=100 km/h)

Tractor mass (kg)	Peak errors in path tracking measures		
	Y_{em} (m)	Y_e (m)	Ψ_e (deg)
5162.5	0.48	1.13	8.28
7269.6	0.54	1.22	8.67
9375.7	0.58	1.31	9.09

Table 5.7: Influence of variations in tractor mass on peak directional responses of the driver-vehicle system (speed=100 km/h)

Tractor mass (kg)	Peak directional responses						
	a_{y1} (m/s^2)	r_1 (deg/s)	a_{y2} (m/s^2)	r_2 (deg/s)	$\dot{\gamma}$ (deg/s)	δ_F (deg)	$\dot{\delta}_F$ (deg/s)
5162.5	3.43	8.98	3.79	7.81	5.26	41.69	141.18
7269.6	3.39	8.85	3.71	7.65	4.87	46.96	142.71
9375.7	3.35	8.56	3.61	7.44	4.59	53.72	142.92

Tractor Wheelbase

The various weight and dimensions regulations limit the tractor wheelbase (L_1) in the 3 to 6.25 m range [160]. The nominal value of the wheelbase of the tractor unit (L_1=3.6 m) is thus decreased by 17 percent to the minimum allowable value of 3.0 m. This value is also increased by 17 percent to obtain the longer value of the tractor wheelbase of 4.2 m. It

should be noted that the steering characteristics of the tractor unit tend to vary from understeer to oversteer, if the vehicle cg is permitted to move toward the rear tandem axle. This would increase the possibility of a directional instability of the trailing unit, e.g., jackknifing, if the driving speed approaches the critical value of the tractor.

Figure 5.9 illustrates influence of variations in the tractor wheelbase on the driver model parameters, which are identified through minimization of the performance index under the double lane change maneuver at 100 km/h. The results show trends similar to those observed with increasing the tractor mass. The results suggest that increasing of the tractor wheelbase yields slightly lower lateral position compensatory gains (K_1) but slightly higher orientation error compensatory gain (K_2). This suggests that a tractor unit with lower wheelbase will impose a slightly higher lateral position compensation demand on the driver to minimize lateral position error. Increasing the tractor wheelbase also implies slightly lower near preview time, while the far preview time remains nearly constant. This suggests that a slightly lesser near preview distance is required for longer tractor units. The lead time constant, however, increases considerably, while the lag time constant decreases with increasing tractor wheelbase. The driver is thus required to respond faster and employ a higher level of prediction, when driving a vehicle with longer tractor. Figure 5.10 shows time-histories of the front wheels steer angle and coordinates of the tractor cg obtained for three different values of the tractor wheelbase. The results show that the vehicle driver tracks nearly the same trajectory, while applying slightly lower steering effort with a shorter wheelbase tractor unit.

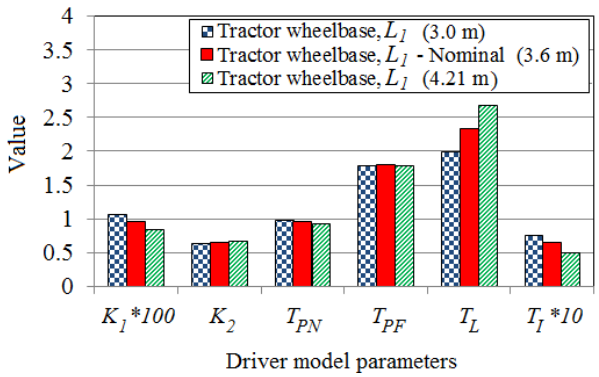

Figure 5.9: Influence of variations in the tractor wheelbase on the driver control parameters during a double lane-change maneuver (speed=100 km/h)

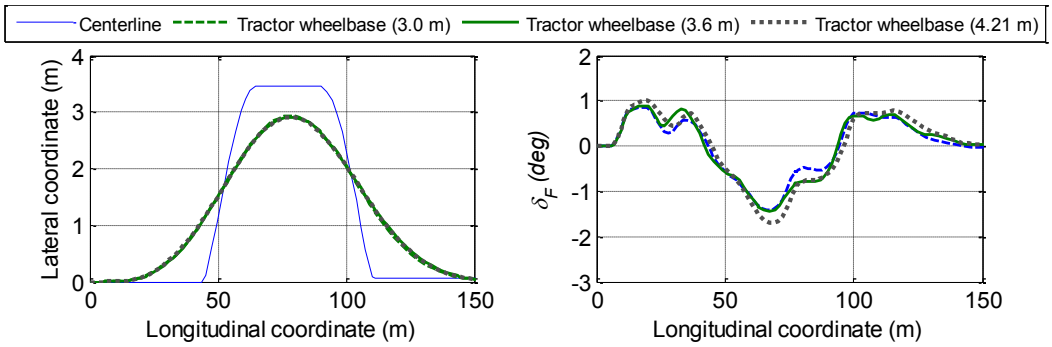

(a) (b)

Figure 5.10: Influence of variations in the tractor wheelbase on: (a) path tracking response; and (b) steer angle during a double lane-change maneuver (speed=100 km/h)

Tables 5.8 and 5.9 summarize the influence of variations in the tractor wheelbase on the peak errors in path tracking measures and peak directional responses of the driver-articulated vehicle system, respectively. In the tables, the grey shaded areas indicate the identified values that are beyond the selected threshold levels in terms of lateral deviation and lateral accelerations of both the units, presented in section 4.5. The results suggest that the peak path deviations, Y_e and Y_{em}, and peak orientation error Ψ_e of the tractor unit increases slightly with increase in the tractor wheelbase (Table 5.8). The peak articulation rate, peak lateral accelerations and peak yaw rates of both the units, however, decrease with increase in the wheelbase (Table 5.9). The similar trends were also

observed from the open-loop step steer maneuver responses (section 5.3.2). The reductions in the directional responses of the vehicle are mostly attributed to increase in the tractor yaw moment of inertia and understeer coefficient of the vehicle with increase in the tractor wheelbase. The results also show that the peak steer angle and peak steer rate increase with increase in the tractor wheelbase, suggesting greater steering effort from the driver when driving a vehicle with relatively more understeer tractor.

Table 5.8: Influence of variations in tractor wheelbase on peak errors in path tracking measures of the driver-vehicle system (speed=100 km/h)

Tractor wheelbase (m)	Peak errors in path tracking measures		
	Y_{em} (m)	Y_e (m)	Ψ_e (deg)
3.00	0.51	1.14	8.55
5.61	0.54	1.22	8.67
4.21	0.55	1.26	8.72

Table 5.9: Influence of variations in tractor wheelbase on peak directional responses of the driver-vehicle system (speed=100 km/h)

Tractor wheelbase (m)	Peak directional responses						
	a_{y1} (m/s^2)	r_1 (deg/s)	a_{y2} (m/s^2)	r_2 (deg/s)	$\dot{\gamma}$ (deg/s)	δ_F (deg)	$\dot{\delta}_F$ (deg/s)
3.00	3.53	9.22	3.83	7.90	4.96	44.07	139.87
5.61	3.39	8.85	3.71	7.65	4.87	46.96	142.71
4.21	3.34	8.67	3.64	7.50	4.70	51.09	147.64

Tractor Tandem Spread

The weights and dimensions regulations permit the tractor tandem axle spread (t_1) in the 1.2 to 1.85 m range [160]. The nominal value of tandem axle spread of the tractor unit (t_1=1.3 m) is thus increased by 42 percent to attain the maximum permissible value of 1.85 m. The sensitivity analysis also considered an alternate spread of 1.6. Figure 5.11 summarizes the influence of variations in the axle spread on the driver control parameters. Figure 5.12 shows the time-histories of the corresponding front wheels steer

angle (δ_F) and path coordinates of the tractor cg. The results suggest only minimal effect of axle spread on the control demands of the driver, except for the lead time constant, T_L, which tends to be lower with higher tandem spread. This suggests some relaxation on the predictive steering control action of the driver when the tractor tandem axle spread is increased. The results also show nearly negligible effect on the front wheels steer angle and the path tracking response.

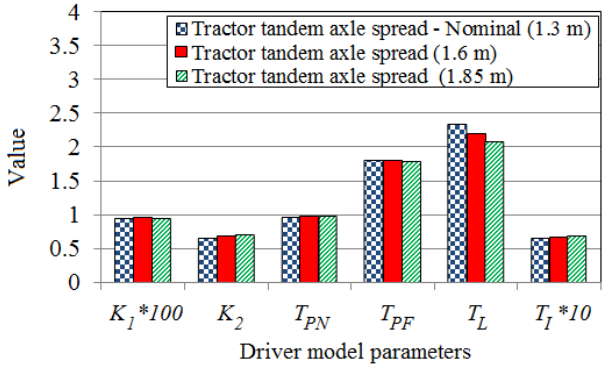

Figure 5.11: Influence of variations in the tractor axle spreads on the driver control parameters during a double lane-change maneuver (speed=100 km/h)

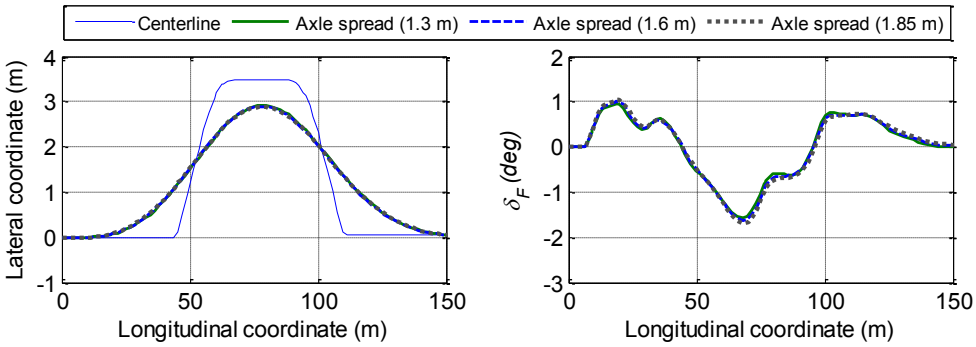

(a) (b)

Figure 5.12: Influence of variations in the tractor axle spreads on: (a) path tracking response; and (b) steer angle during a double lane-change maneuver (speed=100 km/h)

Tables 5.10 and 5.11 summarize the influence of variations in the tractor tandem axle spread on the peak errors in path tracking measures and peak directional responses of the driver-articulated vehicle system. The grey shaded areas indicate that the response

measures in terms of Y_{em}, a_{y1} and a_{y2} exceed the threshold levels, presented in section 4.5. The results suggest that the peak path lateral deviations, Y_e and Y_{em}, and orientation error of the vehicle increase only slightly with increase in the tractor tandem axle spread (Table 5.10), which is mostly attributed to lower lead time constant of the driver. The results also show that the peak steer angle and peak steer rate increase slightly with increase in the tractor tandem axle spread, suggesting greater steering effort demand on the driver. The peak articulation rate, peak lateral accelerations and peak yaw rates of both the units decrease slightly with increase in the tandem axle spread (Table 5.11), as observed for the open-loop step-steer responses. The minimal effect of tandem axle spread on the driver control parameters and thus the directional responses of the vehicle can be attributed to its minimal effect on the steering characteristics and understeer coefficient of the tractor.

Table 5.10: Influence of variations in tractor axle spreads on peak errors in path tracking measures of the driver-vehicle system (speed=100 km/h)

Tractor tandem axle spread (m)	Peak errors in path tracking measures		
	Y_{em} (m)	Y_e (m)	Ψ_e (deg)
1.3	0.54	1.22	8.67
1.6	0.56	1.25	8.79
1.85	0.58	1.27	8.85

Table 5.11: Influence of variations in tractor axle spreads on peak directional responses of the driver-vehicle system (speed=100 km/h)

Tractor tandem axle spread (m)	Peak directional responses						
	a_{y1} (m/s^2)	r_1 (deg/s)	a_{y2} (m/s^2)	r_2 (deg/s)	$\dot{\gamma}$ (deg/s)	δ_F (deg)	$\dot{\delta}_F$ (deg/s)
1.3	3.39	8.85	3.71	7.65	4.87	46.96	142.71
1.6	3.34	8.68	3.64	7.50	4.55	48.89	148.38
1.85	3.30	8.56	3.58	7.39	4.27	50.71	154.06

5.5.3 Variations in Semi-Trailer Design Parameters

Influence of variations in selected semi-trailer design parameters on the driver control and directional responses of the coupled driver-vehicle system are investigated in the similar manner. The design parameters include the semi-trailer mass (m_2), wheelbase (L_2) and tandem axle spread (t_2).

Semi-Trailer Mass

The semi-trailer mass (m_2) includes the mass of the trailing unit with the payload and mass of the rear tandem axles. The nominal value of the semi-trailer mass (26018 kg) is increased by 14 percent, so that the load on the tandem axle of the trailing unit approaches the maximum allowable axle load of 17000 kg [160]. The semi-trailer mass is also decreased by 14 percent to achieve the semi-trailer mass of 22434 kg. A '0 kg' payload condition is also considered to examine the driver control demands and responses of an unloaded vehicle. The semi-trailer mass in this condition is taken as 7602 kg, which includes the mass of the trailing unit and that of rear tandem axles. It should be noted that a higher payload can lead to a greater oversteer tendency of the semi-trailer unit, which may result in lower roll and yaw stability limits of the vehicle combination.

Figures 5.13 and 5.14, respectively, illustrate the influences of variations in the semi-trailer mass on the driver control parameters, and time-histories of the front wheels steer angle (δ_F) and the path coordinates of the tractor cg. The results suggest that increasing the semi-trailer mass can lead to lower lateral position and orientation compensatory gains. This is likely due to lower understeer coefficient of the trailer with greater mass or payload. Increasing the semi-trailer mass, however, would require greater near and far preview times, T_{PN} and T_{PF}, and thus the respective distances. The driver would thus be

required to employ longer preview distances. Furthermore, a heavier trailer would impose a higher level of path prediction by the driver, as it is seen from the increasing lead time constant (T_L). The lag time constant of the driver (T_I), however, decreases with increase in the trailer mass. The results thus suggest that driving a vehicle combination with higher payload would require the driver to employ longer preview distances, faster reaction and higher level of path prediction. The steering and path tracking responses of the driver show that increasing the payload tends to reduce the peak steer angle, while the effect on path tracking performance is minimal, as shown in Figure 5.14.

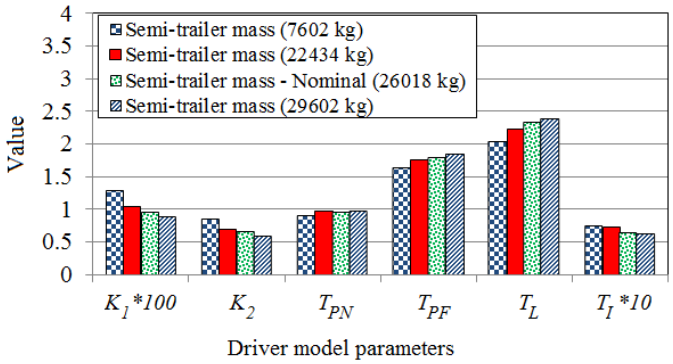

Figure 5.13: Influence of variations in the semi-trailer mass on the driver control parameters during a double lane-change maneuver (speed=100 km/h)

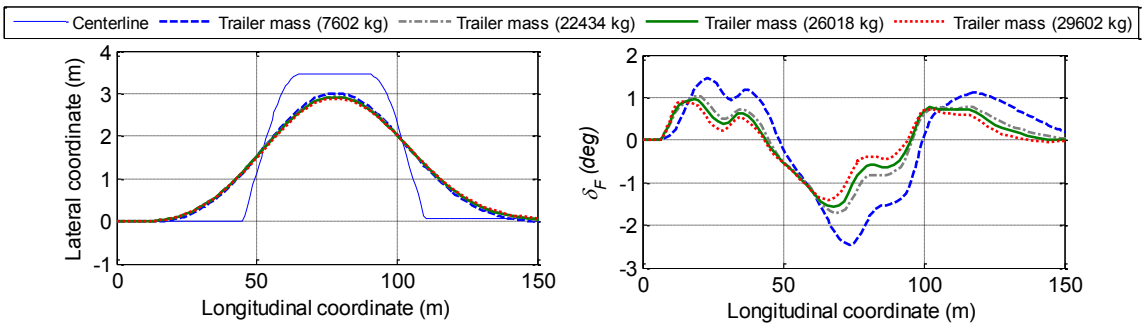

(a) (b)

Figure 5.14: Influence of variations in the semi-trailer mass on: (a) path tracking response; and (b) steer angle during a double lane-change maneuver (speed=100 km/h)

Tables 5.12 and 5.13 summarize variations in the peak errors in path tracking measures and peak directional responses of the coupled driver-articulated vehicle system,

respectively. The grey shaded areas indicate that the response measures in terms of Y_{em}, a_{y1} and a_{y2} exceed the threshold levels, presented in section 4.5. The results suggest that increasing the semi-trailer mass increases the path deviation and orientation error of the vehicle with respect to the desired path (Table 5.12). The results also show that the peak steer angle and peak steer rate of the driver decrease with increase in the semi-trailer mass. This suggests that the driver tends to relax on the path deviation in order to limit the magnitudes of lateral acceleration and yaw rate of the trailing unit. This is also evident from the relatively lower compensation gains (K_1 and K_2), and steer angle and steer rate of the heavier semi-trailer. Increase in the semi-trailer mass also yields higher magnitudes of a_{y2} and r_2. The corresponding tractor yaw rate also increases only slightly. The relatively lower steer angle and rate also results in lower tractor lateral acceleration and articulation rate of the combination.

Table 5.12: Influence of variations in semi-trailer mass on peak errors in path tracking measures of the driver-vehicle system (speed=100 km/h)

Semi-trailer mass (kg)	Peak errors in path tracking measures		
	Y_{em} (m)	Y_e (m)	Ψ_e (deg)
7602	0.45	1.20	8.58
22434	0.53	1.22	8.68
26018	0.54	1.22	8.67
29602	0.57	1.26	8.78

Table 5.13: Influence of variations in semi-trailer mass on peak directional responses of the driver-vehicle system (speed=100 km/h)

Semi-trailer mass (kg)	Peak directional responses						
	a_{y1} (m/s^2)	r_1 (deg/s)	a_{y2} (m/s^2)	r_2 (deg/s)	$\dot{\gamma}$ (deg/s)	δ_F (deg)	$\dot{\delta}_F$ (deg/s)
7602	3.93	8.62	3.28	6.77	4.92	73.96	213.76
22434	3.45	8.65	3.56	7.34	4.89	51.51	165.73
26018	3.39	8.85	3.71	7.65	4.87	46.96	142.71
29602	3.26	8.95	3.81	7.86	4.58	42.01	135.73

Semi-Trailer Wheelbase

The various weight and dimensions regulations limit the semi-trailer wheelbase (L_2) in the 6.25 to 12.5 m range [160]. The nominal wheelbase of the trailer unit (L_2=10.4 m) is thus increased by 20 percent to the maximum allowable value of 12.5 m. This value is also decreased by 20 percent to obtain a lower value of the trailer wheelbase of 8.3 m. Figure 5.15 illustrates influence of variations in the semi-trailer wheelbase on the driver control parameters, identified through minimization of the performance index under the double lane change maneuver performed at 100 km/h. The time-histories of the front wheels steering angle and the coordinates of the tractor cg obtained for three different values of the semi-trailer wheelbase are illustrated in Figure 5.16.

The results show that increasing the semi-trailer wheelbase yields lower lateral position compensatory gain (K_1), while orientation error compensatory gain (K_2) remains almost constant. This suggests a lower lateral position compensation demand on driver when driving a vehicle with longer semi-trailer wheelbase. Increasing the semi-trailer wheelbase also implies greater near and far preview times, T_{PN} and T_{PF}, suggesting that more distant near and far target points are required. Further, the compensatory lead time constant (T_L) increases considerably, while the lag time constant (T_1) decreases slightly with increasing semi-trailer wheelbase. It is thus concluded that a shorter trailing unit can be best adapted to a driver with lower prediction skill, slower reaction time and shorter preview distances. Yang et al. [16] also observed a similar trend in a study of driver-adaptive commercial vehicle designs. The results show that the vehicle driver tracks nearly the same trajectory, irrespective of the trailer wheelbase, although a slightly higher steering angle is applied for a longer wheelbase trailing unit.

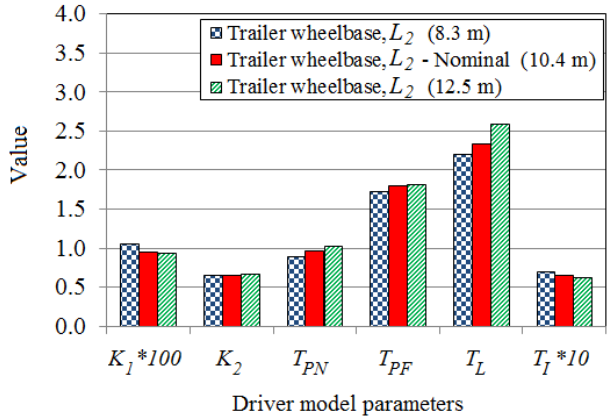

Figure 5.15: Influence of variations in the semi-trailer wheelbase on the driver control parameters during a double lane-change maneuver (speed=100 km/h)

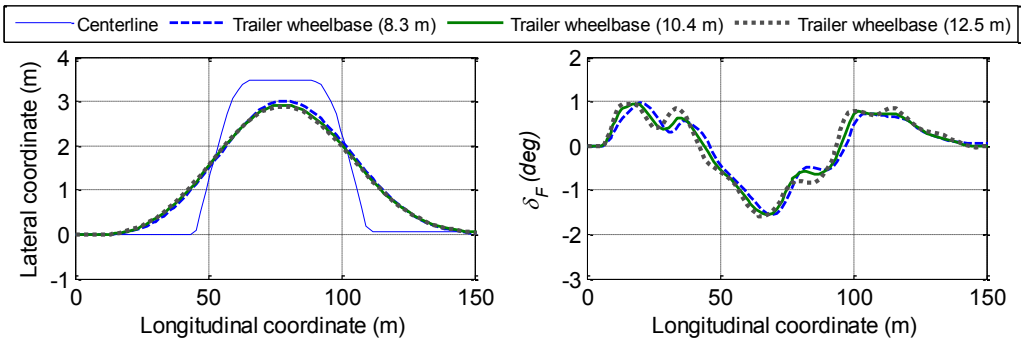

(a) (b)

Figure 5.16: Influence of variations in the semi-trailer wheelbase on: (a) path tracking response; and (b) steer angle during a double lane-change maneuver (speed=100 km/h)

Tables 5.14 and 5.15 summarize the influence of variations in the semi-trailer wheelbase on the peak errors in path tracking measures and peak directional responses of the driver-articulated vehicle system, respectively. The results reveal that a 20 percent decrease in the semi-trailer wheelbase yields considerably lower path deviation in the median segment, in the order of 16%. The peak lateral path deviation and orientation error, Y_e and Ψ_e, of the tractor unit also decreases, although the changes are very small (Table 5.14). The results also suggest that the peak steer angle increases only slightly with increase in the semi-trailer wheelbase, while the peak lateral accelerations and yaw

rates of both the units decrease (Table 5.15). The articulation rate of the vehicle, however, increases with the semi-trailer wheelbase, which is mostly attributed to increase in the peak steer rate. The similar trends were also observed from the open-loop step steer maneuver responses presented in section 5.3.2. The substantial reductions in directional responses of the vehicle with increase in the trailer wheelbase are mostly due to considerable increase in the semi-trailer yaw moment of inertia.

Table 5.14: Influence of variations in semi-trailer wheelbase on peak errors in path tracking measures of the driver-vehicle system (speed=100 km/h)

Semi-trailer wheelbase (m)	Peak errors in path tracking measures		
	Y_{em} (m)	Y_e (m)	Ψ_e (deg)
8.3	0.45	1.20	8.65
10.4	0.54	1.22	8.67
12.5	0.57	1.23	8.76

Table 5.15: Influence of variations in semi-trailer wheelbase on peak directional responses of the driver-vehicle system (speed=100 km/h)

Semi-trailer wheelbase (kg)	Peak directional responses						
	a_{y1} (m/s^2)	r_1 (deg/s)	a_{y2} (m/s^2)	r_2 (deg/s)	$\dot{\gamma}$ (deg/s)	δ_F (deg)	$\dot{\delta}_F$ (deg/s)
8.3	3.74	9.53	4.28	8.83	4.10	46.42	130.51
10.4	3.39	8.85	3.71	7.65	4.87	46.96	142.71
12.5	3.15	8.28	3.28	6.76	5.51	47.75	166.67

Semi-Trailer Tandem Spread

The weights and dimensions regulations permit the semi-trailer tandem axle spread (t_2) in the 1.2 to 1.85 m range [160]. The nominal tandem axle spread of the trailer unit (t_2=1.3 m) is thus increased to attain the maximum permissible value of 1.85 m. The sensitivity analysis also considered an alternate spread of 1.6 m. Figure 5.17 summarizes the influence of variations in the semi-trailer tandem axle spread on the driver control parameters, while Figure 5.18 shows time-histories of the corresponding front wheels

steer angle and path coordinates of the tractor cg under the double-lane change maneuvers at 100 km/h.

The results suggest that increasing the semi-trailer axle spread yields greater lateral position compensatory gains (K_1), while the orientation error compensatory gain (K_2) remains nearly constant. This suggests that a trailing unit with longer axle spread will impose greater lateral position compensation demand on the driver to minimize the lateral position error. Variations in the semi-trailer axle spread also yield only minimal effect on the near as well as far preview times. While the compensatory lead time constant decreases considerably, the lag time constant increases slightly with increase in the trailer axle spread. The driver is thus required to respond faster and employ a higher level of prediction, when driving a vehicle with shorter semi-trailer axle spread. The results also show nearly negligible effect on the front wheels steer angle and path tracking responses.

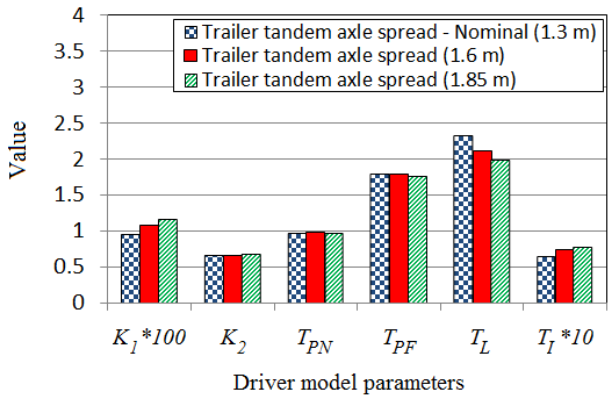

Figure 5.17: Influence of variations in the semi-trailer axle spreads on the driver control parameters during a double lane-change maneuver (speed=100 km/h)

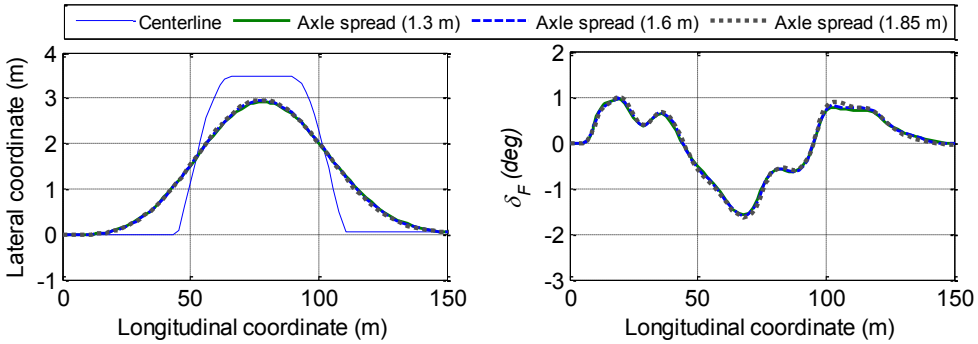

(a) (b)

Figure 5.18: Influence of variations in the semi-trailer axle spreads on: (a) path tracking response; and (b) steer angle during a double lane-change maneuver (speed=100 km/h)

Tables 5.16 and 5.17 summarize the influence of variations in the semi-trailer tandem axle spread on the peak errors in path tracking measures and peak directional responses of the driver-articulated vehicle system. The results suggest that the peak lateral deviations, Y_e and Y_{em}, and orientation error of the vehicle (Ψ_e) decrease with increase in the semi-trailer tandem axle spread (Table 5.16), which is mostly attributed to greater lateral position compensation gain (K_1). The improved path tracking performance, however, is achieved at the expense of increase in the peak articulation rate, peak lateral accelerations and peak yaw rates of both the units. The peak steer angle and peak steer rate also increase, suggesting greater steering effort demand on the driver with increase in axle spread of the trailing unit (Table 5.17).

Table 5.16: Influence of variations in semi-trailer axle spread on peak errors in path tracking measures of the driver-vehicle system (speed=100 km/h)

Semi-trailer tandem spread (m)	Peak errors in path tracking measures		
	Y_{em} (m)	Y_e (m)	Ψ_e (deg)
1.3	0.54	1.22	8.67
1.6	0.52	1.20	8.62
1.85	0.49	1.20	8.54

Table 5.17: Influence of variations in semi-trailer axle spread on peak directional responses of the driver-vehicle system (speed=100 km/h)

Semi-trailer tandem spread (m)	Peak directional responses						
	a_{y1} (m/s^2)	r_1 (deg/s)	a_{y2} (m/s^2)	r_2 (deg/s)	$\dot{\gamma}$ (deg/s)	δ_F (deg)	$\dot{\delta}_F$ (deg/s)
1.3	3.39	8.85	3.71	7.65	4.87	46.96	142.71
1.6	3.49	9.06	3.79	7.82	5.06	47.88	154.05
1.85	3.61	9.34	3.90	8.04	5.34	49.08	158.99

5.6 Summary

A yaw-plane model of a five-axle articulated vehicle is developed and coupled with a two-stage preview driver model, referred to as the 'baseline driver model', which involves simultaneous control of lateral position and orientation errors of the vehicle. The driver's control limits are investigated considering variations in a number of selected vehicle design parameters under the standardized double lane-change maneuver performed at different forward speeds.

The results suggested that at the higher speeds of 100 and 120 km/h, the lateral path deviation and the lateral accelerations of both the tractor and semi-trailer units are beyond the defined threshold limits. The results further showed that a light-weight tractor with shorter wheelbase and shorter tandem axle spread yields improved path tracking performance of the vehicle and reduced steering effort of the driver. The results also suggest that the driver can effectively track the desired roadway while driving a shorter semi-trailer with lower payload. Increasing the tandem axle spread of the semi-trailer unit can also improve the path tracking performance of the vehicle, while it may result in greater rate of tire wear. Table 5.17 summarizes the influences of variations in the forward speed and vehicle design parameters on the peak path deviation, and peak steer angle and peak steer rate of the driver. The positive and negative signs indicate increase

and decrease in a response quantity with increasing of a design or operating variable, respectively.

It has been suggested that enhancing the driver's perception of vehicle motion variables may help the driver to improve its path tracking performance. Considering different motion feedbacks to improve the path tracking and directional responses of the vehicle will be examined in the subsequent chapter.

Table 5.18: Influences of variations in the forward speed and vehicle design parameters on path tracking performance and steering response of the driver

Vehicle unit	Variable	Peak lateral deviation	Peak steer angle	Peak steer rate
Tractor	Forward speed	+	-	+
	Mass	+	+	+
	Wheelbase	+	+	+
	Axle spread	+	+	+
Semi-trailer	Payload	+	-	-
	Wheelbase	+	+	+
	Axle spread	-	+	+

CHAPTER 6

IDENTIFICATION OF EFFECTIVE MOTION CUES PERCEPTION

6.1 Introduction

Under certain driving speeds, a severe vehicle response may occur as the driver tracks the desired roadway, such as rollover or excessive articulation rate of the articulated vehicle. The vehicle driver, in general, controls these critical responses of the vehicle by decreasing the forward speed of the vehicle or by relaxing the path tracking error requirements. These imply that the human driver control actions depend not only to the path information, but also on the driver's perception of directional responses of both the tractor and trailing units. It is thus suggested that considering or enhancing the driver's perception of vehicle motion variables may help the driver to improve its path tracking performance while limiting its control demands. This can be examined by involving different motion states of the vehicle in formulation of the driver model and in evaluating the driver's steering effort demands and the path tracking performance of the coupled driver-vehicle system. For this purpose, the proposed two-stage preview driver model, referred to as the baseline driver model, is modified by adding the driver's perception of different vehicle motion cues.

A number of driver model structures are formulated by integrating different combinations of perceived motion cues to the baseline driver model coupled with the yaw-plane articulated vehicle model. The relative contributions of additional sensory feedbacks are investigated through careful examinations of the directional response quantities and corresponding performance measures in order to identify secondary cues

that could facilitate vehicle path tracking. The driver control parameters are identified through minimization of the generalized performance index, Eq. (4.19), subject to constraints imposed by the human driver's compensation limits (Table 1.7). The sensory feedback cues that help to reduce path deviation and steering effort demands of the driver can be utilized as additional sensory feedbacks that provide important guidance for designs of driver-assist systems (DAS).

6.2 Perception of Different Vehicle States by the Human Driver

It is hypothesized that under medium- and low-speed steering maneuvers the driver is able to track the desired path by considering only the lateral position and orientation errors of the vehicle relative to its surroundings. These errors can be predicted and perceived through the driver's path prediction process and visual sensory cues, respectively [7,8,10]. At higher speeds, the human drivers, however, exhibit limited control performance that generally impose greater demands on the drivers' decisions and control abilities. It is suggested that in these situations, a qualitative perception of additional vehicle states can help the driver to improve its path tracking performance [11]. In the case of articulated vehicles, the human driver can perceive the linear acceleration and rotational velocity of the tractor unit in a qualitative manner through its vestibular and body-distributed kinesthetic cues [32]. The perception of the various motion states of the trailing units also assists the human driver to undertake effective steering control actions. These feedback cues may include articulation rate, lateral accelerations, yaw velocities, roll angles and roll rates of both the units, which can be perceived through in-vehicle sensors or from the driver's experience [9]. Considering only the lateral dynamics of the articulated vehicle, additional vehicle states in this study

are limited to lateral accelerations and yaw rates of the tractor and semi-trailer units (a_{y1}, a_{y1}, r_1 and r_2) and articulation rate ($\dot{\gamma}$).

A total of 10 model structures are formulated by adding different motion cues corresponding to directional responses of both the units of the vehicle to the baseline model, as illustrated in Table 6.1. The baseline driver model (structure 1) only involves the driver's perception of the lateral position and orientation errors that have been commonly employed in reported driver models. Nine combinations of motion cues perception, which are described by structures 2 to 10, describe the driver's perception of different motion cues in a sequential manner.

Table 6.1: The proposed driver model structures employing driver's perceptions of different motion cues

Structure	Path information		Perceived feedback variables				
			Tractor unit		Semi-trailer unit		
	Y_e Lateral position error	Ψ_e Heading error	a_{y1} lateral acceleration	r_1 yaw rate	a_{y2} lateral acceleration	r_2 yaw rate	$\dot{\gamma}$ articulation rate
Structure 1	■	■					
Structure 2	■	■					■
Structure 3	■	■	■				
Structure 4	■	■		■			
Structure 5	■	■			■		
Structure 6	■	■				■	
Structure 7	■	■	■	■			
Structure 8	■	■			■	■	
Structure 9	■	■	■			■	
Structure 10	■	■	■		■		■

The human perception of instantaneous vehicle states is invariably described considering two essential characteristics: (i) perception delay time [5]; and (ii) perception threshold value [32], as described in section 1.2.1. The simulations are performed

assuming a constant perception delay time, selected as 0.1 s. The minimum perceivable linear accelerations and yaw rates of both the units, which can be perceived either by the driver's body-distributed sensors or via in-vehicle sensors, are set as 0.06 m/s^2 and 0.7 deg/s, respectively [5,32].

6.3 Identification of Effective Motion Cues Perception

Relative significance of additional sensory feedbacks related to the path tracking performance and directional dynamic measures of the vehicle is examined by adding different motion cues to the baseline driver model structure (structure 1). These feedback variables, which are related to the selected tractor and semi-trailer motions cues, are integrated in the decision making function, $G_3(s)$, described in Eq. (4.13). Considering a clear visibility condition, simulations are performed to determine the vehicle responses and the individual performance indices while considering nine different combinations of perceived motion cues (Table 6.1). For this purpose, the driver control parameters for each structure are identified through minimization of the generalized performance index, Eq. (4.19), within the practical ranges of control gains that relate to the human driver's characteristics, which are summarized in Table 6.2. The peak directional responses and different performance measures of the vehicle coupled with different driver model structures are then compared to those obtained using the baseline driver model in order to evaluate the relative significance of each set of motion perception at different speeds and various vehicle design parameters. The vehicle design parameters include the variations in the wheelbases, masses and tandem axle spreads of the tractor and the semi-trailer units.

Table 6.2: Range of human driver's control parameters

Control variables	Unit	Range
Near and far preview times, T_N and T_F	s	0.10 - 2.50
Lead time constant, T_L	s	0.02 – 3.00
Lag time constant, T_I	s	0.02 - 0.80
Lateral position error compensatory gain, K_1	rad/m	1e-5 - 1.40
Orientation error compensatory gain , K_2	rad/rad	0.10 - 1.85
Lateral acceleration compensatory gains, K_3 and K_4	rad.s^2/m	0.00 - 1.00
Yaw rate compensatory gains, K_5 and K_6	rad.s/rad	0.00 - 1.00
Articulation rate compensatory gain, K_7	rad.s/rad	0.00 - 1.00

6.3.1 Influence of Additional Feedback Cues - High Speed Driving

During double lane-change maneuvers at the higher speeds of 100 and 120 km/h, the baseline driver model coupled with the articulated vehicle model suggested that the path deviation of the tractor cg in the median segment is greater than the permissible threshold value, 0.5 m (Table 5.4). Further, at 120 km/h the vehicle driver is required to employ a considerably low lag time constant beyond its limit constraints and the driver failed to perform the selected maneuver. The results thus suggest that the vehicle driver exhibits limited control capabilities to perform the selected maneuver at the speeds of 100 and 120 km/h. In such situations, introducing the perception of the vehicle motion variables may help the driver to improve its path tracking performance and to perform the desired maneuver in a controlled and stable manner. Contributions of additional feedback cues to improve the path tracking performance and directional response measures of the coupled driver-vehicle system are discussed considering nine combinations of vehicle motions cues that are integrated with the baseline driver model.

Table 6.3 summarizes the influence of integrating different motion variables to the baseline driver model on the total performance index (J_t) together with its various constituents during double lane-change maneuvers at the speed of 100 km/h. Table 6.4 presents the percent changes in the peak errors of the path tracking measures and peak

directional responses of the vehicle relative to those obtained using the baseline model structure (structure 1) at 100 km/h. A negative and positive value of the percent change indicates a decrease and increase in the response quantity compared to that of the baseline model, respectively. The grey shaded areas in the tables indicate the notable variations in the selected measures when different motion states of the vehicle are involved in formulation of the driver model.

Table 6.3: Variations in the total performance index and its constituents by considering different driver model structures considering nominal vehicle parameters at a constant speed of 100 km/h

Structure	Performance index constituents									
	J_Y	J_Ψ	$J_{a_{y1}}$	$J_{a_{y2}}$	J_{r1}	J_{r2}	$J_{\dot{\gamma}}$	J_δ	$J_{\dot{\delta}}$	J_t
Structure 1	0.7515	0.0758	0.1906	0.2119	0.0916	0.0779	0.0513	0.0068	0.0028	1.4603
Structure 2	0.7542	0.0780	0.1889	0.2095	0.0904	0.0770	0.0499	0.0067	0.0029	1.4577
Structure 3	0.7520	0.0786	0.1901	0.2100	0.0891	0.0772	0.0454	0.0063	0.0020	1.4509
Structure 4	0.7336	0.0753	0.1960	0.2181	0.0942	0.0802	0.0525	0.0069	0.0027	1.4595
Structure 5	0.7332	0.0763	0.1953	0.2167	0.0931	0.0797	0.0505	0.0068	0.0026	1.4541
Structure 6	0.7065	0.0749	0.2040	0.2271	0.0979	0.0835	0.0544	0.0071	0.0027	1.4582
Structure 7	0.7372	0.0777	0.1942	0.2150	0.0914	0.0790	0.0470	0.0065	0.0019	1.4500
Structure 8	0.7183	0.0772	0.1980	0.2191	0.0933	0.0806	0.0484	0.0066	0.0021	1.4436
Structure 9	0.7192	0.0776	0.1996	0.2210	0.0940	0.0813	0.0487	0.0067	0.0021	1.4502
Structure 10	0.7504	0.0790	0.1902	0.2099	0.0891	0.0772	0.0454	0.0063	0.0022	1.4497

At the constant speed of 100 km/h, involving the lateral acceleration of the tractor unit (a_{y1}) alone, as seen in structure 3, and the lateral accelerations of both the units (a_{y1} and a_{y2}) together with the articulation rate of the vehicle ($\dot{\gamma}$), structure 10, yield the most beneficial effects to enhance the performance indices related to a_{y1}, a_{y2}, r_1, r_2, $\dot{\gamma}$ and δ, and corresponding peak directional responses (Tables 6.3 and 6.4). The results further suggest that the lowest values of the path tracking performance (J_Y and J_Ψ) and peak path deviation in the median segment (Y_{em}), can be achieved by using the yaw rate (r_2) of the trailing unit alone (structure 6). Including the r_1 and r_2 also reduce the peak steer rate of

the driver, while its effect on peak steer angle is minimal. It can be thus suggested that combining the trailer yaw rate and lateral accelerations of the tractor and trailing units may leads to considerable improvement in path tracking and performance indices corresponding to directional responses of the vehicle. Employing a_{y2} and r_2 (structure 8) and a_{y1} and r_2 (structure 9) in addition to the lateral position and orientation errors of the baseline driver model greatly improve the total performance index of the vehicle (J_t), and considerably reduce the path deviation (Y_{em}) of the coupled driver-vehicle system.

Table 6.4: Relative changes in path tracking and directional response measures of the coupled driver-vehicle system integrating different feedback cues compared to those obtained from the baseline model (structure 1) considering nominal vehicle parameters at constant speed of 100 km/h

Structure	Percentage variations in the peak path deviations and peak directional responses (%)								
	Y_{em} (m)	Ψ_e (deg)	a_{y1} (m/s^2)	r_1 (deg/s)	a_{y2} (m/s^2)	r_2 (deg/s)	$\dot{\gamma}$ (deg/s)	δ (deg)	$\dot{\delta}$ (deg/s)
Structure 2	0.28	-0.01	-0.73	-1.16	-1.27	-1.27	0.25	-1.47	6.83
Structure 3	2.61	-0.89	-3.24	-10.27	-5.98	-5.98	-17.95	-10.52	19.79
Structure 4	-3.41	-0.66	0.76	0.68	0.79	0.79	0.45	0.73	-2.62
Structure 5	-2.13	-0.91	-2.42	-2.05	-1.65	-1.65	-2.30	-1.65	5.56
Structure 6	-7.86	-1.28	3.01	1.84	2.48	2.48	3.38	0.85	-2.16
Structure 7	-1.40	-1.23	-0.57	-8.72	-3.59	-3.59	-14.71	-10.07	9.38
Structure 8	-4.53	-0.72	-2.30	-5.72	-2.55	-2.55	-9.80	-5.87	6.10
Structure 9	-3.41	-1.47	0.19	-8.56	-3.42	-3.42	-12.25	-9.52	12.58
Structure 10	3.44	-0.80	-3.10	-10.36	-6.28	-6.28	-17.80	-10.52	24.01

Table 6.5 summarizes the influence of involving different combinations of feedback cues on the total performance index (J_t) together with its various elements at 120 km/h. At the same driving speed, Table 6.6 presents the percent changes in the peak errors and peak directional responses of the vehicle relative to those obtained using the baseline model structure (structure 1). A negative and positive value of the percent change in the table indicates a decrease and increase in the response quantity, respectively. The grey

shaded areas indicate the significant variations in the selected response quantities compared to those obtained from the baseline driver model.

The results suggest that including the feedback cues from lateral accelerations and yaw rates of both the units (structures 7 to 10) improves the total performance index of the coupled driver-vehicle system (Table 6.5). At the higher speed of 120 km/h, employing only the lateral position and heading angle errors, as described in structure 1, yields the lowest performance measure related to the tractor lateral acceleration (J_{ay1}), while its peak path deviation (Y_{em}) is greater than the maximum permissible value, 0.5 m (Table 5.4).

Table 6.5: Variations in the total performance index and its constituents by considering different driver model structures considering nominal vehicle parameters at a constant speed of 120 km/h

Structure	Performance index constituents									
	J_Y	J_Ψ	$J_{a_{y1}}$	$J_{a_{y2}}$	J_{r1}	J_{r2}	$J_{\dot{\gamma}}$	J_δ	$J_{\dot{\delta}}$	J_t
Structure 1	0.9391	0.0797	0.2081	0.2750	0.0793	0.0702	0.0541	0.0040	0.0060	1.7155
Structure 2	0.9247	0.0796	0.2114	0.2796	0.0806	0.0714	0.0550	0.0040	0.0055	1.7118
Structure 3	0.8901	0.0785	0.2192	0.2892	0.0831	0.0738	0.0557	0.0041	0.0060	1.6997
Structure 4	0.8828	0.0794	0.2224	0.2954	0.0854	0.0754	0.0592	0.0043	0.0062	1.7106
Structure 5	0.8933	0.0792	0.2180	0.2888	0.0834	0.0737	0.0572	0.0042	0.0061	1.7040
Structure 6	0.8522	0.0756	0.2373	0.3108	0.0881	0.0793	0.0552	0.0039	0.0041	1.7064
Structure 7	0.8406	0.0764	0.2353	0.3060	0.0863	0.0781	0.0521	0.0037	0.0041	1.6826
Structure 8	0.7814	0.0728	0.2584	0.3374	0.0953	0.0861	0.0584	0.0042	0.0044	1.6982
Structure 9	0.7938	0.0737	0.2535	0.3309	0.0931	0.0844	0.0561	0.0039	0.0041	1.6936
Structure 10	0.9324	0.0737	0.2103	0.2677	0.0751	0.0683	0.0428	0.0033	0.0037	1.6773

At a constant speed of 120 km/h, the simulation results show almost similar trends as those obtained for the different driver model structures at the speed of 100 km/h and summarized in Tables 6.3 and 6.4. For instance, employing the yaw velocity of the trailing unit (r_2) alone (structure 6) or combinations of the lateral accelerations of both the units (a_{y1} or a_{y2}) and yaw rate of the trailing unit (structures 8 and 9, respectively)

yield substantial enhancement in Y_{em} and Ψ_e (Table 6.6) and a good improvement of corresponding performance measures, J_Y and J_Ψ (Table 6.5). These improvements, however, are achieved at the expense of increasing the peak directional responses of the vehicle (a_{y1}, r_1, a_{y2} and r_2). Further, adding the lateral accelerations of both the units together with the articulation rate, as seen in structure 10, yields the greatest improvement in the total performance index (J_t) and also improve the performance indices related to $a_{y2}, r_1, r_2, \dot{\gamma}, \delta$ and $\dot{\delta}$, while the contribution of these feedbacks to the path tracking performance are minimal. At 120 km/h, the peak the articulation rate of the vehicle can be effectively reduced by adding the feedback cues of a_{y1} and r_1 (structure 7), a_{y2} and r_2 (structure 8), and a_{y1}, a_{y2} and $\dot{\gamma}$ (structure 10) to the baseline driver model.

Table 6.6: Relative changes in path tracking and directional response measures of the coupled driver-vehicle system integrating different feedback cues compared to those obtained from the baseline model (structure 1) considering nominal vehicle parameters at a constant speed of 120 km/h

Structure	Percentage variations in the peak path deviations and peak directional responses (%)								
	Y_{em} (m)	Ψ_e (deg)	a_{y1} (m/s^2)	r_1 (deg/s)	a_{y2} (m/s^2)	r_2 (deg/s)	$\dot{\gamma}$ (deg/s)	δ (deg)	$\dot{\delta}$ (deg/s)
Structure 2	-1.94	-0.35	0.55	1.00	0.98	0.98	0.29	1.85	0.66
Structure 3	-0.01	-0.87	3.76	0.55	1.39	1.39	0.49	4.44	3.69
Structure 4	-4.12	-1.24	3.67	1.96	2.52	2.51	6.68	3.83	0.34
Structure 5	0.17	-0.72	3.21	1.13	1.89	1.89	3.40	3.52	2.21
Structure 6	-12.19	-3.82	6.40	3.55	4.47	4.46	-6.03	2.21	-7.79
Structure 7	-1.25	-2.85	6.28	-3.41	-0.55	-0.55	-10.26	-3.11	1.83
Structure 8	-11.57	-6.11	10.20	5.52	7.17	7.16	-11.34	5.75	-1.06
Structure 9	-8.34	-4.68	10.75	2.09	5.21	5.20	-7.39	0.95	-2.84
Structure 10	1.80	-3.22	-0.76	-19.51	-13.47	-13.45	-10.78	-20.65	-3.27

The simulation results suggested considerably low lag time constant (T_l) was demanded to perform the selected steering maneuver at the higher speed of 120 km/h, as described in section 5.5.1. Relative significance of involving different motion cues on the lag time

constant of the driver model is investigated (Figure 6.1). The results suggest that introducing the driver's perception from each feedback cue invariably increases the lag time constant of the driver. The most significant increase is observed for structures 7 and 10 of the driver model involving perceptions of a_{y1} and r_1, and a_{y1}, a_{y2} and $\dot{\gamma}$, respectively.

The results for employing additional feedback cues show a number of commonalities between two driving speeds of 100 and 120 km/h: (i) the total performance index can be invariably improved by introducing the driver's perception from each one of the vehicle motion cue; (ii) Involving the yaw rate of the trailing unit (r_2), which can be seen in structures 6, 8 and 9, is most beneficial when improvement in peak errors of path tracking measures (Y_{em} and Ψ_e) has the highest priority, as shown in Tables 6.4 for 100 km/h and 6.6 for 120 km/h; (iii) Perception of the lateral accelerations of both the units and the articulation rate (structure 10) is most desirable when the driver aims to reduce its steering efforts and the peak directional responses of the vehicle, namely, a_{y1}, r_1, a_{y2}, r_2 and $\dot{\gamma}$.

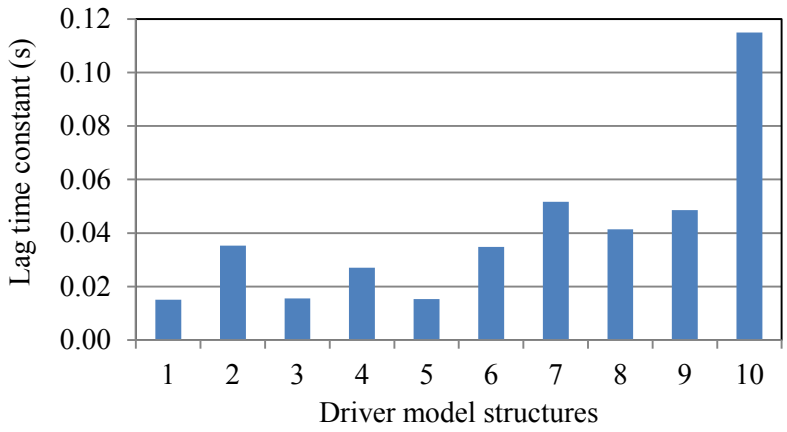

Figure 6.1: Influence of employing different combinations of feedback cues on variations in the lag time constant (T_l) at a constant speed of 120 km/h

6.3.2 Influence of Additional Feedback Cues - Heavier Tractor Unit

The peak errors in path tracking measures of the coupled driver-vehicle system, as summarized in Table 5.6, suggested that increasing the tractor mass generally increases the path deviation and the peak steer angle and the peak steer rate of the driver, while decreases slightly the peak responses of the vehicle in terms of a_{y1}, a_{y2}, r_1, r_2 and $\dot{\gamma}$. Influences of different combinations of feedback cues, when integrated to the baseline driver model, on variations in the path tracking performance and peak directional responses of the vehicle are examined considering the higher tractor mass (m_1=9376 kg) during a double lane-change maneuver at the constant speed of 100 km/h. Table 6.7 summarizes the variations in total performance index (J_t) together with its various elements obtained for each driver model structures. The grey shaded areas indicate the significant variations in the performance measures compared to those obtained from the baseline driver model.

Table 6.7: Variations in the total performance index and its constituents by considering different driver model structures for a heavier tractor unit (100 km/h)

Structure	Performance index constituents									
	J_Y	J_ψ	$J_{a_{y1}}$	$J_{a_{y2}}$	J_{r1}	J_{r2}	$J_{\dot{\gamma}}$	J_δ	$J_{\dot{\delta}}$	J_t
Structure 1	0.8377	0.0803	0.1717	0.1921	0.0835	0.0706	0.0491	0.0089	0.0030	1.4969
Structure 2	0.7687	0.0780	0.1887	0.2117	0.0926	0.0778	0.0560	0.0099	0.0037	1.4870
Structure 3	0.7589	0.0783	0.1873	0.2084	0.0903	0.0766	0.0518	0.0097	0.0038	1.4651
Structure 4	0.7823	0.0780	0.1851	0.2076	0.0906	0.0763	0.0544	0.0097	0.0034	1.4875
Structure 5	0.7470	0.0764	0.1915	0.2038	0.0926	0.0786	0.0535	0.0098	0.0033	1.4666
Structure 6	0.7433	0.0767	0.1946	0.2181	0.0951	0.0802	0.0567	0.0101	0.0035	1.4783
Structure 7	0.7444	0.0764	0.1922	0.2145	0.0927	0.0789	0.0530	0.0098	0.0032	1.4652
Structure 8	0.7237	0.0765	0.1981	0.2208	0.0955	0.0812	0.0545	0.0101	0.0035	1.4638
Structure 9	0.7476	0.0767	0.1907	0.2131	0.0924	0.0784	0.0537	0.0098	0.0034	1.4659
Structure 10	0.7511	0.0791	0.1892	0.2100	0.0903	0.0772	0.0498	0.0096	0.0034	1.4597

The results show that the driver's perception of only the lateral position and orientation errors, referred to as the baseline driver model, yield the lowest performance measures

related to directional responses of the vehicle and steering effort of the driver. Employing only these two visual feedbacks, however, results in a high level of path deviation, which is seen from the terms J_Y and J_Ψ in Table 6.7. The results suggest that the total performance index is invariably improved by adding each of the vehicle feedback cues combination. The most significant decrease is observed for structures 8 and 10 involving perceptions of a_{y2} and r_2, and a_{y1}, a_{y2} and $\dot{\gamma}$, respectively. Integrating yaw rate of the trailing unit alone (structure 6) and the lateral acceleration and yaw rate of the trailing unit (structure 8) yields the most beneficial effect on the path tracking performance of the vehicle (J_Y) and also decreasing the peak path deviation in the median segment (Y_{em}). These two model structures, however, have minimal contributions to improve the performance indices related to the lateral acceleration and yaw rate of both the units.

Considering the driver's perception of different motion cues, Table 6.8 summarizes the percentage variations in the peak errors of the path tracking measures as well as peak directional responses of the coupled driver-vehicle systems compared to the baseline driver model. A negative and positive value of the percent change in the table indicates a decrease and increase in the response quantity, respectively, and the grey shaded areas indicate the significant percent variations. The results show that the driver's perceptions of only the yaw rate of the trailing unit (structure 6) and the lateral acceleration and yaw rate of the semi-trailer (structure 8) yield the most significant reduction of the peak path deviation, in the order of 12%, while these sensory cues help the driver to reduce its peak steer rate, which is desirable in sudden steering maneuvers. Addition of the lateral acceleration of the tractor unit, as seen in structures 3, 7 and 10, is most beneficial to decrease the peak orientation error of the vehicle. Further, the model structure 10, which

integrates the lateral accelerations of both the units and articulation rate of the vehicle to the baseline driver model, yield significant reductions in the peak directional responses of the vehicle as well as decreasing the peak steer angle and peak steer rate.

It can be concluded that in the case of a heavy tractor mass, structures 6 and 8, which employs the lateral acceleration and yaw velocity of the trailing unit, can be most beneficial to improve the path tracking performance of the vehicle. The driver's perception of the lateral accelerations of both the units and articulation rate (structure 10), on the other hand, would be most beneficial when the driver's aim is to reduce the peak directional responses of the vehicle in high speed driving. In addition, the results suggested that incorporating a feedback from lateral acceleration of each vehicle unit yield significant decrease in peak lateral acceleration of the corresponding unit (Table 6.8). This is mostly attributed to greater compensatory actions of the driver with respect to a certain state of the vehicle, when integrated as a secondary feedback cue. This further suggests the driver may use the feedback from critical states of each unit to effectively control the vehicle.

Table 6.8: Relative changes in path tracking and directional response measures of the coupled driver-vehicle system with respect to those obtained from the baseline model (structure 1) considering different feedback cues for a heavier tractor unit (100 km/h)

Structure	Percentage variations in the peak path deviations and peak directional responses (%)								
	Y_{em} (m)	Ψ_e (deg)	a_{y1} (m/s^2)	r_1 (deg/s)	a_{y2} (m/s^2)	r_2 (deg/s)	$\dot{\gamma}$ (deg/s)	δ (deg)	$\dot{\delta}$ (deg/s)
Structure 2	-8.30	-1.79	7.12	7.16	6.88	6.88	5.76	7.07	-44.12
Structure 3	-3.58	-3.57	-4.18	-0.16	-1.62	-1.62	9.39	0.82	-29.07
Structure 4	-6.58	-2.07	6.30	6.83	6.29	6.29	0.91	6.76	-48.07
Structure 5	-7.35	-5.71	-4.18	2.48	-2.59	1.59	4.08	3.44	-35.53
Structure 6	-11.82	-2.49	7.42	7.80	7.60	7.59	7.14	7.98	-44.68
Structure 7	-8.79	-5.46	-1.10	1.77	1.17	1.17	3.94	1.97	-36.67
Structure 8	-11.77	-4.89	0.23	2.80	2.07	2.07	9.39	3.89	-37.29
Structure 9	-5.83	-3.13	-0.20	2.64	1.99	1.99	4.68	2.83	-34.46
Structure 10	-5.42	-5.15	-4.92	-2.42	-2.50	-2.50	-0.47	-1.59	-26.63

6.3.3 Influence of Additional Feedback Cues - Longer Tractor Unit

The path tracking responses of the baseline driver model (structure 1) coupled with the articulated vehicle model suggest that increasing the tractor wheelbase increases the peak path deviation (Table 5.8), while decreases slightly the peak responses of the vehicle related to a_{y1}, a_{y2}, r_1, r_2 and $\dot{\gamma}$ (Table 5.9). During a double lane-change maneuver at a constant speed of 100 km/h, contributions of different feedback cues to improve the path tracking performance and peak directional responses of the vehicle are carefully examined by integrating nine combinations of vehicle motion cues to the baseline driver model considering the longer tractor wheelbase (L_1=4.2 m). Table 6.9 summarizes the variations in the total performance index (J_t) together with its various constituents obtained for each driver model structure during the selected maneuver at 100 km/h. Table 6.10 summarizes the percentage variations of the peak errors in path tracking measures and peak directional responses for different driver model structures compared to the baseline driver model. The grey shaded areas in these tables indicate the significant variations in the selected response quantities compared to those obtained from the baseline driver model.

It is evident that the performance index is invariably enhanced by adding feedback from each feedback cues. The most significant decrease is observed when the baseline driver model is integrated to the lateral acceleration of the tractor unit alone (structure 3), lateral acceleration and yaw rate of the tractor unit (structure 7) and lateral accelerations of both the units and articulation rate (structure 10). This emphasizes the significance of employing the lateral acceleration of the tractor unit to improve the total performance index of the vehicle, and performance measure related to the path tracking (J_Y) and steer

rate ($J_{\dot{\delta}}$), as seen in Table 6.9. Employing the tractor lateral acceleration (structures 3, 7 and 10) also yields the greatest reduction in peak steer angle of the driver (Table 6.10). These suggest that introducing the lateral acceleration of the tractor units as an additional feedback cue could help the driver to improve its path tracking performance while reduces its steering workload in a high demanding steering maneuver. Adding only the yaw rate of the trailing unit (structure 6) is most beneficial to reduce the path tracking performance of the vehicle, J_Y and J_Ψ (Table 6.9), and the peak path deviations of the tractor cg, Y_{em} and Ψ_e (Table 6.10). The similar trends have been seen for heavier tractor unit and higher driving speeds of 100 and 120 km/h.

Table 6.9: Variations in the total performance index and its constituents by considering different driver model structures for a longer tractor unit (100 km/h)

Structure	Performance index constituents									
	J_Y	J_Ψ	$J_{a_{y1}}$	$J_{a_{y2}}$	J_{r1}	J_{r2}	$J_{\dot{\gamma}}$	J_δ	$J_{\dot{\delta}}$	J_t
Structure 1	0.7800	0.0764	0.1826	0.2043	0.0875	0.0751	0.0482	0.0080	0.0030	1.4651
Structure 2	0.7557	0.0764	0.1890	0.2115	0.0905	0.0778	0.0495	0.0082	0.0030	1.4615
Structure 3	0.7432	0.0785	0.1920	0.2138	0.0905	0.0786	0.0469	0.0081	0.0026	1.4543
Structure 4	0.7338	0.0755	0.1957	0.2194	0.0941	0.0807	0.0524	0.0086	0.0032	1.4633
Structure 5	0.7363	0.0772	0.1947	0.2168	0.0921	0.0797	0.0483	0.0083	0.0032	1.4567
Structure 6	0.6969	0.0745	0.2073	0.2322	0.0993	0.0854	0.0544	0.0090	0.0032	1.4623
Structure 7	0.7271	0.0777	0.1966	0.2194	0.0930	0.0807	0.0486	0.0083	0.0026	1.4541
Structure 8	0.7291	0.0767	0.1967	0.2192	0.0930	0.0806	0.0487	0.0084	0.0030	1.4553
Structure 9	0.7218	0.0764	0.1989	0.2218	0.0942	0.0816	0.0496	0.0085	0.0030	1.4558
Structure 10	0.7540	0.0796	0.1891	0.2101	0.0886	0.0772	0.0447	0.0079	0.0026	1.4538

The driver's perception of only the lateral acceleration of the tractor unit (structure 3) significantly reduces the peak dynamic responses related to a_{y1}, a_{y2}, r_1, r_2 and δ (Table 6.10). The similar trend can be seen in structures 7 and 10 that both use the lateral acceleration of the tractor as one of their feedback cues. Employing the lateral accelerations of both the units and the articulation rate of the vehicle (structure 10) yields the greatest reduction of the peak articulation rate, while it also improves the peak

directional responses of the vehicle. Introducing the feedback cue from the articulation rate of the vehicle thus can helps the driver to satisfy its safety requirements corresponding to the excessive articulation rate that may leads to increasing the possibility of a directional instability of the trailing unit, e.g., jackknifing.

Table 6.10: Relative changes in path tracking and directional response measures of the coupled driver-vehicle system with respect to those obtained from the baseline model (structure 1) considering different feedback cues for a longer tractor unit (100 km/h)

Structure	Percentage variations in the peak path deviations and peak directional responses (%)								
	Y_{em} (m)	Ψ_e (deg)	a_{y1} (m/s^2)	r_1 (deg/s)	a_{y2} (m/s^2)	r_2 (deg/s)	$\dot{\gamma}$ (deg/s)	δ (deg)	$\dot{\delta}$ (deg/s)
Structure 2	-1.80	-1.16	1.44	1.36	1.58	1.58	-0.89	1.72	-4.60
Structure 3	-0.75	-2.40	-2.26	-9.80	-4.65	-4.65	-4.16	-9.55	20.47
Structure 4	-4.30	-1.47	2.74	2.78	3.31	3.30	3.40	2.90	-0.97
Structure 5	-1.18	-1.20	-1.74	-4.89	-2.51	-2.51	-7.98	-3.86	15.03
Structure 6	-10.06	-4.78	3.09	3.38	4.11	4.11	6.83	3.74	1.83
Structure 7	-2.39	-2.77	-1.27	-7.79	-3.44	-3.44	-3.64	-7.56	17.15
Structure 8	-4.92	-2.46	-0.95	-3.09	-0.24	-0.24	-4.94	-2.59	9.95
Structure 9	-3.90	-2.64	0.81	-7.33	-2.70	-2.70	-2.99	-7.04	16.69
Structure 10	0.02	-0.82	-1.81	-7.85	-3.67	-3.67	-13.67	-7.74	17.96

6.3.4 Influence of Additional Feedback Cues - Higher Tractor Tandem Spread

Considering the baseline driver model coupled with the articulated vehicle model, higher tandem axle spreads in the tractor unit yields increasing the peak path deviation of the tractor cg in the median segment of the double lane-change maneuver at 100 km/h. Relative significance of additional feedback cues to improve the path tracking performance of the vehicle is examined considering the maximum tractor tandem axle spread (t_1=1.85 m). Table 6.11 summarizes the total performance index (J_t) together with its various constituents obtained for each driver model structure during a double lane-change maneuver at 100 km/h. The grey shaded areas in the table indicate the significant variations in the performance measures compared to those obtained from the baseline driver model.

The results clearly suggest that the total performance index (J_t) and the path tracking performance measures of the vehicle (J_Y and J_Ψ) are invariably enhanced by adding feedback from each of the feedback cues. The most significant decrease in the total performance index is observed for structure 10 of the driver model involving perceptions of a_{y1}, a_{y2} and $\dot{\gamma}$. Employing the driver model structure 10 further results in the lowest performance measures related to $\dot{\gamma}$ and $\dot{\delta}$. Further, integrating the yaw rate of the trailing unit alone to the baseline driver model (structure 6) yields the greatest decrease in the path tracking performance (J_Y and J_Ψ), while its contribution to improve the performance indices related to the directional responses of the vehicle is minimal.

Table 6.11: Variations in the total performance index and its constituents by considering different driver model structures for higher tandem axle spread of the tractor (100 km/h)

Structure	Performance index constituents									
	J_Y	J_Ψ	$J_{a_{y1}}$	$J_{a_{y2}}$	J_{r1}	J_{r2}	$J_{\dot{\gamma}}$	J_δ	$J_{\dot{\delta}}$	J_t
Structure 1	0.8036	0.0790	0.1760	0.1947	0.0837	0.0716	0.0444	0.0076	0.0028	1.4633
Structure 2	0.7621	0.0773	0.1874	0.2075	0.0892	0.0763	0.0475	0.0081	0.0026	1.4580
Structure 3	0.7249	0.0762	0.1978	0.2182	0.0934	0.0803	0.0485	0.0085	0.0033	1.4510
Structure 4	0.7402	0.0757	0.1940	0.2151	0.0926	0.0791	0.0498	0.0084	0.0029	1.4579
Structure 5	0.7396	0.0768	0.1929	0.2129	0.0912	0.0783	0.0475	0.0083	0.0030	1.4504
Structure 6	0.7145	0.0755	0.2013	0.2229	0.0958	0.0820	0.0509	0.0087	0.0031	1.4548
Structure 7	0.7315	0.0761	0.1957	0.2160	0.0922	0.0794	0.0474	0.0083	0.0030	1.4498
Structure 8	0.7154	0.0768	0.1992	0.2211	0.0938	0.0826	0.0498	0.0086	0.0029	1.4502
Structure 9	0.7202	0.0759	0.1992	0.2200	0.0941	0.0809	0.0487	0.0085	0.0031	1.4505
Structure 10	0.7537	0.0790	0.1889	0.2080	0.0882	0.0765	0.0435	0.0078	0.0022	1.4479

Considering different driver model structures, Table 6.12 presents the percentage variations of the peak path deviations together with the peak direction responses of the vehicle compared to the baseline model when the tractor tandem axle spread is selected as 1.85 m. The results show that perception of the yaw rate of the trailing unit alone, r_2, in structures 6 would help the driver to significantly reduces the peak path deviations measures (Y_{em} and Ψ_e). Further, involving the lateral acceleration from each unit of the

vehicle in structures 3 and 5 yields the greatest reduction in peak lateral acceleration of the corresponding units, suggesting significance of enhancing the driver's perception from critical states of the vehicle. This is mostly attributed to greater compensatory actions of the driver to minimize the lateral accelerations of each unit. Considering only the articulation rate in structure 2 and yaw rate of the tractor unit alone as of structure 4 are most beneficial to decrease the driver's peak steer rate and thus its steering effort. The model structure 10, which employs the lateral accelerations of both the units together with the articulation rate of the vehicle yields considerable decrease in the peak values of the directional responses of the vehicle (a_{y1}, r_1, a_{y2}, r_2 and $\dot{\gamma}$) and peak steer angle.

Table 6.12: Relative changes in path tracking and directional response measures of the coupled driver-vehicle system with respect to those obtained from the baseline model (structure 1) considering different feedback cues for higher tandem axle spread of the tractor (100 km/h)

Structure	Percentage variations in the peak path deviations and peak directional responses (%)								
	Y_{em} (m)	Ψ_e (deg)	a_{y1} (m/s^2)	r_1 (deg/s)	a_{y2} (m/s^2)	r_2 (deg/s)	$\dot{\gamma}$ (deg/s)	δ (deg)	$\dot{\delta}$ (deg/s)
Structure 2	-6.93	-1.41	4.26	3.15	3.54	3.54	3.94	2.12	-9.77
Structure 3	-7.11	-3.75	-2.05	-4.79	-2.52	-2.52	7.31	-4.30	14.71
Structure 4	-9.26	-2.84	4.88	4.09	4.53	4.53	9.73	3.32	-9.72
Structure 5	-6.58	-2.33	-0.63	0.24	-3.03	0.23	5.27	0.61	13.41
Structure 6	-11.29	-4.22	4.38	4.61	4.78	4.77	10.56	4.74	-1.92
Structure 7	-6.74	-3.72	0.32	-6.40	-3.02	-3.02	6.15	-6.92	11.85
Structure 8	-9.80	-3.75	1.69	1.69	2.66	2.66	6.80	1.76	2.63
Structure 9	-9.02	-3.92	0.84	-4.11	-1.35	-1.35	8.24	-4.48	12.55
Structure 10	-5.25	-1.85	-2.04	-6.03	-2.35	-2.35	-4.96	-7.41	12.48

6.3.5 Influence of Additional Feedback Cues - Heavier Trailer Unit

The peak errors in path tracking measures of the coupled driver-vehicle system, as summarized in Table 5.12, suggested that increasing the semi-trailer mass increases the path deviation and also the peak responses of the vehicle in terms of a_{y2} and r_2. Influences of additional feedback cues, when integrated to the baseline driver model, on

variations in the path tracking performance and directional response measures of the vehicle are examined considering the higher value of the trailer (m_2=29602 kg) during a double lane-change maneuver at the constant speed of 100 km/h. Table 6.13 summarizes the total performance index (J_t) together with its various constituents obtained for each driver model structure. Considering different combinations of motion feedback cues, Table 6.14 summarizes the percentage variations in the peak errors of the path tracking measures and peak directional responses of the coupled driver-vehicle systems compared to the baseline driver model.

Table 6.13: Variations in the total performance index and its constituents by considering different driver model structures for a heavier trailer unit (100 km/h)

Structure	Performance index constituents									
	J_Y	J_Ψ	$J_{a_{y1}}$	$J_{a_{y2}}$	J_{r1}	J_{r2}	$J_{\dot{\gamma}}$	J_δ	$J_{\dot{\delta}}$	J_t
Structure 1	0.7795	0.0775	0.1840	0.2169	0.0910	0.0797	0.0517	0.0052	0.0026	1.4882
Structure 2	0.7751	0.0765	0.1848	0.2175	0.0912	0.0800	0.0515	0.0052	0.0026	1.4843
Structure 3	0.7522	0.0792	0.1922	0.2230	0.0900	0.0820	0.0472	0.0047	0.0010	1.4715
Structure 4	0.7516	0.0757	0.1921	0.2269	0.0949	0.0834	0.0535	0.0053	0.0023	1.4856
Structure 5	0.7502	0.0796	0.1909	0.2226	0.0919	0.0818	0.0473	0.0049	0.0019	1.4713
Structure 6	0.7294	0.0764	0.1970	0.2317	0.0965	0.0852	0.0527	0.0053	0.0022	1.4764
Structure 7	0.7345	0.0784	0.1963	0.2292	0.0946	0.0843	0.0490	0.0051	0.0019	1.4733
Structure 8	0.7230	0.0772	0.1994	0.2329	0.0962	0.0856	0.0499	0.0051	0.0019	1.4711
Structure 9	0.7372	0.0778	0.1956	0.2284	0.0943	0.0840	0.0488	0.0050	0.0019	1.4730
Structure 10	0.7617	0.0801	0.1874	0.2184	0.0901	0.0803	0.0462	0.0048	0.0017	1.4706

The results suggest that the total performance index (J_t) and the path tracking performance of the vehicle (J_Y) invariably improves by considering different combinations of feedback cues. The most significant decrease is observed for structures 8 and 10 of the driver model involving perceptions of a_{y2} and r_2, and a_{y1}, a_{y2} and $\dot{\gamma}$, respectively. In addition, considering the lateral acceleration of the tractor unit, as seen in driver model structures 3 and 10, improves the performance measures related to the steering effort of driver (J_δ and $J_{\dot{\delta}}$), tractor yaw rate (J_{r1}) and articulation rate ($J_{\dot{\gamma}}$) of the

vehicle compared to the baseline driver model (Table 6.13). Integrating the yaw rate of the trailing unit alone (structure 6) and the lateral acceleration and yaw rate of the trailing unit (structure 8) yield the greatest reduction of the path tracking performance (J_Y). These feedbacks, however, have minimal contribution to improve the performance indices corresponding to the lateral acceleration and yaw rate of both the units.

Table 6.14: Relative changes in path tracking and directional response measures of the coupled driver-vehicle system with respect to those obtained from the baseline model (structure 1) considering different feedback cues for a heavier trailer unit (100 km/h)

Structure	Percentage variations in the peak path deviations and peak directional responses (%)								
	Y_{em} (m)	Ψ_e (deg)	a_{y1} (m/s^2)	r_1 (deg/s)	a_{y2} (m/s^2)	r_2 (deg/s)	$\dot{\gamma}$ (deg/s)	δ (deg)	$\dot{\delta}$ (deg/s)
Structure 2	-1.08	-0.42	0.23	-0.85	-0.55	-0.55	1.53	-0.84	15.60
Structure 3	-0.57	-0.73	-1.04	-13.37	-4.59	-5.59	-9.72	-15.90	-1.23
Structure 4	-4.09	-1.10	2.27	0.83	1.68	1.68	1.76	0.82	10.10
Structure 5	-1.87	-0.37	-0.06	-9.16	-5.43	-4.43	-7.89	-10.48	25.05
Structure 6	-7.76	-1.30	4.04	-4.39	-1.19	-1.19	6.29	-5.46	10.95
Structure 7	-4.29	-1.27	5.65	-11.56	-4.15	-4.15	-5.89	-14.02	22.31
Structure 8	-8.21	-2.99	4.98	-6.72	-2.16	-2.16	-2.98	-8.05	14.58
Structure 9	-5.08	-2.59	5.20	-11.39	-3.89	-3.89	-6.55	-14.70	16.76
Structure 10	-1.65	-0.34	3.54	-9.88	-4.26	-4.26	-8.54	-11.97	20.66

The results suggest that the driver's perception of only the lateral acceleration of the tractor unit (structure 3) yield significant decrease in the peak directional responses related to a_{y2}, r_1, r_2 and $\dot{\gamma}$ as well as the peak steer angle of the driver. Integration of the lateral acceleration of the trailer unit alone (structure 5) to the baseline driver model further yields greatest reduction in peak lateral acceleration of the corresponding unit (a_{y2}) as well as decrease in peak yaw rate of the trailer and peak articulation rate of the vehicle. Almost similar trends of decreasing the peak directional responses of the vehicle can be seen for structure 10 that employs the lateral acceleration feedbacks from both the units together with the articulation rate. Employing of the yaw rate of the trailing unit (structures 6 and 8) substantially reduces the peak path deviation Y_{em} and orientation

error Ψ_e of the tractor unit. As it would be expected, involving both the yaw rate of the trailing unit and the lateral acceleration of the tractor unit to the baseline driver model (structure 9) results notable decrease in the peak path deviation and peak directional response of the vehicle as well as the peak steer angle of the driver.

6.3.6 Influence of Additional Feedback Cues - Longer Trailer Unit

The path tracking responses of the driver-vehicle system suggest that increasing the trailer wheelbase increases the peak path deviation (Table 5.14) as well as the peak articulation rate of the vehicle (Table 5.15). Considering the longer semi-trailer (L_2=12.5 m), different combinations of feedback cues are studied to identify influences of integrating different feedback cues to the baseline driver model on variations in path tracking performance and peak directional responses of the vehicle. Table 6.15 summarizes the variations in the total performance index together with its various constituents obtained for each driver model structure. Table 6.16 presents the percentage variations in the peak errors in path tracking measures and peak directional responses of the different driver model structures compared to the baseline driver model.

Table 6.15: Variations in the total performance index and its constituents by considering different driver model structures for a longer trailer unit (100 km/h)

Structure	Performance index constituents									
	J_Y	J_Ψ	$J_{a_{y1}}$	$J_{a_{y2}}$	J_{r1}	J_{r2}	$J_{\dot{\gamma}}$	J_δ	$J_{\dot{\delta}}$	J_t
Structure 1	0.7783	0.0774	0.1825	0.1881	0.0895	0.0692	0.0631	0.0077	0.0035	1.4593
Structure 2	0.7490	0.0756	0.1909	0.1968	0.0934	0.0724	0.0655	0.0080	0.0035	1.4550
Structure 3	0.7237	0.0779	0.1992	0.2054	0.0964	0.0755	0.0650	0.0081	0.0035	1.4546
Structure 4	0.7195	0.0747	0.1998	0.2062	0.0981	0.0759	0.0693	0.0084	0.0034	1.4554
Structure 5	0.7650	0.0803	0.1862	0.1923	0.0894	0.0707	0.0588	0.0074	0.0023	1.4525
Structure 6	0.7080	0.0750	0.2032	0.2095	0.0994	0.0771	0.0694	0.0085	0.0038	1.4539
Structure 7	0.7410	0.0780	0.1939	0.2000	0.0936	0.0736	0.0626	0.0078	0.0031	1.4537
Structure 8	0.7311	0.0771	0.1954	0.2019	0.0945	0.0743	0.0635	0.0078	0.0026	1.4480
Structure 9	0.7267	0.0776	0.1979	0.2043	0.0957	0.0751	0.0646	0.0080	0.0030	1.4529
Structure 10	0.7617	0.0789	0.1873	0.1935	0.0898	0.0712	0.0585	0.0074	0.0022	1.4505

The results suggest that the total performance index (J_t) is invariably improved by adding feedback from each of the vehicle motion cues. The most significant decrease in the total performance index is observed for structure 5, 8 and 10, which involve perceptions of a_{y2} alone and a_{y2} and r_2, and a_{y1}, a_{y2} and $\dot{\gamma}$, respectively. The results imply that the driver's perception of only the yaw rate of the tractor (structure 4) and the yaw rate the semi-trailer unit (structure 6) yield the most significant decrease of the path tracking performance, which can be seen from the terms J_Y and J_Ψ in Table 6.15 and the peak path error measures Y_{em} and Ψ_e in Table 6.16. Further, integrating only the lateral acceleration of the trailing unit (structures 5) helps the driver to reduce the performance indices related to its steer angle and steer rate as well as articulation rate of the vehicle. The similar reductions can be seen from the peak steer angle, the peak steer rate and the peak articulation rate of the vehicle (Table 6.16). This suggests significance of this feedback in high speed steering maneuvers to decrease the articulation rate of the vehicle while reducing the driver's steering effort.

Table 6.16: Relative changes in path tracking and directional response measures of the coupled driver-vehicle system with respect to those obtained from the baseline model (structure 1) considering different feedback cues for a longer trailer unit (100 km/h)

Structure	Percentage variations in the peak path deviations and peak directional responses (%)								
	Y_{em} (m)	Ψ_e (deg)	a_{y1} (m/s^2)	r_1 (deg/s)	a_{y2} (m/s^2)	r_2 (deg/s)	$\dot{\gamma}$ (deg/s)	δ (deg)	$\dot{\delta}$ (deg/s)
Structure 2	-5.83	-2.22	2.87	2.90	2.27	2.27	1.61	3.08	-3.13
Structure 3	-9.02	-2.52	10.54	-5.76	6.79	6.80	-12.72	-11.60	1.07
Structure 4	-9.20	-3.03	5.64	5.20	5.05	5.05	3.75	4.31	-1.17
Structure 5	-4.57	-1.36	5.19	-1.40	4.41	4.41	-20.75	-14.89	-1.94
Structure 6	-11.64	-3.52	4.54	2.70	3.86	3.86	3.58	2.51	3.59
Structure 7	-6.88	-3.22	8.72	-7.81	4.93	4.93	-14.58	-11.15	-0.16
Structure 8	-8.72	-3.79	3.91	2.60	4.58	4.58	-11.01	1.09	-7.50
Structure 9	-7.64	-2.43	8.65	-5.99	5.24	5.24	-12.08	-8.22	-1.10
Structure 10	-3.27	-0.82	1.85	-2.63	1.91	1.91	-17.51	-4.76	2.26

6.3.7 Influence of Additional Feedback Cues - Higher Trailer Tandem Spread

Considering the baseline driver model coupled with the articulated vehicle model, increasing the tandem axle spreads in the semi-trailer unit yields decreasing the peak path deviation of the tractor during the double lane-change maneuver at 100 km/h. The path tracking enhancement is, however, obtained at the expense of increasing the peak directional responses and corresponding performance measures of the vehicle. Relative significance of additional feedback cues to improve directional responses of the vehicle is examined considering the maximum tandem axle spread of the semi-trailer (t_2=1.85 m). Table 6.17 summarizes the total performance index (J_t) together with its various constituents obtained for each driver model structure. Table 6.18 presents the percentage variations of the peak path deviations together with the peak direction responses of different driver model structures compared to the baseline model.

Table 6.17: Variations in the total performance index and its constituents by considering different driver model structures for higher tandem axle spread of the trailer (100 km/h)

Structure	Performance index constituents									
	J_Y	J_Ψ	$J_{a_{y1}}$	$J_{a_{y2}}$	J_{r1}	J_{r2}	$J_{\dot{\gamma}}$	J_δ	$J_{\dot{\delta}}$	J_t
Structure 1	0.6982	0.0747	0.2079	0.2317	0.1013	0.0852	0.0592	0.0075	0.0032	1.4690
Structure 2	0.7044	0.0739	0.2059	0.2288	0.0995	0.0841	0.0565	0.0073	0.0031	1.4634
Structure 3	0.7006	0.0749	0.2055	0.2286	0.0962	0.0841	0.0545	0.0070	0.0025	1.4539
Structure 4	0.7029	0.0741	0.2064	0.2298	0.0996	0.0845	0.0560	0.0072	0.0024	1.4629
Structure 5	0.7109	0.0787	0.2060	0.2259	0.0978	0.0831	0.0507	0.0069	0.0028	1.4627
Structure 6	0.6765	0.0731	0.2145	0.2383	0.1035	0.0876	0.0585	0.0076	0.0032	1.4626
Structure 7	0.6971	0.0756	0.2073	0.2296	0.0985	0.0844	0.0533	0.0070	0.0022	1.4570
Structure 8	0.6929	0.0747	0.2091	0.2315	0.0998	0.0851	0.0542	0.0072	0.0027	1.4573
Structure 9	0.6998	0.0756	0.2062	0.2285	0.0982	0.0840	0.0526	0.0070	0.0023	1.4543
Structure 10	0.6985	0.0752	0.2066	0.2290	0.0983	0.0842	0.0526	0.0070	0.0022	1.4536

The results suggest that while the total performance index is invariably improved by adding feedback from each of the motion cues, the most significant decrease is observed for structure 3 and 10, which both involve perception of the lateral acceleration of the

tractor unit. The greatest reductions in performance indices related to lateral acceleration and yaw rate of the tractor unit and corresponding peak responses are further obtained by considering the lateral accelerations of the tractor alone, as seen in Table 6.17 and Table 6.18, respectively. As it would be expected, involving the lateral acceleration of the semi-trailer unit yields the greatest decrease in the performance measures related to the lateral acceleration and yaw rate of the trailing unit as well as the articulation rate (Table 6.17). The similar trends can be seen for the corresponding peak responses of the vehicle (a_{y2}, r_2 and $\dot{\gamma}$), as seen in Table 6.18. Influence of a_{y2} to improve the path tracking performance of the vehicle is, however, minimal. The results imply that the driver's perception of only the yaw rate of the semi-trailer unit (structure 6) yields the most significant improvement in the path tracking performance. This can be seen from the term J_Y in Table 6.17 and the greatest reduction of the peak path deviation (Y_{em}) in Table 6.18. The results further show that driver's perception of the yaw rate of the tractor unit alone, as for structure 4, yields significant decrease in the peak steer angle and peak steer rate by -14% and -22%, respectively, suggesting that employing this feedback cue is most beneficial when the driver's aim is to minimize its path tracking performance. Perception of the lateral accelerations of both units and the articulation rate (structure 10) and lateral acceleration and yaw rate of the semi-trailer unit (structure 8), on the other hand, would be most beneficial when the driver aims to reduce its demanded steering effort and the peak directional measures of the vehicle related to a_{y1}, r_1, a_{y2}, r_2 and $\dot{\gamma}$ in a critical driving situation.

Table 6.18: Relative changes in path tracking and directional response measures of the coupled driver-vehicle system with respect to those obtained from the baseline model (structure 1) considering different feedback cues for higher tandem axle spread of the trailer (100 km/h)

Structure	Percentage variations in the peak path deviations and peak directional responses (%)								
	Y_{em} (m)	Ψ_e (deg)	a_{y1} (m/s^2)	r_1 (deg/s)	a_{y2} (m/s^2)	r_2 (deg/s)	$\dot{\gamma}$ (deg/s)	δ (deg)	$\dot{\delta}$ (deg/s)
Structure 2	-1.25	-0.92	-3.09	-3.04	-2.63	-2.63	-1.23	-2.17	1.31
Structure 3	3.01	-0.98	-7.15	-14.43	-7.21	-6.21	-10.75	-8.38	2.66
Structure 4	-1.35	-1.09	-0.86	-0.89	-0.29	-0.30	-9.87	-14.06	-22.00
Structure 5	-0.20	0.24	-1.85	-9.78	-7.86	-7.85	-12.35	-1.09	-2.58
Structure 6	-3.62	-1.73	-4.17	-3.26	-2.70	-2.70	0.83	-2.10	0.65
Structure 7	-1.44	-1.87	-5.01	-10.13	-6.54	-6.54	-11.78	-10.51	-9.21
Structure 8	-2.53	-1.86	-6.48	-7.83	-6.08	-6.08	-5.19	-6.19	-6.97
Structure 9	-0.97	-0.34	-5.80	-9.92	-6.86	-6.86	-11.57	-9.95	-4.10
Structure 10	-0.32	-0.98	-4.54	-11.53	-6.68	-6.67	-9.81	-12.48	-7.69

6.4 Summary

The primary goal of this work was to identify vehicle motion cues that, when integrated to a coupled driver-vehicle model, could yield enhanced directional control performance of the vehicle. The results show that the proposed driver model structures could serve effective tools to determine the most effective motion feedback cues. The results further suggest that the lateral position and heading angle of the lead unit are the most essential sensory cues to achieve satisfactory guidance and control of the vehicle, while the total performance index of the coupled driver-vehicle system can be invariably improved by adding feedback from each of the motion cues. The most significant reduction of the total performance index is generally observed for structure 10, which involves perceptions of a_{y1}, a_{y2} and $\dot{\gamma}$. These feedback cues can be perceived via a driver assist system capable of monitoring and displaying the vehicle state to the driver.

The relative changes in the peak path deviations and peak directional responses of the vehicle are also investigated. These investigations suggest that the peak responses of the vehicle are strongly dependent upon the driver's motion cues feedbacks. The human

driver can thus effectively control a critical state of the articulated vehicle by perceiving certain feedback cues of the vehicle. For instance, the tractor lateral acceleration for heavier semi-trailer unit and the trailer lateral acceleration for the vehicle with longer trailing unit can serve as a secondary cue to reduce the peak articulation rate of the vehicle. These can be mostly attributed to greater compensatory actions of the vehicle driver to minimize the lateral accelerations of the tractor and semi-trailer units, which is achieved by a slower steering action. The results also imply that perceiving certain feedback cues may help the vehicle driver to improve its demanded steering effort. It should be noted that the lower steering effort does not necessarily lead to a higher level of path deviation; but a more effective steering control action, which can also reduce the total performance index and the path tracking performance of the vehicle. Table 6.19 presents the model structures that, when integrated to the baseline driver model, results in significant improvements in path deviation, steering effort and the total performance index of the coupled driver-vehicle system.

Table 6.19: The most effective combinations of feedback cues to improve the path deviation, steering effort and the total performance index of the coupled driver-vehicle system

Vehicle unit	Variable	The driver model structure		
		Path deviation	Steering effort	Total performance index
Tractor	Speed (100 km/h)	6	3 and 10	8 and 10
	Speed (120 km/h)	6 and 8	10	7 and 10
	Heavier mass	6 and 8	4 and 6	8 and 10
	Longer wheelbase	6	3, 7 and 10	3, 7 and 10
	Higher axle spread	6	2 and 10	10
Semi-trailer	Heavier mass	8	3	8 and 10
	Longer wheelbase	4 and 6	5	8 and 10
	Higher axle spread	6	4	3, 10

CHAPTER 7

CONCLUSIONS AND RECOMMENDATIONS

7.1 Highlights and Major Contributions of the Dissertation Research

This dissertation research presents concerns the development of a two-stage preview driver model and its integration to single as well as multiple unit articulated vehicles. A baseline driver model, employing the previewed path information based on instantaneous lateral position and orientation, was formulated with an objective to maintain central lane position of vehicle together with control of vehicle orientation. The baseline driver model was integrated to the yaw-plane models of single and multiple unit vehicles to derive coupled driver-vehicle system models. The resulting coupled driver-vehicle models were analyzed to identify human driver control characteristics subject to the control limits obtained from the reported studies. The control performance limits of the human driver are evaluated under wide ranges of vehicle design parameters and forward speed. The results are discussed in view of human driver control demands and adoptability to the given vehicle.

Relative contributions of different sensory feedbacks were further investigated by integrating driver's perception of selected states of the vehicle combination to the baseline driver model. The contributions of different motion cues to human driver control performance and directional responses of the coupled driver-vehicle system were thoroughly investigated through simulations. The results are discussed so as to build guidance on the designs of driver-assist systems (DAS) for commercial vehicle combinations. The major highlights of the dissertation work are summarized below:

- The reported studies relevant to human driving cognitive behaviors and sensory feedbacks corresponding to different driver model structures were reviewed and analyzed to establish ranges of human driver control parameters, including the driver perception, preview and compensation.

- Relative performance characteristics of reported driver models based on different preview, prediction and control strategies were analyzed in order to establish significance of different control and preview features of the human driver. The driver control performance measures were thoroughly examined so as to assess the contributions of different control strategies and to identify the most effective strategy for application to heavy vehicles drivers.

- A series of experiments were conducted on a driving simulator to identify different control properties of the human drivers as functions of participants' driving experience and forward speed of the vehicle. These included the drivers' reaction times under different steering and braking inputs, and magnitude and rate of steering effort of drivers. The experiments involved different directional maneuvers such as slalom maneuver, abrupt braking, obstacle avoidance and standardized double lane-change maneuvers at different driving speeds.

- The measured data were used to establish correlations between the human driver control performance and the driving experience. The data were further used to obtain regression models describing driver control properties as functions of the speed and driving experience.

- A modified two-stage preview driver model, referred to as the baseline driver model, was formulated and integrated with the single- and multiple-unit articulated vehicle models. Validity of the driver coupled with the single-unit vehicle model was examined by comparing the path tracking and steering responses of the driver-vehicle system with the simulator-measured data for three different forward speeds and two different visibility conditions. The steering responses of the coupled driver-articulated vehicle model were also compared with the reported measured data to illustrate its validity.

- The human drive model parameters were identified through minimization of a composite cost function of selected vehicle states and directional characteristics subject to a set of limit constraints that were defined on the basis of known control limits.

- Simulations were performed to establish the human driver control characteristics and limits considering variations in selected vehicle design parameters and forward speed. The results were discussed in view of control demands imposed on the vehicle driver to achieve desirable path tracking performance and directional dynamics of the articulated vehicle.

- The significance of driver's perception of different motion states of the vehicle were investigated through developments and analyses of a series of human driver model structures. The importance of different motion cues were discussed in view of vehicle control in terms of path tracking and control demands of the driver using a driver assist system capable of monitoring and displaying the desired states to the driver.

7.2 Conclusions

The major conclusions drawn from the dissertation research work are summarized below:

- Human driver models incorporating a roadway preview and a path prediction strategy yield improved path tracking performance and reduced steering effort demand, particularly at higher driving speeds.

- A two-stage preview strategy coupled with the 'internal vehicle model' path predictor can provide most effective path tracking performance over a wide range of variations in speed and vehicle parameters, compared to the single- and multi-point preview strategies.

- The simulator-measured data suggested good correlations of the driving experience with various performance measures acquired during slalom maneuvers. These included: (i) maneuver accomplishment at 70 km/h; (ii) peak steer angle and rate of steering; (iii) crest factors of steer angle and its rate; (iv) steering profile area; and (v) the 'mean' and 'peak' speed variations at the higher speed of 70 km/h.

- The simulator-measured data obtained during abrupt braking and obstacle avoidance maneuvers implied that the drivers' steering response time varies with variations in the forward speed of the vehicle. Human driver steering response time could be described by a regression function in forward speed.

- The data obtained from simulator measurements also implied that the magnitude and rate of steering responses of drivers are strongly affected by the forward speed and the participants' driving experience. Peak steer angle and the peak steer rate could be described as a square function of both the speed and the driving experience.

- A two-stage preview can adequately describe human drivers' near and far path preview strategy. The far and near preview distances strongly depend upon forward speed and road geometry.

- Comparison of the proposed two-stage preview driver model responses and the simulator-measured data suggested that the baseline driver model based on path position and orientation could provide relatively good predictions of the drivers'

steering responses under clear as well as limited visibility conditions at different forward speeds.

- The steering response of an articulated vehicle coupled with the baseline human driver model showed reasonably good agreements with the reported field measure data. Considering a set of limit constraints on the driver control parameters, the model parameters were identified through minimization of a composite performance index comprising lateral position and orientation errors, articulation rate, lateral accelerations and yaw rates of both the units as well as steering effort of the driver.

- The lateral position and heading angle of the tractor unit form the most essential sensory cues for the driver to achieve satisfactory guidance and control of the vehicle at lower driving speeds. The baseline human driver model based on lateral position and orientation errors alone, however, yields path deviation and lateral accelerations of both the tractor and semi-trailer units beyond the defined permissible thresholds at speeds near and above 100 km/h. This suggested the need for additional motion cues to the driver for enhanced path prediction and control performance.

- The control demands of the human driver strongly depend on various vehicle design parameters and operating speed. The path tracking performance of the baseline driver model could be enhanced by reducing the mass and wheelbase of both the lead and trailing units.

- Increasing the tandem axle spread of the semi-trailer unit resulted in improved path tracking performance of the vehicle, while an opposite trend was evident for tractor drive-axle spread.

- The results suggested that freight vehicle combinations with longer and heavier tractor and semi-trailer units can be best adapted to a driver with greater prediction skill, faster reaction and longer preview distances, which generally describe a driver with superior driving and compensations skills.

- The simulations suggested lower compensation gains and thus a relaxed path control in order to limit directional responses of the vehicle such as lateral accelerations and yaw rates of both the units, particularly for longer and heavier semi-trailer units. The driver, however, demands longer preview distance, a higher level of prediction and faster steering response.

- Enhancing human driver's perception of semi-trailer’s lateral acceleration and yaw rate resulted in improved path tracking and control performance of the driver. Driver's perception of these motion cues could be realized through on-line measurements and displays.

- The driver's knowledge of the articulation rate, in addition to the tractor and trailer lateral accelerations, could provide most significant improvement in the driver control performance.

- The perceptions of vehicle directional responses, in-particular, the lateral acceleration of the two units permit greater lag time for the driver's compensation and reduce the steering effort demands on the driver.

- The perceptions of the vehicle lateral acceleration also permit improved adaptation of the human driver to articulated vehicle with relatively higher cargo loads.

- The integration of yaw rates of the two units to the driver's matrix of perceptions was found most beneficial for control of longer articulated vehicles.

- The lateral acceleration and yaw rate responses of the long articulated vehicle combinations are the most essential cues for design of advanced driver assist systems (ADAS).

7.3 Recommendations for Future Studies

This dissertation research proposed a two-stage human driver model structure for applications in control of articulated commercial vehicles. The model simulations permitted the study of control limits of the human driver with regards to selected weights and dimensional design parameters of the vehicle and the forward speed. The results attained from alternate driver model structures, involving human driver's perception of additional motion states of the vehicle, provided valuable design guidance for design of effective commercial vehicle driver assist systems. Characterization and modeling of the human driver, however, involve thorough understanding of cognitive behaviors under a range of driving scenarios, which are not only challenging but also most difficult to measure. Furthermore, only very little knowledge exists on interactions between human cognitive measures and operational dynamics of commercial vehicle. Far more systematic studies in human driver and vehicle interactions are thus desirable,

particularly, for the designs of ADAS for commercial vehicles. Some of these are briefly summarized below:

- Comprehensive field- and simulator-measurements under a range of realistic driving scenarios are vital for characterizing human drivers' responses in terms of path preview, path prediction and compensation strategies, and limb dynamic responses. The data reported thus far have shown wide discrepancies and thereby broad ranges of different cognitive measures.

- More effective measurement techniques such as eye-tracking and visual-field scanning systems need to be developed for accurate measurements of human driver preview. Moreover, alternate concepts should be explored for qualifying the near and far preview characteristics of the driver. The currently available slip-preview method is not considered reliable.

- Alternate methods for characterizing the human driver's error compensation need to be explored. The method based on path error and steering effort, as applied in this thesis, is strongly affected by many confounders such as driving skill, driving experience, age, speed, gender, road curvature and visibility.

- Owing to several confounders, the experiment designs must involve appropriate considerations of driving experience, gender, age and visibility for a set of defined road curvature and steering maneuvers. Moreover, critical directional maneuvers and environmental conditions need to be defined so as to characterize critical limits of human driver cognition.

- The effect of different motion and sound cues on human driver cognition and control should be systematically investigated in order to identify most beneficial cues for designs of ADAS.

- The human driver models generally describe drivers' control and compensation abilities considering human as an ideal controller. It is shown that consideration of target directional responses and permissible deviations allows for realization of the controller within known limits. It is, however, essential to incorporate driving skill and environmental condition within the model, which substantially alter the human driver control characteristics. Furthermore, reported driver models focus on steering behavior of the driver alone assuming a constant forward speed. Considering that most critical maneuvers involve simultaneous steering and braking, alternate model need to be developed to characterize human driver responses in terms of braking and steering actions.

- Further efforts are also needed to investigate the driver model coupled with a more comprehensive vehicle model (with roll, pitch and longitudinal degrees of freedom) so as to enhance understanding of driver's interaction with the vehicle

under more realistic motion cues. These would also permit effective developments in driver assist technologies for future commercial vehicles.

- A more refined model of the steering mechanism is highly desirable to fully describe the nonlinear dynamics of the steering system and to examine the significance of steering torque feedback on steering responses of the human driver, particularly for power steering systems that use hydraulic or electric actuators.

REFERENCES

[1] Evans, L. (1991) Traffic safety and the driver. Van Nostrand Reinhold, New York.

[2] Commercial motor vehicle facts (2013) Federal Motor Carrier Safety Administration (FMCSA).

[3] Fatality analysis reporting system general estimates system: 2011 Data summary (2013) National Highway Traffic Safety Administration (NHTSA), Washington DC.

[4] Hendricks D, Freedma M, Zador PL, Fell J (2001) The relative frequency of unsafe driving acts in serious traffic crashes. Technical Report: National Highway Traffic Safety Administration (NHTSA), Washington DC.

[5] Macadam CC (2003) Understanding and modeling the human driver. Vehicle System Dynamics, 40(1-3): 101 – 134.

[6] McRuer DT, Krendel ES (1957) Dynamic response of human operators. Technical Report: The Franklin Institute, Air Force Flight Dynamics Labaoratory (AFFDL), Ohio.

[7] Plöchl M, Edelmann J (2007) Driver models in automobile dynamics application. Vehicle System Dynamics, 45: 699 – 741.

[8] Guo K (1993) Modelling of driver/vehicle directional control system. Vehicle System Dynamics, 22: 141 – 184.

[9] Yang X (1999) A closed-loop driver/vehicle directional dynamic predictor. PhD Thesis, Concordia University, Montreal, Canada.

[10] McRuer D, Graham D, Krendel ES, Reisener W (1965) Human pilot dynamics in compensatory systems: theory, models and experiments with controlled-element and forcing function variations. Technical Report: The Franklin Institute, Air Force Flight Dynamics Labaoratory (AFFDL), Ohio.

[11] Yang X, Rakheja S, Stiharu I (2002) Structure of the driver model for articulated vehicles. International Journal of Heavy Vehicle Systems, 9(1): 27 – 51.

[12] Edelmann J, Plöchl M, Reinalter W, Tieber W (2007) A passenger car driver model for higher lateral accelerations. Vehicle System Dynamics, 45(12): 1117 – 1129.

[13] Habib MS (1993) Identification of vehicle-driver stability domain using human pilot structural model. American Control Conference, San Francisco, CA, USA.

[14] MacAdam CC (2001) Development of a driver model for near/at-limit vehicle handling. University of Michigan, Transportation Research Institute, UMTRI-2001-43.

[15] Sharp R (2000) A mathematical model for driver steering control, with design, tuning and performance results. Vehicle System Dynamics, 33(5): 289 – 326.

[16] Yang X, Rakheja S, Stiharu I (2001) Adapting an articulated vehicle to its drivers. Journal of Mechanical Design, 123 (1): 132 – 140.

[17] Ishio J, Ichikawa H, Kano Y, Abe M (2008) Vehicle-handling quality evaluation through model-based driver steering behavior. Vehicle System Dynamics, 46: 549 – 560.

[18] Ungoren AY, Peng HM (2005) An adaptive lateral preview driver model. Vehicle Dystem Dynamics, 43(4): 245 – 259.

[19] Iguchi M (1959) A study of manual control. Journal of mechanic Society of Japan, 62(481).

[20] Cole DJ, Pick AJ, Odhams AMC (2006) Predictive and linear quadratic methods for potential application to modelling driver steering control. Vehicle System Dynamics, 44(3): 259 – 284.

[21] Menhour L (2009) Steering control based on a two-level driver model: experimental validation and robustness tests. IEEE Multi-Conference on Systems and Control, Saint Petersburg, Russia.

[22] Keen SD, Cole DJ (2011) Application of time-variant predictive control to modelling driver steering skill. Vehicle System Dynamics, 49(4): 527 – 559.

[23] Guan H, Guo K (1993) A comparison of two optimal preview driver models for automobile directional control. SAE Technical Paper 931932.

[24] MacAdam CC (1988) Development of driver/vehicle steering interaction models for dynamic analysis. University of Michigan, Transportation Research Institute, UMTRI-86 – 41.

[25] Liu Z (2007) Characterisation of optimal human driver model and stability of a tractor-semitrailer vehicle system with time delay. Mechanical Systems and Signal Processing, 21(5): 2080 – 2098.

[26] MacAdam CC, Fancher P (1986) Study of the closed-loop directional stability of various commercial vehicle configurations. Vehicle System Dynamics: International Journal of Vehicle Mechanics and Mobility, 15(1): 367 – 382.

[27] McRuer DT (1967) A review of quasi-linear pilot models. IEEE Trans. on Human Factors in Electronics, 8(3): 231 – 249.

[28] Erséus A (2010) Driver-vehicle interaction, identification, characterization and modelling of path tracking skill. Ph.D. Thesis, KTH Univeristy, School of Engineering Sciences, Stockholm, Sweden.

[29] Weir DH, McRuer DT (1970) Dynamics of driver vehicle steering control. Automatica, 6(1): 87 – 98.

[30] Guo KH, Fancher P (1983) Preview-Follower method for modelling closed-loop vehicle directional control. Symposium of 19th Annual Conference on Manual Control, Cambridge, Massachusetts, USA.

[31] Land MF, Lee L (1994) Where we look when we steer. Nature 369: 742 – 744.

[32] Bigler RS, Cole DJ (2011) A review of mathematical models of human sensory dynamics relevant to the steering task. Proceedings of 22nd IAVSD Symposium on the Dynamics of Vehicles on Roads and Tracks, Manchester, UK.

[33] Teichner WH (1954) Recent studies of simple reaction time. Psychological Bulletin, 51(2): 128 – 149.

[34] Wallis G, Chatziastros A, Bülthoff H (2002) An unexpected role for visual feedback in vehicle steering control. Current Biology, 12(4): 295 – 299.

[35] Grabherr L, Nicoucar K, Mast FW, Merfeld DM (2008) Vestibular thresholds for yaw rotation about an earth-vertical axis as a function of frequency. Experimental Brain Research, 186: 677 – 681.

[36] Huang J, Young LR (1981) Sensation of rotation about a vertical axis with a fixed visual field in different illuminations and in the dark. Experimental Brain Research, 41: 172 – 183.

[37] Kingma H (2005) Thresholds for perception of direction of linear acceleration as a possible evaluation of the otolith function. BMC Ear, Nose Throat Disorders, 5(5):1 – 6.

[38] Teichner WH, Krebs ML (1972) Laws of the simple visual reaction time. Psychology Review, 79(4): 344 – 358.

[39] Weir DH, Mcruer DT (1968) Models for steering control of motor vehicles. Proceedings of the 4th annual NASA-University conference on manual control (NASA SP-192), Washington DC, USA, 135 – 169.

[40] MacAdam CC (1981) Application of an optimal preview control for simulation of closed-loop automobile driving. IEEE Transactions on Systems, Man, and Cybernetics, 393 – 399.

[41] Kondo M, Ajimine A (1968) Driver's sight point and dynamics of the driver-vehicle-system related to it. SAE Technical Paper 680104.

[42] Yoshimoto K (1968) Simulation of driver/vehicle system including preview control. Journal of Mechanics Society Japan, 71.

[43] McRuer D (1980) Human dynamics in man-machine systems. Automatica, 16(3): 237 – 253.

[44] Afonso J, Brandelon B, Huerre B, Sa Da Costa J (1993) Analysis of driver's visual behavior. SAE Technical Paper No 931931.

[45] Donges E (1978) A two-level model of driver steering behavior. Human Factors, 20(6): 393 – 413.

[46] Connolly P (1966) Visual considerations of man, the vehicle, and the highway. SAE Technical Paper 660164.

[47] Schnell T, Zwahlen H (1999) Driver preview distances at night based on driver eye scanning recordings as a function of pavement marking retroreflectivities. Journal of the Transportation Research Board, 1692: 129 – 141.

[48] Sharp RS (2005) Driver steering control and a new perspective on car handling qualities. Journal of Mechanical Engineering Science, 219(C): 1041-1051.

[49] McLean JR, Hoffmann ER (1973) The Effect of restricted preview on driver steering control and performance. Human Factors, 15(4): 421 – 430.

[50] Cloete S, Wallis G (2010) Visuomotor control of steering: The artifact of the matter. Experimental Brain Research, 208(4): 475 – 489.

[51] Myers J (2002) The effects of near and far visual occlusion upon a simulated driving task. Master's Thesis, South Dakota State University, Madison, USA.

[52] Gordon A (1966) Experimental isolation of the driver's visual input. Public Roads 33(12): 266 – 273.

[53] Liu A, Salvucci D (2001) Modeling and prediction of human driver behavior. Proceedings of the 9th International Conference on Human-Computer Interaction, New Orleans.

[54] Reid LD, Solowka EN (1981) A systematic study of driver steering behaviour. Ergonomics, 24(6): 447 – 462.

[55] Harbluk JL, Noy YI, Eizenman M (2002) The impact of cognitive distraction on driver visual behaviour and vehicle control. Report No. TP13889E: Transport Canada, Ontario.

[56] Neumann H, Deml B (2011) The two-point visual control model of steering - new empirical evidence.Digital Human Modeling, LNCS 6777:493 – 502.

[57] Land MF, Tatler BW (2001) Steering with the head: the visual strategy o a racing driver. Current Biology, 11(15): 1215 – 1220.

[58] Robertshaw KD, Wilkie RM (2008) Does gaze influenc steering around a bend. Journal of Vision, 8(4): 18.1 – 13.

[59] Boer ER (1996) Tangent point oriented curve negotiation. IEEE Proceedings of the intelligent vehicles symposium, Tokyo.

[60] Nevalainen S, Sajaniemi J (2004) Comparison of three eye tracking devices in psychology of programming research. 16th Annual workshop of the psychology of programming interest group, Ireland.

[61] Wallis G (2006) The temporal and spatial limits of compensation for fixational eye movements. Vision Research, 46(18): 2848 – 2858

[62] Rahimi M, Briggs RP, Thom DR (1990) A field evaluation of driver eye and head movement strategies toward environmental targets and distractors. Applied Ergonomics, 21(4): 267 – 274.

[63] Macadam CC (1980) An optimal preview control for linear systems. ASME Journal of Dynamic Systems, Measurement And Control, 102: 188 – 190.

[64] Leglouis T (1986) Characterization of dynamic vehicle stability using two models of the human pilot behaviour. Vehicle System Dynamics, 15(1): 1 – 18.

[65] Mitschke M (1993) Driver-vehicle-lateral dynamics under regular driving. Vehicle System Dynamics, 22(5-6): 483 – 492.

[66] Moon C, Choi SB (2011) A driver model for vehicle lateral dynamics. International Journal of Vehicle Design, 56(1-2): 49 – 80.

[67] Pick AJ, Cole DJ (2008) A mathematical model of driver steering control including neuromuscular dynamics. Journal of Dynamic Systems, Measurement, and Control, 130(3): 1 – 9.

[68] Sharp RS, Valtetsiotis V (2001) Optimal preview car steering control. Vehicle System Dynamics, 35: 101 – 117.

[69] Odhams A, Cole D (2009) Application of linear preview control to modelling human steering control. Journal of Automobile Engineering, 223(D): 835 – 853.

[70] Land M, Horwood J (1995) Which parts of the road guide steering. Nature, 377: 339 – 340.

[71] Billington J, Field DT, Wilkiec, RM, Wanna JP (2010) An fMRI Study of parietal cortex involvement in the visual guidance of locomotion. Journal of Experimental Psychology: Human Perception and Performance, 36(6): 1495 – 1507.

[72] Sentouh C, Chevrel P, Mars F, Claveau F (2009) A Sensorimotor driver model for steering control. Proceedings of the 2009 IEEE International Conference on Systems, Man, and Cybernetics, San Antonio, USA.

[73] Menhour L, Lechner D, Charara A (2011) Two degrees of freedom PID multi-controllers to design a mathematical driver model: experimental validation and robustness tests. Vehicle System Dynamics: International Journal of Vehicle Mechanics and Mobility, 49(4): 595 – 624.

[74] Irmscher M, Willumeit HP, Juergensohn T (1999) Driver models in vehicle development. Vehicle System Dynamics Supplement, 33: 83 – 93.

[75] McRuer DT, Hofmann LG, Jex H, Moore G, Phatak A, Weir DH, Wolkovitch J (1968) New approaches to human-pilot/vehicle dynamic analysis. Technical Report: Air Force Flight Dynamics Labaoratory (AFFDL), Ohio.

[76] Hess RA (1985) A model based theory for analyzing human control behavior. Advances in Man-Machine Systems Research, 2: 129 – 175.

[77] Mcruer DT, Allen RE, Weir DH, Klein RH (1977) New results in driver steering control models. The Journal of the Human Factors and Ergonomics Society, 19: 381 – 397.

[78] Horiuchi S, Yuhara N (2000) An analytical approach to the prediction of handling qualities of vehicles with advanced steering control system using multi-input driver model. Journal of Dynamic Systems, Measurement, and Control, 22(3): 490 – 497.

[79] Salvucci D, Gray R (2004) A two-point visual control model of steering. Perception, 33(10): 1233 – 1248.

[80] Fildes B, Triggs Tj (1985) The effect of changes in curve geometry on magnitude estimates of road-like perspective curvature. Perception & Psychophysics, 37(3): 218 – 224.

[81] Allen R, Rosenthal T, Szostak H (1988) Analytical modeling of driver response in crash avoidance maneuvering-Volume I. Technical Background: National Highway Traffic Safety Administration (NHTSA), Washington DC, USA.

[82] Allen RW, Szostak HT, Rosenthal TJ (1987) Analysis and computer simulation of driver/vehicle interaction. SAE Technical Paper 871086.

[83] Savkoor AR, Ausejo S (1999) Analysis of driver steering and speed control strategies in curve negotiation. Vehicle System Dynamics Supplement, 33: 94 – 109.

[84] Chandler RE, Herman R, Montroll E (1958) Traffic dynamics studies in car following. Operation Research, 6(2): 165 – 184.

[85] Gazis DC, Herman R, Potts B (1959) Car following Theory of steady-state traffic flow. Operation Research, 7(4): 499 – 505.

[86] Pipes LA (1953) An operational analysis of traffic dynamics. Journal of Applied Physics, 24(3): 274 – 281.

[87] Reymond G, Kemeny A, Droulez J, Berthoz A (2001) Role of lateral acceleration in curve driving: driver model and experiments on a real vehicle and a driving simulator. Human factors, 43(3): 483 – 495.

[88] Adams L (1994) Review of the literature on obstacle avoidance maneuvers: braking versus steering. University of Michigan, Transportation Research Institute, UMTRI-94-19.

[89] Dewar RE, Olson P (2007) Human factors in traffic safety. Lawyers & Judges Publishing Company Inc.

[90] Pick A (2004) Neuromuscular dynamics and the vehicle steering task. PhD thesis, University of Cambridge, Cambridge, UK.

[91] Barrett G, Kobayashi M, Fox B (1968) Feasibility of studying driver reaction to sudden pedestrian emergencies in an automobile simulator. The Journal of the Human Factors and Ergonomics Society, 10(1): 19 – 26.

[92] Green M (2000) How Long does it take to stop? methodological analysis of driver perception-brake times. Transportation Human Factors, 2(3): 195 – 216.

[93] Lockhart T (2010) Effects of age on dynamic accommodation. Ergonomics, 53(7): 892 – 903.

[94] Davies B, Waits J (1969) Preliminary investigation of movement time between brake and accelerator pedals in automobiles. The Journal of the Human Factors and Ergonomics Society, 11(4): 407 – 410.

[95] Hoffmann E (1991) Accelerator-to-brake movement times. Ergonomics, 34(3): 277 – 287.

[96] Warshawsky-Livne L, Shinar D (2002) Effects of uncertainty, transmission type, driver age and gender on brake reaction and movement time. Journal of Safety Research, 33(1): 117 – 128.

[97] Hancock PA, Simmons L, Hashemi L, Howarth H, Ranney T (1999) The effects of in-vehicle distraction on driver response during a crucial driving maneuver. Transportation Human Factors, 1(4): 295 – 309.

[98] Lenne MG, Triggs TJ, Redman JR (1999) Alcohol, time of day, and driving experience: effects on simulated driving performance and subjective mood. Transportation Human Factors, 1(4): 331 – 346.

[99] Mehmood R, Easa S (2009) Modeling reaction time in car-following behaviour based on human factors. International Journal of Engineering and Applied Sciences, 5(2): 93 – 101.

[100] Olson P, Sivak M (1986) Perception-response time to unexpected roadway hazards. The Journal of the Human Factors and Ergonomics Society, 28(1): 91 – 96.

[101] Young M (2007) Back to the future: brake reaction times for manual and automated vehicles. Ergonomics, 50(1): 46 – 58.

[102] Hess RA (1981) Pursuit tracking and higher levels of skill development in the human pilot. IEEE transactions on systems, man, and cybernetics, 11(4): 262 – 273.

[103] Hess RA, Modjtahedzadeh A (1989) A preview control model of driver steering behavior. IEEE Control Systems Magazine, 504 – 509.

[104] Johansson G (1971) Drivers' brake reaction times. Human Factors, 13(1): 23 – 27.

[105] Klemmer ET (1956) Time uncertainty in simple reaction time. Journal of Experimental Psychology, 51(3): 179 – 184.

[106] Summala H (1981) Drivers' steering reaction to a light stimulus on a dark road. Ergonomics, 24(2): 125 – 131.

[107] Summala H (1981) Driver/Vehicle steering response latencies. The Journal of the Human Factors and Ergonomics Society, 23(6): 683 – 692.

[108] McGehee DV, Mazzae EN, Baldwin GHS (2000) Driver reaction time in crash avoidance research: validation of a driving simulator study on a test track. Proceedings of the IEA 2000/HFES 2000 Congress, San Diego, USA

[109] Magdaleno R (1971) Experimental validation and analytical elaboration for models of the pilot's neuromuscular subsystem in tracking tasks. NASA Contractor Report CR1757

[110] Hoult V (2008) A neuromuscular model for simulating driver steering torque. PhD thesis, University of Cambridge, Cambridge

[111] Droogendijk C (2010) A new neuromuscular driver model for steering system development. Master's thesis, Delft University of Technology, Delft, Netherlands.

[112] de Vulgt E (2004) Identification of spinal reflexes. PhD thesis, Delft University of Technology, Delft, Netherlands.

[113] McRuer D, Magdaleno R, Moore G (1967) A neuromuscular actuation system model. IEEE Transactions On Man-Machine Systems, 9(3): 61 – 71.

[114] Jonsson S, Jonsson B (1975) Function of the muscles of the upper limb in car driving. Ergonomics, 18(4): 375 – 388.

[115] Pick AJ, Cole DJ (2006) Measurement of driver steering torque using electromyography. Journal of Dynamic Systems, Measurement and Control, 128(4): 960-968

[116] Hoult W, Cole DJ (2008) A neuromuscular model featuring co-activation for use in driver simulation. Vehicle System Dynamics, 46(1): 175 – 189.

[117] Modjtahedzadeh A, Hess RA (1993) A model of driver steering control behaviour for use in assessing vehicle handling qualities. Journal of Dynamic Systems, Measurement And Control, 115(3): 456-464.

[118] Pick A, Cole D (2007) Dynamic properties of a driver's arms holding a steering wheel. Journal of Automobile Engineering, 221(D): 1475 – 1486.

[119] Burdet E, Tee KP, Mareels I, Milner TE, Chew CM, Franklin DW, Osu R, Kawato M (2006) Stability and motor adaptation in human arm movements. Biological Cybernetics, 94: 20 – 32.

[120] Cheong D (2006) Steering torque feedback. Master's thesis, Cambridge University, Cambridge, UK.

[121] Chai YW (2004) A study of effect of steering gain and steering torque on driver's feeling for sbw vehicle. Proceedings of FISITA world automotive congress, Barcelona, Spain.

[122] Cole DJ (2011) Influence of steering torque feedback and neuromuscular dynamics on driver and vehicle response to lateral force disturbance. Proceeding of 22nd IAVSD Symposium on the Dynamics of Vehicles on Roads and Tracks, Manchester, UK.

[123] Toffin D, Reymond G, Kemeny A, Droulez J (2003) Influence of steering wheel torque feedback in a dynamic driving simulator. Proceedings of the Driving Simulation Conference, Dearborn, USA.

[124] Wong JY (2001) Theory of ground vehicles. John Wiley & Sons Inc.

[125] Pacejka HB (2005) Tire and vehicle dynamics. Society of Automotive Engineers Inc.

[126] Hirsch P (2012) 'pierro.hirsch@viragesimulation.com', Virage simulation Inc.

[127] ISO 3888-1, passenger cars - test track for a severe lane-change maneuver - part 1: double lane-change, International Standards Organization, 1999.

[128] Abe M, Yoshio K (2008) A study on vehicle handling evaluation by model based driver steering behavior. Proceedings of FISITA world automotive congress, Munich, Germany.

[129] Guo K (2004) Development of a longitudinal and lateral driver model for autonomous vehicle control. International Journal of Vehicle Design, 36(1): 50 – 65.

[130] Hildreth EC, Beusmans JMH, Boer ER, Royden CS (2000) From vision to action: experiments and models of steering control during driving. Joumal of Experimental Psychology: Human Perception and Performance, 26(3): 1106 – 1132.

[131] Waard DD (1996) The measurement of drivers' mental workload. PhD thesis, University of Groningen, Netherlands.

[132] Breuer J (1998) Analysis of driver-vehicle-interactions in an evasive manoueuvre - results of Moose test studies. 16th International Technical Conference on the Enhanced Safety of Vehicles (ESV), Windsor, Canada.

[133] Forkenbrock G, Elsasser D (2005) An assessment of human driver steering capability. Report: National Highway Traffic Safety Administration (NHTSA), Washington DC.

[134] Horton D, Crolla D (1992) Application of linear sensitivity methods to vehicle dynamics problems. Vehicle System Dynamics: International Journal of Vehicle Mechanics and Mobility, 20(1): 269 – 283.

[135] Nalecz A (1989) Application of sensitivity methods to analysis and synthesis of vehicle dynamic systems. Vehicle System Dynamics: International Journal of Vehicle Mechanics and Mobility, 18(1-3): 1 – 44.

[136] Guo KH, Zong CF, Kong FS, Chen ML (2002) Objective evaluation correlated with human judgment - An approach to the optimization of vehicle handling control system. International Journal of Vehicle Design, 29(1-2): 96 – 111.

[137] Transport Canada (2008) Hybrid technologies electric conversion: Test plan. Transport Canada, ecoTECHNOLOGY for Vehicles (eTV) Program, Vancouver, Canada.

[138] McCauley ME (1984) Research issues in simulator sickness: Proceedings of a workshop. National Academy Press, Washington DC.

[139] Zhang Y, Lin WC, Chin YS (2010) A pattern-recognition approach for driving skill characterization. IEEE transactions on intelligent transportation systems, 11(4): 905 – 916.

[140] Zhang Y, Lin WC, Chin YS (2008) Driving skill characterization: A feasibility study. IEEE international conference on robotics and automation, Pasadena, USA.

[141] Tang X (2009) Driving skill recognition: New approaches and their comparison. American Control Conference, St. Louis, USA.

[142] Oscarsson M (2003) Variable vehicle dynamics design - objective design methods. Master's thesis, Linköping University, Linköping, Sweden.

[143] Heger R (1995) Driver behaviour and driver mental workload as criteria of highways geometric design quality. International Symposium on Highway Geometric Design Practices, Boston, USA.

[144] Triggs TJ, Harris WG (1982) Reaction time of drivers to road stimuli. Monash University, Human Factors Report No HFR-12.

[145] Evans L, Schwing RC (1985) Human behavior and traffic safety. Plenum Press, New York.

[146] Hoffmann M, Fischer E, Richter B (1992) The incorporation of tire models into vehicle simulations. Vehicle System Dynamics: International Journal of Vehicle Mechanics and Mobility, 21(1): 49 – 57.

[147] Ranganathan R, Aia A (1995) Development of heavy vehicle dynamic stability analysis model using MATLAB/SIMULINK. SAE Technical Paper 952638.

[148] Ervin R, Guy Y (1986) The influence of weights and dimensions on the stability and control of heavy-duty trucks in Canada. University of Michigan, Transportation Research Institute, UMTRI-86-35/II

[149] Fancher PS, Mallikarjunarao C, Nisonger RL (1979) Simulation of the directional response characteristics of tractor-semitrailer vehicles. University of Michigan, Highway Safety Research Institute, UM-HSRI-79-9

[150] El-Gindy M, Wong JY (1987) A comparison of various computer simulation models for predicting the directional responses of articulated vehicles. Vehicle System Dynamics, 16(5): 249 – 268.

[151] Leucht PM (1970) The directional dynamics of the commercial tractor-semitrailer vehicle during braking. SAE Technical Paper 700371.

[152] Fancher PS, Bareket Z (1992) Including roadway and tread factors in a semi-empirical model of truck tires. Vehicle System Dynamics: International Journal of Vehicle Mechanics and Mobility, 21(1): 92 – 107.

[153] Bakker E, Nyborg L, Pacejka H (1987) Tyre modelling for use in vehicle dynamics studies. SAE Technical Paper 870421.

[154] Palkovics L, El-Gindy M (1993) Neural network representation of tyre characteristics: The neuro-tyre. Intenational Jornal of Vehicle Design, 14(5-6): 563 – 591.

[155] Bareket Z, Fancher PS (1989) Representation of truck tire properties in braking and handling studies: The influence of pavement and tire conditions on frictional characteristics. University of Michigan, Transportation Research Institute, UMTRI-89-33.

[156] Vullurupalli RK (1993) Directional dynamic analysis of an articulated vehicle with articulation dampers and forces-steering. PhD Thesis, Concordia University, Montreal, Canada.

[157] Conner D, Bieber-Tregear M, Tregear S (2012) Visual field loss and commercial motor vehicle driver safety. The Federal Motor Carrier Safety Administration, Washington DC, USA.

[158] Dunn AL (2003) Jackknife stability of articulated tractor-semitrailer vehicles with high-output brakes and jackknife detection on low coefficient surfaces. PHD thesis, Ohio State University, Ohio, USA.

[159] Karkee M (2009) Modeling, identification and analysis of tractor and single axle towed implement system. PhD Thesis, Iowa State University, Iowa, USA.

[160] El-Gindy M, Woodrooffe JHF (1990) Study of rollover threshold and directional stability of log hauling trucks. National Research Council Canada, Division of Mechanical Engineering, Ottawa, Ontario, TR-VDL-002.

[161] Ervin RD (1983) The influence of size and weight variables on the roll stability of heavy duty trucks. SAE Technical Paper 831163.

[162] Winkler C (2000) Rollover of heavy commercial vehicles. UMTRI Research Review, October-December 2000, Vol. 31(4).

[163] Tianjun Z, changfu Z (2009) Modelling and active safe control of heavy tractor semi-trailer, Second International Conference on Intelligent Computation Technology and Automation, Handan, China.

[164] Schulman JF (2003) Heavy truck weight and dimension limits in canada. The Railway Association of Canada.

[165] Task Force on Vehicle Weights and Dimensions Policy (2011) Heavy truck weight and dimension limits for interprovincial operations in canada: resulting from the federal-provincial-territorial memorandum of understanding on interprovincial weights and dimensions.

Appendix A

A.1 Yaw-Plane Model of the Single-Track Articulated Vehicle

The equations of motion of the constant speed single-track yaw-plane model of the articulated vehicle (Figure A.1), describing the lateral and yaw velocities of the tractor (unit 1), v_{y1} and r_1, and yaw velocity of the semi-trailer (unit 2), r_2, are obtained as:

$$m_1(\dot{v}_{y1} + r_1 v_{x1}) = F_{y1}\ cos\,\delta_F + F_{y2} + F_{y3} + F_{YA} \tag{A.1}$$

$$I_{zz1}\dot{r}_1 = (F_{y1}\ cos\,\delta_F)a_1 - F_{y2}a_2 - F_{y3}a_3 + M_1 + M_2 + M_3 + M_{DT2} + M_{DT3} - F_{YA}c_1 \tag{A.2}$$

$$I_{zz2}\dot{r}_2 = -(F_{YA}\ cos\,\gamma)c_2 - F_{y4}\,a_4 - F_{y5}\,a_5 + M_4 + M_5 + M_{DT4} + M_{DT5} \tag{A.3}$$

where m_j and I_{zzj} are the mass and yaw moment of inertia of unit j ($j = 1,2$), respectively, and v_{xj} is forward speed of unit j. F_{yk} , M_k and M_{DTk} are, respectively, the cornering and longitudinal forces, aligning moment and dual tire moment of the k^{th} axle tires (k=1,2,3,4,5). a_k is the longitudinal distance from k^{th} axle tires to the center of gravity of the associated unit, and c_j is the longitudinal distance between the articulation joint and the center of gravity of unit j. F_{XA} and F_{YA} are the longitudinal and lateral forces at the articulation point, which are derived from the following constraint equations:

$$\begin{aligned} F_{XA} &= -m_2(\dot{v}_{x2} + r_2 v_{y2})\ cos\,\gamma - m_2(\dot{v}_{y2} + r_2 v_{x2})\ sin\,\gamma + (F_{y4} + F_{y5})\ sin\,\gamma \\ F_{YA} &= \ \ m_2(\dot{v}_{x2} + r_2 v_{y2})\ sin\,\gamma - m_2(\dot{v}_{y2} + r_2 v_{x2})\ cos\,\gamma + (F_{y4} + F_{y5})\ cos\,\gamma \end{aligned} \tag{A.4}$$

where γ is the articulation angle. From the above constraint relations in the lateral and longitudinal directions, assuming small articulation angles, the longitudinal and lateral velocities of the semi-trailer unit can be related to those of the tractor unit in the following manner:

$$\begin{aligned} v_{x2} &= v_{x1}\ cos\,\gamma + (c_1 r_1 - v_{y1})\ sin\,\gamma \\ v_{y2} &= -c_2 r_2 + v_{x1}\ sin\,\gamma + (v_{y1} - c_1 r_1)\ cos\,\gamma \end{aligned} \tag{A.5}$$

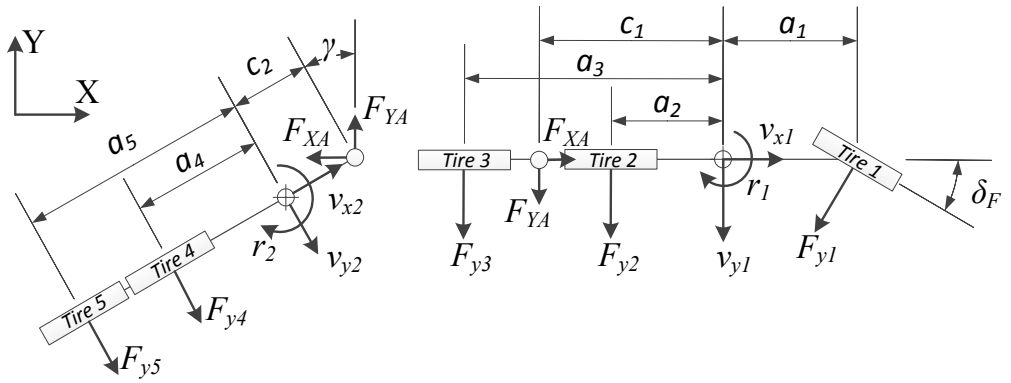

Figure A.1: Three DoF yaw-plane model of the single-track articulated vehicle

Assuming linear cornering characteristics of the tire for small side-slip angles, the cornering force of the tire on axle k^{th} is expressed as:

$$F_{yk} = C_k \alpha_{kj} \tag{A.6}$$

where α_{kj} is the average side-slip angle developed at the tires mounted on axle k of the unit j. C_k is the cornering stiffness of tires mounted on axle k. The side-slip angle of the tires on axle k can be expressed as:

$$\begin{aligned} \alpha_1 &= \delta_f - \frac{v_{y1}+a_1 r_1}{v_{x1}} && \text{For the front wheel of tractor (unit 1)} \\ \alpha_{ij} &= \frac{a_k r_j - v_{yj}}{v_{xj}} && \text{For } j = 1;\ k = 2 \\ & && \quad j = 2;\ k = 3,4,5 \end{aligned} \tag{A.7}$$

At small side-slip angles, the cornering force on the ground plane is normally behind the wheel center on the contact patch, giving rise to a moment which tends to align the wheel plane with the direction of motion during cornering, widely referred to as the "aligning moment". The aligning moment of the tire is obtained from the cornering force and 'pneumatic trail' of the tire, as [158]:

$$M_K = t_k F_{yk} \tag{A.8}$$

where t_k is the pneumatic trail of tires on axle k, which may be estimated from the normal load acting on the tire, as [158]:

$$t_k = 0.05334 + 3.175 * 10^{-6}(0.2248 * F_{zk} - 6040) \tag{A.9}$$

In the above relation, considering single-track vehicle model, F_{zk} is the normal load on the tire corresponding to axle k in newtons and t_k is in meters. Furthermore, in heavy articulated trucks each axle can be equipped with single or dual tires. Dual tire aligning moment arises from the relative slip of inside and outside tires, given by:

$$M_{DTk} = -\frac{D^2}{v_{xj}} C_{xk}\, r_j \qquad \begin{matrix} \text{For } j = 1;\ k = 2{,}3 \\ j = 2;\ k = 4{,}5 \end{matrix} \tag{A.10}$$

where C_{xk} is the longitudinal stiffness of tires mounted on axle k of the vehicle. Equations (A.1) to (A.10) yield the linear equations of motions of the single-track articulated vehicle that can be used to derive the state-space vehicle model as follow:

$$\begin{aligned} &(m_1 + m_2)\,\dot{v}_{y1} - (m_2 c_1 + m_2 c_2)\,\dot{r}_1 + m_2 c_2 \dot{\gamma}_2 \\ &\quad = \frac{-\sum_{k=1}^{5} C_k}{v_{x1}}\, v_{y1} + \frac{\left(-(m_1 + m_2) v_{x1}^2 + (c_1 + c_2)(C_4 + C_5)\right)}{v_{x1}}\, r_1 \\ &\quad + \frac{(-a_1 C_1 + a_2 C_2 + a_3 C_3 + a_4 C_4 + a_5 C_5)}{v_{x1}}\, r_1 \\ &\quad - \frac{(c_2(C_4 + C_5) + a_4 C_4 + a_5 C_5)}{v_{x1}}\, \dot{\gamma} - (C_4 + C_5)\,\gamma + C_1 \delta_F \end{aligned} \tag{A.11}$$

$$\begin{aligned} &(-m_2 c_1)\,\dot{v}_{y1} + (I_{zz1} + m_2 c_1^2 + m_2 c_1 c_2)\,\dot{r}_1 - m_2 c_1 c_2 \dot{\gamma}_2 \\ &\quad = \frac{(-(a_1 + t_1)C_1 + (a_2 - t_2)C_2 + (a_3 - t_3)C_3 + c_1 C_4 + c_1 C_5)}{v_{x1}}\, v_{y1} \\ &\quad + \frac{(-m_2 c_1 v_x^2 - (a_1 + t_1) a_1 C_1 - (a_2 - t_2) a_2 C_2 - (a_3 - t_3) a_3 C_3)}{v_{x1}}\, r_1 \\ &\quad + \frac{\left(-c_1 a_4 C_4 - c_1 a_5 C_5 - c_1 (c_1 + c_2)(C_4 + C_5) - D^2 (C_{x2} + C_{x3})\right)}{v_{x1}}\, r_1 \\ &\quad - \frac{(c_1 (a_4 + c_2) C_4 + c_1 (a_5 + c_2) C_5)}{v_{x1}}\, \dot{\gamma} + (c_1 C_4 + c_1 C_5)\,\gamma + a_1 C_1 \delta_F \end{aligned} \tag{A.12}$$

$$
\begin{aligned}
&(-m_2c_2)\,\dot{v}_{y1} + (I_{zz2} + m_2c_2^2 + m_2c_1c_2)\,\dot{r}_1 - (m_2c_2^2 + I_{zz2})\dot{\gamma}_2 \\
&\quad = \frac{\big((a_4 - t_4)C_4 + (a_5 - t_5)C_5 + c_2(C_4 + C_5)\big)}{v_{x1}}\, v_{y1} \\
&\quad + \frac{\big(m_2c_2v_x^2 - \big(c_2^2 + 2a_4c_2 + a_4(a_4 + t_4)\big)C_4\big)}{v_{x1}}\, r_1 \\
&\quad + \frac{\big(-\big(c_2^2 + (a_4 + a_5)c_2 + a_5(a_5 + t_5)\big)C_5\big)}{v_{x1}}\, r_1 \\
&\quad + \frac{\big(-(a_4 + c_2)c_1C_4 - (a_5 + c_2)c_1C_5 - D^2(C_{x4} + C_{x5})\big)}{v_{x1}}\, r_1 \\
&\quad - \frac{(a_4(a_4 - t_4)C_4 + c_2^2C_4 + a_5(a_5 + t_5)C_5 - c_2^2C_5)}{v_{x1}}\, \dot{\gamma} \\
&\quad + \big((a_4 + c_2 - t_4)C_4 + (a_5 + c_2 + t_5)C_5\big)\,\gamma
\end{aligned}
\tag{A.13}
$$

The equations of motions of the vehicle are then described as the first-order matrix form:

$$
[M]\dot{\vec{x}}(t) = [K]\vec{x}(t) + [I]\vec{u}(t) \tag{A.14}
$$

where the state vector $\vec{x}(t)$ is given as:

$$
\vec{x}(t) = \begin{bmatrix} v_{y1}(t) \\ r_1(t) \\ \dot{\gamma}(t) \\ \gamma(t) \end{bmatrix} \tag{A.15}
$$

In Eq. (A.14), $[M]$, $[K]$ and $[I]$ are the mass, stiffness and input matrices, respectively, which are given as follow:

$$
[M] = \begin{bmatrix} m_1 + m_2 & -m_2(c_1 + c_2) & m_2c_2 & 0 \\ -m_2c_1 & I_{zz1} + m_2c_1^2 + m_2c_1c_2 & -m_2c_1c_2 & 0 \\ -m_2c_2 & I_{zz2} + m_2c_2^2 + m_2c_1c_2 & -(m_2c_2^2 + I_{zz2}) & 0 \\ 0 & 0 & 0 & 1 \end{bmatrix} \tag{A.16}
$$

$$
[I] = \begin{bmatrix} C_1 \\ a_1C_1 \\ 0 \\ 0 \end{bmatrix} \tag{A.17}
$$

$$
[K] = \begin{bmatrix} \vec{K}_1 & \vec{K}_2 & \vec{K}_3 & \vec{K}_4 \end{bmatrix} \tag{A.18}
$$

In above equation, vectors $\vec{K}_1$, $\vec{K}_2$, $\vec{K}_3$ and $\vec{K}_4$ are described as

$$\vec{K}_1 = \frac{1}{v_{x1}}\begin{bmatrix} -\left(\sum_{k=1}^{5} C_k\right) \\ -(a_1+t_1)C_1 + \sum_{k=2}^{3}((a_k-t_k)C_k) + \sum_{k=4}^{5} c_1 C_k \\ \left(c_2(C_4+C_5) + \sum_{k=4}^{5}(a_k-t_k)C_k\right) \\ 0 \end{bmatrix} \tag{A.19}$$

$$\vec{K}_2 = \frac{1}{v_{x1}}\begin{bmatrix} -(m_1+m_2)v_{x1}^2 - a_1C_1 + \sum_{k=2}^{5} a_k C_k + \sum_{k=4}^{5}(c_1+c_2)C_k \\ -m_2c_1v_x^2 - (a_1+t_1)a_1C_1 - \sum_{k=2}^{3}\left((a_k-t_k)a_kC_k - D^2C_{xk}\right) - \sum_{k=4}^{5}(c_1a_kC_k - c_1(c_1+c_2)C_k) \\ m_2c_2v_x^2 - \sum_{k=4}^{5}\left((a_k+c_2)c_1C_k - \left(c_2^2 + (a_4+a_k)c_2 + a_k(a_k+t_k)\right)C_k - D^2C_{xk}\right) \\ 0 \end{bmatrix} \tag{A.20}$$

$$\vec{K}_3 = -\frac{1}{v_{x1}}\begin{bmatrix} c_2(C_4+C_5) + \sum_{k=4}^{5} a_k C_k \\ \sum_{k=4}^{5} c_1(a_k+c_2)C_k \\ \sum_{k=4}^{5}(a_k(a_k+(-1)^{k+1}t_k)C_k + (-1)^k c_2^2 C_5) \\ 0 \end{bmatrix} \tag{A.21}$$

$$\vec{K}_4 = \begin{bmatrix} -(C_4+C_5) \\ c_1C_4 + c_1C_5 \\ \sum_{k=4}^{5}(a_k+c_2+t_k)C_k \\ 1 \end{bmatrix} \tag{A.22}$$

The state-space model of the articulated vehicle is derived from Eqs. (A.14) to (A.22) using $[A_2] = [M]^{-1}[K]$ and $[B_2] = [M]^{-1}[I]$, as:

$$\dot{\vec{x}}(t) = [A_2]\vec{x}(t) + [B_2]\vec{u}(t) \tag{A.23}$$

A.2 Yaw-Plane Articulated Vehicle Model

The equations of motion of the yaw-plane vehicle model, as shown in Figure A.2, describing the lateral and yaw velocities of the tractor and yaw velocity of the semi-trailer unit are obtained as:

$$m_1\left(\dot{v}_{y1} + r_1 v_{x1}\right) = \sum_{i=1}^{2} F_{y\,1i}\ cos\,\delta_F + \sum_{k=2}^{3}\sum_{i=1}^{4} F_{y\,ki} + F_{YA} \tag{A.24}$$

$$I_{zz1}\dot{r}_1 = \sum_{i=1}^{2} F_{y1i}\ a_1\ cos\,\delta_F + \sum_{i=1}^{2}(-1)^i\ F_{y1i}\frac{T_1}{2} sin\,\delta_F\ - \sum_{k=2}^{3}\sum_{i=1}^{4} F_{y\,ki}\ a_k + \sum_{k=1}^{2}\sum_{i=1}^{4} M_{ki} + \sum_{k=2}^{3}\sum_{i=1}^{4} M_{ki} - F_{YA}c_1 + \sum_{i=1}^{2} M_{DTk} \tag{A.25}$$

$$I_{zz2}\dot{r}_2 = -(F_{XA}\ sin\,\gamma)c_2 - (F_{YA}\ cos\,\gamma)\ c_2 - \sum_{k=4}^{5}\sum_{i=1}^{4} F_{y\,ki}\ a_k + \sum_{k=4}^{5}\sum_{i=1}^{4} M_{ki} + \sum_{i=3}^{5} M_{DTk} \tag{A.26}$$

where F_{yki} and M_{ki} are respectively the cornering force and the aligning moment of the i^{th} tire on axle k (i=1,2 for k=1; i=1,2,3,4 for k=2,3,4,5). T_k is the distance between the tires on the tractor front axle, and the longitudinal and lateral forces at the articulation point, as shown in Figure A.3, F_{XA} and F_{YA}, are derived from the constraint equations, as:

$$\begin{aligned} F_{XA} &= -m_2\left(\dot{v}_{x2} + r_2 v_{y2}\right)\ cos\,\gamma - m_2\left(\dot{v}_{y2} + r_2 v_{x2}\right)\ sin\,\gamma + \sum_{j=4}^{5}\sum_{i=1}^{4} F_{y\,ji}\,sin\,\gamma \\ F_{YA} &= m_2\left(\dot{v}_{x2} + r_2 v_{y2}\right)\ sin\,\gamma - m_2\left(\dot{v}_{y2} + r_2 v_{x2}\right)\ cos\,\gamma + \sum_{j=4}^{5}\sum_{i=1}^{4} F_{y\,ji}\,cos\,\gamma \end{aligned} \tag{A.27}$$

The vehicle parameters used in the study are summarized in Table A.1.

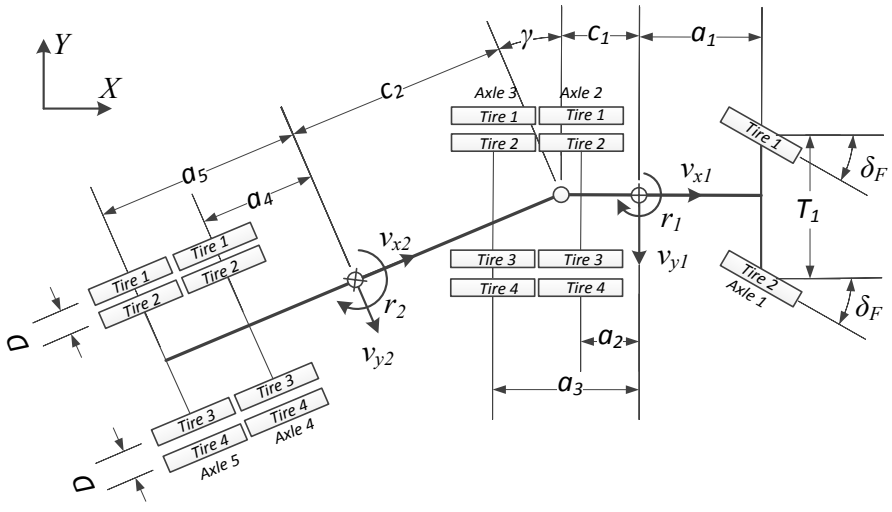

Figure A.2: Dimensional parameters of the yaw-plane articulated vehicle model

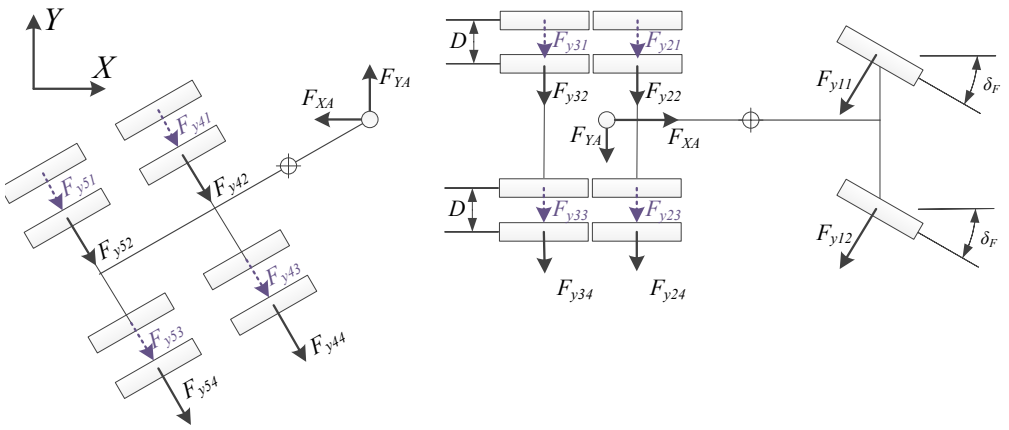

Figure A.3: Cornering forces of the tires and articulation forces of the yaw-plane articulated vehicle model

Table A.1. Design parameters of the selected articulated vehicle combination

Tractor Unit			
Mass, m_1 (kg)		7269.6	
Yaw moment of inertia of the tractor unit, I_{zz1} (kg.m/sec^2)		7903.9	
Horizontal distance from tractor cg to articulation point, c_1 (m)		2.7	
	Axle 1	Axle 2	Axle 3
Axle load (kN)	39.6	70.2	69.4
Horizontal distance from tractor cg cg, a_k , k=1,2,3 (m)	0.9	2.0	3.3
Dual tire spacing, D (m)	-	0.3	0.3
Track width, T_k , k=1,2,3 (m)	2.0	1.8	1.8
Semi-Trailer Unit			
Mass, m_2 (kg)		26018	
Yaw moment of inertia of the semi-trailer unit, I_{zz2} (kg.m/sec^2)		89243.4	
Horizontal distance from semi-trailer cg to articulation point, c_2 (m)		5.8	
	Axle 4	Axle 5	
Axle load (kN)	74.8	74.8	
Horizontal distance from semi-trailer cg, a_k , k=4,5 (m)	3.7	5.0	
Dual tire spacing, D (m)	0.3	0.3	
Track width, T_k , k=4,5 (m)	1.83	1.83	

The cornering force and aligning moments of the tires are described using the Pacejka's tire model, widely referred to as the "Magic formula" tire model [125] in following manner:

$$Y = S_v + D\sin\{C\arctan[B(X - S_h)(1 - E) + E\arctan[B(X - S_h)]]\} \quad \text{(A.28)}$$

where the dependent variable Y represents quantifiable tire responses, such as cornering, longitudinal forces and aligning moment. The independent variable X is the tire service variable. In the case of the cornering force of the tires, the service variable is the side-slip angle (α). The six constants variables S_h, S_v, B, C, D and E, which are associated with the normal load of tires (F_z), tire/road friction coefficient (μ) and side-slip angle, are identified through a curve fitting process considering the reported measured data [152-155]. The coefficients of the Magic Formula for the cornering force of the tire vary with the normal load and side-slip angle as:

$$\begin{aligned} D &= a_1 F_z^2 + a_2 F_z \\ C &= a_0 \\ B.C.D &= a_3 \, sin\left(2.arctan\left(\frac{F_z}{a_4}\right)\right) \\ E &= (a_6 F_z^2 + a_7).\left(1 - a_5.sgn(\alpha + a_8 F_z + a_9)\right) \\ S_{vy} &= a_{10} F_Z + a_{11} \end{aligned} \tag{A.29}$$

where a_l (l=0 to 11) are constant variable which are determined through a curve fitting process considering the experimental measured data.

The coefficients of the Magic Formula for aligning moment of the tire also vary with the normal load and side-slip angle as:

$$\begin{aligned} D &= m_1 F_z^2 + m_2 F_z \\ C &= m_0 \\ B.C.D &= m_3 \sin\left(2.\arctan\left(\frac{F_z}{m_4}\right)\right) \\ E &= (m_6 F_z^2 + m_7).\left(1 - m_5.sgn(\alpha + m_8 F_z + m_9)\right) \\ S_{vm} &= m_{10} F_Z + m_{11} \end{aligned} \tag{A.30}$$

where m_l (l=0 to 11) are constant variable which are determined through a curve fitting process considering the experimental measured data.

A.3 Simulation Results of Tire Cornering and Aligning Properties

In this study, the measured data of a heavy vehicle tire (Michelin XZA, 11R22.5 radial tire), which represents a new truck tire rolling at a moderate speed, has been used to characterize cornering force and aligning moment of the tire [148]. Figures A.4 compares the cornering force and aligning moment derived from the tire model with the measured data subject to variations in the tire's normal load. The tire model (Magic Formula) parameters are identified using a curve-fitting method. The comparisons illustrate a reasonably good correlation between the measured data and the estimated responses.

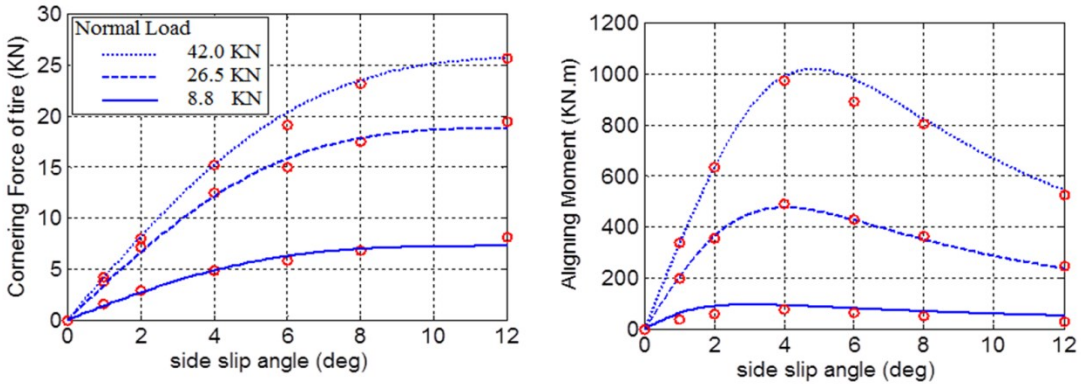

(a) (b)

Figure A.4: Comparison of the measured data (circle dotes) and estimated profile of (a) the cornering forces; and (b) aligning moments of the tire subject to the three different normal loads [148]